ABSTRACT

MCBRYDE, JAMES. Inverter Efficiency Simulation and Measurement for Various Modern Switching Devices. (Under the direction of Dr. Subhashish Bhattacharya).

A power electronics circuit designers most difficult task generally involves loss estimation of power components. The number of variables that must be taken into consideration when calculating power losses can be very overwhelming and a computer based computation tool can be extremely helpful in simplifying the process. The first part of this thesis is an in depth development of a loss computation tool build to speed up, simplify and make more accurate the process of power loss computation in a switching power system. In recent years efficiency has also become a major concern for modern switching power systems. As power devices improve and post-silicon devices become more readily available, it will be increasingly important for power electronics designers to understand key operating principles of these devices. The second part of this thesis explores dynamic switching characteristics for a broad range of switching devices. The switching devices covered include several generations of IGBTs from the same manufacturer, several manufacturers, and several categories of devices. Included in this study are Silicon Carbide JFET devices and Silicon Carbide MOSFET devices, both of which are just hitting the market and are considered to be the next generation of switching devices. The final part of this thesis does an application based study of how the two aforementioned Silicon Carbide devices perform in a real world application as a drop in replacement for traditional Silicon devices.

Inverter Efficiency Simulation and Measurement for Various Modern Switching Devices

by
James McBryde

A thesis submitted to the Graduate Faculty of
North Carolina State University
in partial fulfillment of the
requirements for the degree of
Master of Science

Electrical Engineering

Raleigh, North Carolina

2010

APPROVED BY:

_____	_____
Dr. Subhashish Bhattacharya Committee Chair	Dr. Jayant Baliga
_____	
Dr. Srdjan Lukic	

BIOGRAPHY

James McBryde has been an Electrical Design Engineer at Eaton Corporation since February 2007. He currently designs rectifiers, inverters, dc-dc converters, and other power electronic circuits for Uninterruptible Power Systems (UPS) in the range of 20kVA to 8MVA. Prior to joining Eaton Corporation, James worked for EMC Corporation as a Supplier Quality Engineer managing Switch Mode Power Supplies (SMPS). James graduated Summa Cum Laude from North Carolina State University with a Bachelor of Science Degree in Electrical Engineering in December 2006. This Thesis completes James' requirements for the degree of Master of Science in Electrical Engineering from North Carolina State University.

ACKNOWLEDGMENTS

First of all I would like to thank my advisor, Dr. Subhashish Bhattacharya. Dr. Bhattacharya encouraged me to do the thesis option in the M.S. program and his enthusiasm, knowledge, and advice were extremely helpful throughout my studies. I would then like to thank my thesis committee members Dr. Jayant Baliga and Dr. Srdjan Lukic for their valuable support. I would also like to thank Eaton Corporation for sponsoring my studies at NC State University and my managers Pasi Taimela and Bobby Compton for their support as well. Finally, I would like to thank my wife Brandy for her continued encouragement and support of my career and educational goals; I could not have done this without her encouragement and motivation.

TABLE OF CONTENTS

LIST OF TABLES

LIST OF FIGURES

CHAPTER 1

1 INTRODUCTION

Semiconductor switching devices are the foundation of modern switching power systems. Devices of many voltage and current ratings are available on the market and advances to these devices are being released each year. This study was motivated by the need to understand and characterize modern switching devices in the context of efficiency on a UPS inverter. The first obstacle investigated was the issue of being able to evaluate different devices from a dynamic loss perspective and get a level playing field comparison. Each device manufacturer specifies dynamic loss parameters for their devices using their own values for gate resistor, gate voltage, temperature, current, voltage, and frequency. Additionally, many manufacturers offer a way to compute losses in an inverter but do not have a way of comparing their devices with other manufacturers

In Chapter 2, a loss computation tool has been created that allows the user to evaluate different devices in a carrier based switching power system. A half bridge inverter configuration was used as an example and shown using several devices as test cases. The loss tool takes as inputs standard datasheet parameters that are flexible enough to be read or calculated from any manufacturers' datasheet. The loss computation tool was then extended to a 3-level Neutral-Point-Clamped (NPC) inverter topology to show how flexible the loss simulator can be. Chapter 3 expanded on the tool usefulness by showing through evaluation that it is indeed accurate. Two different semiconductor vendor loss software programs were evaluated with respect to the loss

computation tool created in Chapter 2. It was shown that the loss computation tool created for this project is not only accurate; it allows the user to input parameters that both software programs on the market do not have available. This gives the power electronics engineer an extra degree of freedom in that they can compare one to one different devices without making the drive assumptions forced by the manufacturer.

Chapter 4 takes the loss simulator and does a detailed efficiency evaluation of a 480V, 18kW inverter phase leg. The loss simulator evaluates in detail six devices, two of which are Silicon Carbide JFET devices which have recently been introduced to the. The chapter gives an in depth evaluation of the devices. Further, chapter 4 extends the findings to a 3-level NPC inverter as well.

Chapter 5 begins laboratory experimental testing of the dynamic switching characteristics of several devices. In application, switching losses of power semiconductor devices can depend on a large number of factors. These can include the temperature of the device, the gate drive characteristics, the switched current and voltage, and the stray inductances and capacitances in the test setup. This laboratory setup set out to compare several different switching devices from different technology generations on a baseline scale in order to understand the dynamic performance characteristics of each. Each test in this section utilized the same exact gate driver, power supply, oscilloscope, measurement probes and current sensors, gate resistor, and room temperature. Because the test utilized a single pulse generator, the device was not given time to heat up under test and is at a set room temperature. Fourteen total tests were done, using a

variation of Silicon IGBT's, Silicon MOSFET's, Silicon Carbide JFET's, and Silicon Carbide MOSFET's in addition to antiparallel diodes made with both Silicon and Silicon Carbide.

Chapter 6 took the information obtained from the testing in chapter 5 in addition to research about the devices and further laboratory testing in order optimize the performance of the Silicon Carbide devices (JFET and MOSFET). Both of the Silicon Carbide devices have incredible performance capability but require special gate drive requirements in order to achieve them. In chapter 7, the laboratory data from the previous two chapters is evaluated, compared, and discussed.

Chapters 8 and 9 respectively, take the knowledge learned from the previous 7 chapters and apply them to a laboratory experiment. Chapter 8 takes a 300W two switch flyback supply and replaces the two 1000V MOSFET devices with 1200V SiC MOSFET devices in order to analyze in a real world application how the SiC MOSFET performs in a real system. Chapter 9 does the same with a 6kVA, 4.2kW double conversion true online Uninterruptible Power Supply. The data from the two chapters is analyzed and summarized explaining how much, if any, improvement can be achieved by converting an existing design to SiC devices.

CHAPTER 2

2 CREATION OF LOSS SIMULATOR IN MATLAB

One of the most important aspects of analyzing power electronic circuits is the ability to calculate loss components. There are several reasons why a simulation tool can be very useful in computing these losses. In particular, when dealing with AC waveforms, there can be a limit to how accurate one can calculate loss components by hand. For each device the most important parameter that determines the number of watts lost is the instantaneous current flowing through the semiconductor device. Because the current waveform in a sinusoidal AC power supply is constantly changing, one must breakdown the waveform into parts and analyze each point in order to get an accurate estimate of conduction and switching losses. This process can be very tedious if not automated, and computational tools such as Matlab make the process much quicker.

There are several semiconductor vendors with commercial applications on the market designed to estimate losses for particular devices at specific operating conditions. Infineon Technologies has a program called Iposim, Semikron International has a program called SemiSel, and PowerEx Semiconductor has a program called MelcoSim. Each of these programs has one or more of the following flaws preventing it from being flexible enough for everyday use:

1) The program will only calculate losses for devices made by that particular semiconductor vendor.
2) The program does not allow multiple devices to be paralleled.

3) The program does not allow other configurations besides a typical half bridge configuration (three level NPC for example, is not supported)

4) The program does not allow for adjusting key parameters such as gate resistor, output filter inductance, DC Link voltage, or temperature.

This project addresses these concerns by creating a generic but easy to use simulation tool for computing semiconductor losses. A Matlab script was used as the engine for the calculations with a typical inverter phase leg as the initial target. The loss simulator takes as inputs several key parameters which should be readily available off of a standard datasheet. The standard device used in a typical inverter phase leg is generally an IGBT with anti-parallel diode. As a benchmark, a standard phase leg was used. The exercise was then extended to a three level Neutral Point Clamped (NPC) inverter to show the flexibility of the tool with minor modification. All simulations were run for a unity power factor, although power factor could easily be adjusted. It is important to note that each layer of flexibility that was added to the simulation made the run time significantly longer.

2.1 Two Level Loss Simulator Inputs and Operation

The two level loss simulator takes inputs which should be readily available from IGBT and diode datasheets. The key parameters are as follows:

1) IGBT conduction loss – read directly from the IGBT I vs. V curve on the datasheet. This is expressed in the Matlab script as two constants; the knee voltage and the on resistance. These values are listed as IGBT_V and IGBT_R.

2) Diode Conduction loss – read directly from the Diode I vs. V curve on the datasheet. This is expressed in the Matlab script as two constants; the knee voltage and the on resistance. These values are listed as Diode_V and Diode_R.

3) IGBT turn on switching loss – this loss is usually read directly off of the datasheet for an IGBT, but may have to be calculated for a MOSFET or other switch. This is expressed in the Matlab script as two constants; the intercept (IGBT_Eon_int) and the slope (IGBT_Eon_sl). The slope is the only parameter required since the intercept will generally be zero. The slope is simply the delta E divided by the delta I.

4) IGBT turn off switching loss – this loss is usually read directly off of the datasheet for an IGBT, but may have to be calculated for a MOSFET or other switch. This is expressed in the Matlab script as two constants; the intercept (IGBT_Eoff_int) and the slope (IGBT_Eoff_sl). The slope is the only parameter required since the intercept will generally be zero. The slope is simply the delta E divided by the delta I.

5) Diode reverse recovery switching loss – this loss is usually read directly off of the datasheet for a co-pack with an IGBT and diode, but may have to be

calculated for other configurations. This is expressed in the Matlab script as two constants; the intercept (Diode_Err_int) and the slope (Diode_Err_sl). The slope is the only parameter required since the intercept will generally be zero. The slope is simply the delta E divided by the delta I.

The key parameters must be compared at similar operating conditions when comparing two different devices for use in the same application. For example, different semiconductor manufacturers may use different gate resistors when drawing the switching loss curves for their devices. Also, various temperatures are usually given on the datasheet. For accurate simulation results, the power electronics engineer must understand these parameters and be able to use similar assumptions when evaluating two devices. In some datasheets, semiconductor manufacturers will combine the turn on loss of the IGBT with the recovery loss in the diode, since much of the turn on loss for the IGBT is actually due to the recovery current for the diode charge recombination. For this case, the value can be put into either the Eon or Err keeping the other zero. The loss simulator also takes as inputs eight design constants. The user can adjust the following design constants:

1) n = number of parallel devices

2) f = operating frequency of output sinusoid in Hz

3) fs = switching frequency of converter in Hz

4) L = output filter inductor in Henry's

5) R = output load resistance in Ohms

6) VDC = DC voltage of inverter in Volts

7) mod_index = modulation index of the inverter

8) simulation_step = time step for the simulation in seconds

2.2 Two Level Simulator Example and Results

In order to demonstrate the operation of the simulator, a case is shown for a 18kW, 480V inverter. The inverter uses the following key parameters:

1) DC Link is 820V
2) Output Voltage is 277V L-N, 480V L-L
3) Output power factor is 1
4) Full resistive load is 18kW
5) Full load current for one phase is (18,000/3)/277 = 21.7Arms
6) Resistive load is 277V/21.7A = 12.8Ohms
7) Switching frequency is 20kHz

The inverter uses two 1200V 50A devices in parallel, and uses International Rectifier IRG4PH50KD co-packs with anti-parallel diode built in. Because the device is a co-pack with IGBT and Diode in the same package, the manufacturer has included the reverse recovery losses together with the turn on loss. The datasheet for this device has been attached and is in

Appendix A. The entire Matlab script for this exercise is also attached and is shown in Appendix B. The datasheet key parameters and the design constants are as follows:

```
%%Datasheet Inputs
IGBT_V = 1.3;
IGBT_R = 80e-3;
Diode_V = 1.6;
Diode_R = 40e-3;
IGBT_Eon_int = 0;
IGBT_Eon_sl = 0.1785;
IGBT_Eoff_int = 0;
IGBT_Eoff_sl = 0.1785;
Diode_Err_int = 0;
Diode_Err_sl = 0;

%%Design Constants
n = 2;
f = 50;
fs = 20000;
L = 1000e-6;
R = 12.8;
VDC = 410;
mod_index = 0.9;
simulation_step = 0.5e-6;
```

Using the datasheet parameters and the design constants the simulator creates a sinusoidal reference voltage and triangular carrier signal. It uses sine-triangle modulation with these two signals to generate the pwm patterns for the switching devices. Figure 1 shows a zoomed in portion of the sinusoidal reference voltage in purple and triangular carrier signal in blue. A zoomed in portion of the generated pwm signal is shown in Figure 2.

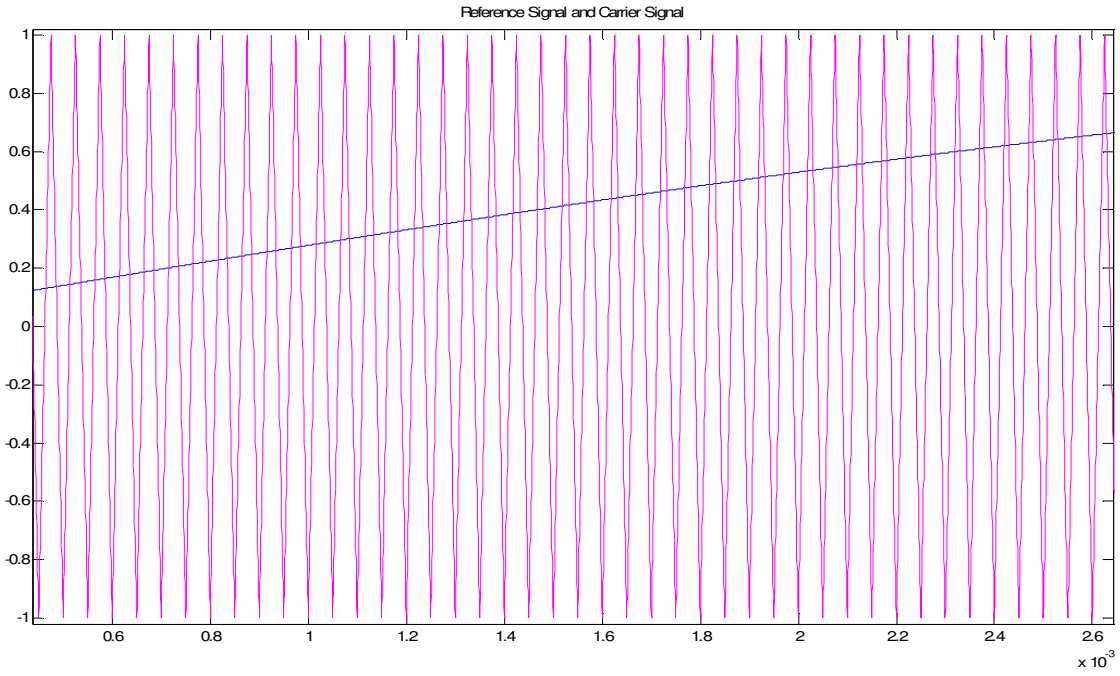

Figure 1: Sinusoidal Reference Voltage and Triangular Carrier Signal

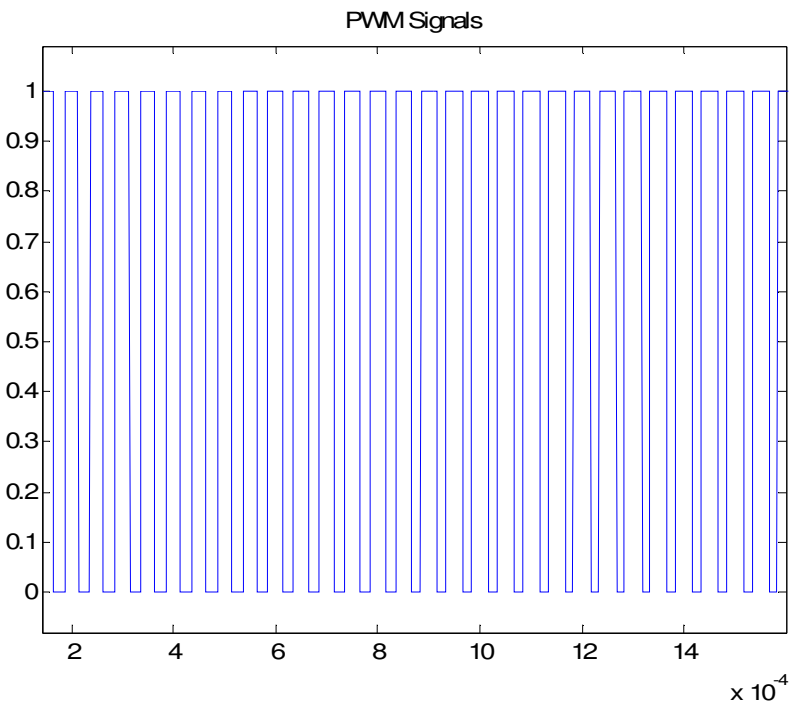

Figure 2: Generated PWM Signal

The current waveform is then calculated using the known inductance value and the reference voltage at each instant. The current waveform is shown below in Figure 3. The simulator keeps track of the instantaneous current at each point in time and computes the conduction losses in either the IGBT or Diode, depending on the direction of the current and instantaneous PWM signal. The conduction losses are computed using the instantaneous current, V, and R for the particular device. The IGBT conduction losses are plotted in Figure 4 below and the Diode conduction losses are plotted in Figure 5 below.

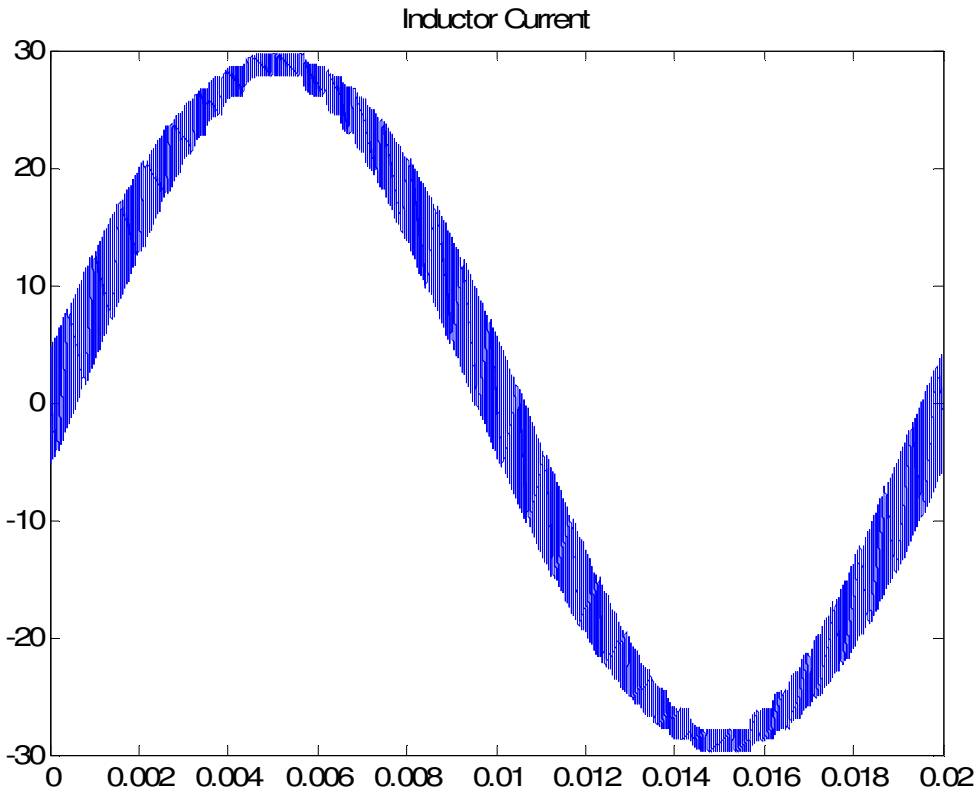

Figure 3: Instantaneous Inductor Current

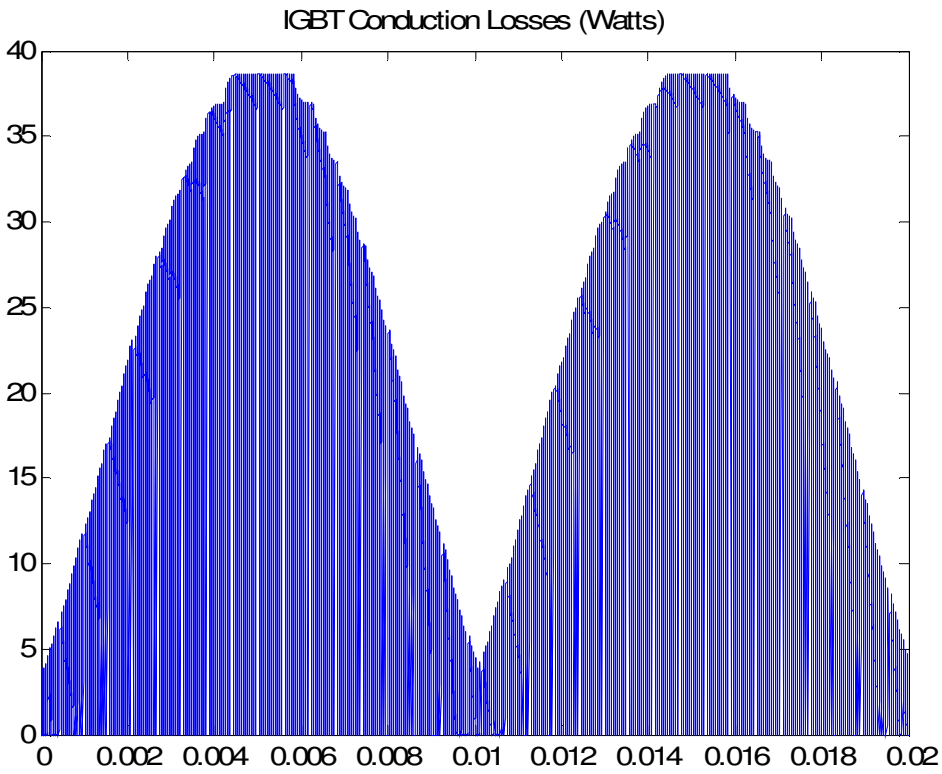

Figure 4: IGBT Instantaneous Conduction Losses

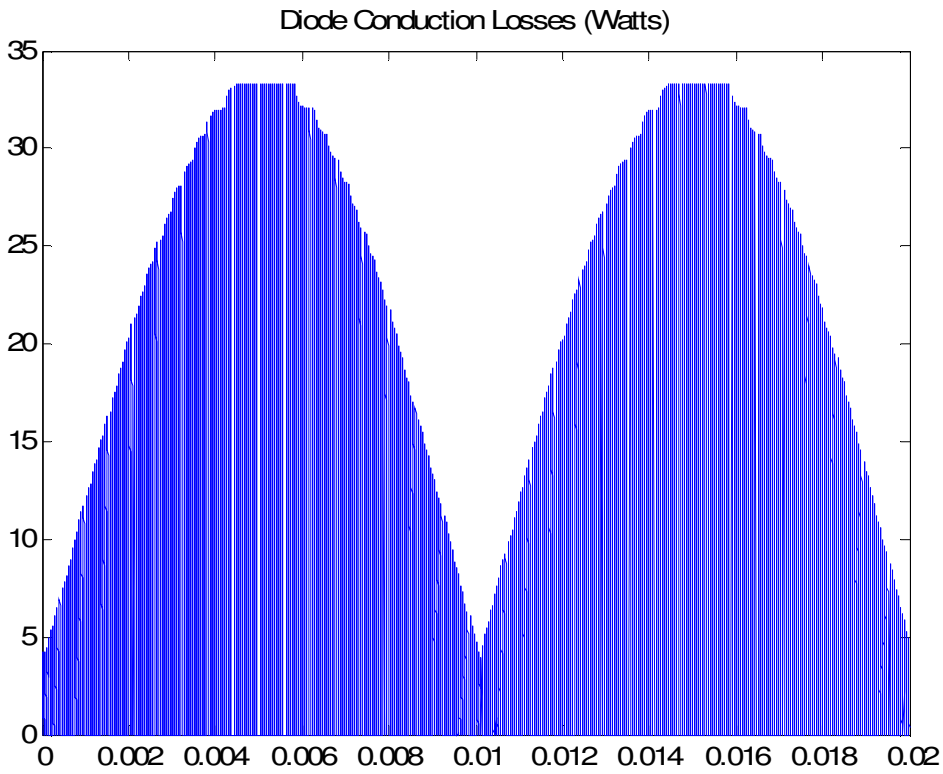

Figure 5: Diode Instantaneous Conduction Losses

Finally, the simulator keeps track of the previous PWM command so that it knows exactly the instant when the PWM command switches and switching losses occur. For each switching event, the simulator calculates either the IGBT turn off loss or the IGBT turn on and Diode reverse recovery losses (depending on the direction of the current and the PWM command). The instantaneous turn on losses are plotted in Figure 6 below and the instantaneous turn off losses (including reverse recovery) are plotted in Figure 7 below.

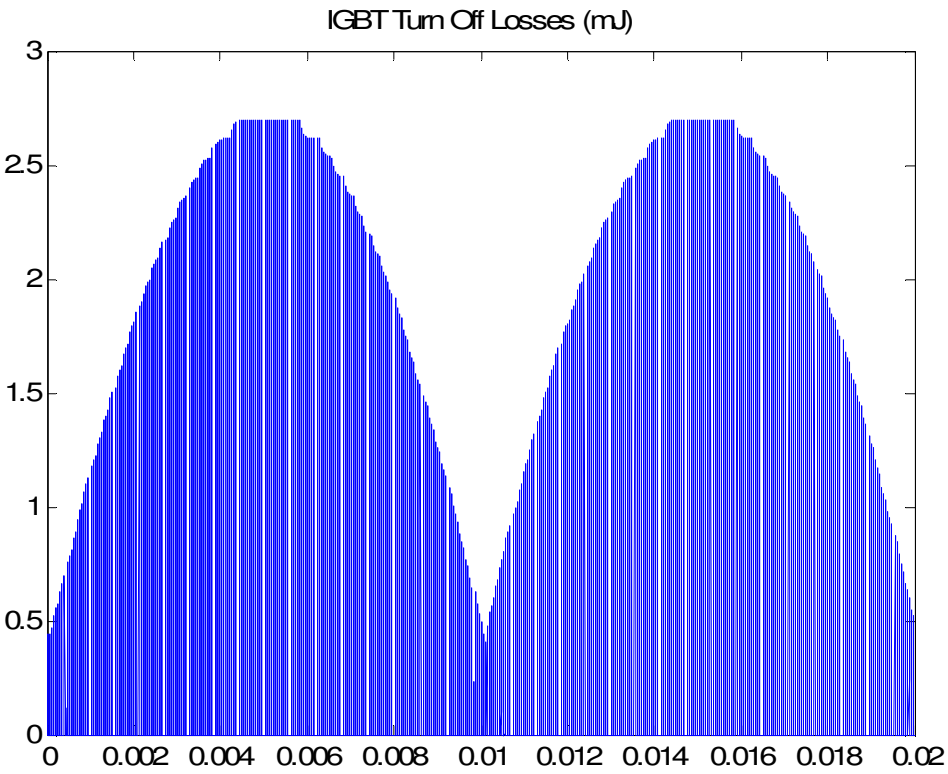

Figure 6: Instantaneous IGBT turn off losses

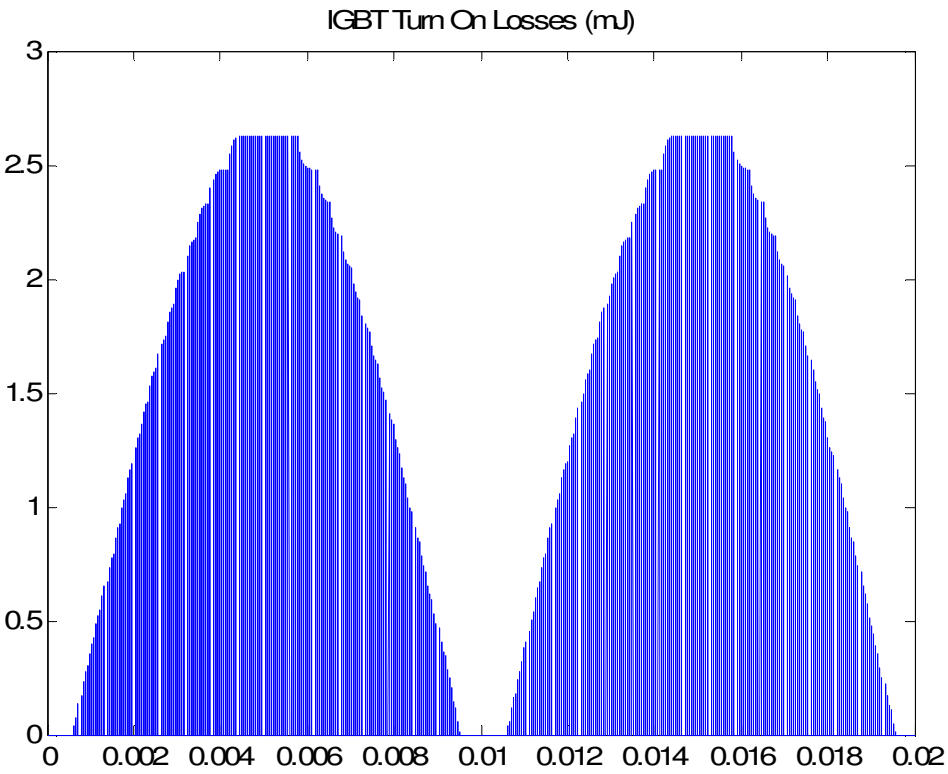

Figure 7: Instantaneous IGBT turn on & Diode reverse recovery losses

The final calculation the simulator must make is to calculate the average of each of the loss elements and print them to the output of the Matlab command window. For this example exercise, the outputs were shown to be 39 Watts for the IGBT conduction losses, 4.8 Watts for the Diode conduction losses, and 189 Watts for the total switching losses.

2.3 Three Level Simulator Example and Results

The above simulation exercise can fairly simply be extended to the case where the inverter is a different topology. One example is the Three Level Neutral-Point-Clamped (NPC)

topology. In this exercise, the Three Level topology is evaluated in a similar manner as done in Section 2.2 for a Two Level inverter. This case study is shown again for a 18kW, 480V inverter. This Three Level inverter uses the following key parameters:

1) DC Link is 820V
2) Output Voltage is 277V L-N, 480V L-L
3) Output power factor is 1
4) Full resistive load is 18kW
5) Full load current for one phase is (18,000/3)/277 = 21.7Arms
6) Resistive load is 277V/21.7A = 12.8Ohms
7) Switching frequency is 20kHz

The inverter uses two 600V 30A devices in parallel, and uses International Rectifier IRG4PC30KD co-packs with anti-parallel diode built in. For the extra diodes required in the Three Level NPC topology, the same diode was used that is internal to the IRB4PC30KD co-pack. Because the device is a co-pack with IGBT and Diode in the same package, the manufacturer has included the reverse recovery losses together with the turn on loss. The datasheet for this device has been attached and is in Appendix C. The entire Matlab script for this exercise is also attached and is shown in Appendix D. The datasheet key parameters and the design constants are as follows:

```
%%Datasheet Inputs
IGBT_V = 1.1;
IGBT_R = 85e-3;
Diode_V = 1;
Diode_R = 42e-3;
```

```
IGBT_Eon_int = 0;
IGBT_Eon_sl = 0.0451;
IGBT_Eoff_int = 0;
IGBT_Eoff_sl = 0.0451;
Diode_Err_int = 0;
Diode_Err_sl = 0;

%%Design Constants
n = 2;
f = 50;
fs = 20000;
L = 1000e-6;
R = 12.8;
VDC = 410;
mod_index = 0.9;
simulation_step = 0.5e-6
```

The simulator again creates a sinusoidal reference voltage and compares it to the carrier signal. The difference here, however, is that a Three Level NPC topology requires two carrier signals to be used. One during the positive half cycle and one during the negative half cycle. Two pwm signals are also generated, since there are four total switches in this topology. Again, using the datasheet parameters and the design constants the simulator generates the PWM patterns for the switching devices and using the PWM patterns, generates a current waveform through the inductor. Figure 8 below shows the current waveform through the inductor, with Figures 9, 10, 11, and 12 respectively being the instantaneous loss components of IGBT conduction, Diode conduction, IGBT turn on, and IGBT turn off with Diode reverse recovery included. Figure 12b shows a schematic of a single phase three level NPC inverter topology.

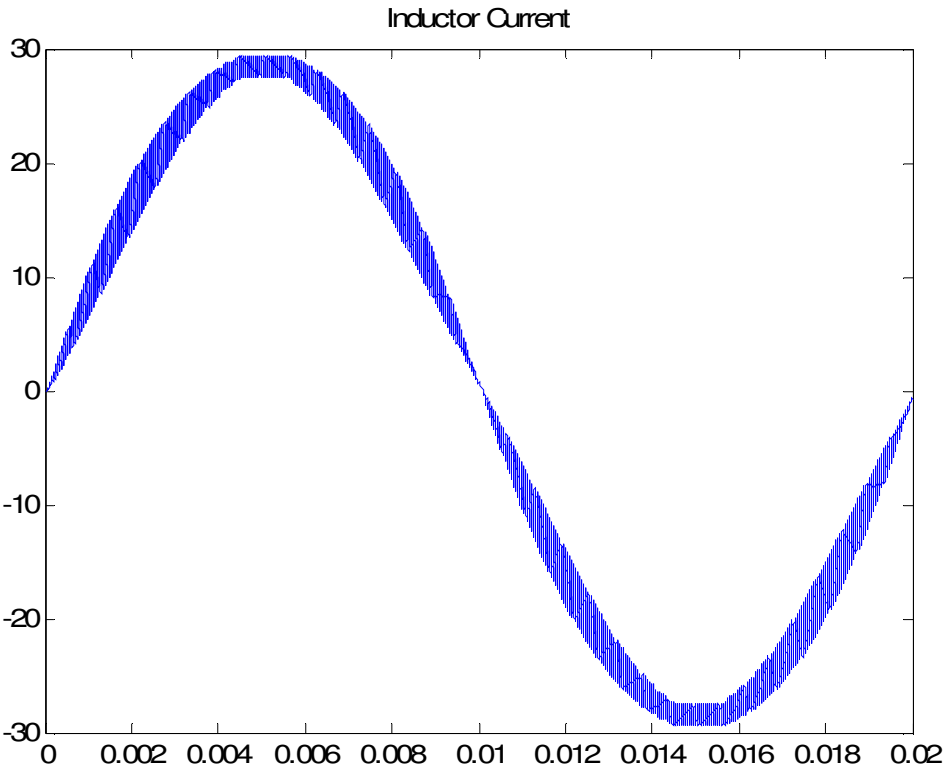

Figure 8: Three Level Inductor Current Waveform

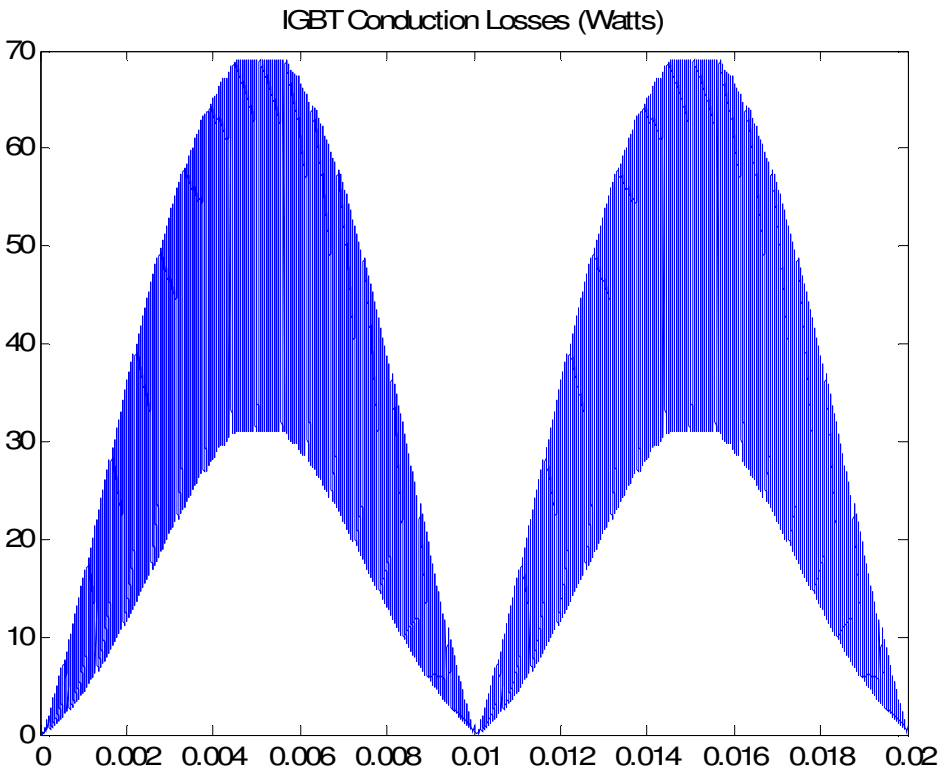

Figure 9: IGBT Instantaneous Conduction Losses

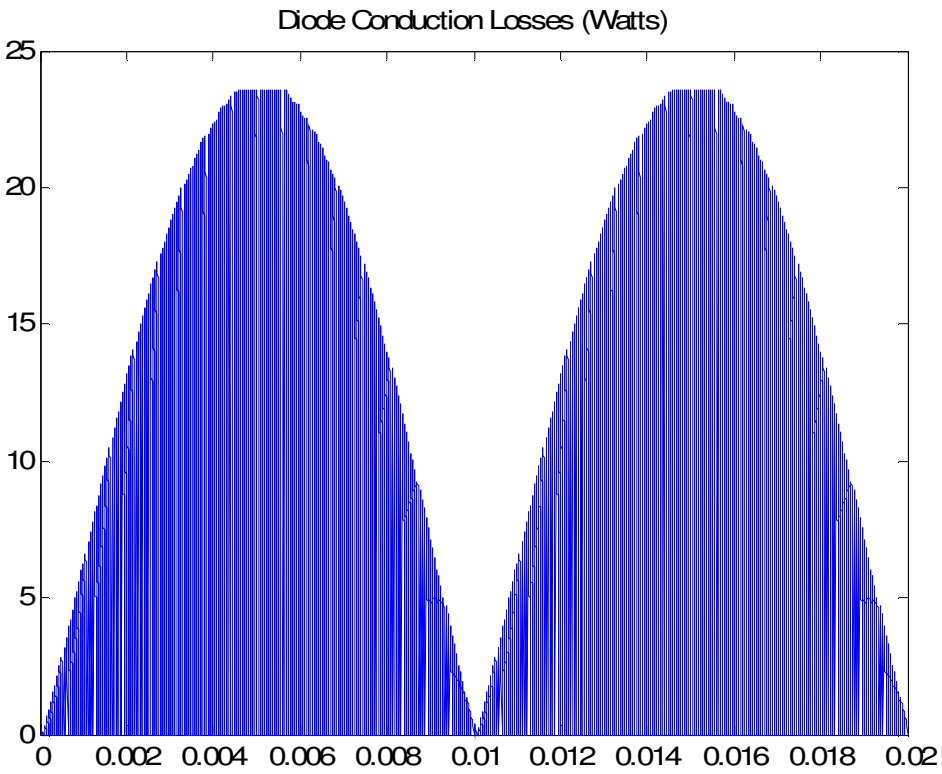

Figure 10: Diode Instantaneous Conduction Losses

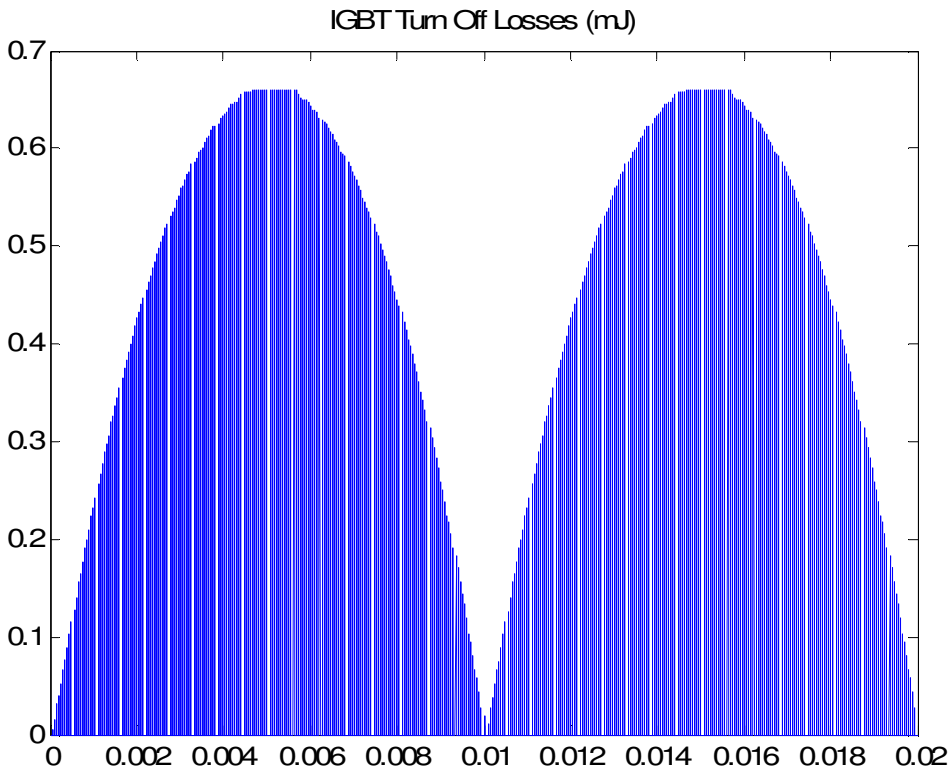

Figure 11: IGBT Instantaneous Turn Off Losses

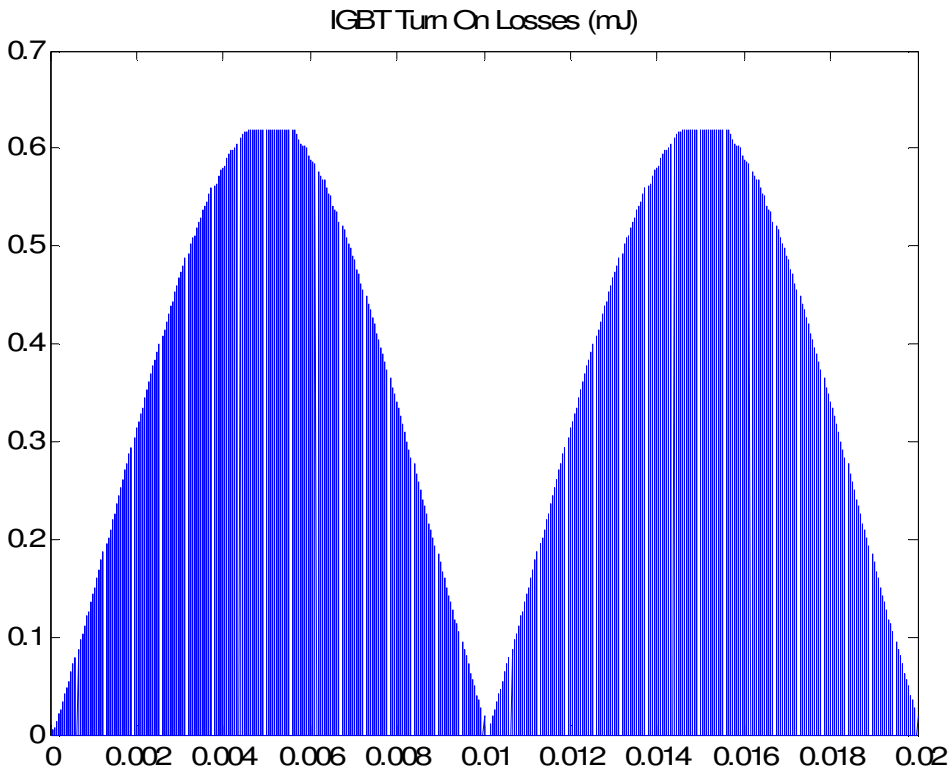

Figure 12: IGBT Instantaneous Turn On Losses With Diode Reverse Recovery

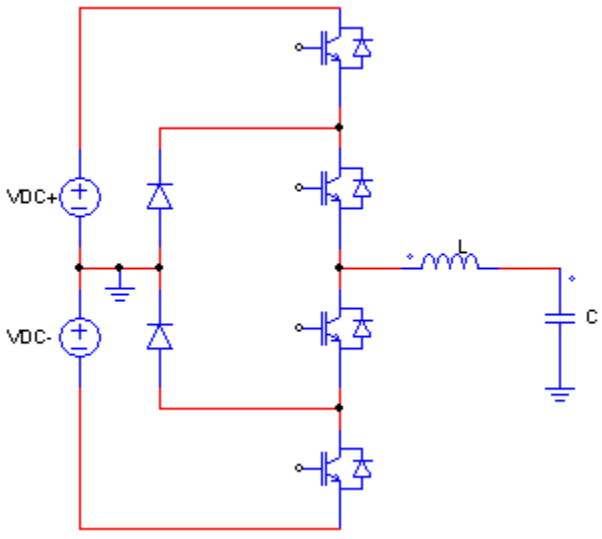

Figure 12b: Schematic of Single Phase Three Level NPC Inverter Topology

Again, the final calculation the simulator must make is to calculate the average of each of the loss elements and print them to the output of the Matlab command window. For this example Three Level exercise, the outputs were shown to be 66 Watts for the IGBT conduction losses, 7.4 Watts for the Diode conduction losses, and 45 Watts for the total switching losses. It can be seen that as we would expect when using a three level topology, the conduction losses roughly double and the switching losses go down by a factor of 3-4 times.

CHAPTER 3

3 EVALUATION OF LOSS SIMULATOR

It is imperative that once an Engineering tool has been created it is evaluated and proven before being used as a benchmark for calculations. As mentioned earlier in this paper, many semiconductor vendors have their own loss computation programs each of which has one of more distinct flaws that prevent it from being flexible enough for comparison. Those tools, however, are a valuable way to check the calculations made in this paper.

3.1 Comparison of Loss Simulator with Infineon Iposim Tool

The loss simulator was evaluated for accuracy by comparing it to the Infineon Technologies Iposim loss calculator. The device chosen was the Infineon part number FF100R12YT3; a 100 Amp 1200 Volt IGBT co-pack in the Easy2B package. Parameters for comparison were input identically for both the Matlab simulator and the Iposim tool. A summary of the input parameters is as follows:

1) DC Link is 800V
2) Output Voltage is 277V L-N, 480V L-L
3) Output power factor is 1
4) Full resistive load is 20kW
5) Full load current for one phase is (20,000/3)/277 = 24Arms
6) Resistive load is 277V/24A = 11.5Ohms

7) Switching frequency is 20kHz

8) Turn on/off Gate Resistor = 6.8 Ohms

The Infineon FF100R12YT3 datasheet is attached in Appendix E and the Iposim simulator output results are shown in Appendix F. The key datasheet parameters for the Infineon device that were input into the Matlab script file are as follows:

```
%%Inputs Needed Are As Follows
IGBT_V = 0.75;
IGBT_R = 9e-3;
Diode_V = 1.2;
Diode_R = 30e-3;
IGBT_Eon_int = 1.2;
IGBT_Eon_sl = 0.15;
IGBT_Eoff_int = 0;
IGBT_Eoff_sl = 0.17;
Diode_Err_int = 1.6;
Diode_Err_sl = 0.1833;
```

The final results of the Matlab simulator were shown to be accurate within 5% of the results the Infineon Iposim tool gave (most of which could have been attributed to rounding). A summary of the final loss breakdown is shown below in Figure 13:

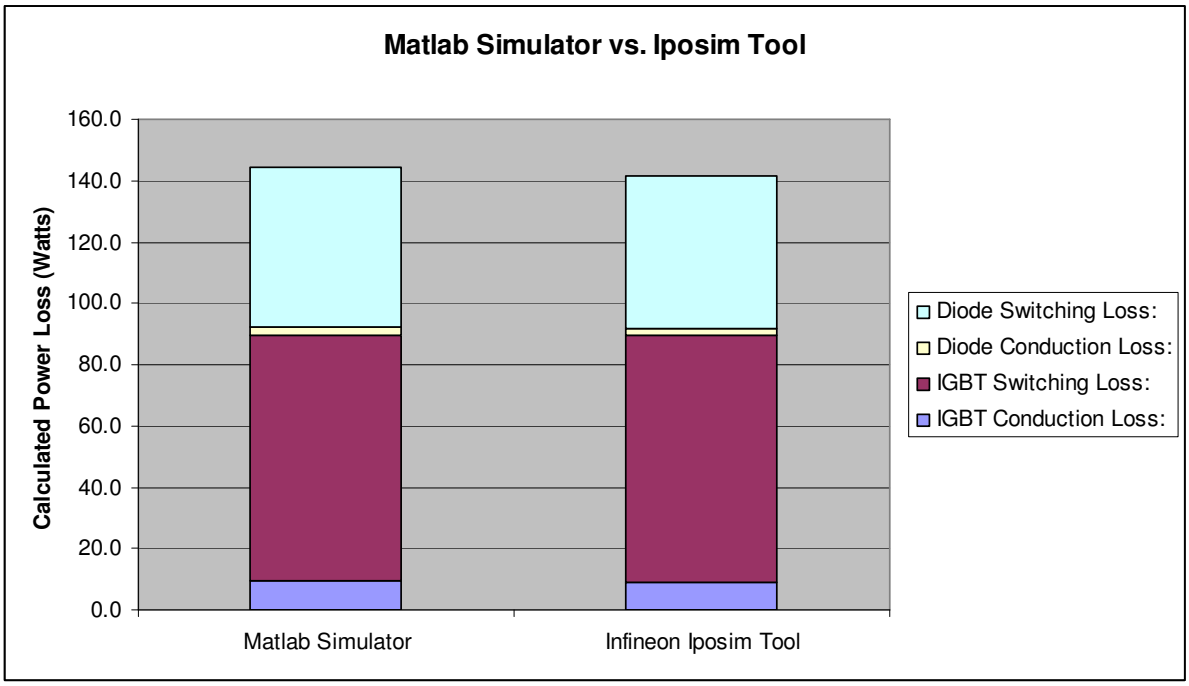

Figure 13: Loss Breakdown for Matlab vs. Iposim

Table 1: Loss Breakdown for Matlab vs. Iposim

	Matlab Simulator	Infineon Iposim Tool
IGBT Conduction Loss:	9.4 Watts	9.0 Watts
IGBT Switching Loss:	80.3 Watts	80.4 Watts
Diode Conduction Loss:	2.5 Watts	2.4 Watts
Diode Switching Loss:	52.2 Watts	50.0 Watts

3.2 Comparison of Loss Simulator with Semikron Semisel Tool

The loss simulator was evaluated for accuracy a second time by comparing it to the Semikron International Semisel loss calculator. The device chosen was the Semikron part number SK100GB12T4T; a 100 Amp 1200 Volt IGBT co-pack in the Semitop 3 package. Parameters for comparison were input identically for both the Matlab simulator and the Semisel tool. A summary of the input parameters is as follows:

1) DC Link is 800V
2) Output Voltage is 277V L-N, 480V L-L
3) Output power factor is 1
4) Full resistive load is 20kW
5) Full load current for one phase is (20,000/3)/277 = 24Arms
6) Resistive load is 277V/24A = 11.5Ohms
7) Switching frequency is 20kHz
8) Turn on/off Gate Resistor = 16 Ohms

The Semikron SK100GB12T4T datasheet is attached in Appendix G and the Semikron simulator output results are shown in Appendix H. The key datasheet parameters for the Semikron device that were input into the Matlab script file are as follows:

```
%%Inputs Needed Are As Follows
IGBT_V = 1;
IGBT_R = 12e-3;
Diode_V = 0.8;
Diode_R = 19e-3;
IGBT_Eon_int = 0;
IGBT_Eon_sl = 0.22;
IGBT_Eoff_int = 0;
IGBT_Eoff_sl = 0.17;
Diode_Err_int = 0;
Diode_Err_sl = 0.075;
```

The final results of the Matlab simulator were shown to be accurate within 5% of the results the Semikron Semisel tool gave (most of which could have been attributed to rounding). A summary of the final loss breakdown is shown below in Figure 14:

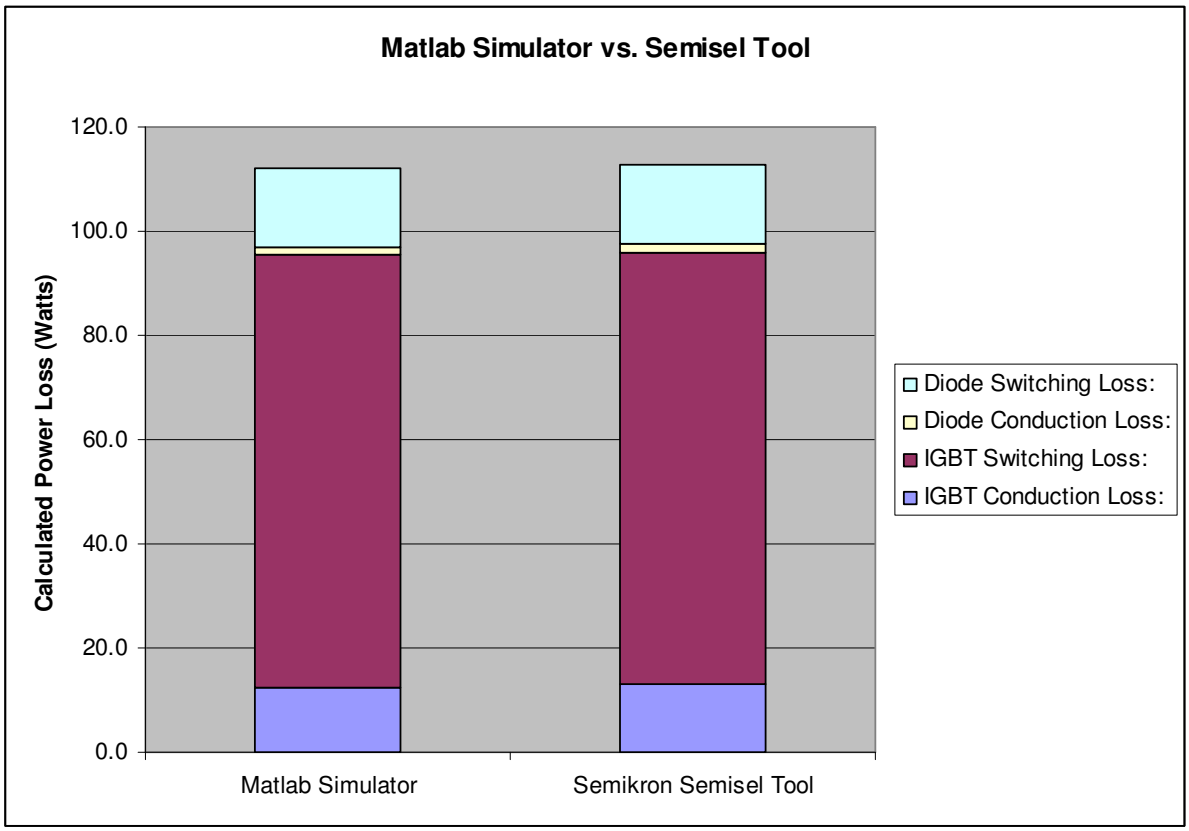

Figure 14: Loss Breakdown for Matlab vs. Semisel

Table 2: Loss Breakdown for Matlab vs. Semisel

	Matlab Simulator	Semikron Semisel Tool
IGBT Conduction Loss:	12.5 Watts	13.0 Watts
IGBT Switching Loss:	82.9 Watts	83.0 Watts
Diode Conduction Loss:	1.6 Watts	1.6 Watts
Diode Switching Loss:	15.1 Watts	15.0 Watts

CHAPTER 4

4 EVALUATION OF VARIOUS SWITCHING DEVICES IN A HALF BRIDGE CONFICURATION

The previous loss computation tool gives the power electronics engineer the flexibility to compare and contrast various power electronic devices from different manufacturers, with different parameters, and of different technology families. The next stage of this project utilizes the above described loss computation tool in order to compare and contrast various technologies for a half bridge inverter. The half bridge inverter is the industry standard for UPS inverters, solar inverters, and AC power supplies. This chapter will initially compare devices in a two level half bridge inverter configuration, and then in a three level half bridge inverter configuration.

4.1 Two Level Switching Device Evaluation

Six switching device configurations are used for comparison in this section of the project. All six switching configurations use two devices in parallel in order to handle the 21.7 amp RMS current of an 18kW phase leg. 1200V devices are used in order to handle an 820V DC Link, with a switching frequency of 20kHz. The key parameters are as follows:

1) DC Link is 820V
2) Output Voltage is 277V L-N, 480V L-L

3) Output power factor is 1

4) Full resistive load is 18kW

5) Full load current for one phase is (18,000/3)/277 = 21.7Arms

6) Resistive load is 277V/21.7A = 12.8Ohms

7) Switching frequency is 20kHz

8) Two IGBT's and two Diodes in parallel for each switch

The investigation begins with a 50 Amp International Rectifier (IR) short circuit rated generation 4 IGBT part (IRG4PH50KD). The part includes an UltraFast Soft Recovery Diode as a co-pack. The device is then replaced with the same part minus the co-packaged diode. The device part number from IR is IRG4PH50K, and it is now mated with a separate C2D20120 Silicon Carbide (SiC) diode from Cree. The Cree device has virtually zero reverse recovery and enables the half bridge switching losses to be reduced drastically. The total losses with the Cree diode are reduced from 235.45 Watts to 192.82 Watts, a decrease in losses of 18%. A table showing the breakdown of losses is shown in Table 3 below.

The next stage of calculations uses another 50 Amp IR IGBT and Diode co-pack (IRG4PH50UD). The device sacrifices its short circuit rating for the ability to switch much faster than the previous device. The device is again compared with and then without its co-packaged Silicon diode, the latter time using the same Cree diode used in the first experiment. The device part number without the co-packaged diode is IRG4PH50U and is used with a C2D20120 SiC diode. As can be seen from the loss breakdown results in Table 3, the use of SiC diode reduces the losses by roughly 31% in this case.

The final evaluation was done with a new emerging device technology. The switch used is made by a small startup company called SemiSouth Laboratories, a spin-off company from the Mississippi State University in Starkville, MS. The device is a SiC JFET transistor, in a normally-on configuration. The device optimizes the switching speed of a MOSFET without the drive complications of a normally-off configuration switch. The device also exhibits very low conduction losses. Two such devices were evaluated, a 125mOhm device which has extremely low switching losses but slightly higher conduction losses than its standard silicon counterparts. Finally, a 63mOhm device was used which has almost as low switching losses as the 125mOhm device yet much lower conduction losses as well. Both devices were mated with the Cree C2D20120 SiC diodes providing exceptional switching characteristics. The SiC JFET's showed to have much lower losses compared to both the standard silicon counterparts. The higher loss SiC JFET dissipated less than half the losses of the best Silicon switch with SiC diode combination.

A summary of all the loss components for each configuration is shown in Table 3 below. The table includes the total losses along with the efficiency of the whole inverter were it to be used in a 3-phase configuration with these devices. Also, a graph showing the relative losses compared between the three is shown in Figure 15 below.

Table 3: Loss Comparison for Two Level Devices (Units are in Watts)

	IRG4PH50KD Internal Diode	IRG4PH50K C2D20120	IRG4PH50UD Internal Diode	IRG4PH50U C2D20120	SJEP120R125 C2D20120	SJEP120R063 C2D20120
IGBT Cond	39.9	39.9	39.9	39.9	43.3	23.8
Diode Cond	4.65	4.52	4.65	4.52	4.52	4.52
Switching	190.9	148.4	145.6	86.7	11.23	14
Total	**235.45**	**192.82**	**190.15**	**131.12**	**59.05**	**42.32**
Inverter Eff	96.08%	96.79%	96.83%	97.81%	99.02%	99.29%

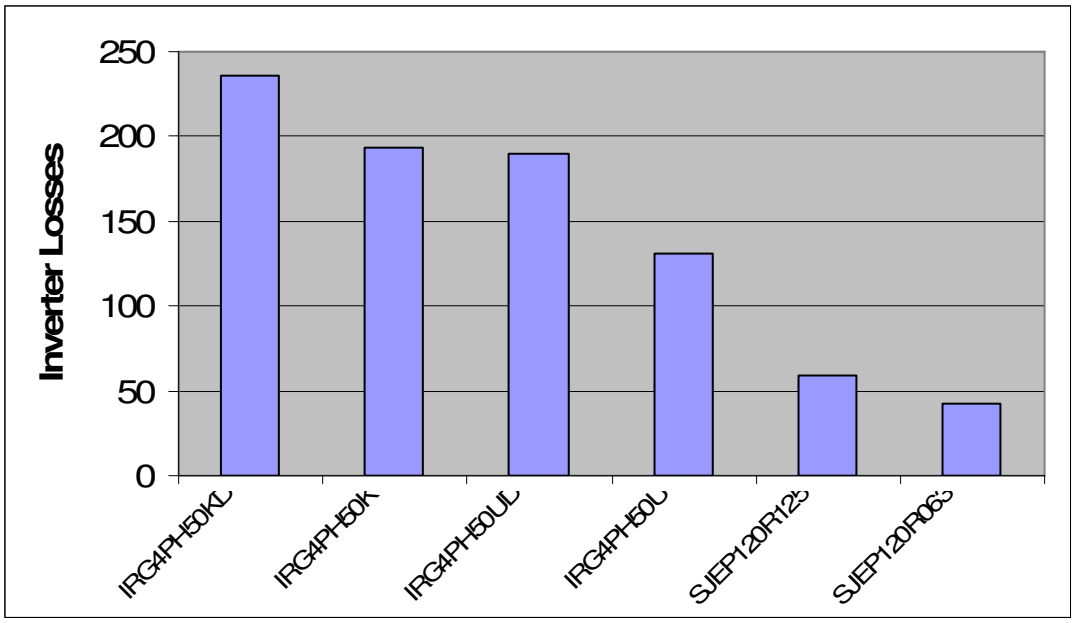

Figure 15: Loss Comparison for Two Level Devices

4.2 Three Level Switching Device Evaluation

The above exercise was then extended to the case where a Three Level inverter topology is used. For this case, four different switch configuarations were used. Each switching configuration again uses two devices in parallel in order to handle the 21.7 amp RMS current of an 18kW phase leg. 1200V devices are used in order to handle an 820V DC Link, with a switching frequency of 20kHz. Each device is 600V rated in order to handle the 410V half DC Link voltage. The key parameters are as follows:

1) DC Link is 820V
2) Output Voltage is 277V L-N, 480V L-L
3) Output power factor is 1
4) Full resistive load is 18kW

5) Full load current for one phase is (18,000/3)/277 = 21.7Arms

6) Resistive load is 277V/21.7A = 12.8Ohms

7) Switching frequency is 20kHz

8) Two IGBT's and two Diodes in parallel for each switch

The investigation begins with a 30 Amp short circuit rated IGBT and Diode co-package from International Rectifier (IRG4PC30KD). The part again uses an UltraFast Soft Recovery Diode as a co-package. The device is then replaced with an identical IGBT without the internal diode. A Cree 600V ZeroRecovery C3D10060A SiC Diode is mated with an IR IRG4PC30K IGBT. For this exercise, the loss breakdown is shown in Table 4 below and we can see that the losses are decreased from 127.8 Watts to 116.5 Watts (an 8.8% reduction) when the SiC diode is used.

Next, as was done for the two level, the same IGBT device was evaluated for a non short circuit rated part. The part is an IR IRG4PC30UD device and has a lower turn off loss compared to the short circuit rated device. The part losses were simulated and then compared to the same device losses when using a Cree C3D10060A diode instead of the internal diode. The IRG4PC30U device was used as the part mated to the SiC diode. Here, we see a loss reduction of only 3.3%. It is important to realize that 600V devices exhibit much lower switching losses than 1200V devices. It is because of this that we get so much less improvement by using a SiC diode at the 600V level. Figure 16 below shows the loss comparison for Three Level devices, on the same scale as was shown in Figure 15 in the last

section. It is easy to see from the graphs that losses are reduced far further in the Two Level case than they are in the Three Level case.

Table 4: Loss Comparison for Three Level Devices (Units are in Watts)

	IRG4PC30KD Internal Diode	IRG4PC30K C3D10060A	IRG4PC30UD Internal Diode	IRG4PC30U C3D10060A
IGBT Cond	75	75	71.3	71.3
Diode Cond	6	8.3	6	8.3
Switching	46.8	33.2	32.9	27
Total	**127.8**	**116.5**	**110.2**	**106.6**
Inverter Eff	97.87%	98.06%	98.16%	98.22%

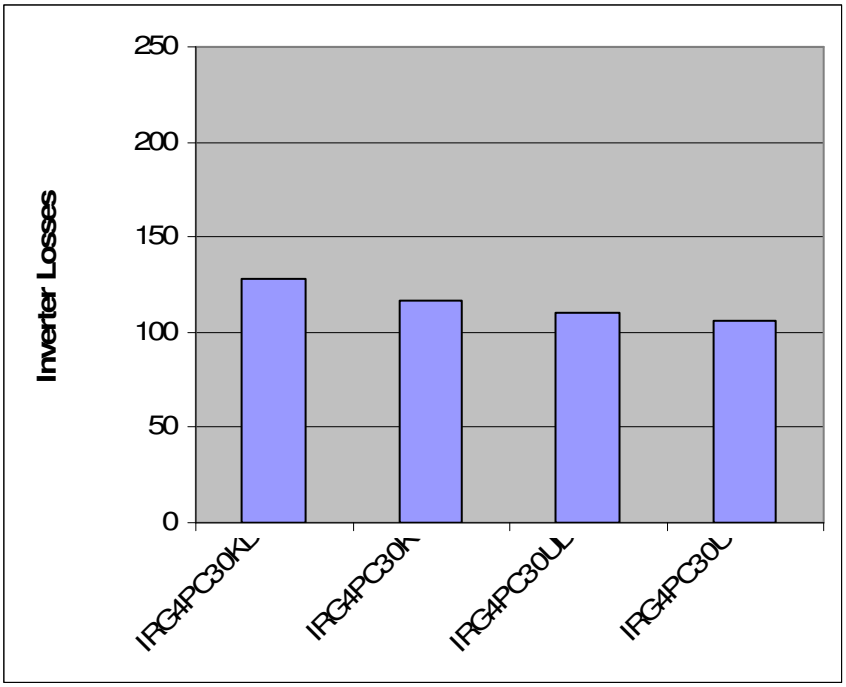

Figure 16: Loss Comparison for Three Level Devices

CHAPTER 5

5 BASELINE DYNAMIC TESTING OF VARIOUS SWITCHING DEVICES

At this point in the project a shift will be made from simulation environment to assessing real lab data for the switching devices discussed in the previous chapters. The following is a detailed analysis of a baseline dynamic test for a variety of devices. The baseline dynamic test attempts to keep all things equal in the test setup so that benefits and drawbacks of each device can be seen on a consistent basis. The optimization with respect to key devices will be covered in later sections of this report.

5.1 Test Circuit Schematic and Setup Description

The test circuit used was developed with the help of International Rectifier, a special thank you goes to Wibawa Chow for his help with this. The setup consists of four parts; a double pulse tester, gate drive circuitry, logic power and dc link power supplies, and a digital oscilloscope. The double pulse tester was donated by International Rectifier and uses a series of 555 timers to generate two pulses. The circuit includes three potentiometers which allow the user to adjust the width of the first pulse, the hold time between pulses, and the width of the second pulse. The two pulse tester is shown in figure 17 below. You can see from the figure that the TO-247 devices mount directly to the board and you can easily see the three potentiometers at the top of the picture. The DC Link power supply is

connected to the left of the large electrolytic capacitors in the figure. Finally, a 200uH inductor is included on the bottom side of the PCB. Figure 18 shows the bottom side of the PCB with the inductor and a trace cut to enable current probe measurement. Figure 19 below shows the schematic of the power board. The power board accepts two TO-247 devices for testing. The upper device was either a co-pack IGBT/diode combination or simply a discrete diode for the purpose of testing the SiC diodes. The lower device is the IGBT under test. The gate driver sends the signal labeled Vgate through a gate resistor which was set to 10 Ohms for this initial testing. The Voltage measurement was made across the lower IGBT's collector-emitter and the current measurement was made as shown through the lower trace of the bottom IGBT. The double pulse tester schematic is attached in Appendix I and the switching tester power board full schematic is attached in Appendix J.

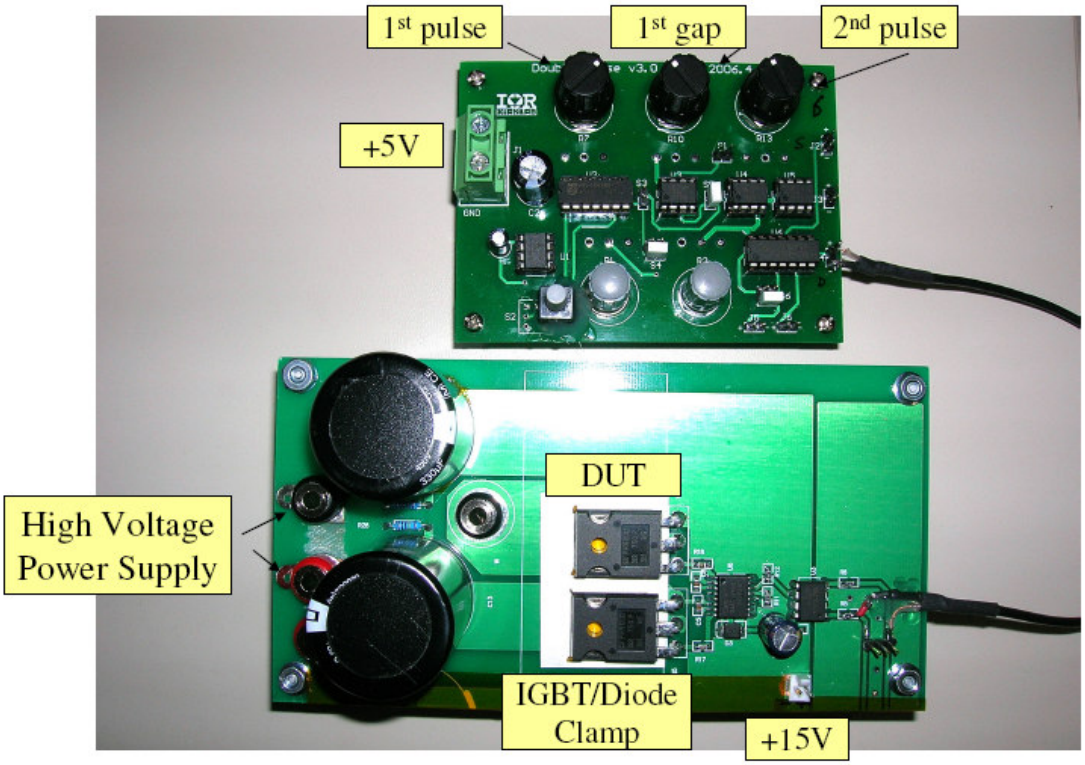

Figure 17: Two Pulse Tester and Power Board

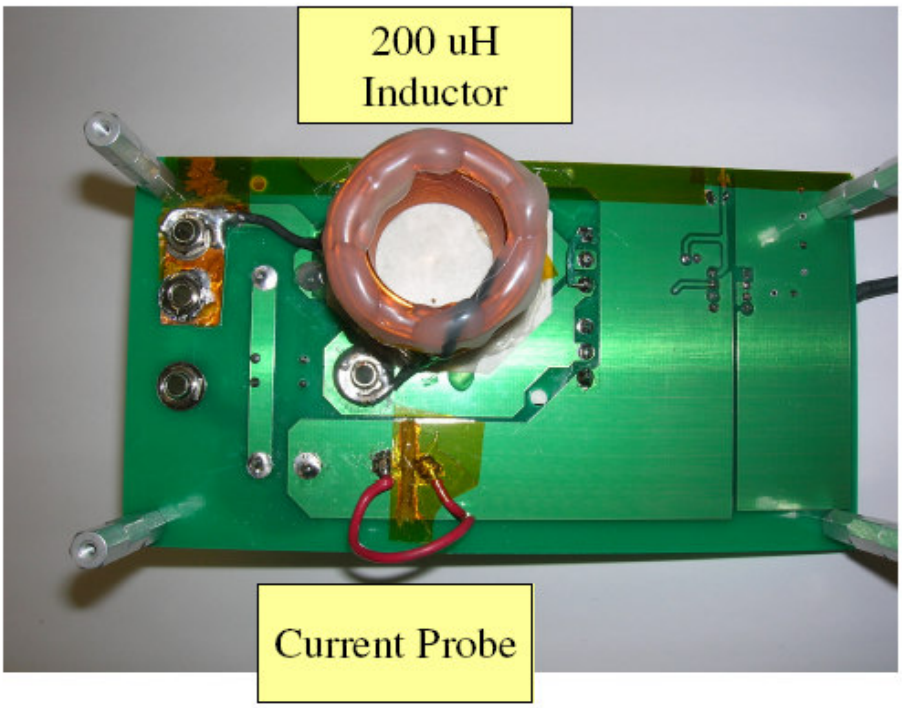

Figure 18: Bottom Side of Power Board

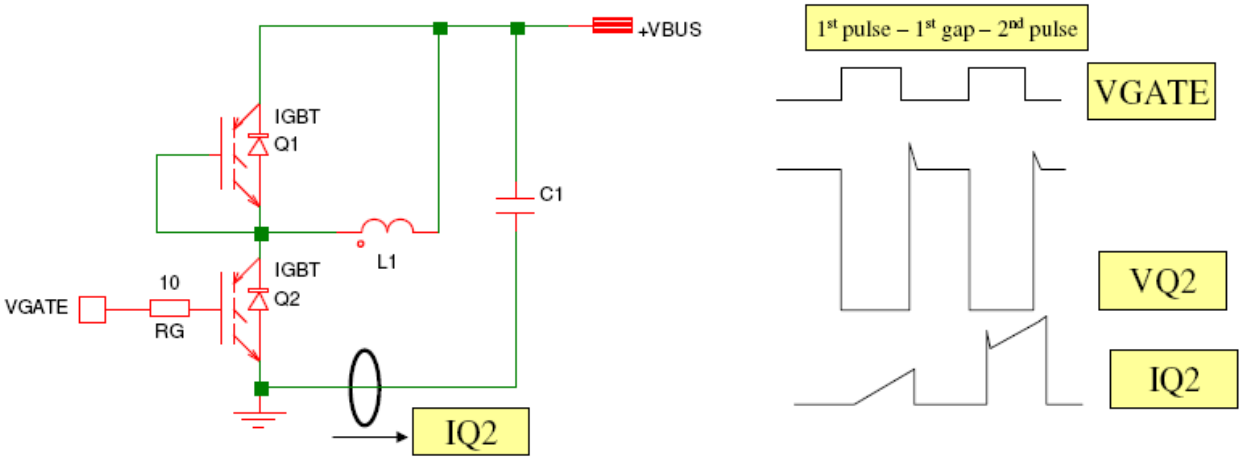

Figure 19: Power Board Schematic and Typical Gate Signals

The baseline comparison of the devices in question was done using a fixed gate drive circuit as described above. The gate drive delivers a +15V signal when the gate is being

commanded on and a 0V signal when the gate is being commanded off. The gate is driven through a 10 Ohm resistor for all cases in this chapter of testing. This provides a 1.5 Amp steady state gate current capability. This is a standard IGBT gate drive configuration and is used here as a baseline to keep with the theme of attempting to use any SiC devices as a drop in replacement initially. Any optimization of the devices will be left as an exercise for a future chapter. In this section 14 different combinations of devices are evaluated.

The end goal for this baseline comparison is to show how the devices compare and if substituting SiC devices directly for Silicon counterparts can yield a significant benefit to the designer. If this is the case, how much benefit for different devices will be a great guide in deciding whether the devices are worth using in future designs as prices for SiC begins to slowly come down to reasonable levels. The testing in the following section of this chapter were done at two different voltage levels (600V and 800V) and at two different current levels (10A and 20A) in order to get a broad view of the devices dynamic behavior. The measurement equipment used for this project was as follows:

1) Tektronix TDS5034B Digital Oscilloscope
    a. 350MHz
    b. 5GS/s
    c. 4 Channels
    d. 16M sample record length
2) Tektronix P5205 High Voltage Differential Probe
    a. Output +/- 2.6V into 1MOhm

b. 1300V maximum differential voltage

c. 100MHz BW

3) Tektronix TCP202 DC Coupled Current Probe

a. 15Amps DC + Peak AC Current

b. 50Amps Peak Pulsed Current

c. 50MHz BW

4) Fluke 87III True RMS Multimeter

5.2 International Rectifier IRG4PH50KD

The IRG4PH50KD was the first device tested. This device is short circuit rated and it compromises some efficiency in the optimization process. The device performance is shown in Figures 21-28. A summary of the performance statistics is given in Table 5 below. This device performed the worst of all IGBT's tested mainly due to the compromise in getting the short-circuit rating.

Table 5: IRG4PH50KD Dynamic Losses (Units are in uJ)

	IRG4PH50KD			
	600V 10A	600V 20A	800V 10A	800V 20A
Eoff	501	876	822	1250
Eon	771	1560	1060	2210
Etotal	**1272**	**2436**	**1882**	**3460**

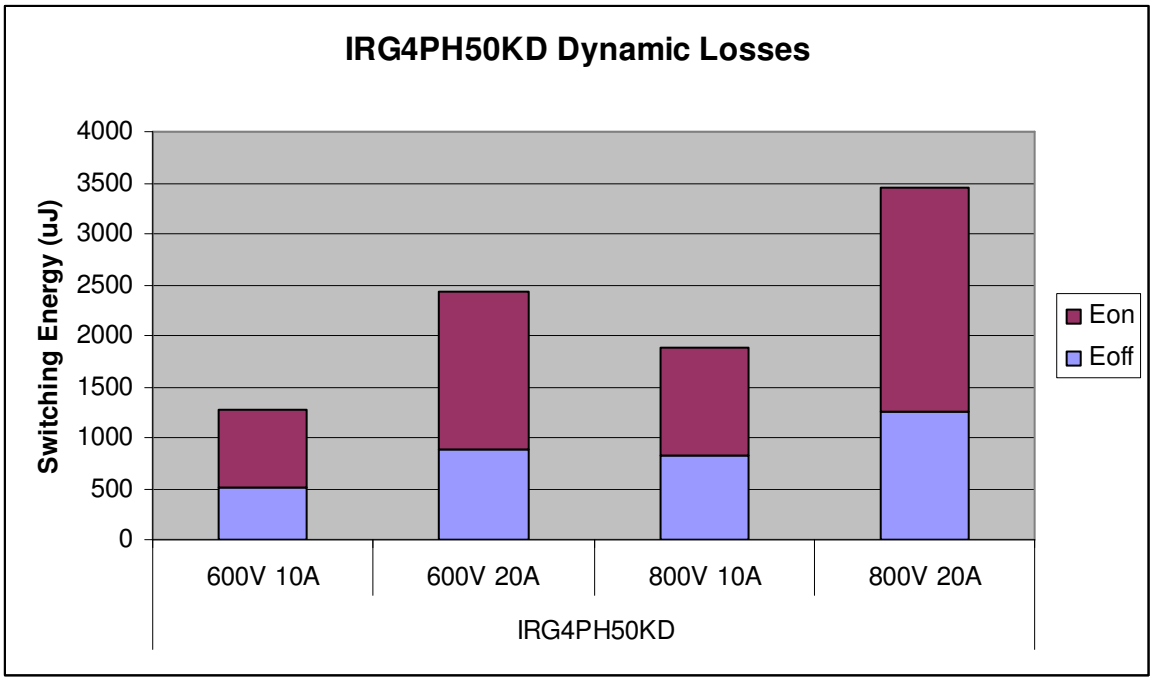

Figure 20: IRG4PH50KD Dynamic Losses (Units are in uJ)

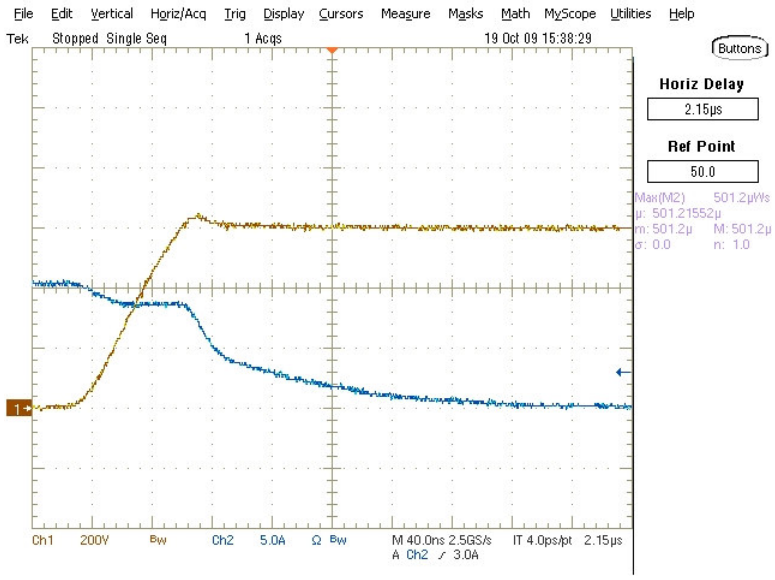

Figure 21: IRG4PH50KD Turn Off Behavior at 600V, 10A
(blue = current, yellow = voltage)

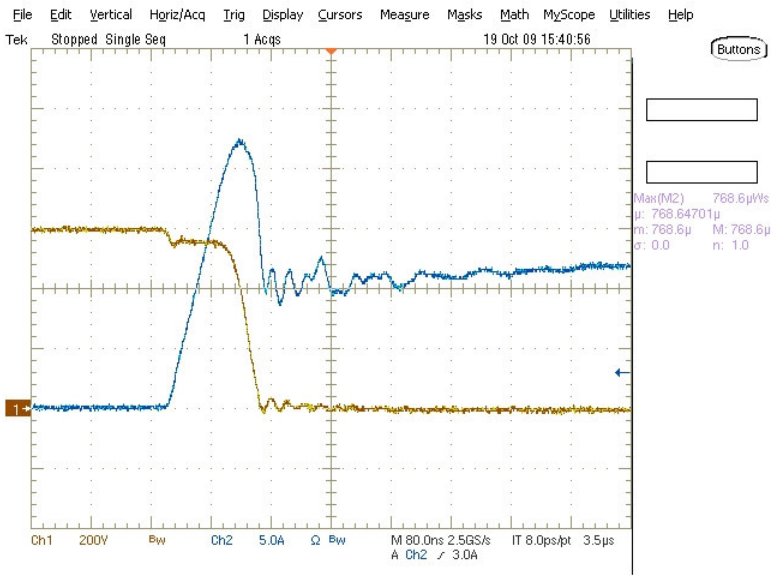

Figure 22: IRG4PH50KD Turn On Behavior at 600V, 10A
(blue = current, yellow = voltage)

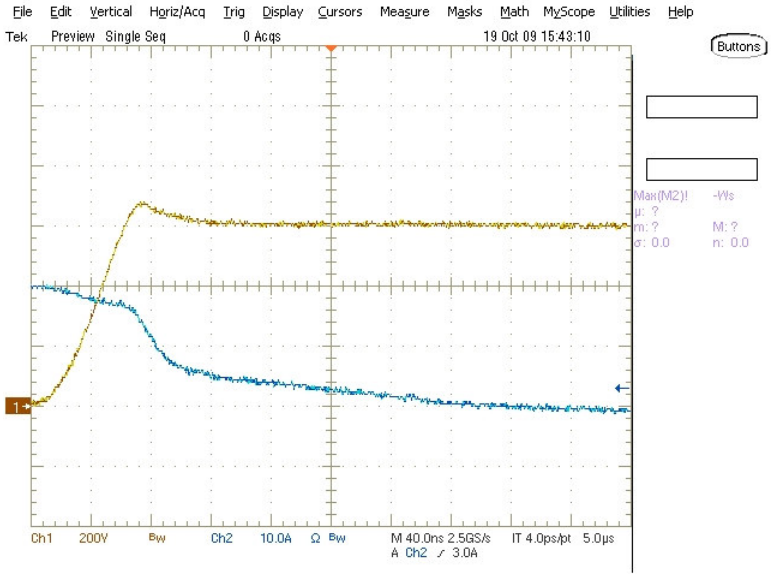

Figure 23: IRG4PH50KD Turn Off Behavior at 600V, 20A
(blue = current, yellow = voltage)

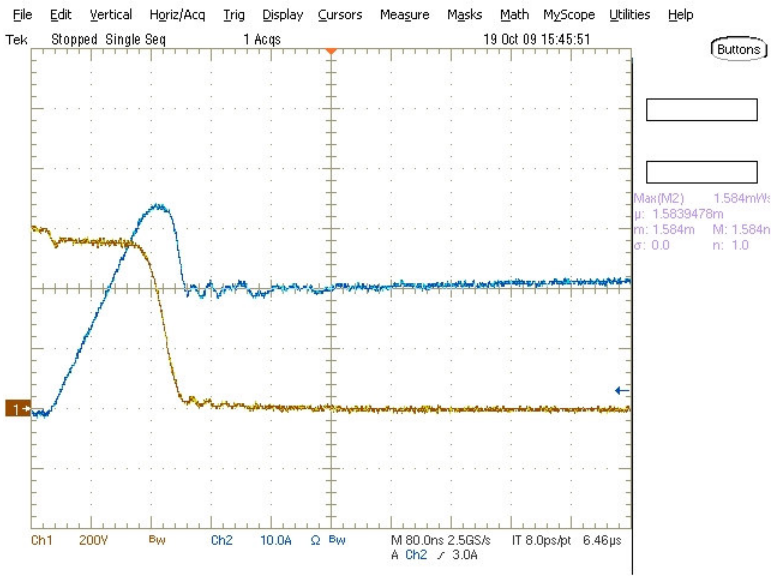

Figure 24: IRG4PH50KD Turn On Behavior at 600V, 20A
(blue = current, yellow = voltage)

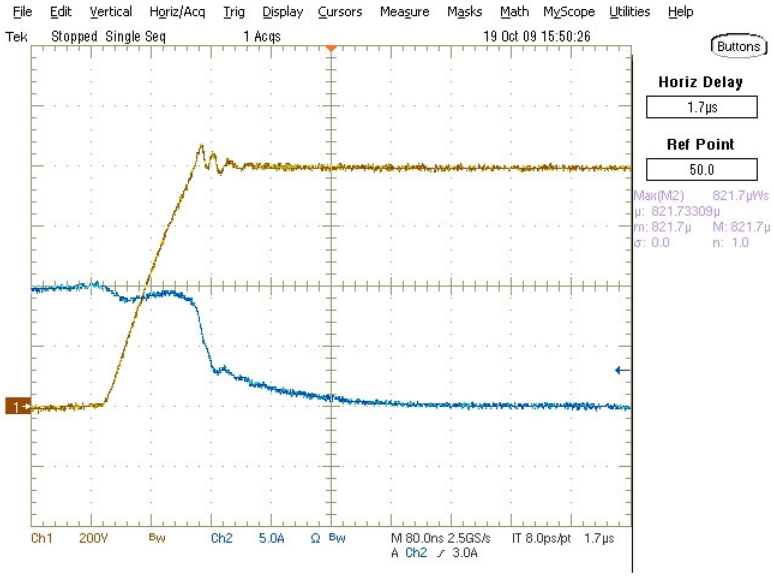

Figure 25: IRG4PH50KD Turn Off Behavior at 800V, 10A
(blue = current, yellow = voltage)

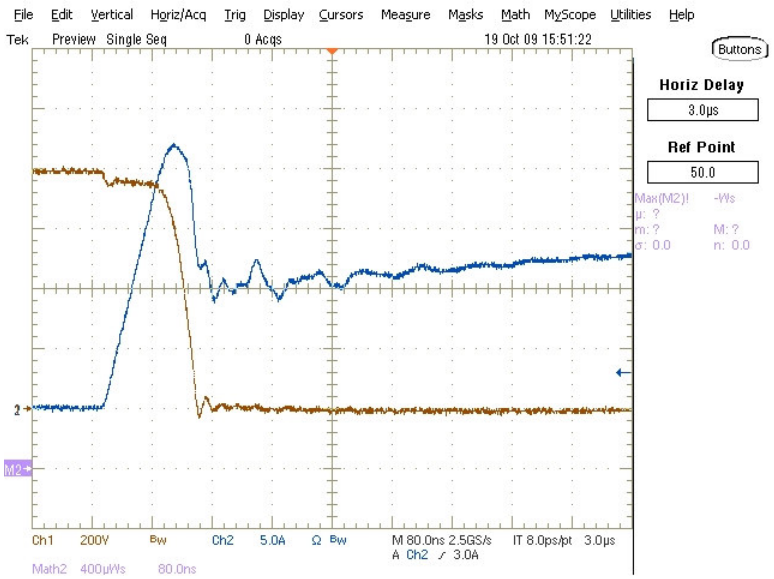

Figure 26: IRG4PH50KD Turn On Behavior at 800V, 10A
(blue = current, yellow = voltage)

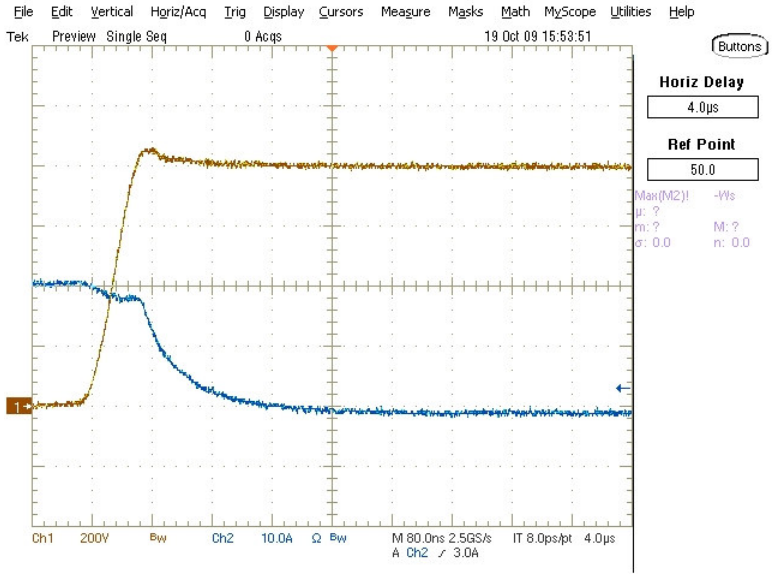

Figure 27: IRG4PH50KD Turn Off Behavior at 800V, 20A
(blue = current, yellow = voltage)

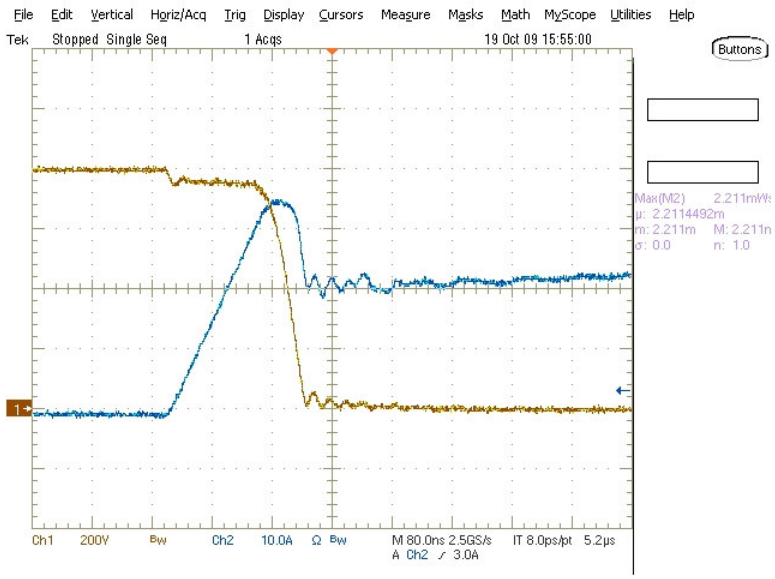

Figure 28: IRG4PH50KD Turn On Behavior at 800V, 20A (blue = current, yellow = voltage)

5.3 International Rectifier IRG4PH50K and Cree C2D20120 SiC Diode

The IRG4PH50K is the identical device to the IRG4PH50KD, except that it does not come co-packaged with an anti-parallel diode. Instead, this testing used a Cree 1200V, 20A Silicon Carbide freewheeling diode. The device performance is shown in Figures 30-37. A summary of the performance statistics is given in Table 6 below.

Table 6: IRG4PH50K Dynamic Losses (Units are in uJ)

	IRG4PH50K & C2D20120D			
	600V 10A	600V 20A	800V 10A	800V 20A
Eoff	472	843	765	1190
Eon	372	891	589	1350
Etotal	**844**	**1734**	**1354**	**2540**

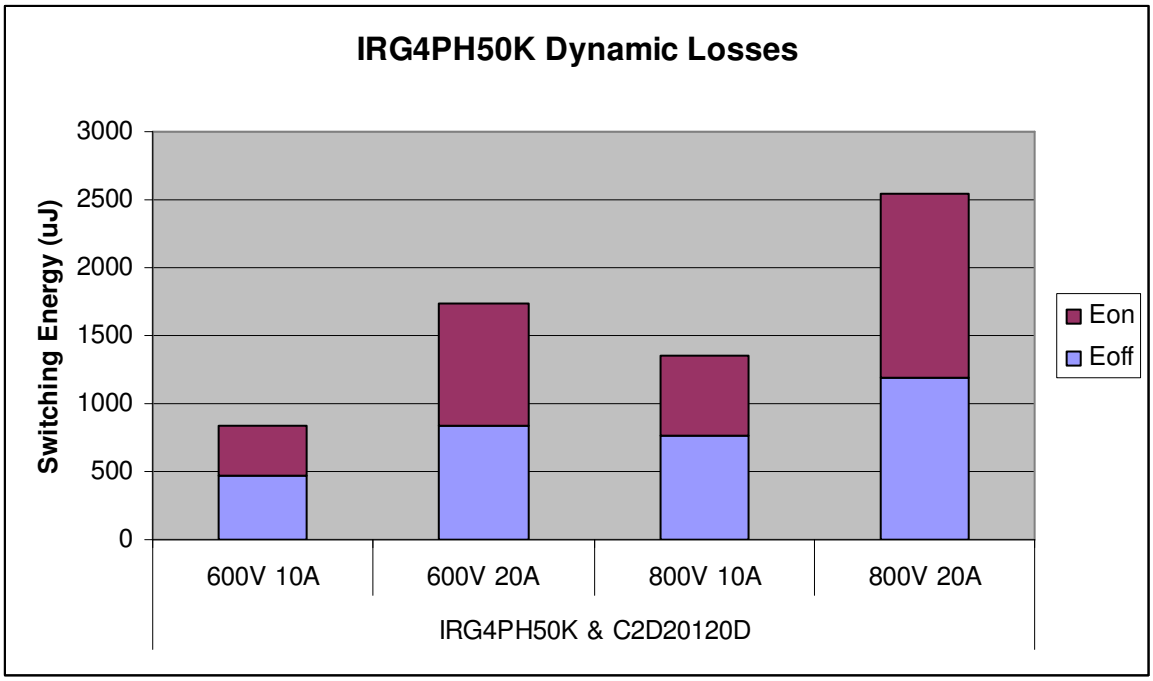

Figure 29: IRG4PH50K Dynamic Losses (Units are in uJ)

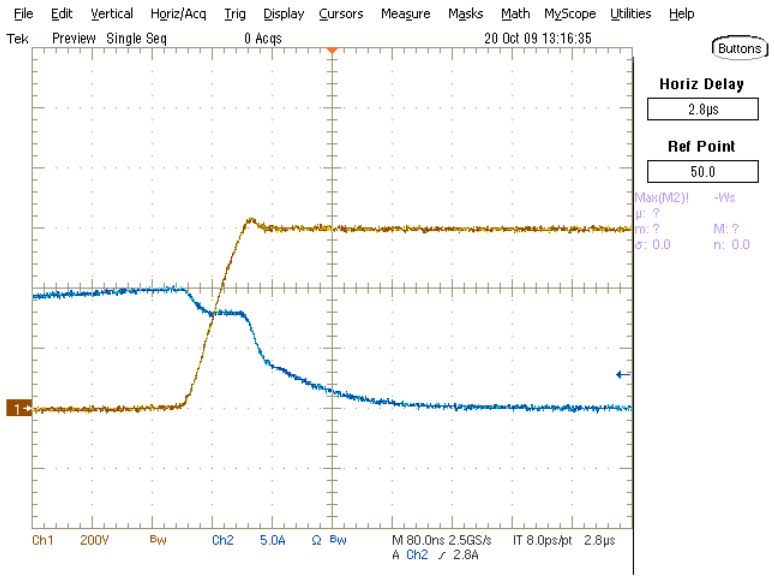

Figure 30: IRG4PH50K Turn Off Behavior at 600V, 10A
(blue = current, yellow = voltage)

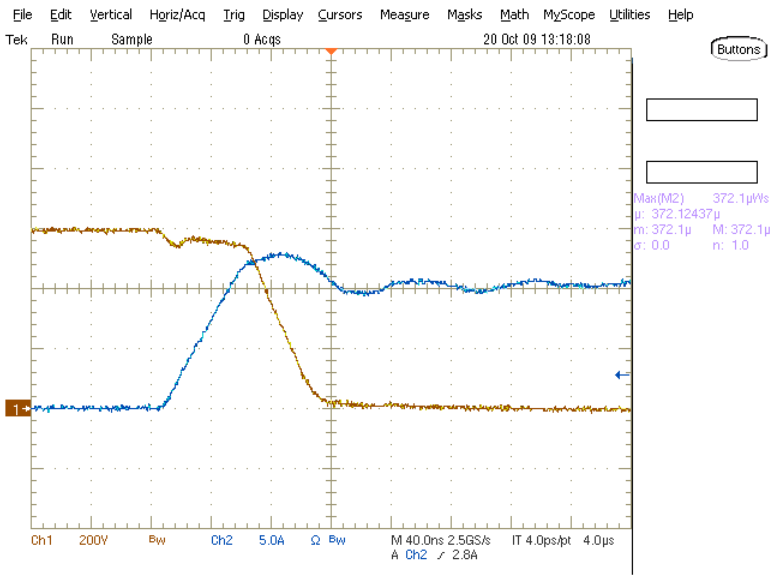

Figure 31: IRG4PH50K Turn On Behavior at 600V, 10A
(blue = current, yellow = voltage)

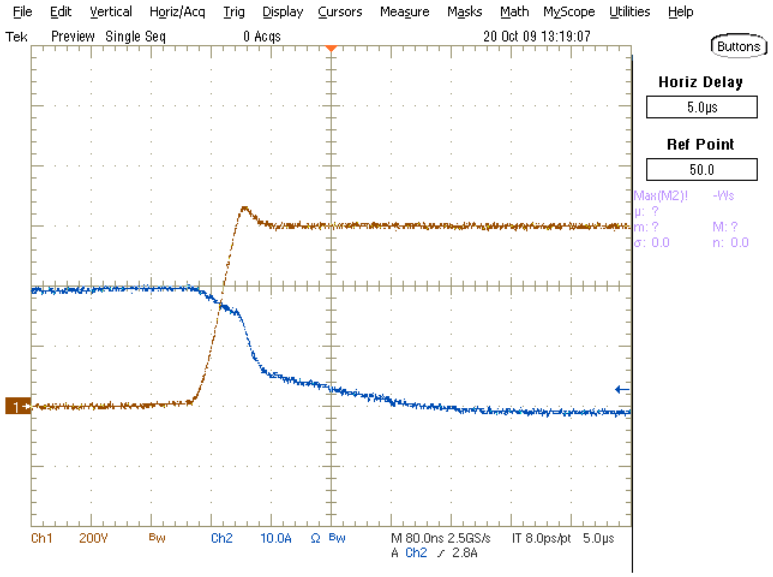

Figure 32: IRG4PH50K Turn Off Behavior at 600V, 20A
(blue = current, yellow = voltage)

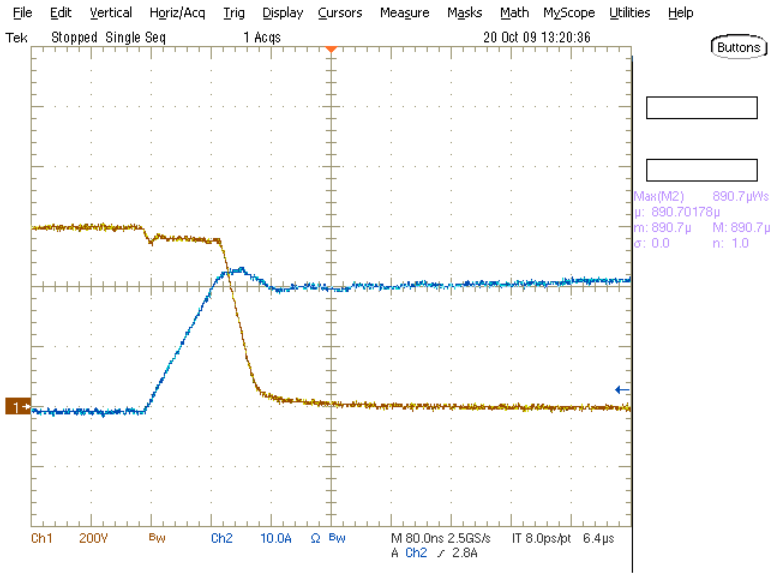

Figure 33: IRG4PH50K Turn On Behavior at 600V, 20A
(blue = current, yellow = voltage)

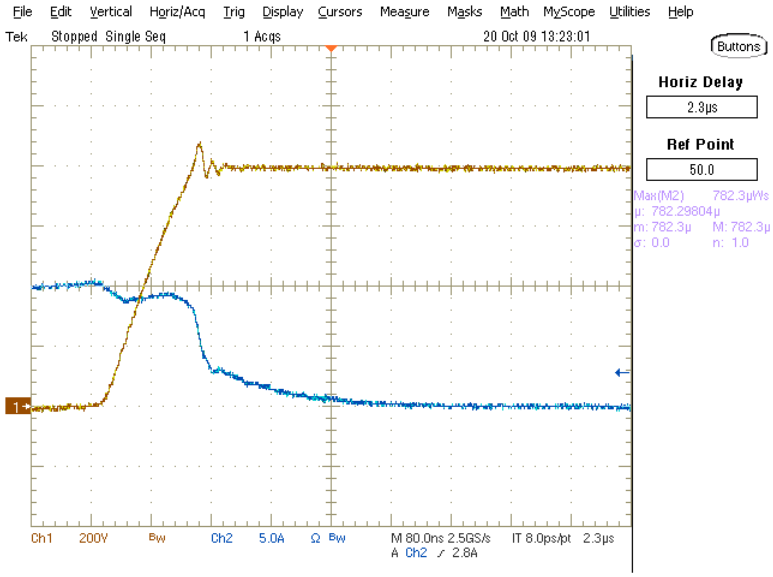

Figure 34: IRG4PH50K Turn Off Behavior at 800V, 10A
(blue = current, yellow = voltage)

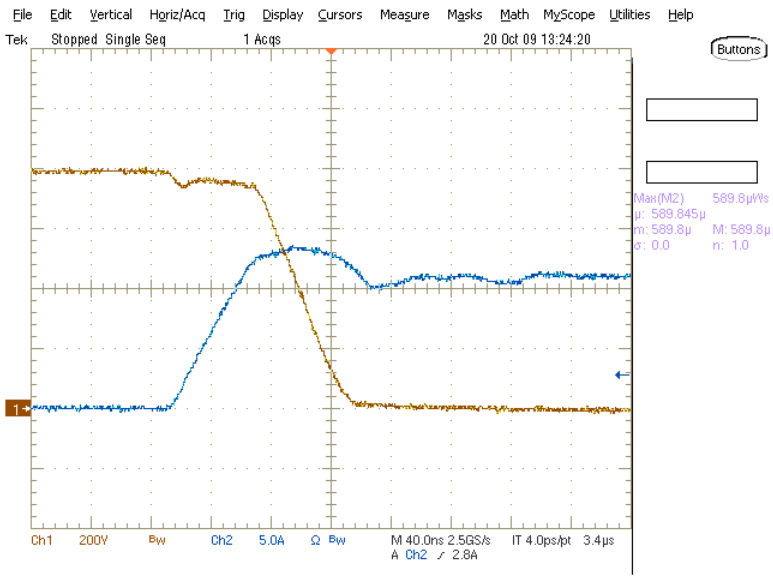

Figure 35: IRG4PH50K Turn On Behavior at 800V, 10A
(blue = current, yellow = voltage)

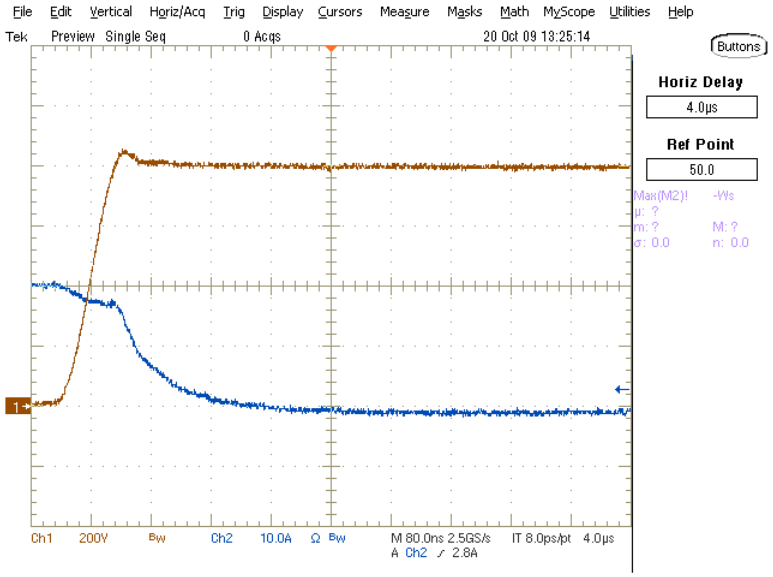

Figure 36: IRG4PH50K Turn Off Behavior at 800V, 20A
(blue = current, yellow = voltage)

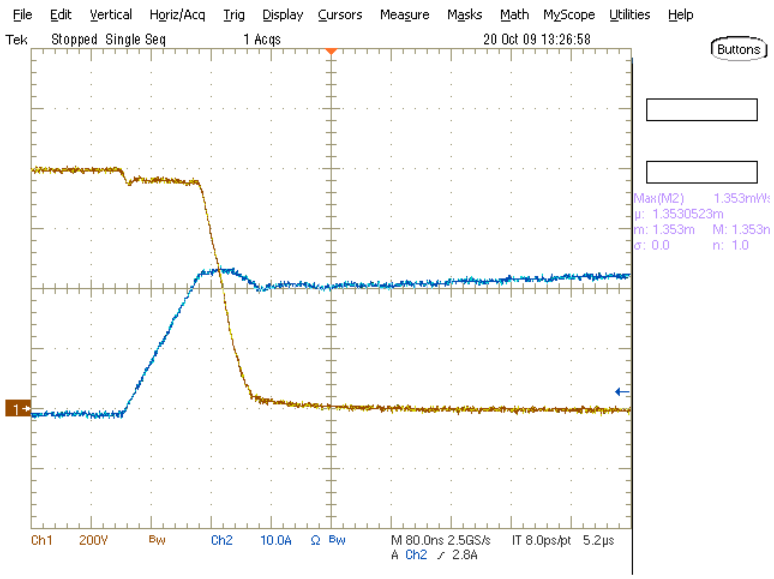

Figure 37: IRG4PH50K Turn On Behavior at 800V, 20A (blue = current, yellow = voltage)

5.4 International Rectifier IRG4PH50UD

The IRG4PH50UD was tested next. This device is not short circuit rated and is optimized for switching losses by increasing the speed at which the device turns on. The device performance is shown in Figures 39-46. A summary of the performance statistics is given in Table 7 below.

Table 7: IRG4PH50UD Dynamic Losses (Units are in uJ)

	IRG4PH50UD			
	600V 10A	600V 20A	800V 10A	800V 20A
Eoff	490	855	797	1178
Eon	598	1153	881	1742
Etotal	**1088**	**2008**	**1678**	**2920**

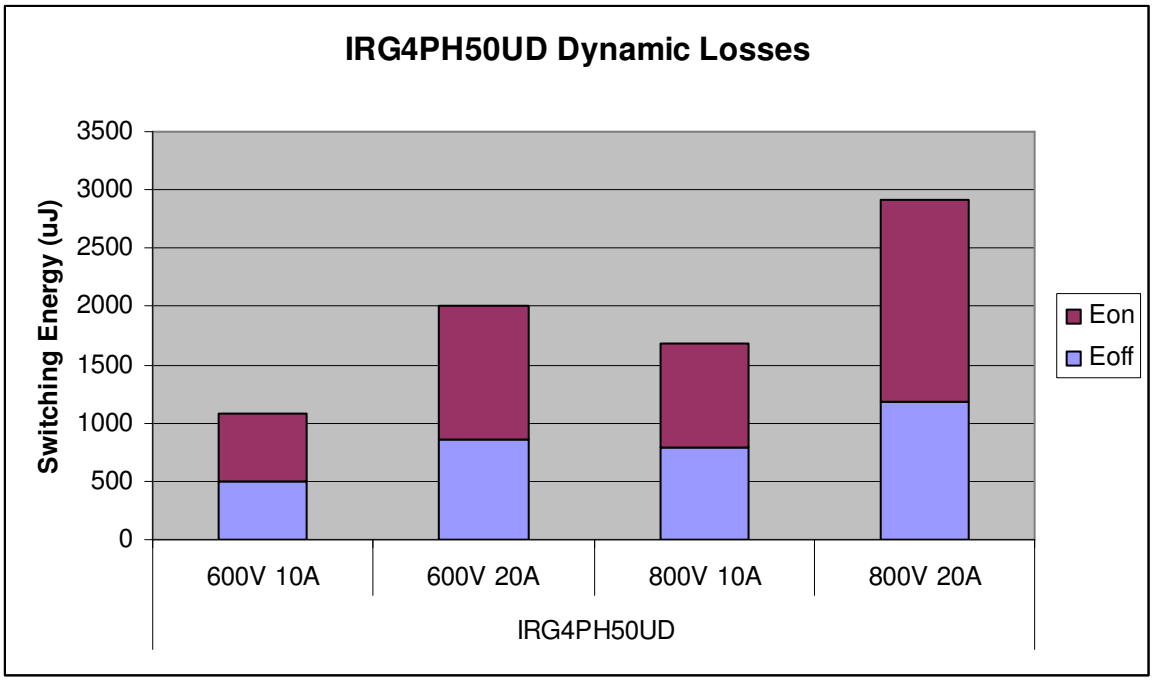

Figure 38: IRG4PH50UD Dynamic Losses (Units are in uJ)

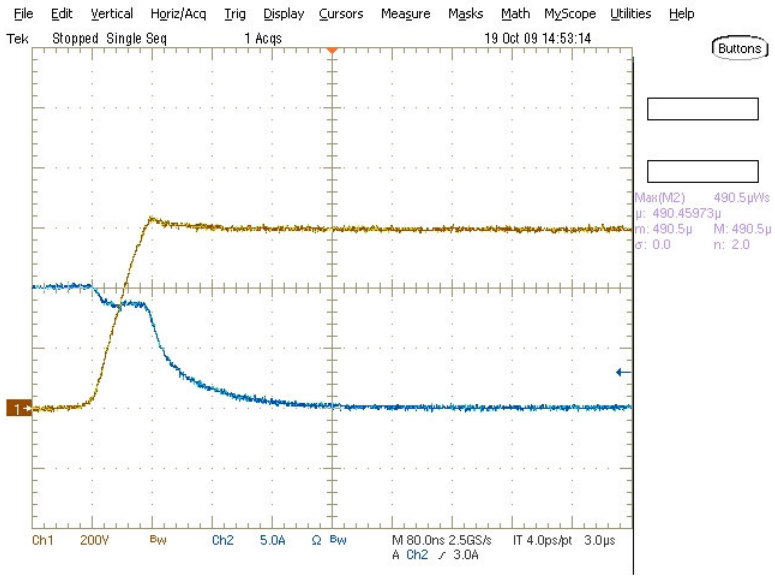

Figure 39: IRG4PH50UD Turn Off Behavior at 600V, 10A
(blue = current, yellow = voltage)

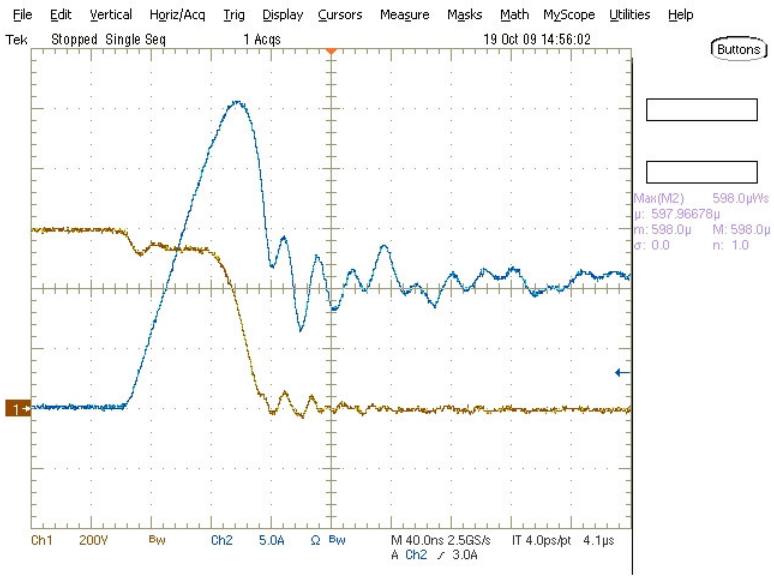

Figure 40: IRG4PH50UD Turn On Behavior at 600V, 10A
(blue = current, yellow = voltage)

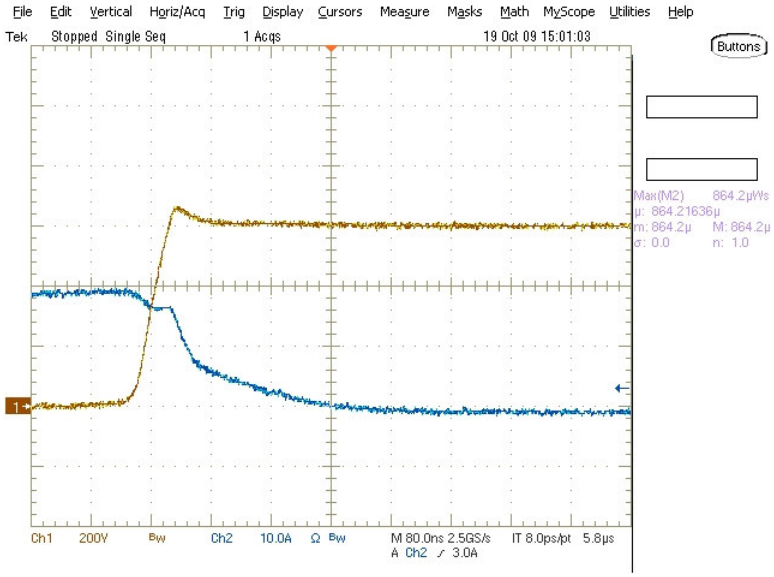

Figure 41: IRG4PH50UD Turn Off Behavior at 600V, 20A
(blue = current, yellow = voltage)

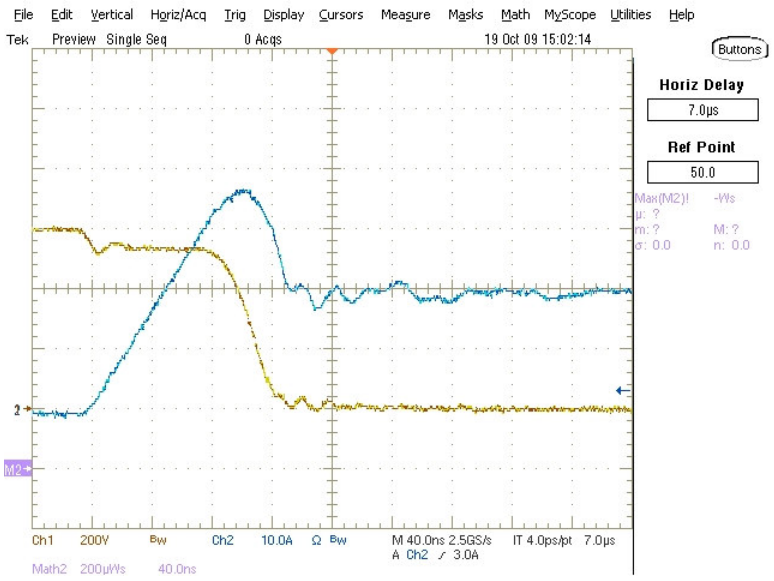

Figure 42: IRG4PH50UD Turn On Behavior at 600V, 20A
(blue = current, yellow = voltage)

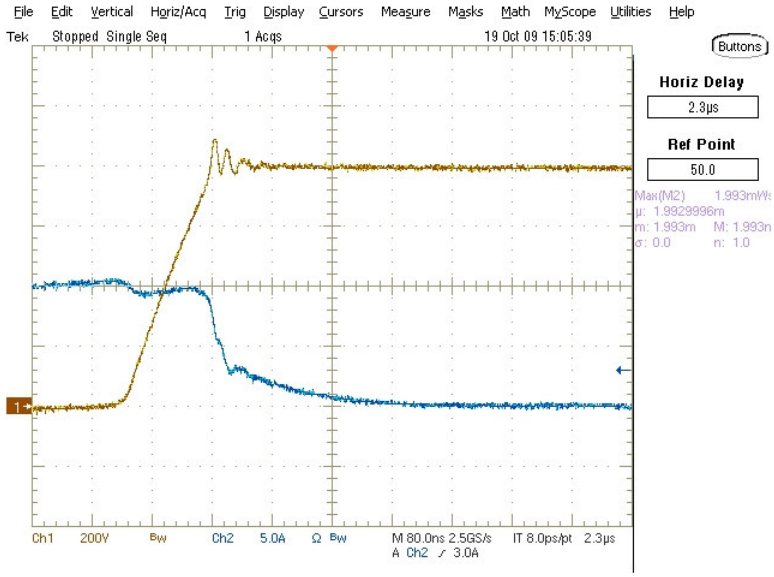

Figure 43: IRG4PH50UD Turn Off Behavior at 800V, 10A
(blue = current, yellow = voltage)

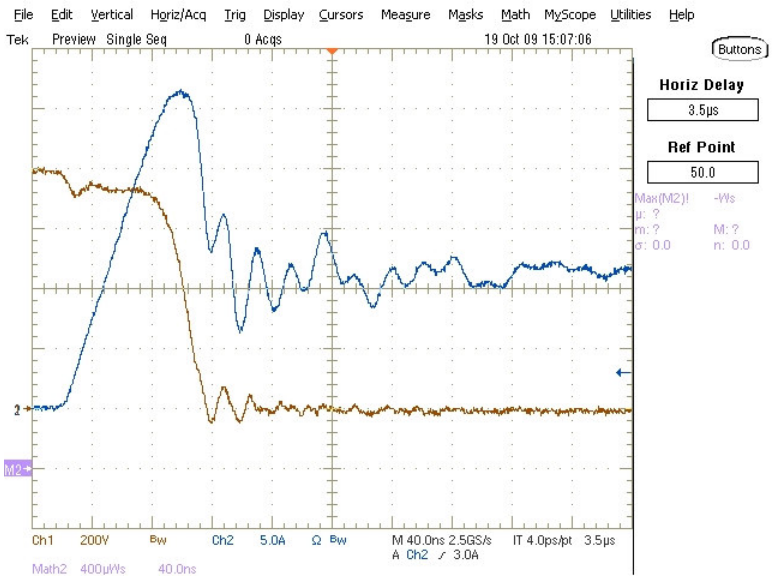

Figure 44: IRG4PH50UD Turn On Behavior at 800V, 10A
(blue = current, yellow = voltage)

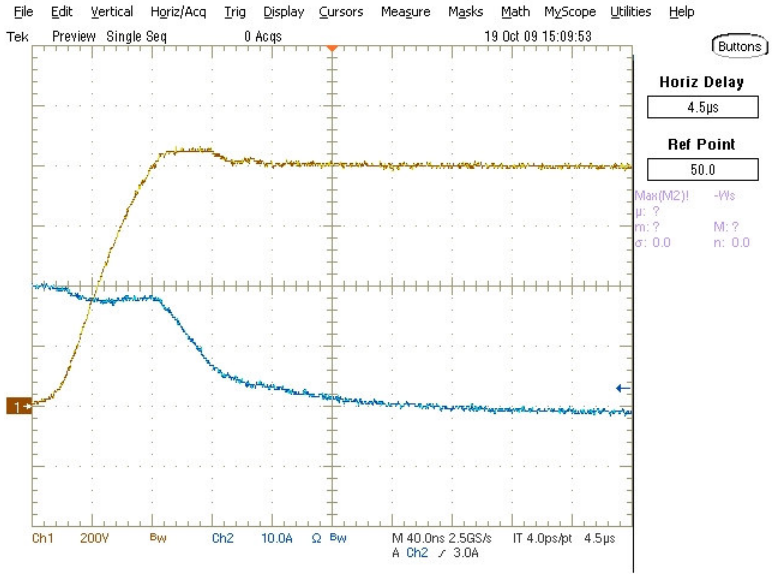

Figure 45: IRG4PH50UD Turn Off Behavior at 800V, 20A
(blue = current, yellow = voltage)

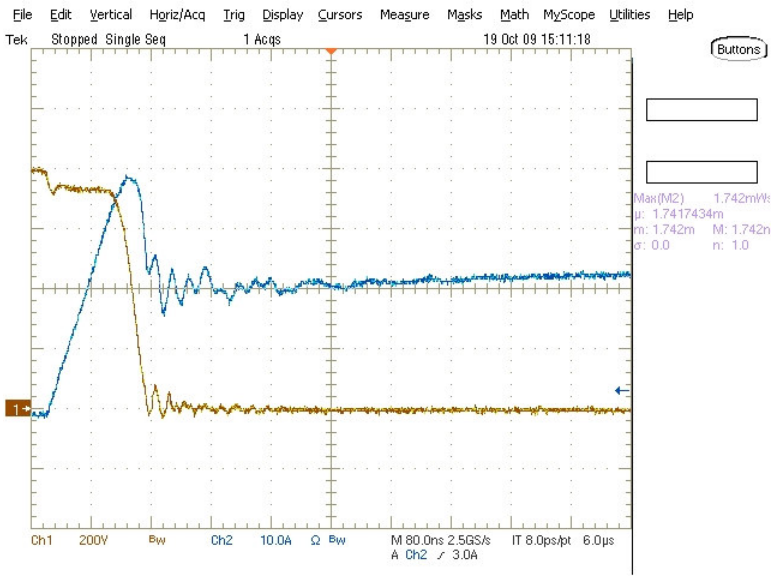

Figure 46: IRG4PH50UD Turn On Behavior at 800V, 20A
(blue = current, yellow = voltage)

5.5 International Rectifier IRG4PH50U and Cree C2D2120 SiC Diode

The IRG4PH50U is the identical device to the IRG4PH50UD, except that it does not come co-packaged with an anti-parallel diode. Instead, this testing used a Cree 1200V, 20A Silicon Carbide freewheeling diode. The device performance is shown in Figures 48-55. A summary of the performance statistics is given in Table 8 below.

Table 8: IRG4PH50U Dynamic Losses (Units are in uJ)

	IRG4PH50U & C2D20120D			
	600V 10A	600V 20A	800V 10A	800V 20A
Eoff	486	936	722	1200
Eon	261	635	411	941
Etotal	**747**	**1571**	**1133**	**2141**

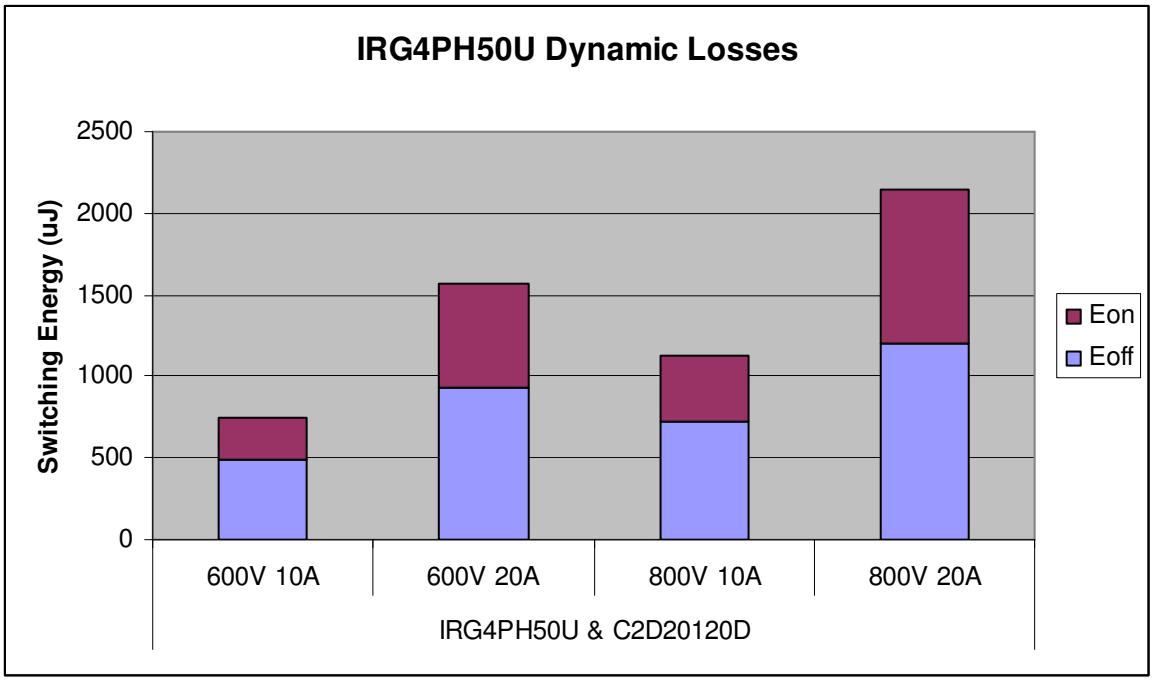

Figure 47: IRG4PH50U Dynamic Losses (Units are in uJ)

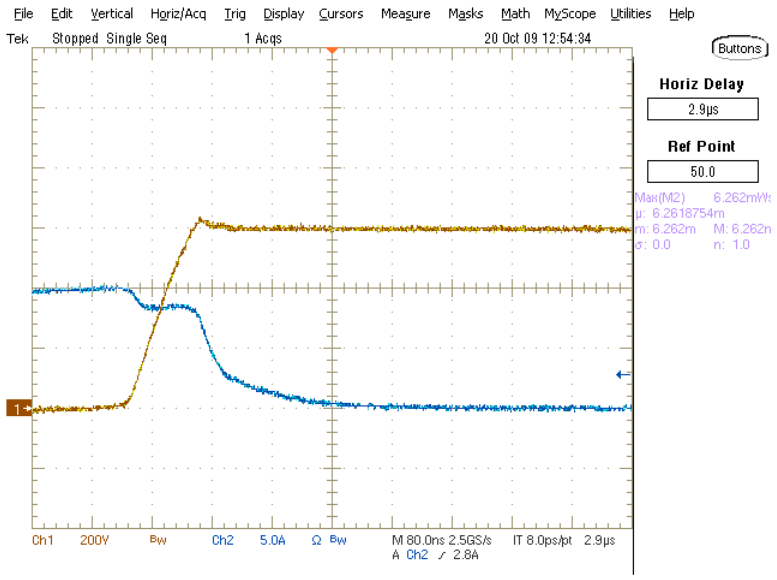

Figure 48: IRG4PH50U Turn Off Behavior at 600V, 10A
(blue = current, yellow = voltage)

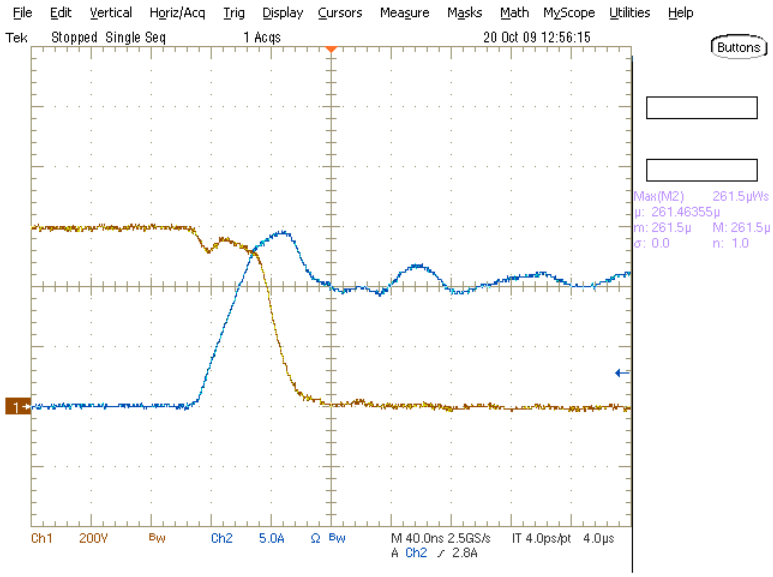

Figure 49: IRG4PH50U Turn On Behavior at 600V, 10A
(blue = current, yellow = voltage)

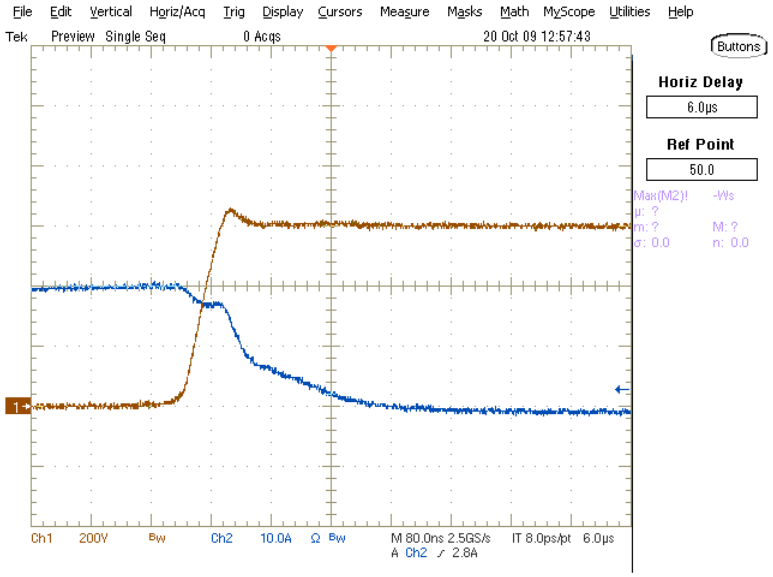

Figure 50: IRG4PH50U Turn Off Behavior at 600V, 20A
(blue = current, yellow = voltage)

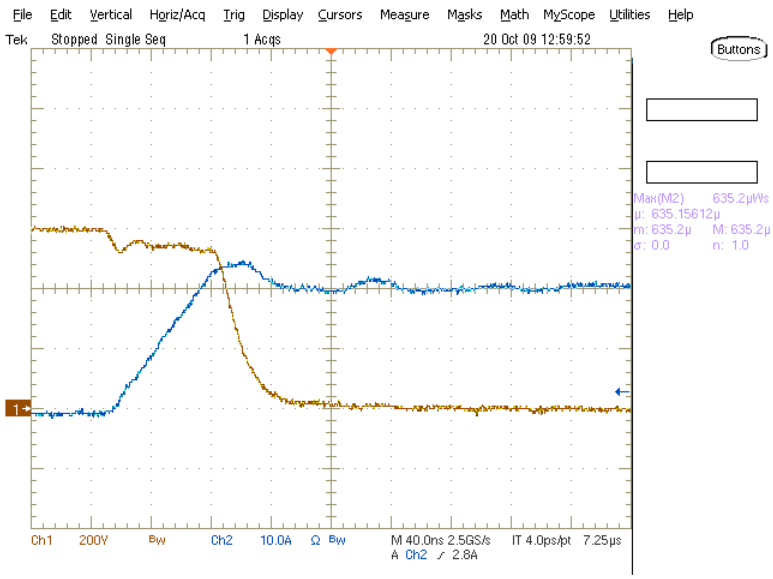

Figure 51: IRG4PH50U Turn On Behavior at 600V, 20A
(blue = current, yellow = voltage)

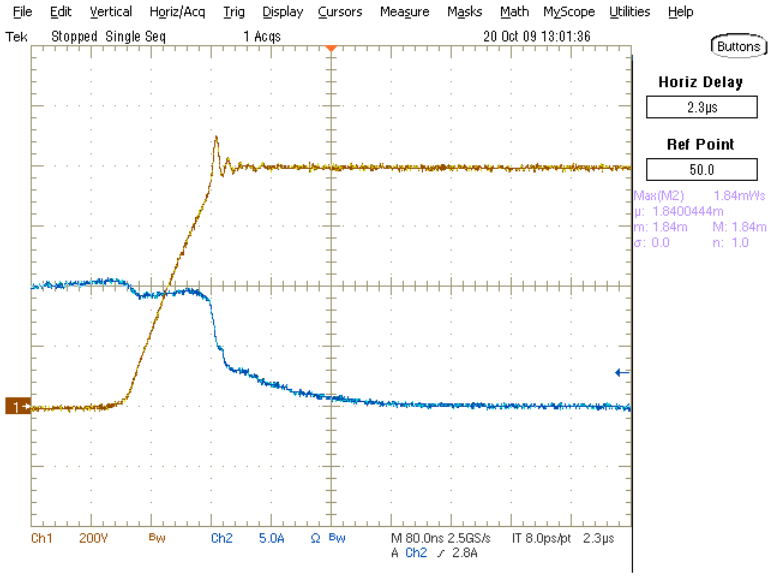

Figure 52: IRG4PH50U Turn Off Behavior at 800V, 10A
(blue = current, yellow = voltage)

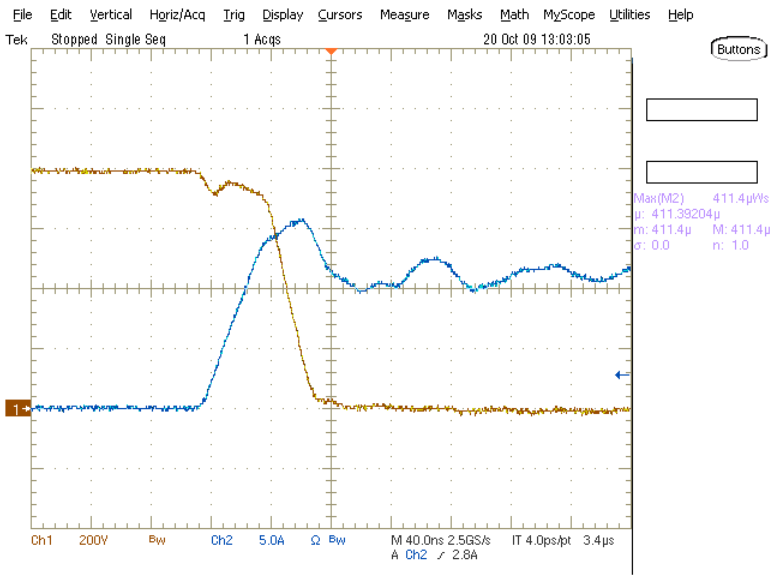

Figure 53: IRG4PH50U Turn On Behavior at 800V, 10A
(blue = current, yellow = voltage)

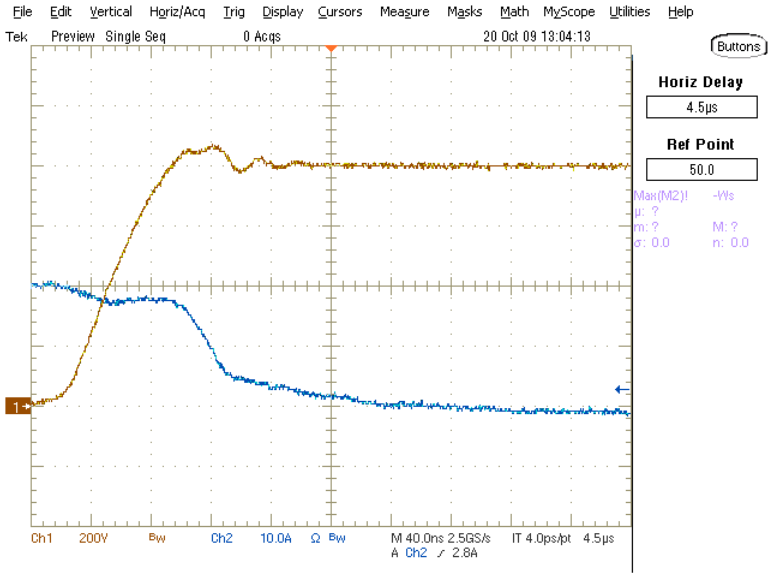

Figure 54: IRG4PH50U Turn Off Behavior at 800V, 20A
(blue = current, yellow = voltage)

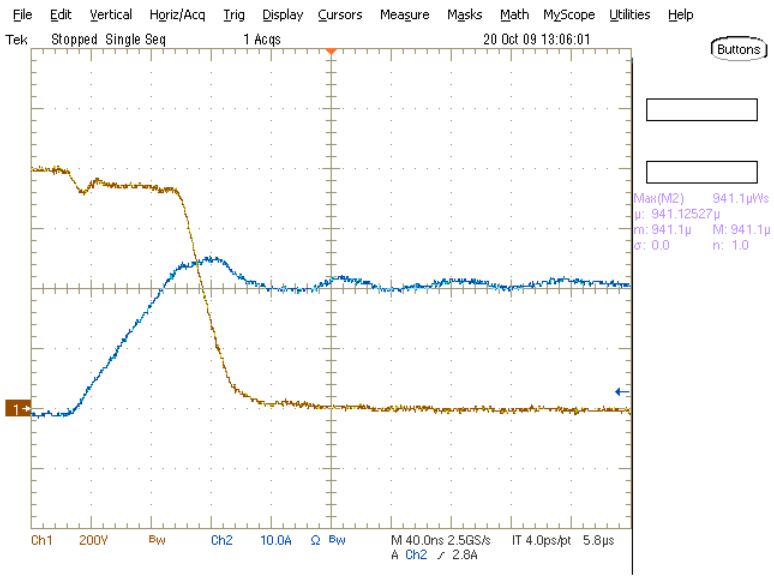

Figure 55: IRG4PH50U Turn On Behavior at 800V, 20A (blue = current, yellow = voltage)

5.6 International Rectifier IRG7PH42UD

This section gives test results for the IRG7PH42UD device. This device is not short circuit rated and is optimized for switching losses by increasing the speed at which the device turns on. This device is a generation seven International Rectifier IGBT, which is their latest generation to date. The device performance is shown in Figures 57-64. A summary of the performance statistics is given in Table 9 below.

Table 9: IRG7PH42UD Dynamic Losses (Units are in uJ)

	IRG7PH42UD			
	600V 10A	600V 20A	800V 10A	800V 20A
Eoff	483	729	709	1010
Eon	634	1290	955	1850
Etotal	**1117**	**2019**	**1664**	**2860**

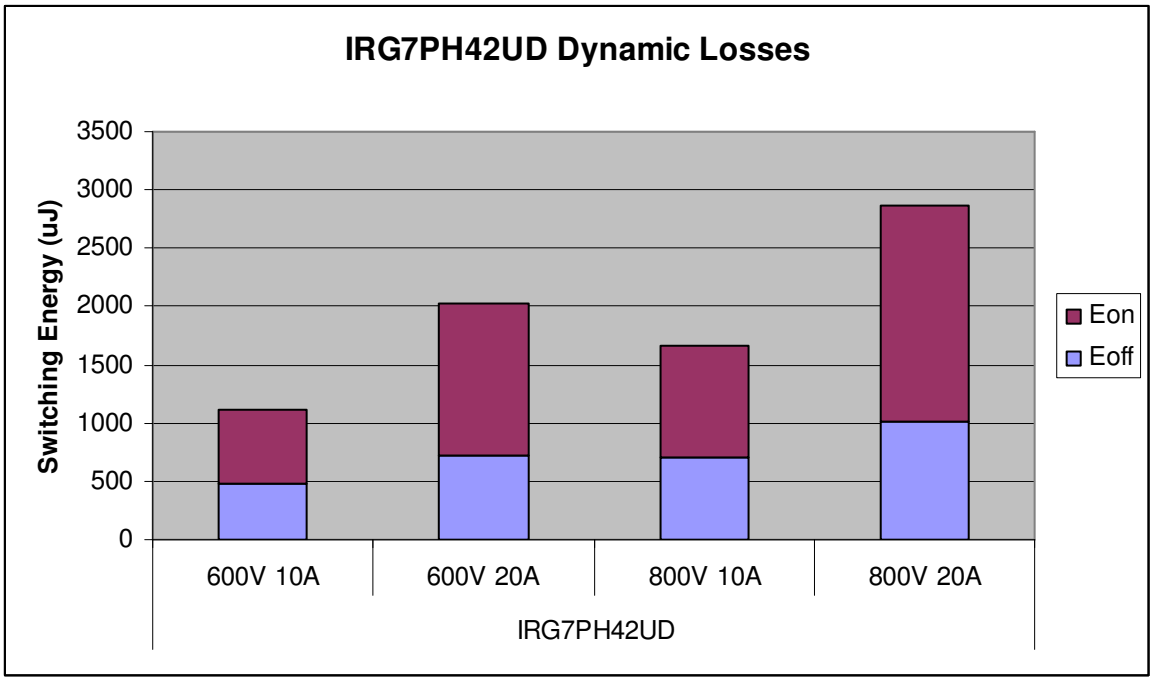

Figure 56: IRG7PH42UD Dynamic Losses (Units are in uJ)

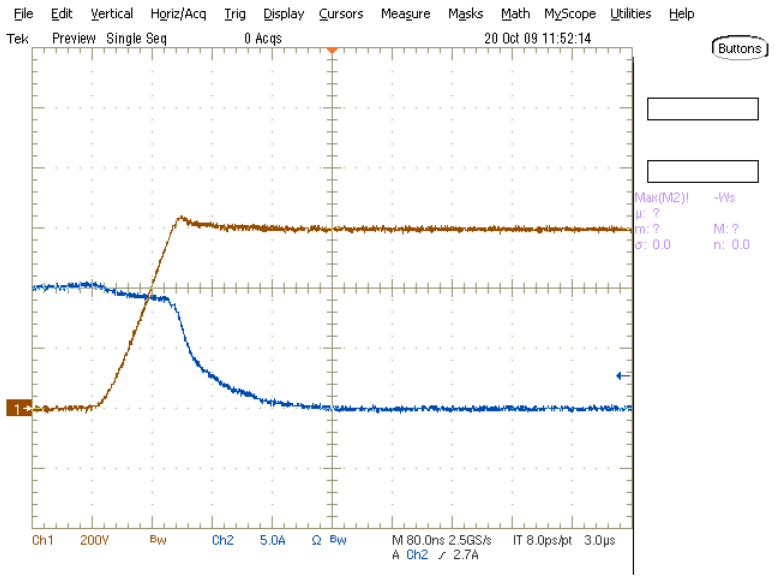

Figure 57: IRG7PH42UD Turn Off Behavior at 600V, 10A
(blue = current, yellow = voltage)

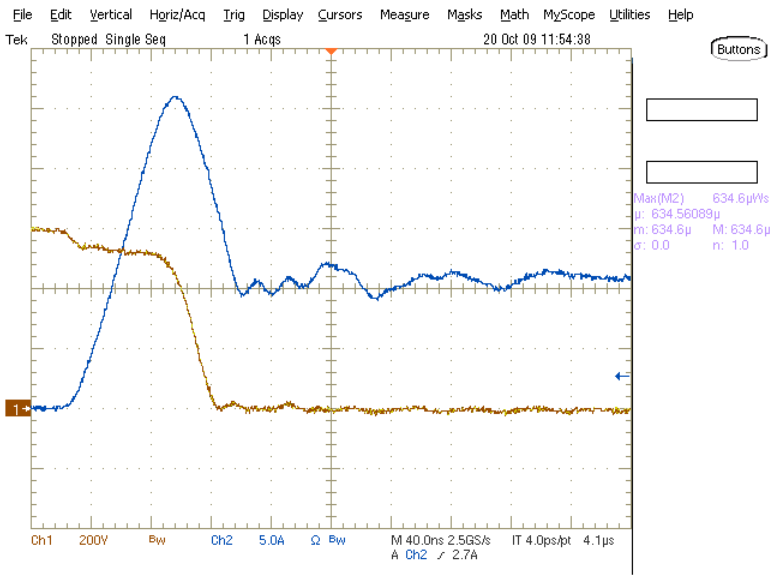

Figure 58: IRG7PH42UD Turn On Behavior at 600V, 10A
(blue = current, yellow = voltage)

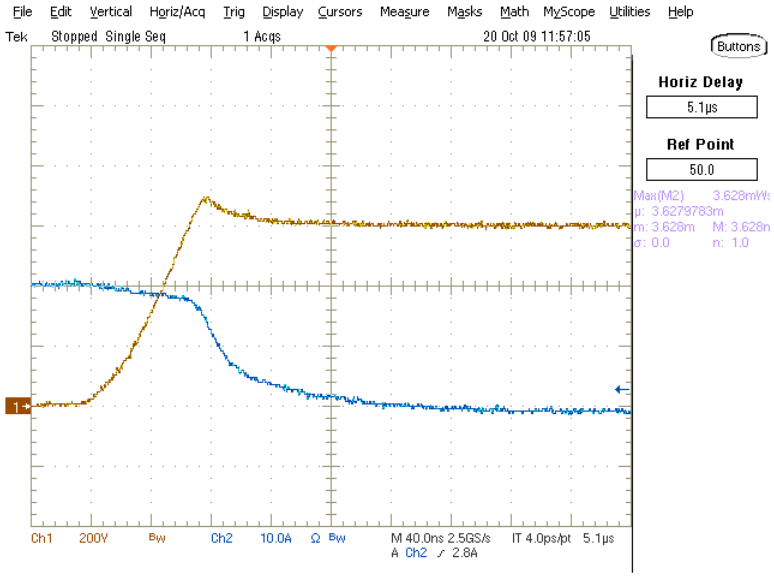

Figure 59: IRG7PH42UD Turn Off Behavior at 600V, 20A
(blue = current, yellow = voltage)

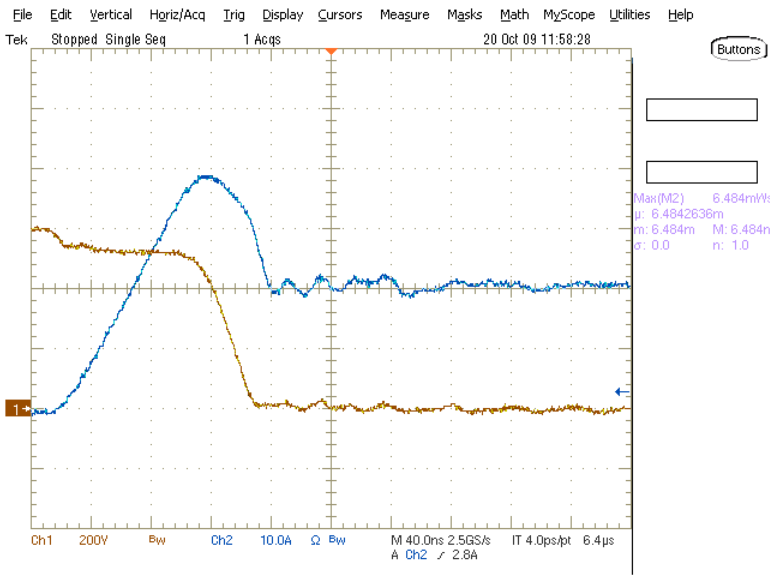

Figure 60: IRG7PH42UD Turn On Behavior at 600V, 20A
(blue = current, yellow = voltage)

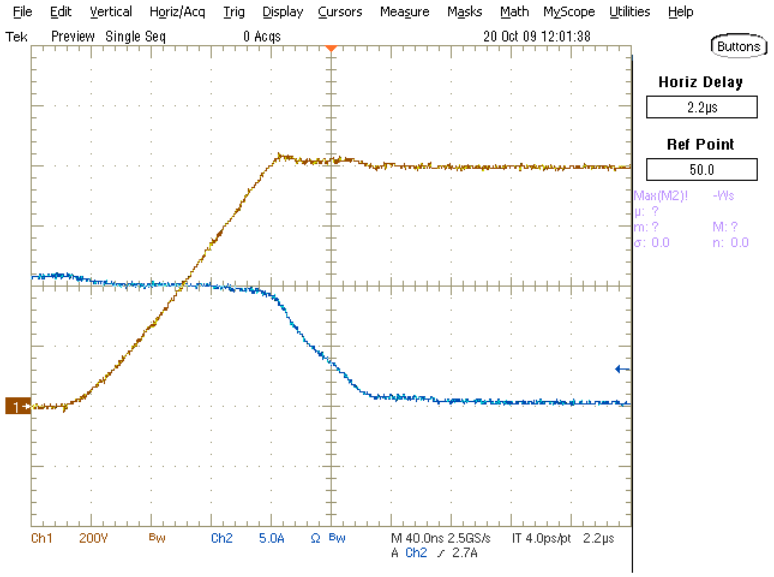

Figure 61: IRG7PH42UD Turn Off Behavior at 800V, 10A
(blue = current, yellow = voltage)

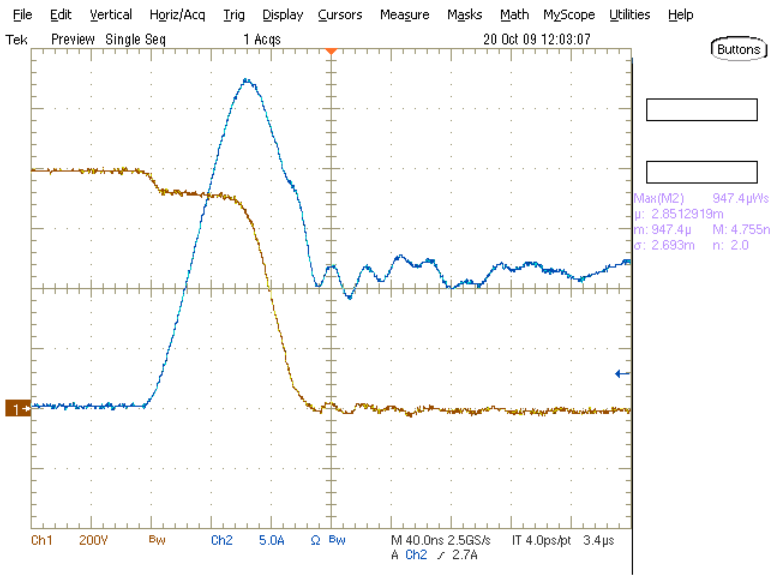

Figure 62: IRG7PH42UD Turn On Behavior at 800V, 10A
(blue = current, yellow = voltage)

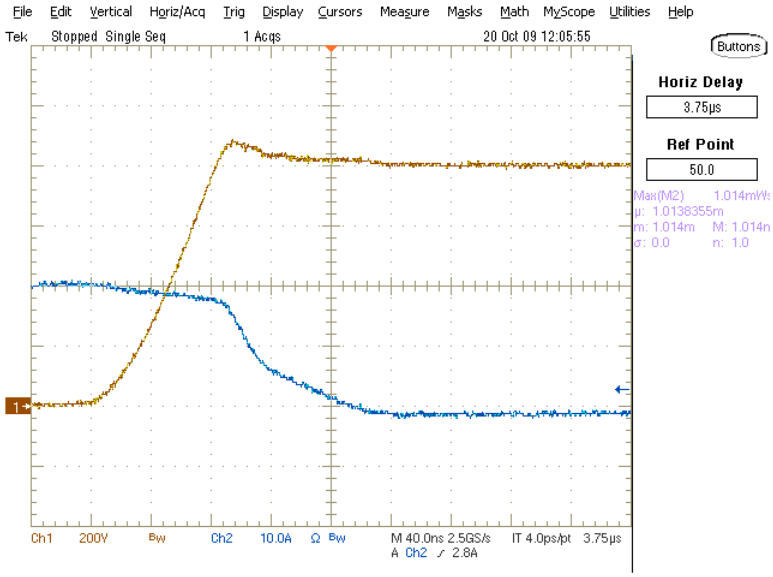

Figure 63: IRG7PH42UD Turn Off Behavior at 800V, 20A
(blue = current, yellow = voltage)

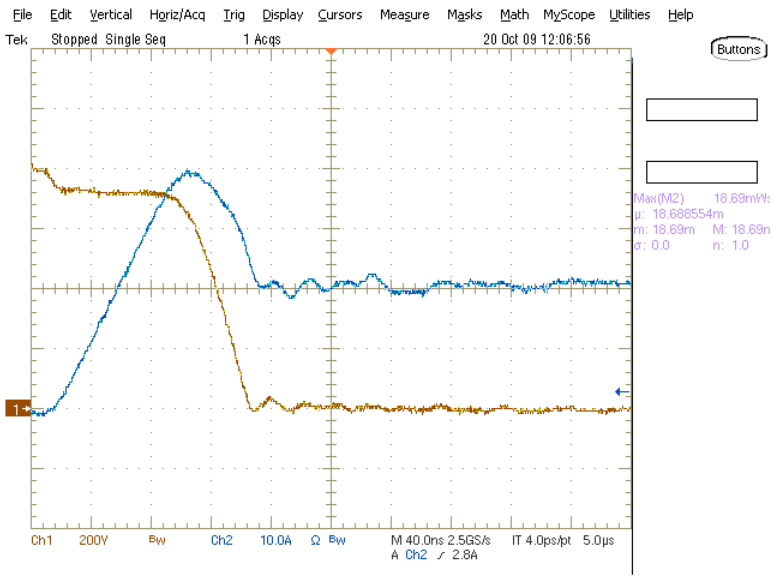

Figure 64: IRG7PH42UD Turn On Behavior at 800V, 20A (blue = current, yellow = voltage)

5.7 International Rectifier IRG7PH42U and Cree C2D20120 SiC Diode

The IRG7PH42U is the identical device to the IRG7PH42UD, except that it does not come co-packaged with an anti-parallel diode. Instead, this testing used a Cree 1200V, 20A Silicon Carbide freewheeling diode. The device performance is shown in Figures 66-73. A summary of the performance statistics is given in Table 10 below.

Table 10: IRG7PH42U Dynamic Losses (Units are in uJ)

	IRG7PH42U & C2D20120D			
	600V 10A	600V 20A	800V 10A	800V 20A
Eoff	465	678	612	952
Eon	272	617	432	925
Etotal	**737**	**1295**	**1044**	**1877**

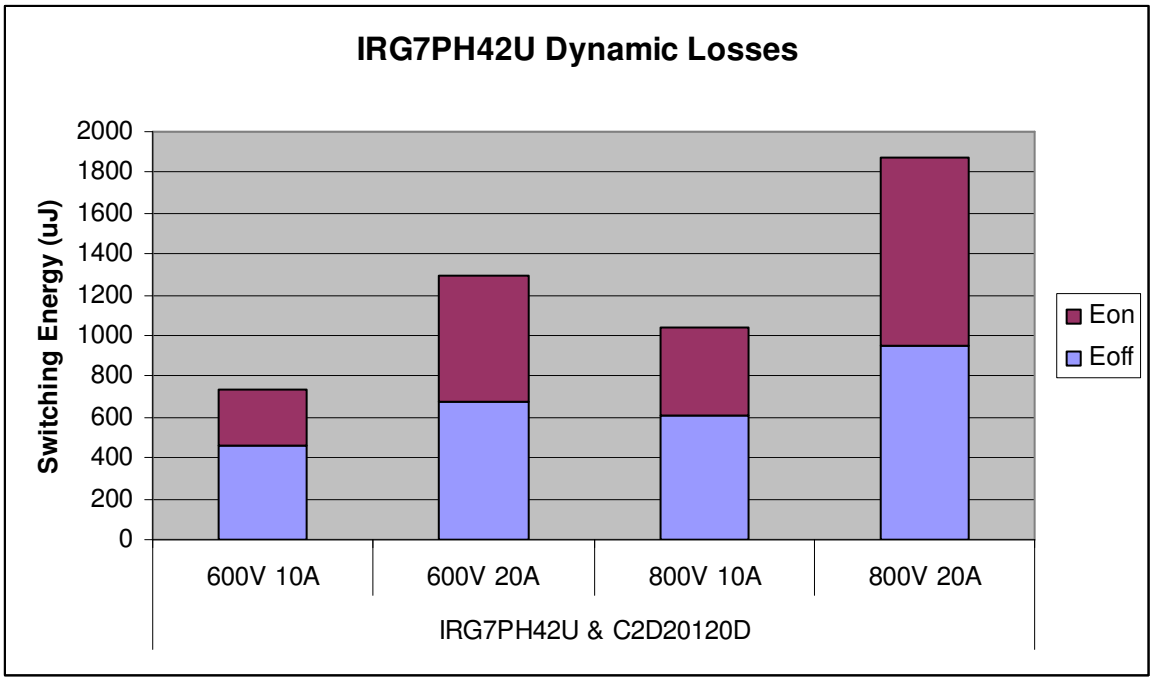

Figure 65: IRG7PH42U Dynamic Losses (Units are in uJ)

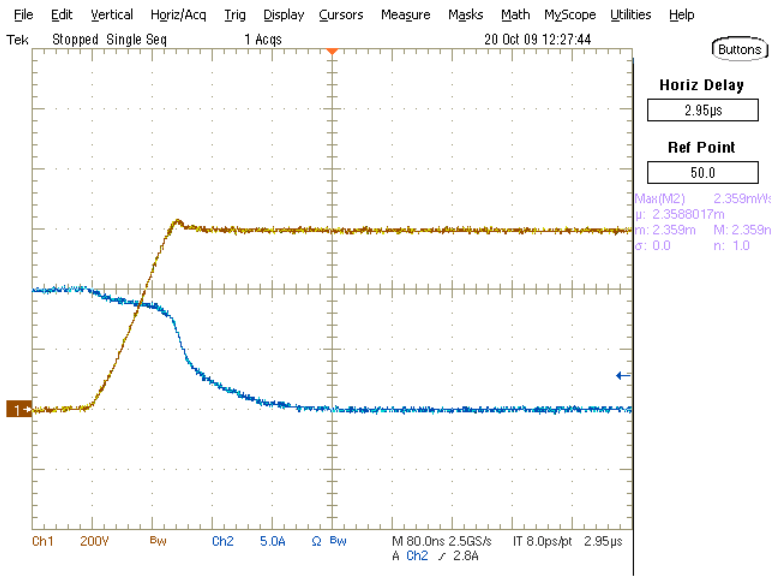

Figure 66: IRG7PH42U Turn Off Behavior at 600V, 10A
(blue = current, yellow = voltage)

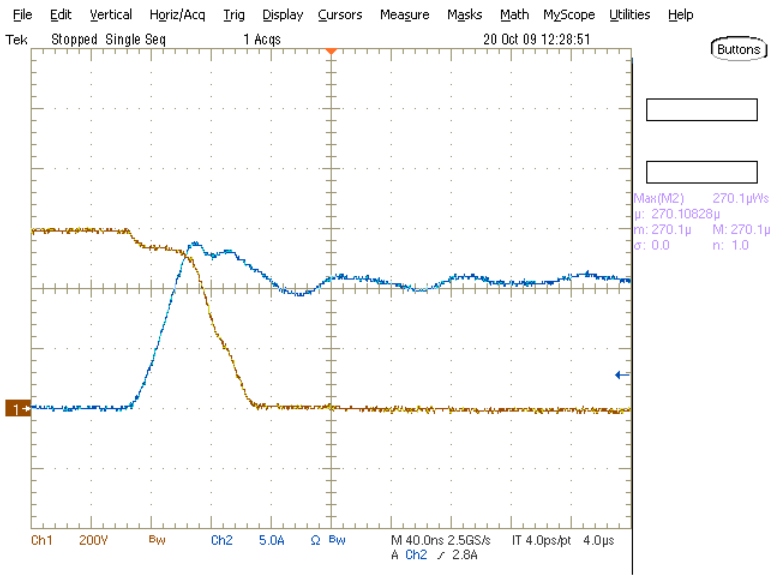

Figure 67: IRG7PH42U Turn On Behavior at 600V, 10A
(blue = current, yellow = voltage)

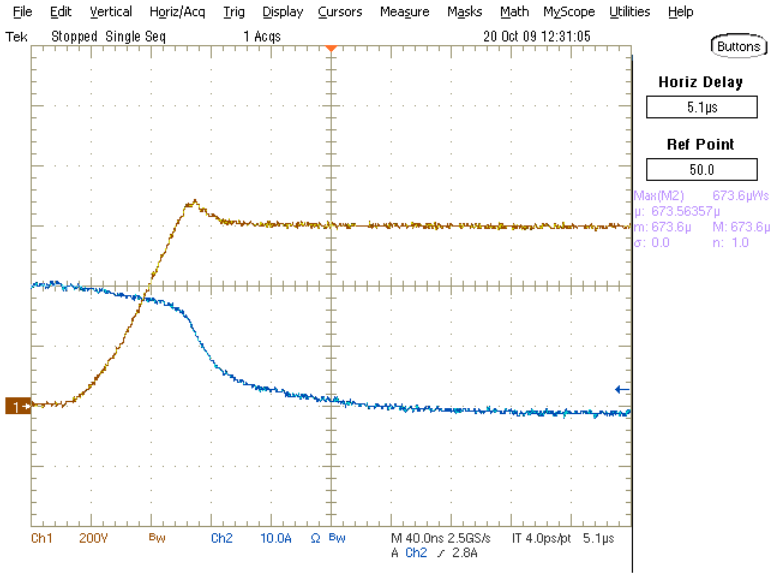

Figure 68: IRG7PH42U Turn Off Behavior at 600V, 20A
(blue = current, yellow = voltage)

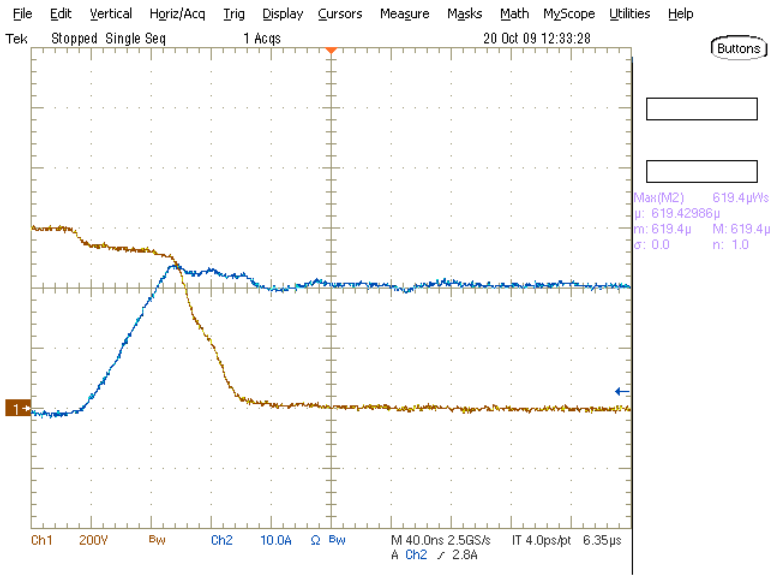

Figure 69: IRG7PH42U Turn On Behavior at 600V, 20A
(blue = current, yellow = voltage)

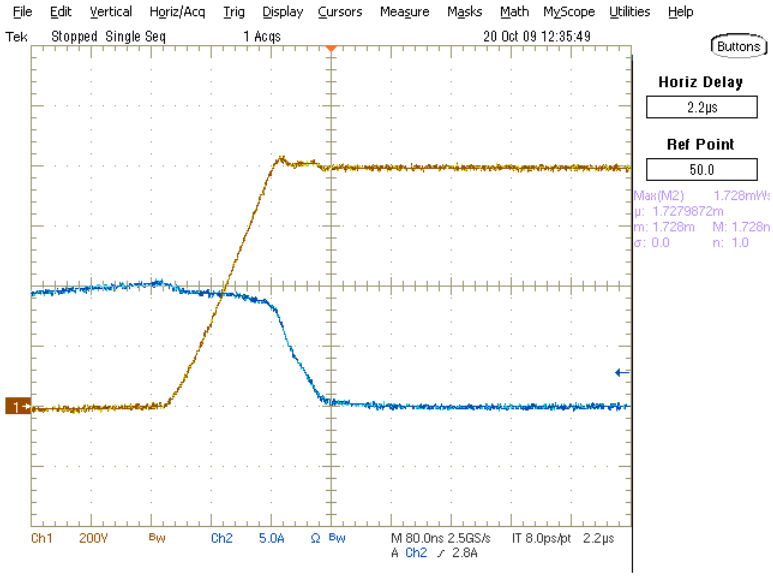

Figure 70: IRG7PH42U Turn Off Behavior at 800V, 10A
(blue = current, yellow = voltage)

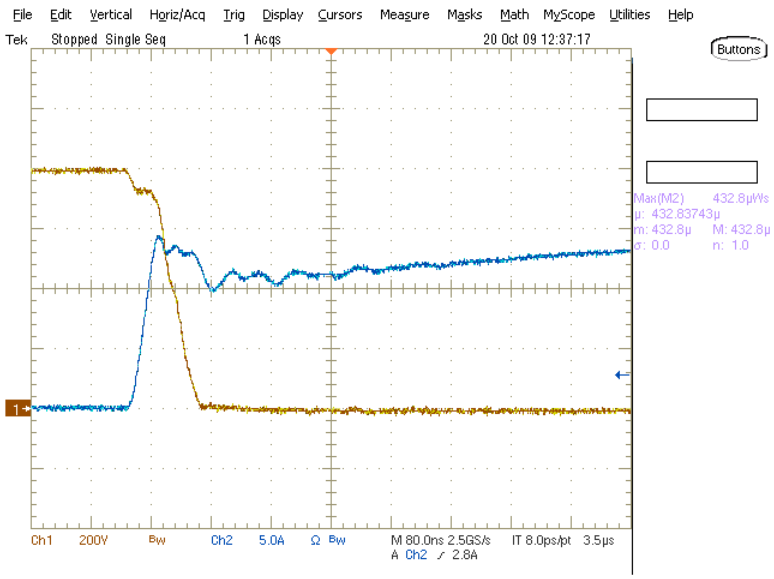

Figure 71: IRG7PH42U Turn On Behavior at 800V, 10A
(blue = current, yellow = voltage)

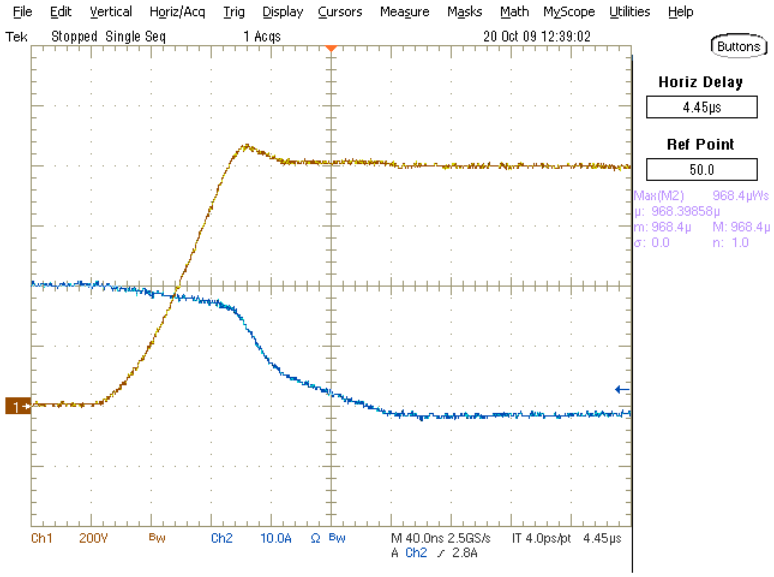

Figure 72: IRG7PH42U Turn Off Behavior at 800V, 20A
(blue = current, yellow = voltage)

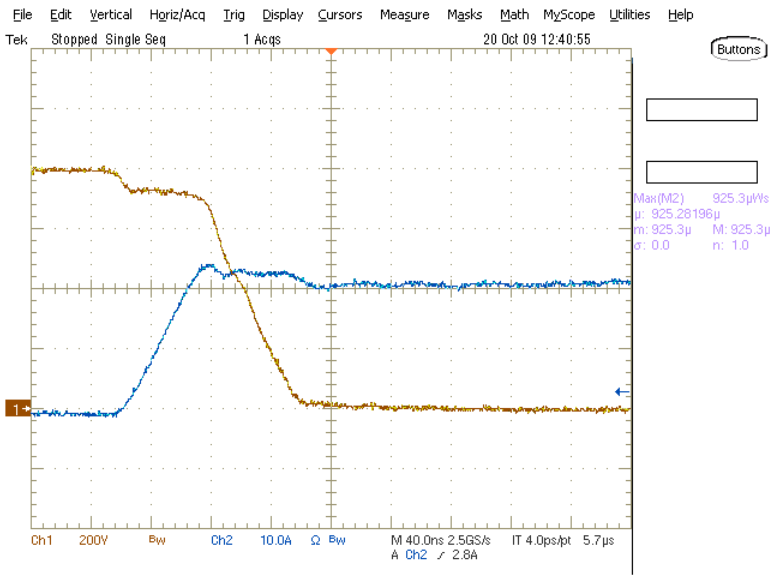

Figure 73: IRG7PH42U Turn On Behavior at 800V, 20A (blue = current, yellow = voltage)

5.8 Fairchild FGL40N120AND

This section gives test results for the FGL40N120AND device. This device is optimized for switching losses by increasing the speed at which the device turns on and decreasing the bipolar tail current of the device during turn off. This device is the latest generation Fairchild IGBT and diode co-pack, which optimizes the device for switching losses while increasing the conduction loss slightly. The device performance is shown in Figures 75-82. A summary of the performance statistics is given in Table 11 below.

Table 11: FGL40N120AND Dynamic Losses (Units are in uJ)

	FGL40N120AND			
	600V 10A	600V 20A	800V 10A	800V 20A
Eoff	328	494	606	684
Eon	572	1180	890	1780
Etotal	**900**	**1674**	**1496**	**2464**

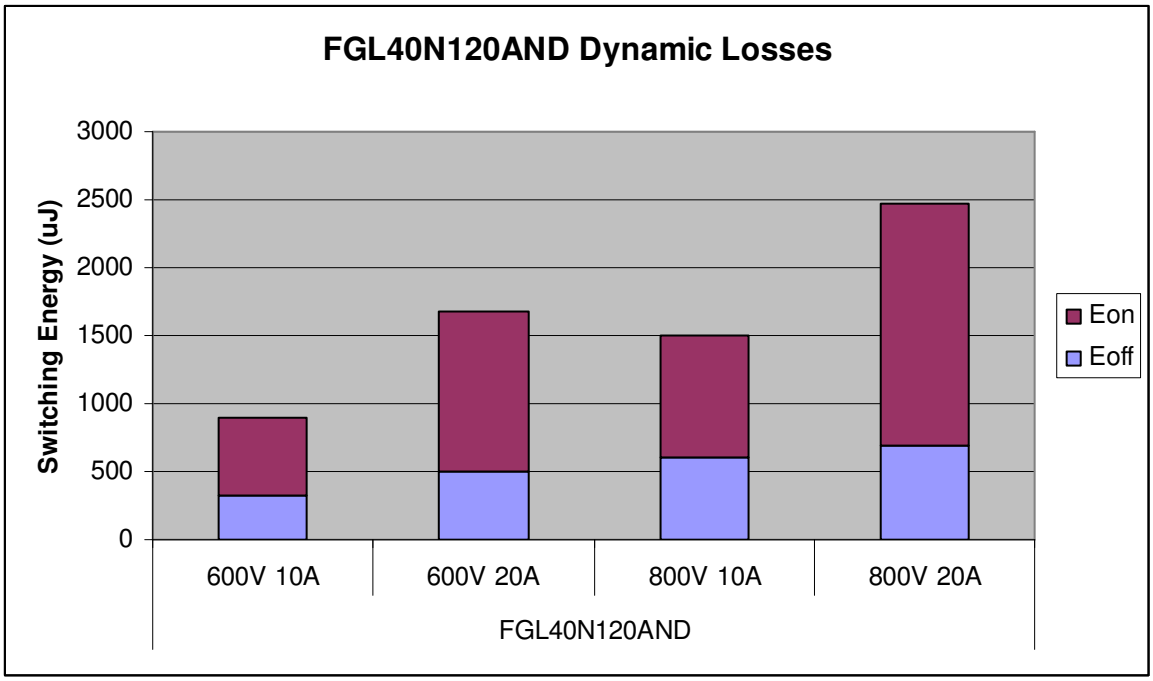

Figure 74: FGL40N120AND Dynamic Losses (Units are in uJ)

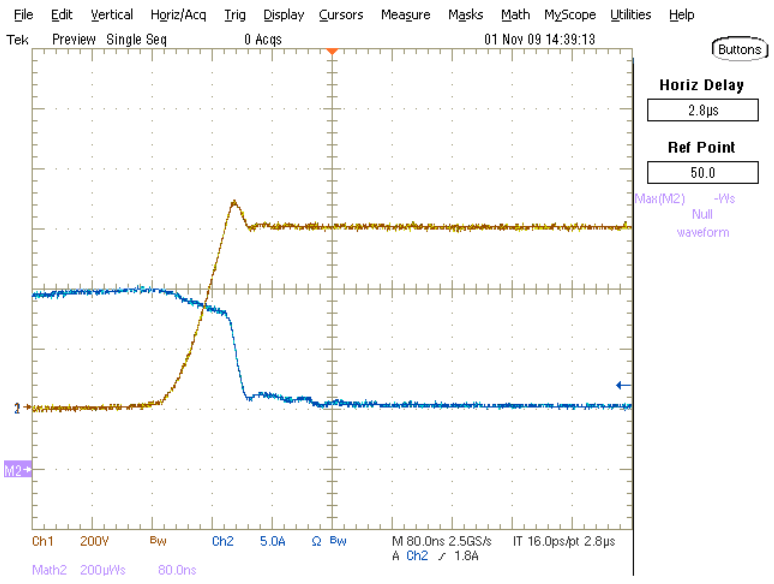

Figure 75: FGL40N120AND Turn Off Behavior at 600V, 10A (blue = current, yellow = voltage)

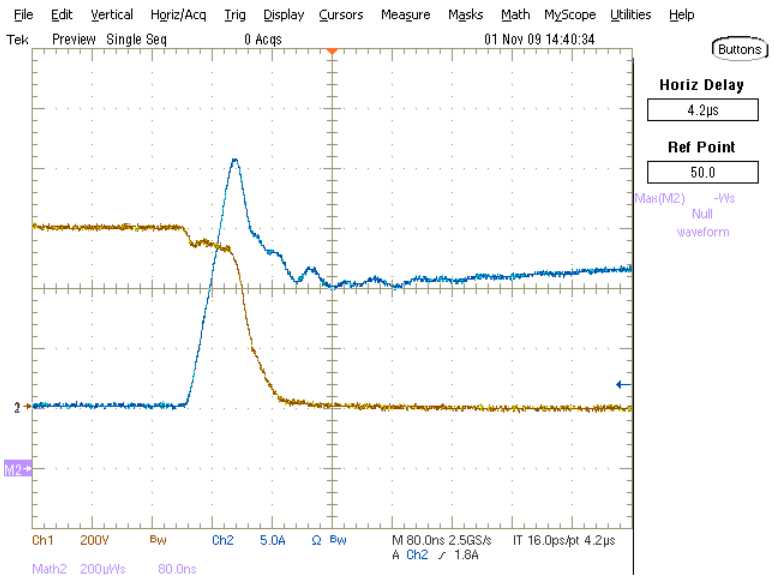

Figure 76: FGL40N120AND Turn On Behavior at 600V, 10A
(blue = current, yellow = voltage)

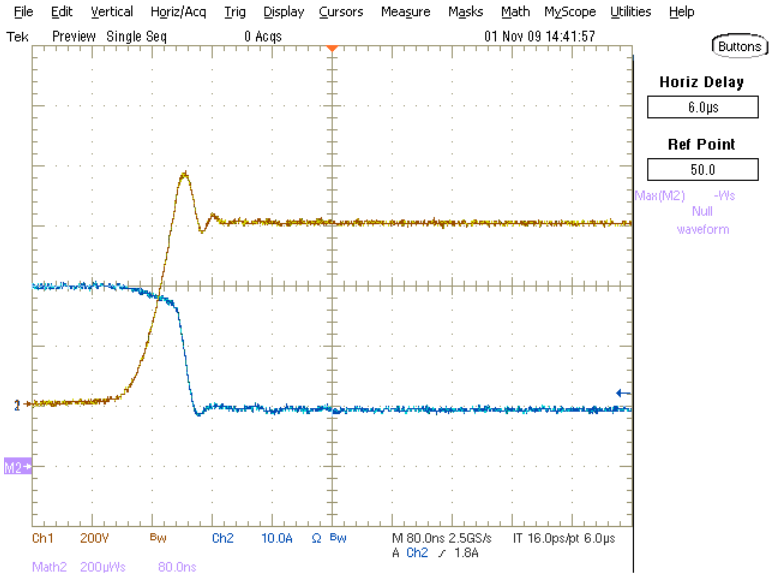

Figure 77: FGL40N120AND Turn Off Behavior at 600V, 20A
(blue = current, yellow = voltage)

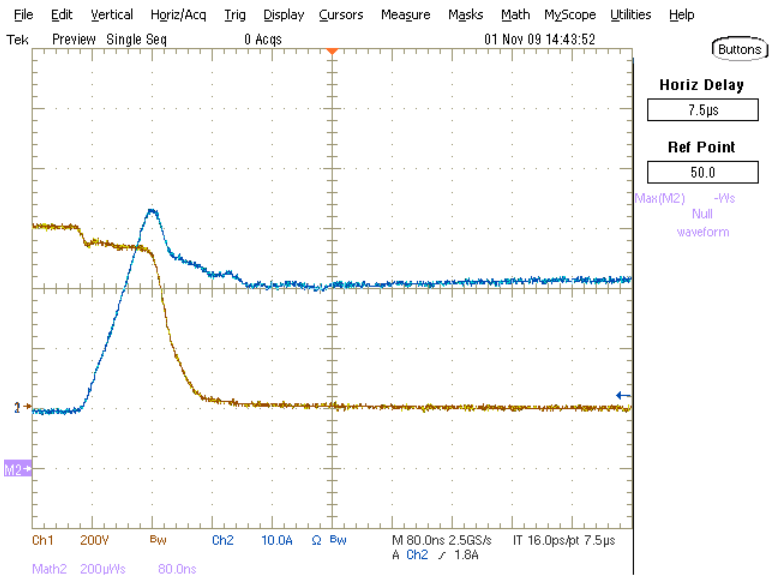

Figure 78: FGL40N120AND Turn On Behavior at 600V, 20A
(blue = current, yellow = voltage)

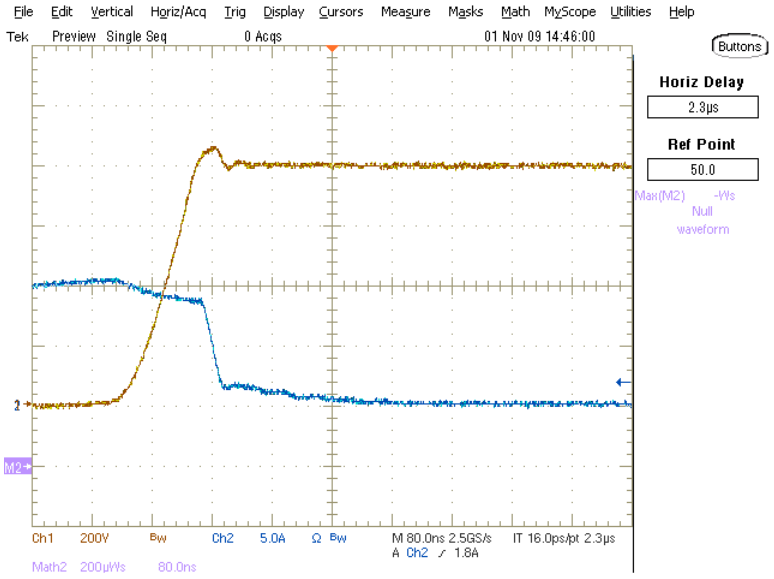

Figure 79: FGL40N120AND Turn Off Behavior at 800V, 10A
(blue = current, yellow = voltage)

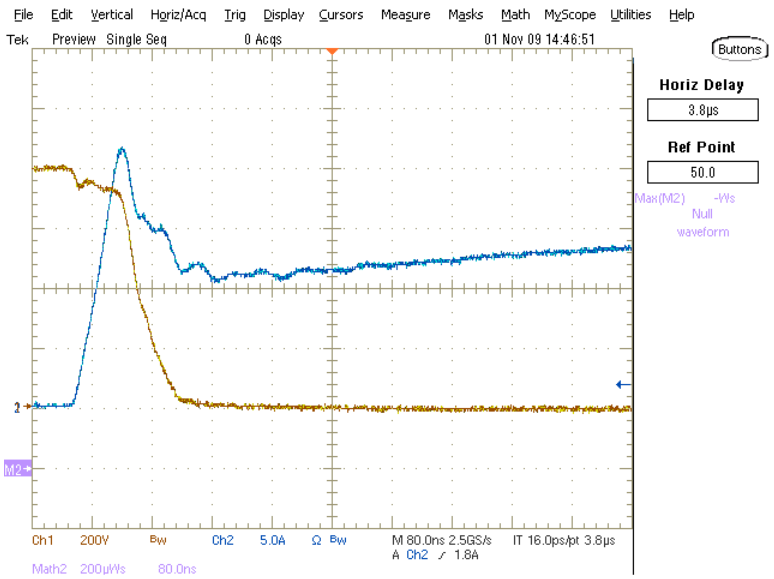

Figure 80: FGL40N120AND Turn On Behavior at 800V, 10A
(blue = current, yellow = voltage)

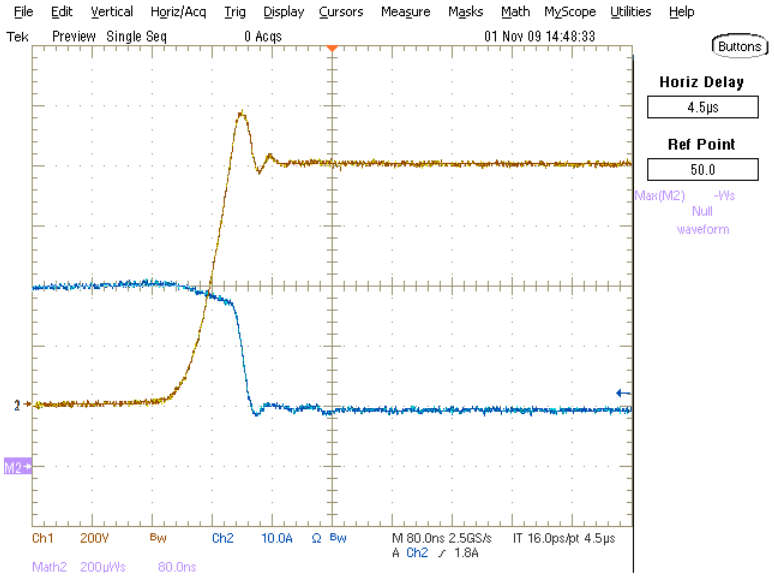

Figure 81: FGL40N120AND Turn Off Behavior at 800V, 20A
(blue = current, yellow = voltage)

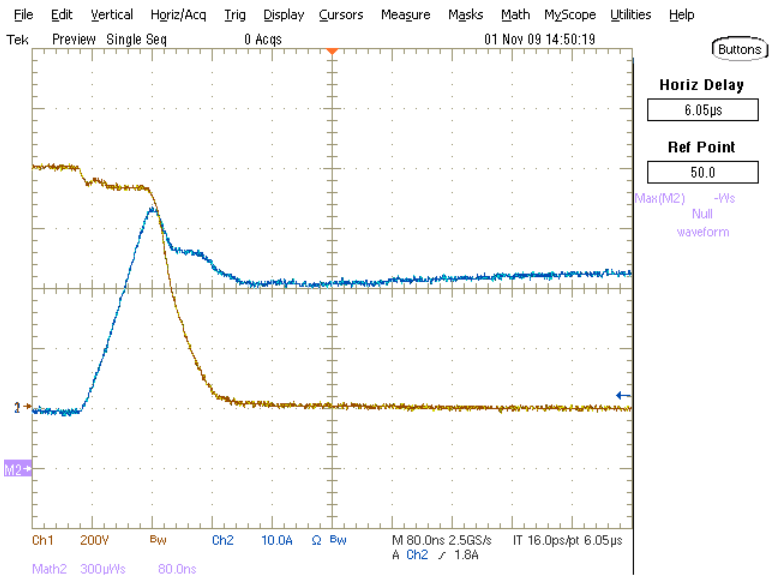

Figure 82: FGL40N120AND Turn On Behavior at 800V, 20A (blue = current, yellow = voltage)

5.9 Fairchild FGL40N120AN and Cree C2D20120 SiC Diode

The FGL40N120AN is the identical device to the FGL40N120AND, except that it does not come co-packaged with an anti-parallel diode. Instead, this testing used a Cree 1200V, 20A Silicon Carbide freewheeling diode. The device performance is shown in Figures 84-91. A summary of the performance statistics is given in Table 12 below.

Table 12: FGL40N120AN Dynamic Losses (Units are in uJ)

	FGL40N120AN & C2D20120D			
	600V 10A	600V 20A	800V 10A	800V 20A
Eoff	313	457	588	641
Eon	359	780	560	1230
Etotal	**672**	**1237**	**1148**	**1871**

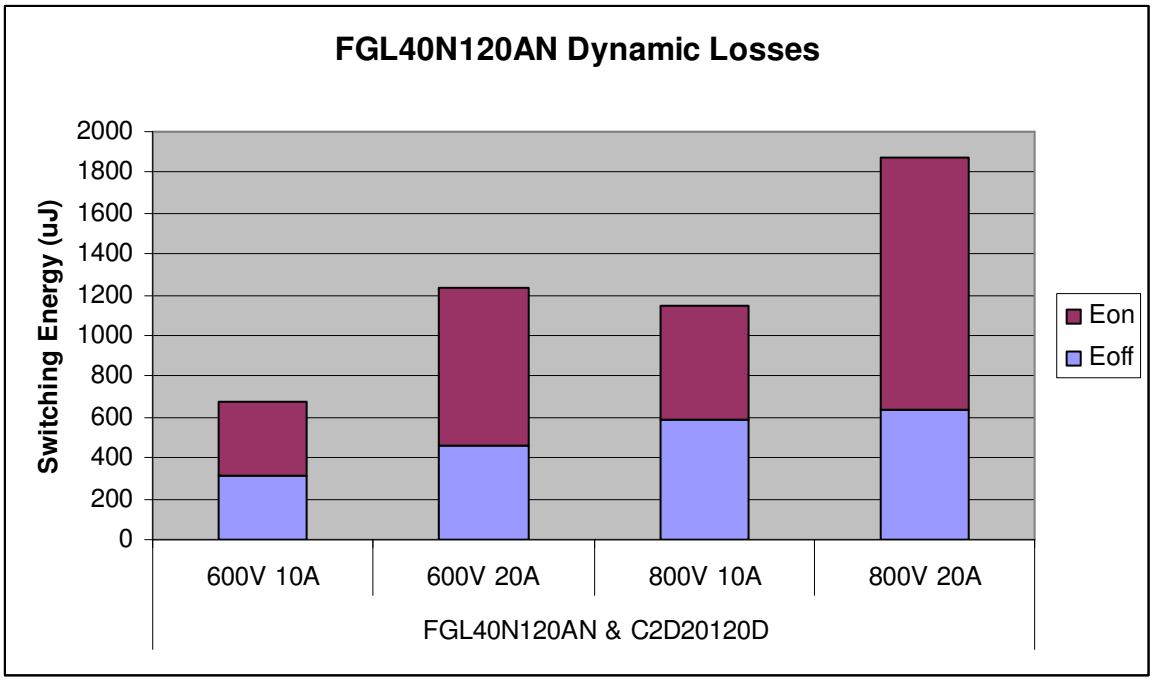

Figure 83: FGL40N120AN Dynamic Losses (Units are in uJ)

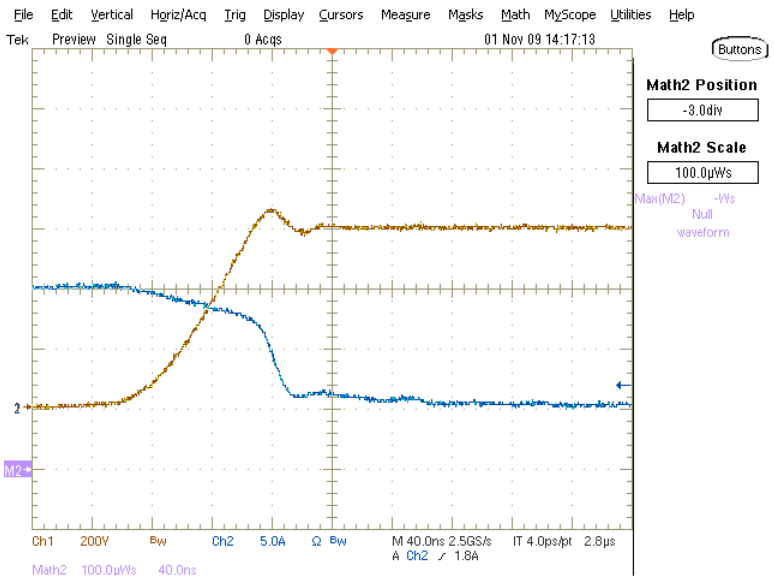

Figure 84: FGL40N120AN Turn Off Behavior at 600V, 10A
(blue = current, yellow = voltage)

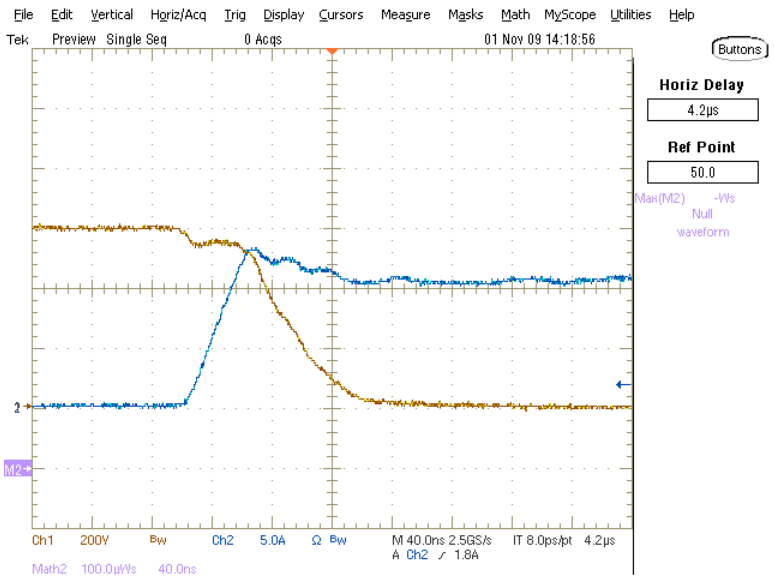

Figure 85: FGL40N120AN Turn On Behavior at 600V, 10A
(blue = current, yellow = voltage)

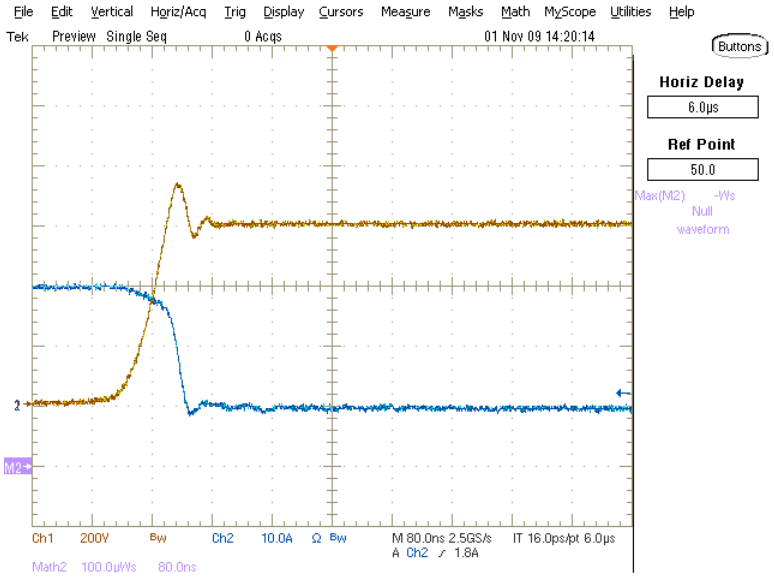

Figure 86: FGL40N120AN Turn Off Behavior at 600V, 20A
(blue = current, yellow = voltage)

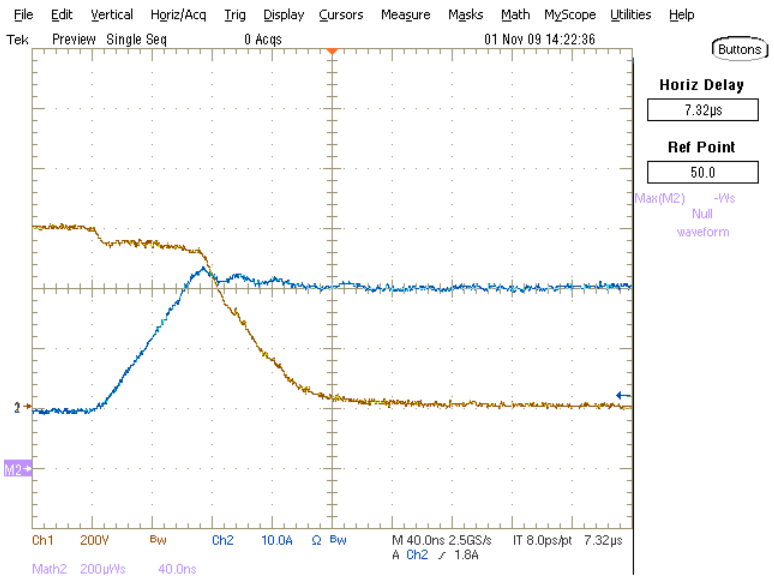

Figure 87: FGL40N120AN Turn On Behavior at 600V, 20A
(blue = current, yellow = voltage)

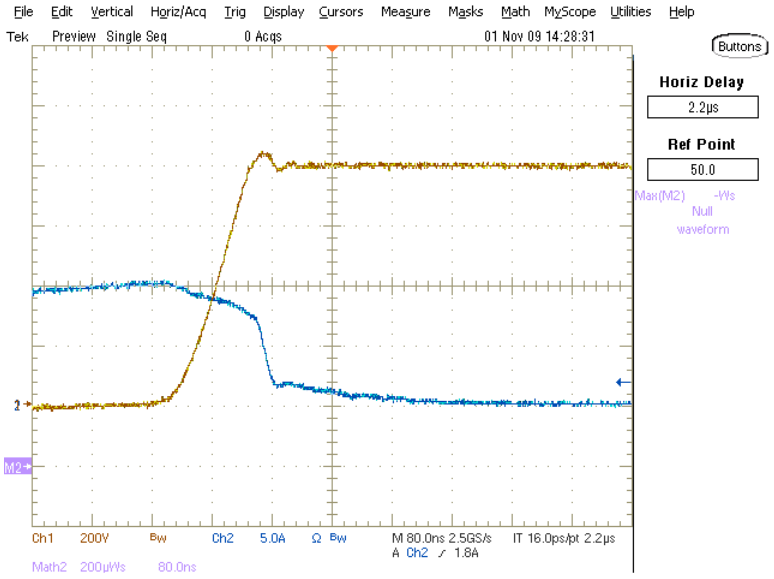

Figure 88: FGL40N120AN Turn Off Behavior at 800V, 10A
(blue = current, yellow = voltage)

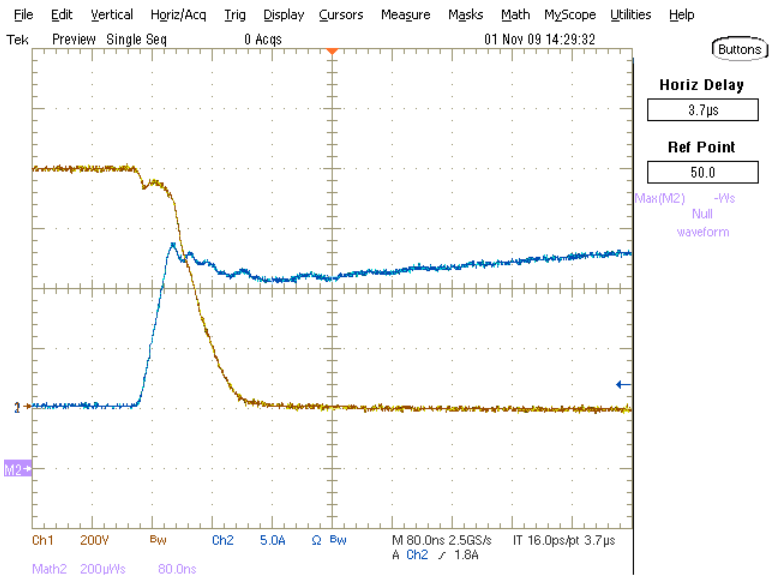

Figure 89: FGL40N120AN Turn On Behavior at 800V, 10A
(blue = current, yellow = voltage)

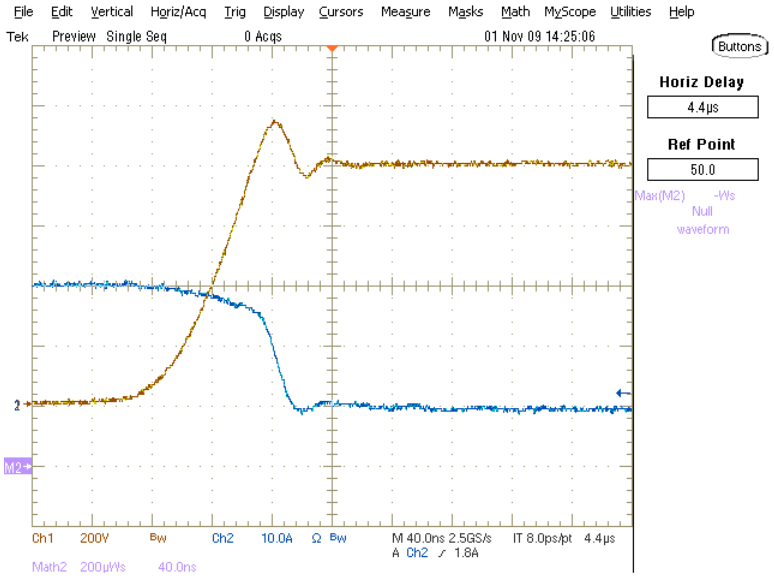

Figure 90: FGL40N120AN Turn Off Behavior at 800V, 20A
(blue = current, yellow = voltage)

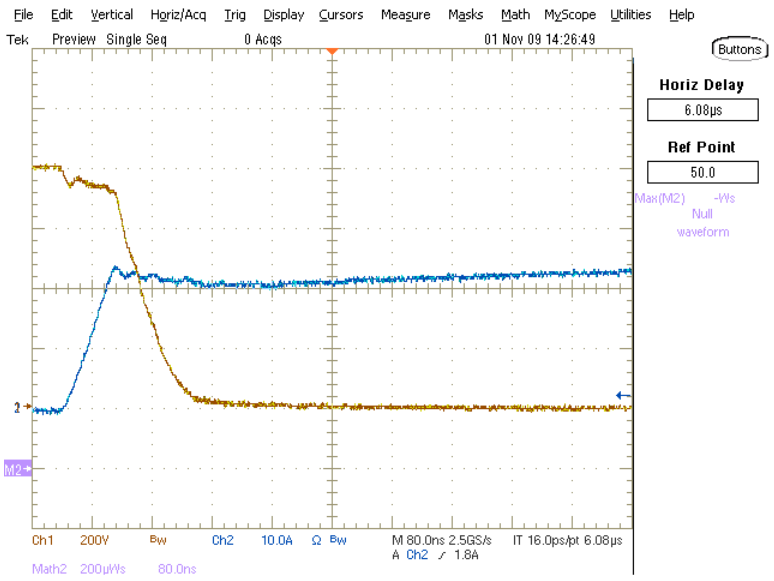

Figure 91: FGL40N120AN Turn On Behavior at 800V, 20A (blue = current, yellow = voltage)

5.10 SemiSouth SJEP120R125 SiC JFET with Cree C2D20120 SiC Diode

This section gives test results for the SJEP120R125 device. This device is designed for extra low switching losses. The device is a normally off Silicon Carbide JFET. The device performance is shown in Figures 93-100. A summary of the performance statistics is given in Table 13 below. It is important to note that this baseline comparison was done with a simple 15V unipolar gate driver through a 10 Ohm resistor. The SemiSouth JFET devices have slightly different gate drive requirements and should be used as such. In Chapter 6 of this report the gate driver for the SemiSouth JFETs have been optimized for best performance and it is clear this baseline test was not a very good reflection of the performance of these devices. It is, however, important to see how the devices serve as a

drop in replacement for IGBT's. It can be concluded from the following results that the devices do not do an extremely poor job of this. It will also be shown in Chapter 6 that the devices can improve by roughly a factor of 5 with a very small gate drive optimization.

Table 13: SJEP120R125 Dynamic Losses (Units are in uJ)

	SJEP120R125 & C2D20120D			
	600V 10A	600V 20A	800V 10A	800V 20A
Eoff	913	1860	1350	2700
Eon	197	392	310	639
Etotal	**1110**	**2252**	**1660**	**3339**

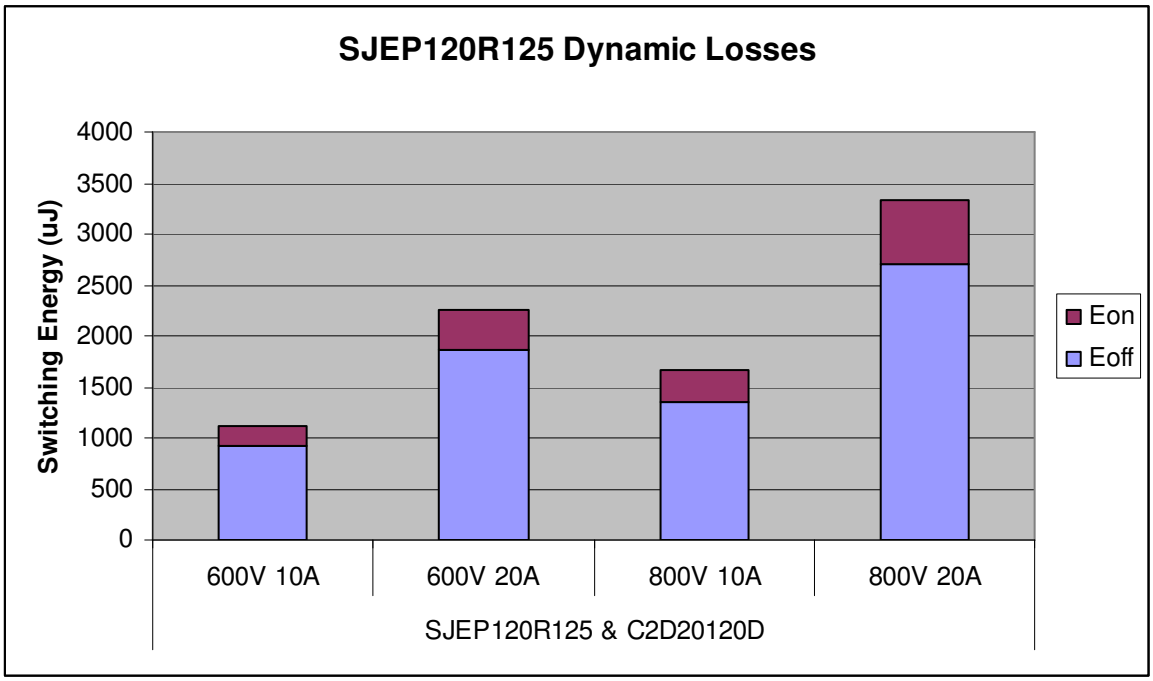

Figure 92: SJEP120R125 Dynamic Losses (Units are in uJ)

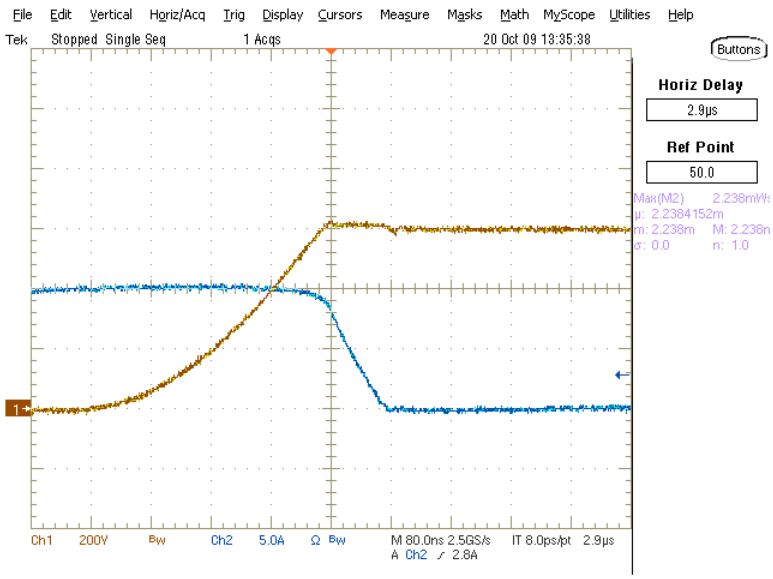

Figure 93: SJEP120R125 Turn Off Behavior at 600V, 10A (blue = current, yellow = voltage)

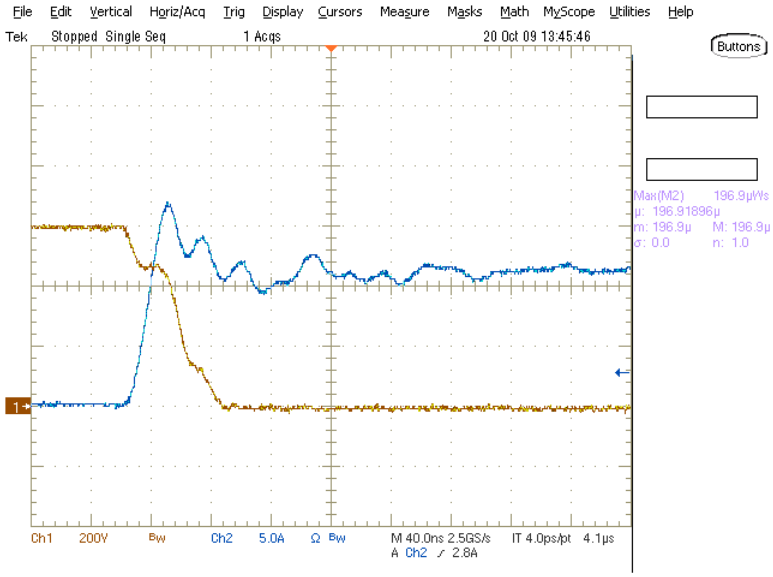

Figure 94: SJEP120R125 Turn On Behavior at 600V, 10A (blue = current, yellow = voltage)

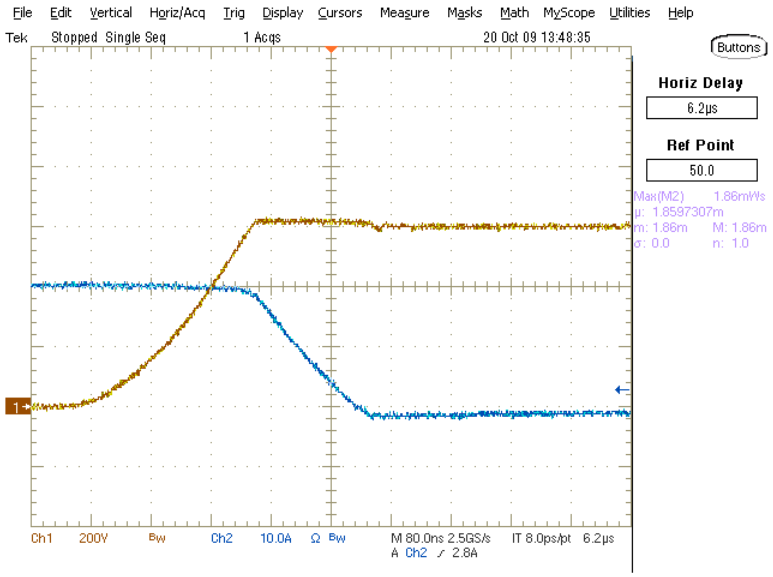

Figure 95: SJEP120R125 Turn Off Behavior at 600V, 20A (blue = current, yellow = voltage)

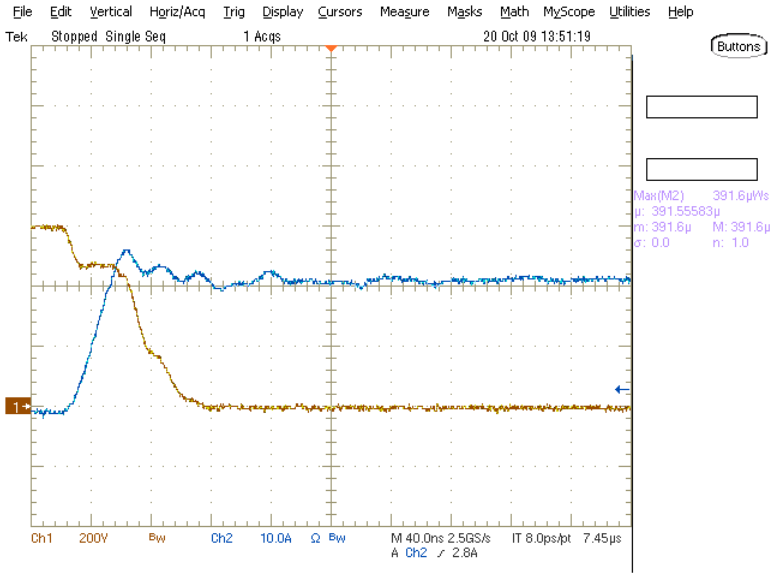

Figure 96: SJEP120R125 Turn On Behavior at 600V, 20A (blue = current, yellow = voltage)

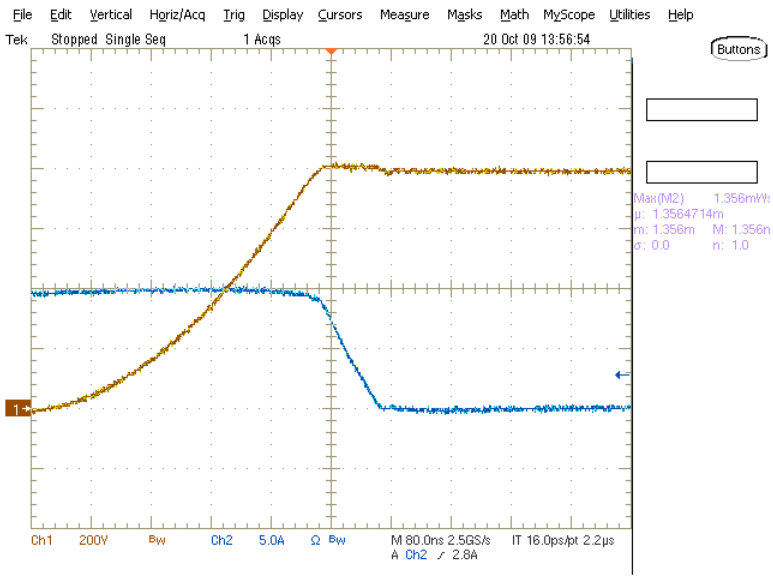

Figure 97: SJEP120R125 Turn Off Behavior at 800V, 10A (blue = current, yellow = voltage)

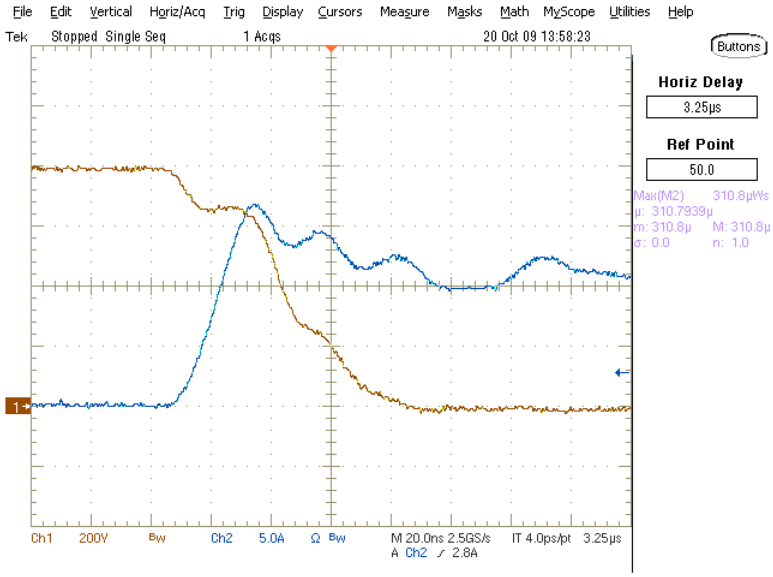

Figure 98: SJEP120R125 Turn On Behavior at 800V, 10A (blue = current, yellow = voltage)

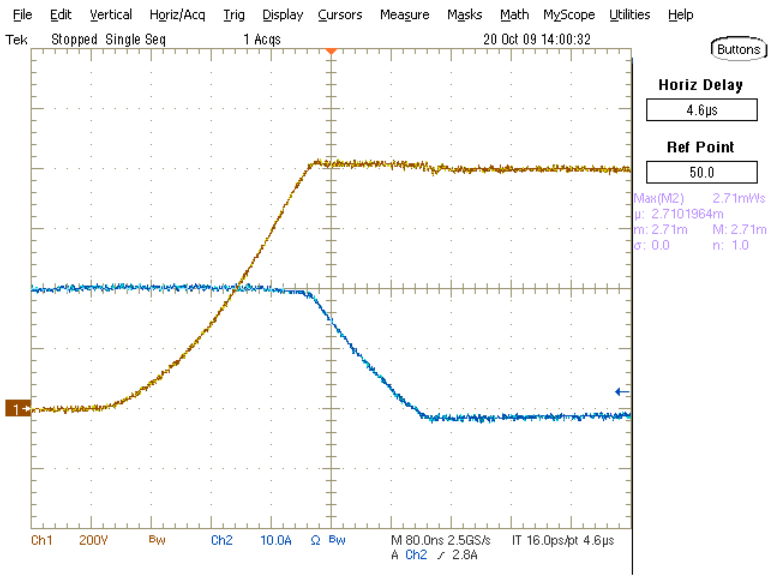

Figure 99: SJEP120R125 Turn Off Behavior at 800V, 20A
(blue = current, yellow = voltage)

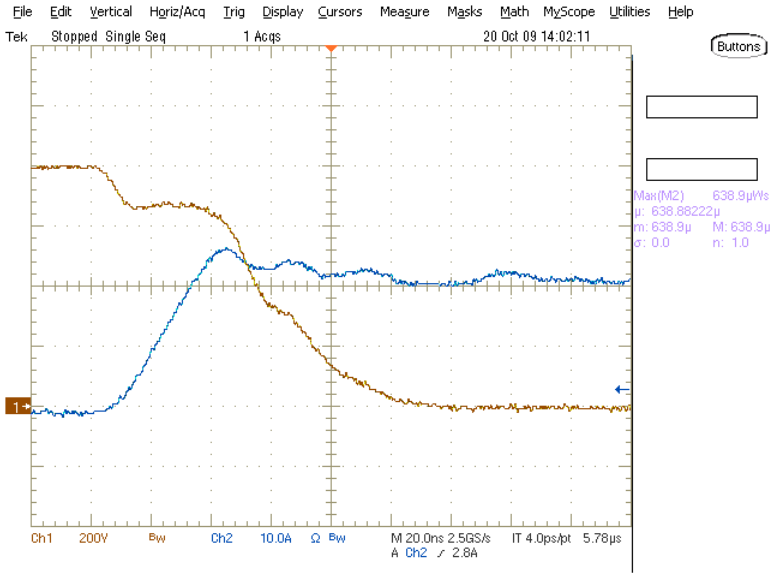

Figure 100: SJEP120R125 Turn On Behavior at 800V, 20A
(blue = current, yellow = voltage)

5.11 SemiSouth SJEP120R063 SiC JFET with Cree C2D20120 SiC Diode

This section gives test results for the SJEP120R063 device. This device is designed for extra low switching losses. The device is a normally off Silicon Carbide JFET. This device is the latest release for SemiSouth and has the lowest Rds of the lineup (63mOhm). It does, however, have slightly higher switching losses than the 125mOhm device. The device performance is shown in Figures 102-109. A summary of the performance statistics is given in Table 14 below. It is important to note that this baseline comparison was done with a simple 15V unipolar gate driver through a 10 Ohm resistor. The SemiSouth JFET devices have slightly different gate drive requirements and should be used as such. In Chapter 6 of this report the gate driver for the SemiSouth JFETs have been optimized for best performance and it is clear this baseline test was not a very good reflection of the performance of these devices. It is, however, important to see how the devices serve as a drop in replacement for IGBT's. It can be concluded from the following results that the devices do not do an extremely poor job of this. It will also be shown in Chapter 6 that the devices can improve by roughly a factor of 5 with a very small gate drive optimization.

Table 14: SJEP120R063 Dynamic Losses (Units are in uJ)

	SJEP120R063 & C2D20120D			
	600V 10A	600V 20A	800V 10A	800V 20A
Eoff	1390	2780	2050	4100
Eon	253	447	418	705
Etotal	**1643**	**3227**	**2468**	**4805**

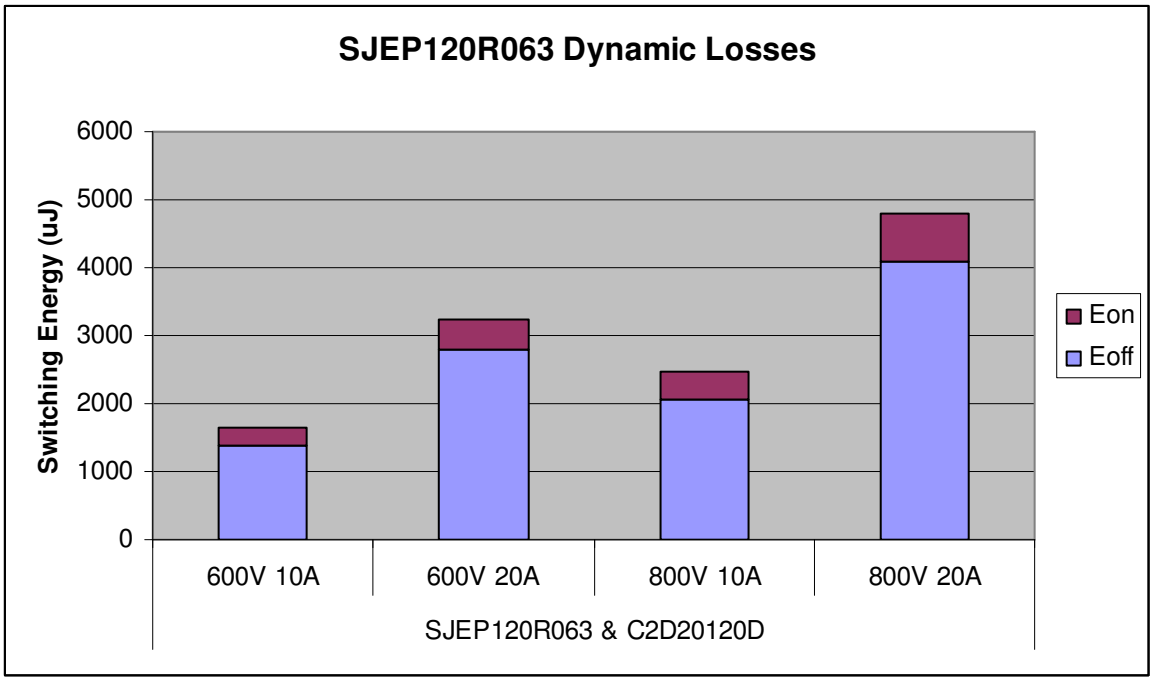

Figure 101: SJEP120R063 Dynamic Losses (Units are in uJ)

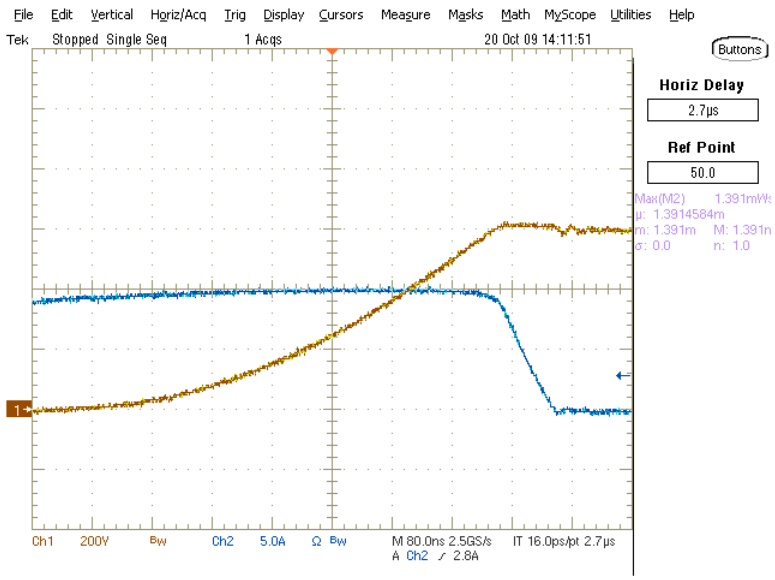

Figure 102: SJEP120R063 Turn Off Behavior at 600V, 10A
(blue = current, yellow = voltage)

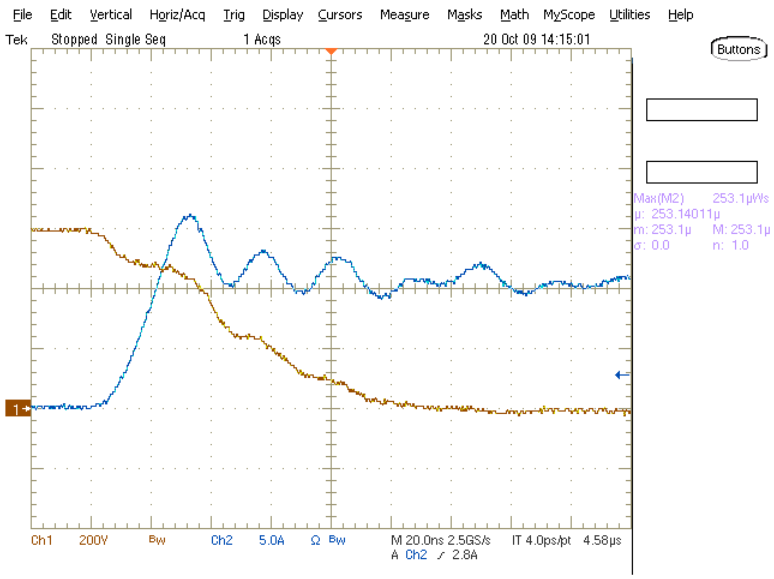

Figure 103: SJEP120R063 Turn On Behavior at 600V, 10A
(blue = current, yellow = voltage)

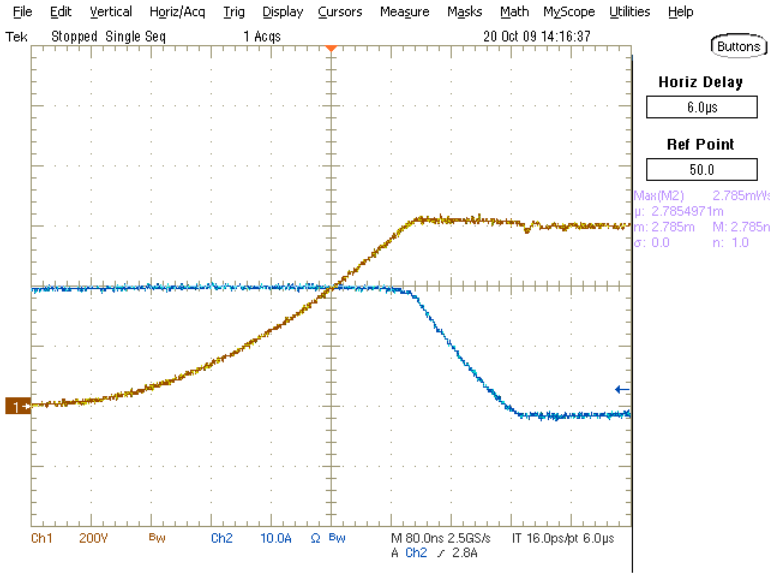

Figure 104: SJEP120R063 Turn Off Behavior at 600V, 20A
(blue = current, yellow = voltage)

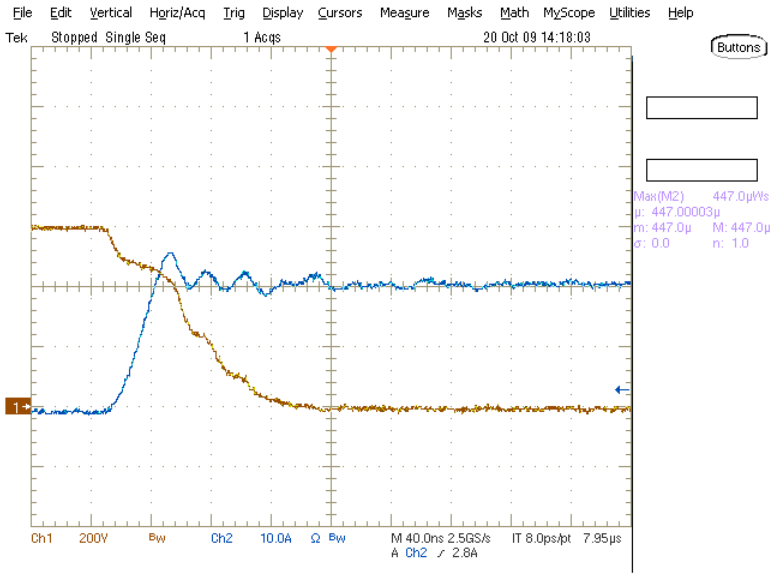

Figure 105: SJEP120R063 Turn On Behavior at 600V, 20A
(blue = current, yellow = voltage)

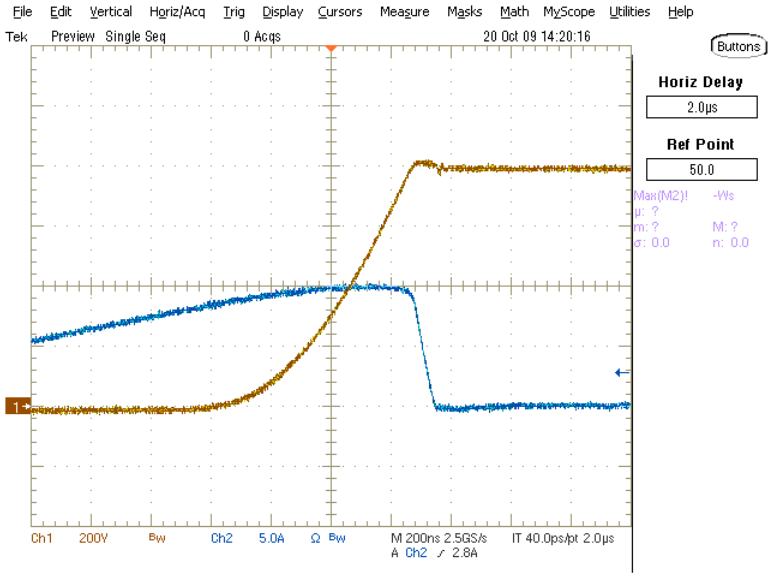

Figure 106: SJEP120R063 Turn Off Behavior at 800V, 10A
(blue = current, yellow = voltage)

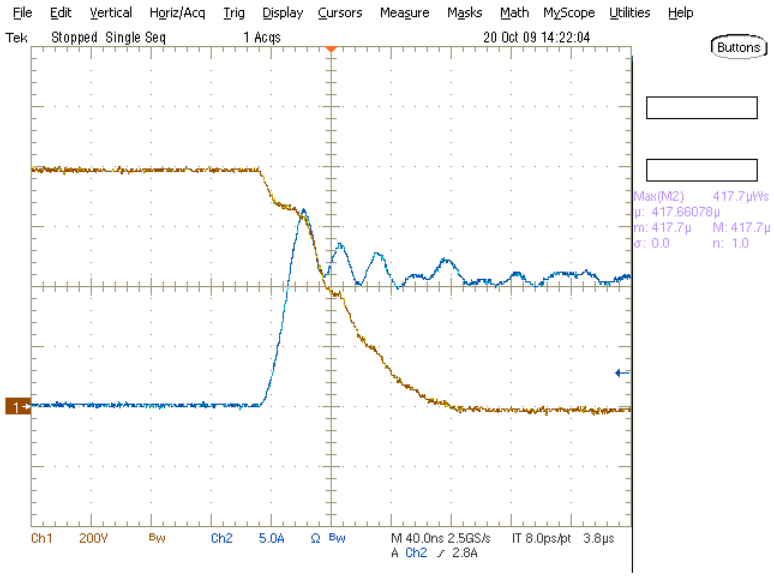

Figure 107: SJEP120R063 Turn On Behavior at 800V, 10A
(blue = current, yellow = voltage)

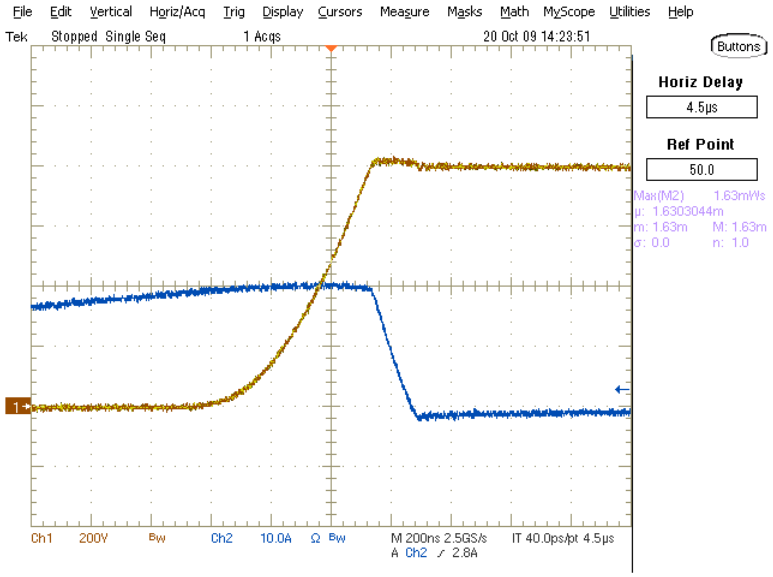

Figure 108: SJEP120R063 Turn Off Behavior at 800V, 20A
(blue = current, yellow = voltage)

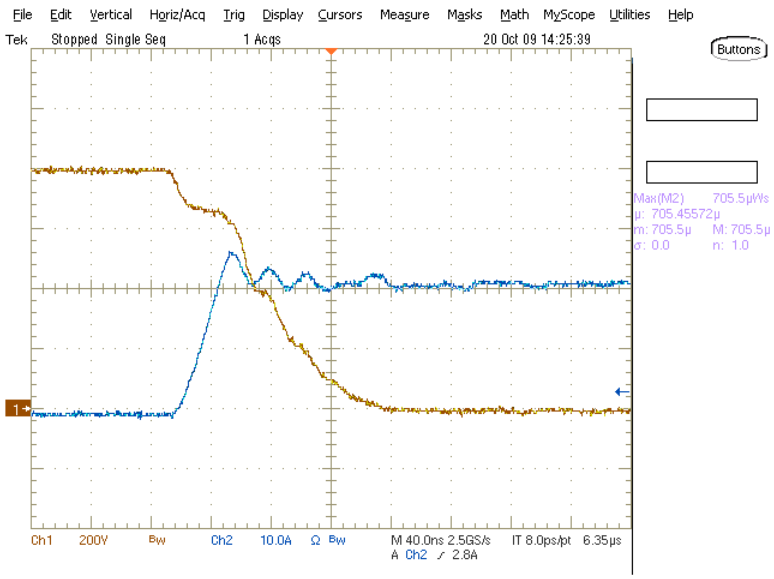

Figure 109: SJEP120R063 Turn On Behavior at 800V, 20A (blue = current, yellow = voltage)

5.12 Infineon IPW90R120C3 MOSFET with Ultrafast Silicon Diode

The IPW90R120C3 is a Super Junction MOSFET made by Infineon. The device it the latest to be released by Infineon in their CoolMOS series. The device can handle up to 900V Vds and is rated for 23 Amps at 100C junction temperature. The device has a maximum Rds,on of 120mOhms and a typical gate charge of 270nC. The device was tested in this section with the International Rectifier diode co-packaged with the IRG7PH42UD device. This diode had the lowest reverse recovery of the Silicon Diodes tested. The device performance is shown in Figures 111118. A summary of the performance statistics is given in Table 15 below. It is important to note the device was tested using only the body diode of the device and failed miserably. The device performed so poorly with the body diode that test results could not even be obtained. The main reason for this was the peak reverse

recovery current of the diode. The datasheet gives a figure of 65 Amps peak reverse recovery current for a 26A forward current. Because of this, the measurement equipment used could not even show the high peak currents. Not only that, when the test was attempted, the peak current was so great that the IPW90R120C3 device could not even turn on without being damaged due to the extremely high peak recovery current. It was determined that this product could never be used in a bridge configuration where the diode of the upper device would conduct current. The main reason of this is that the voltage drop of the body diode is extremely low:

1) Body diode: 0.8V drop at 26A (25C)

2) Si Ultrafast Diode in IRG7PH42UD: 2.5V drop at 20A (25C)

3) SiC Diode C2D20120D: 2.2V at 20A (25C)

Because of this, the body diode would still conduct current even if another device was placed in parallel and the device is essentially useless in a bridge configuration. Testing done in this section is valuable only to a single switch topology such as a boost or buck converter.

Table 15: IPW90R120C3 Dynamic Losses (Units are in uJ)

10Ohm	IPW90R120C3 & Ultrafast Si Diode			
	600V 10A	600V 20A	800V 10A	800V 20A
Eoff	218	607	480	1110
Eon	518	984	791	1450
Etotal	**736**	**1591**	**1271**	**2560**

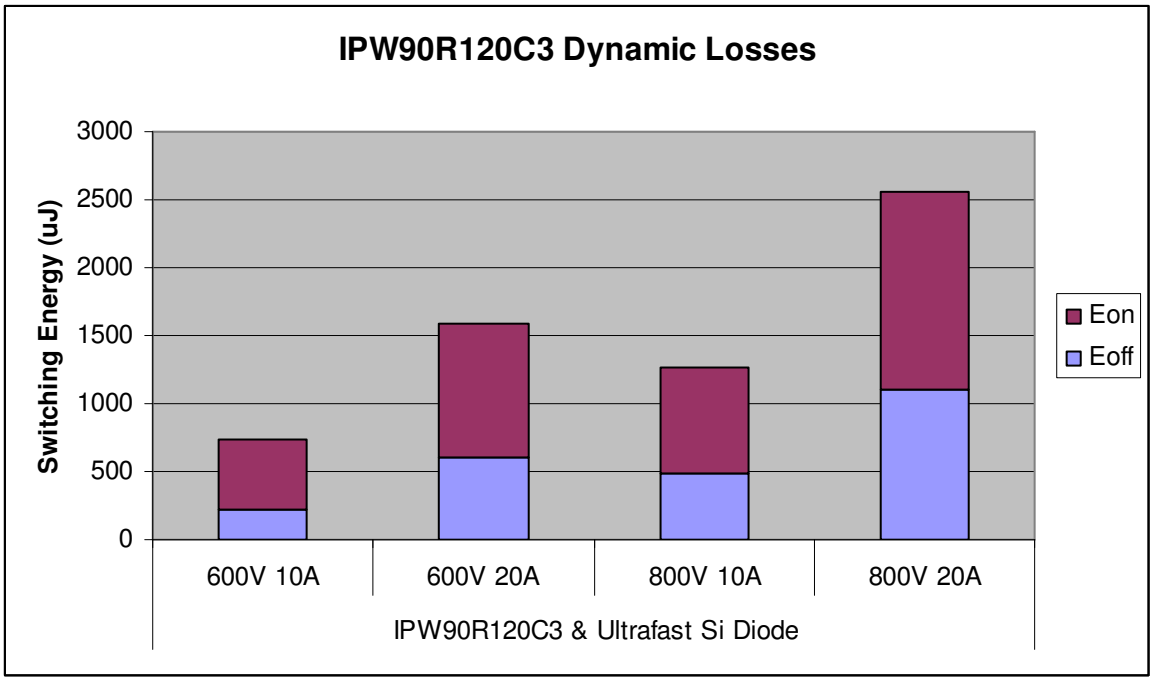

Figure 110: IPW90R120C3 Dynamic Losses (Units are in uJ)

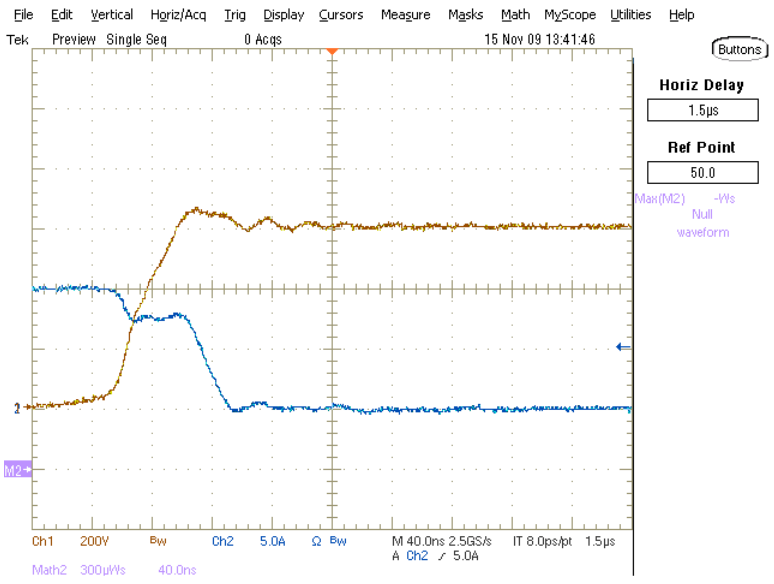

Figure 111: IPW90R120C3 Turn Off Behavior at 600V, 10A
(blue = current, yellow = voltage)

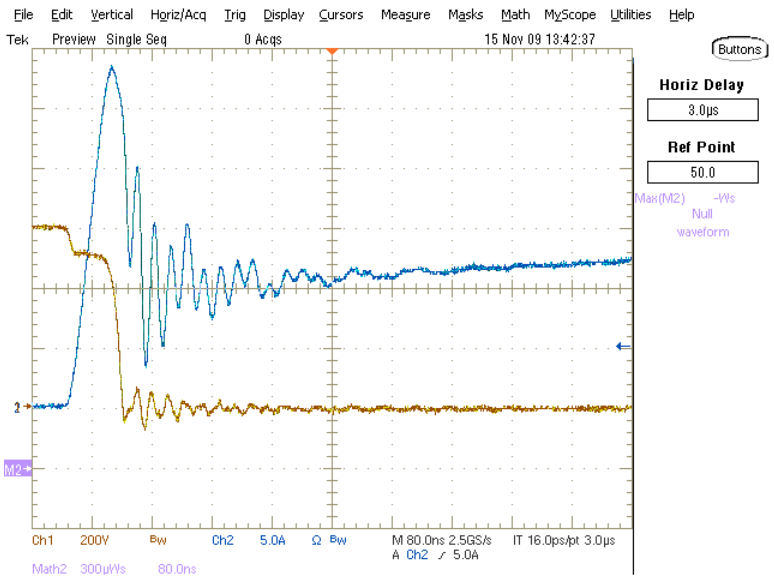

Figure 112: IPW90R120C3 Turn On Behavior at 600V, 10A
(blue = current, yellow = voltage)

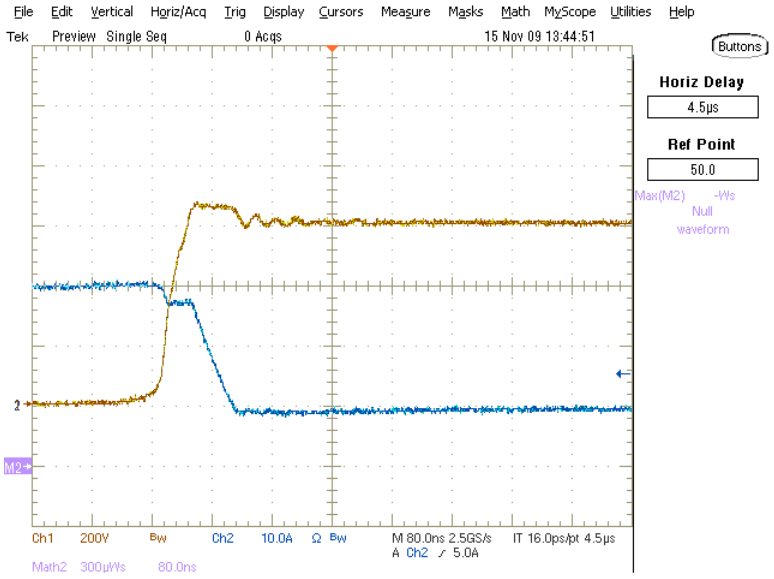

Figure 113: IPW90R120C3 Turn Off Behavior at 600V, 20A
(blue = current, yellow = voltage)

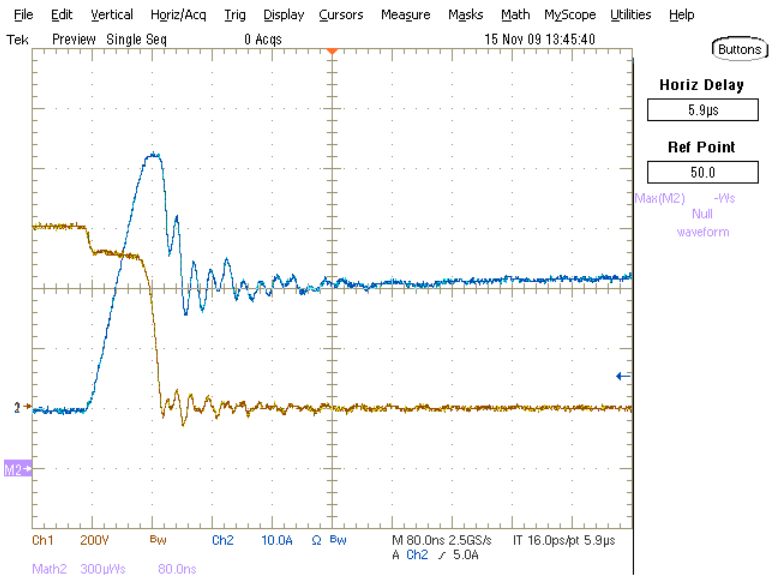

Figure 114: IPW90R120C3 Turn On Behavior at 600V, 20A
(blue = current, yellow = voltage)

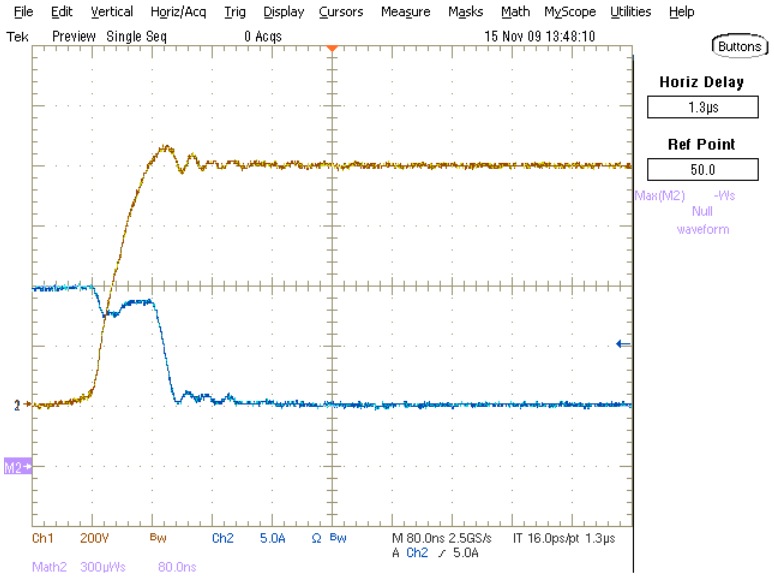

Figure 115: IPW90R120C3 Turn Off Behavior at 800V, 10A
(blue = current, yellow = voltage)

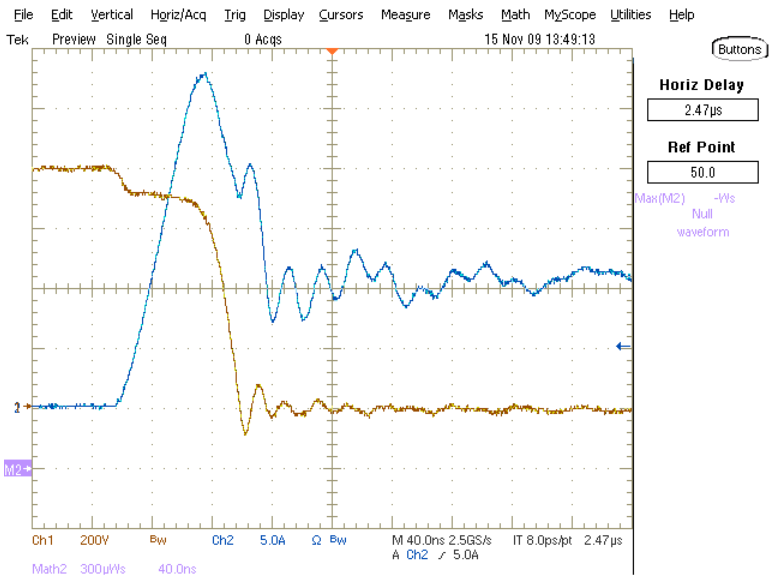

Figure 116: IPW90R120C3 Turn On Behavior at 800V, 10A
(blue = current, yellow = voltage)

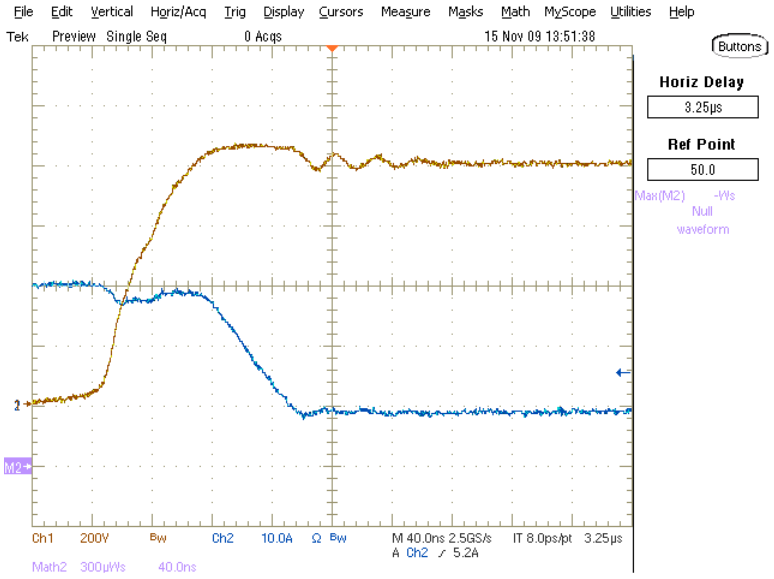

Figure 117: IPW90R120C3 Turn Off Behavior at 800V, 20A
(blue = current, yellow = voltage)

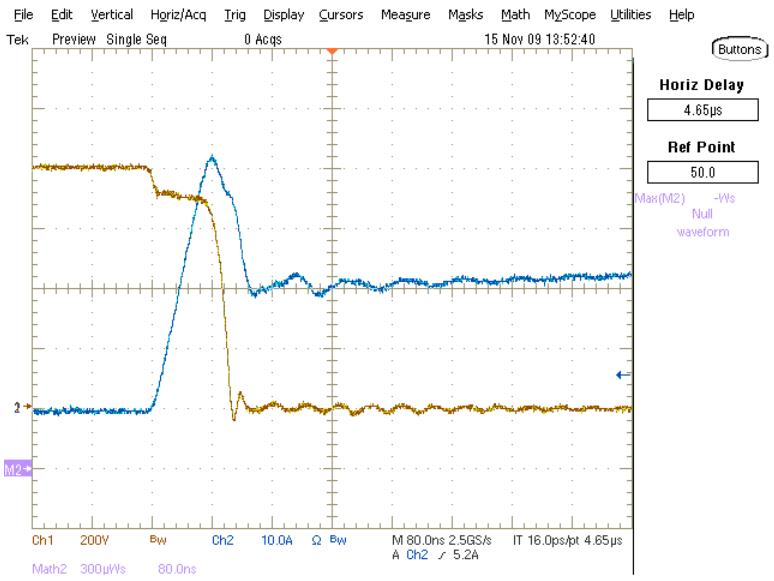

Figure 118: IPW90R120C3 Turn On Behavior at 800V, 20A (blue = current, yellow = voltage)

5.13 Infineon IPW90R120C3 MOSFET with Cree C2D20120 SiC Diode

In this section the IPW90R120C3 MOSFET was tested using a Cree SiC Diode instead of the Silicon ultrafast recovery diode tested in the previous section. The device performance is shown in Figures 120-127. A summary of the performance statistics is given in Table 16 below.

Table 16: IPW90R120C3 Dynamic Losses (Units are in uJ)

10Ohm	IPW90R120C3 & C2D20120D			
	600V 10A	600V 20A	800V 10A	800V 20A
Eoff	194	543	446	1060
Eon	199	388	376	740
Etotal	**393**	**931**	**822**	**1800**

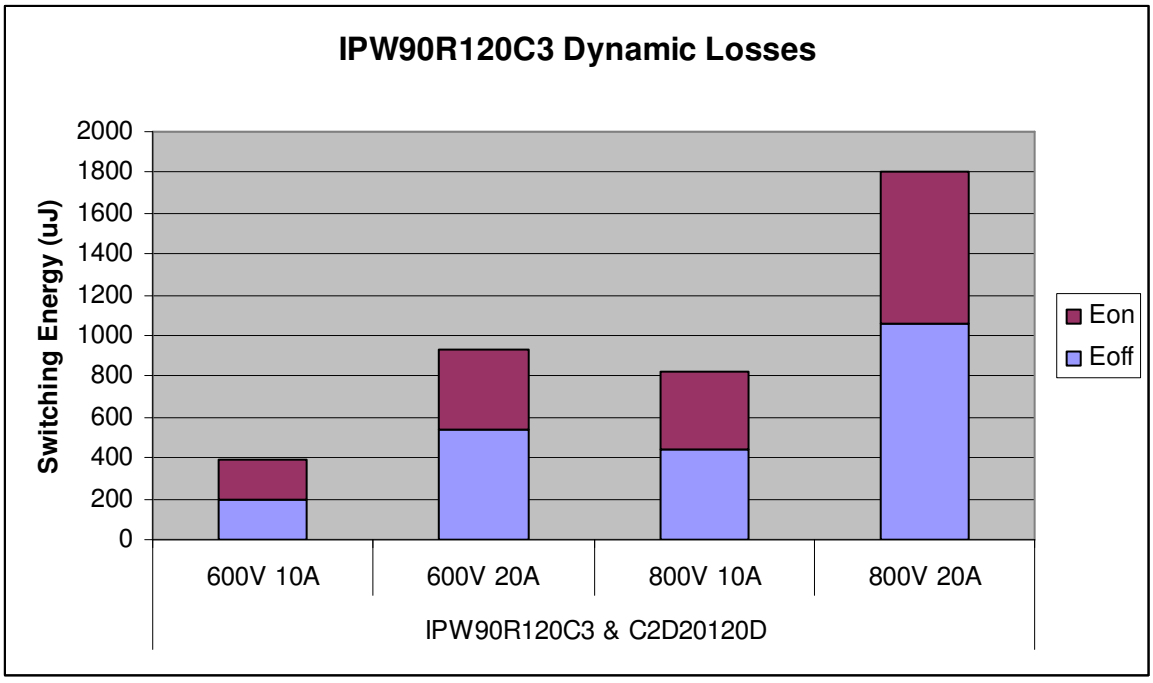

Figure 119: IPW90R120C3 Dynamic Losses (Units are in uJ)

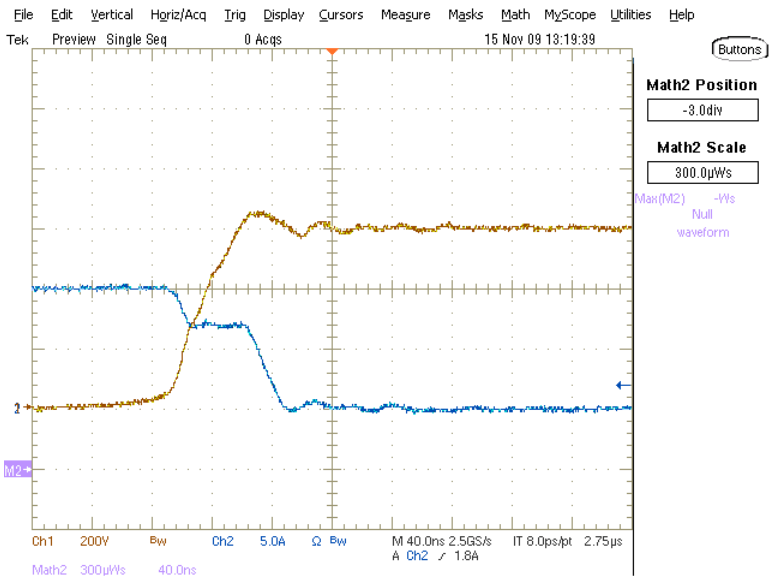

Figure 120: IPW90R120C3 Turn Off Behavior at 600V, 10A (blue = current, yellow = voltage)

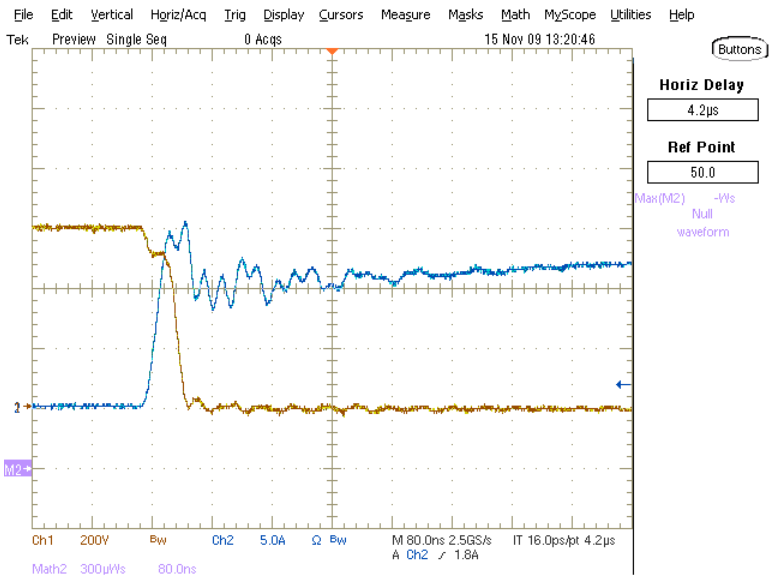

Figure 121: IPW90R120C3 Turn On Behavior at 600V, 10A
(blue = current, yellow = voltage)

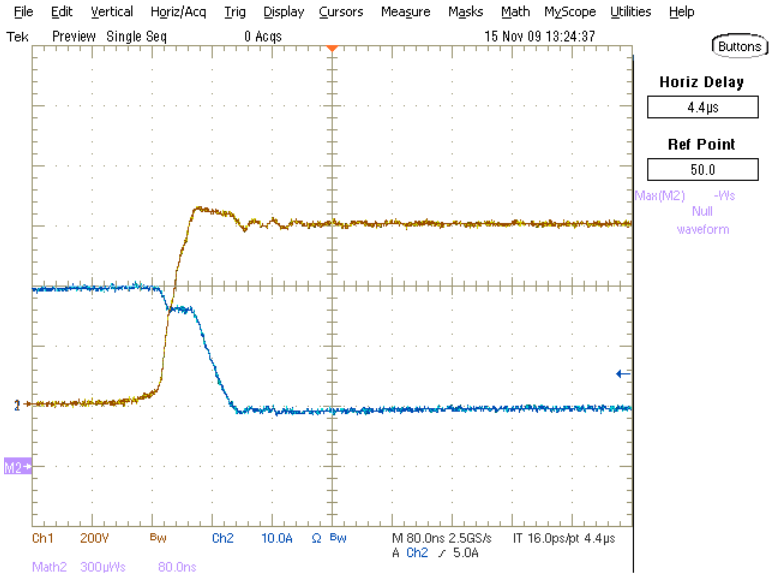

Figure 122: IPW90R120C3 Turn Off Behavior at 600V, 20A
(blue = current, yellow = voltage)

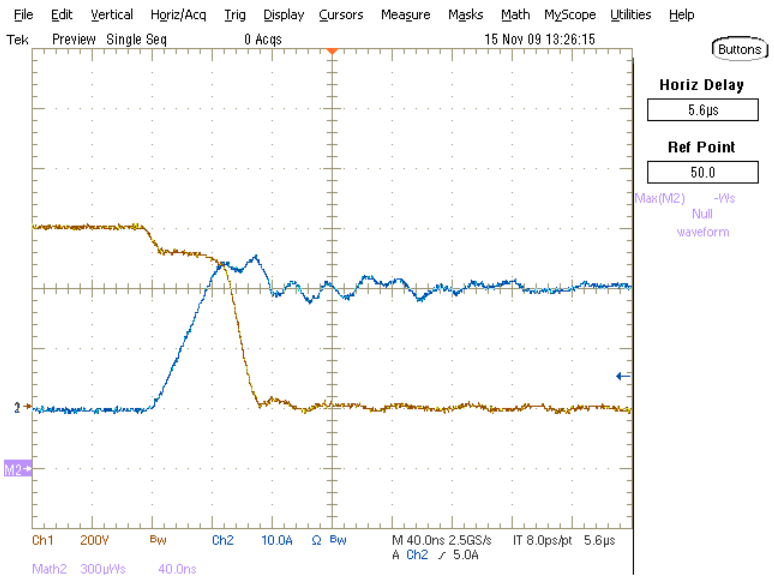

Figure 123: IPW90R120C3 Turn On Behavior at 600V, 20A
(blue = current, yellow = voltage)

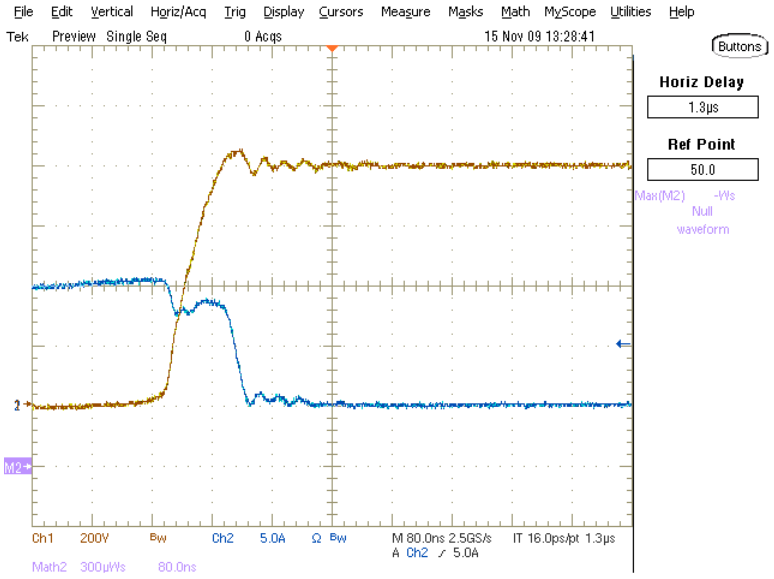

Figure 124: IPW90R120C3 Turn Off Behavior at 800V, 10A
(blue = current, yellow = voltage)

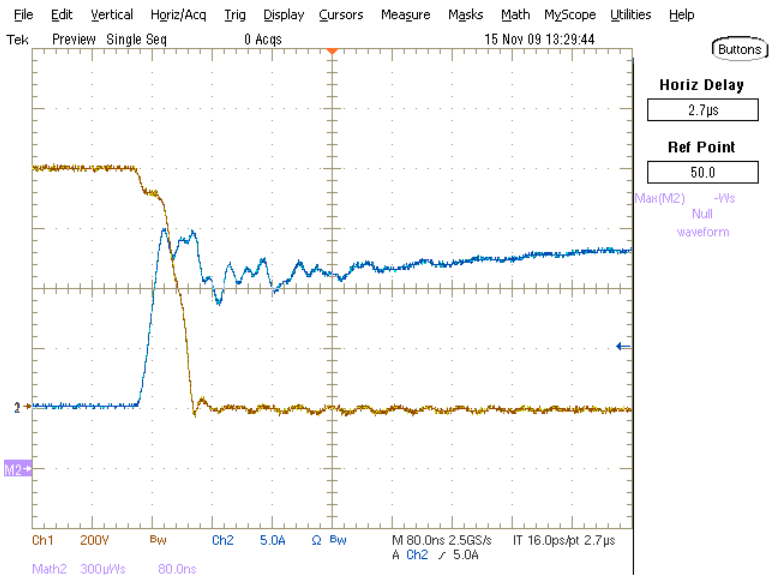

Figure 125: IPW90R120C3 Turn On Behavior at 800V, 10A
(blue = current, yellow = voltage)

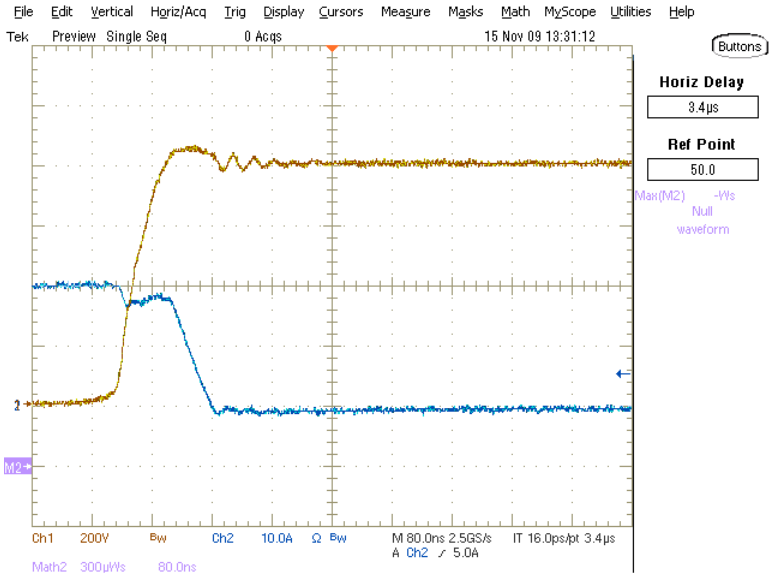

Figure 126: IPW90R120C3 Turn Off Behavior at 800V, 20A
(blue = current, yellow = voltage)

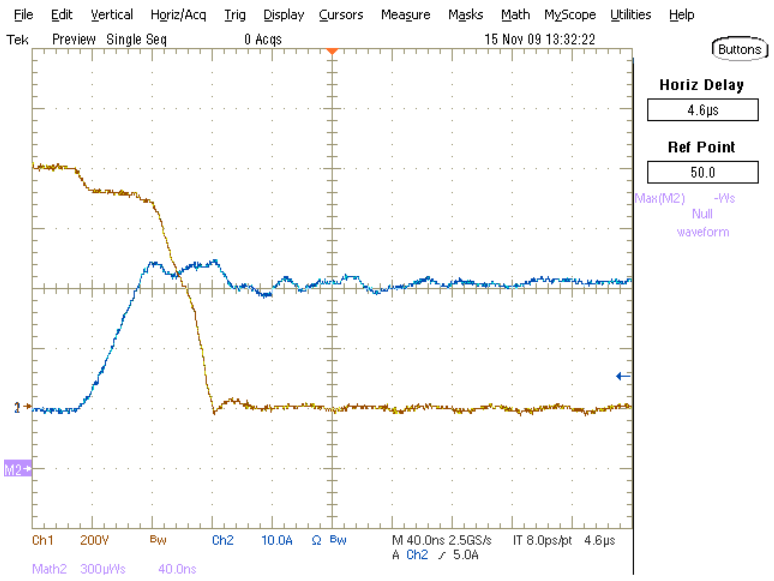

Figure 127: IPW90R120C3 Turn On Behavior at 800V, 20A (blue = current, yellow = voltage)

5.14 Cree CMF20120D SiC MOSFET with Cree C2D20120 SiC Diode

In this section the Cree CMF20120D SiC MOSFET was tested with a Cree C2D20120 SiC Diode. The device was tested using the same baseline gate driver as all other devices in this chapter. The device used +15V unipolar gate driver with a 10Ohm gate resistor. The device performance is shown in Figures 129-136. A summary of the performance statistics is given in Table 17 below.

Table 17: CMF20120D Dynamic Losses (Units are in uJ)

10Ohm	CMF20120D Mosfet & C2D20120D			
	600V 10A	600V 20A	800V 10A	800V 20A
Eoff	130	285	300	430
Eon	400	1005	605	1580
Etotal	**530**	**1290**	**905**	**2010**

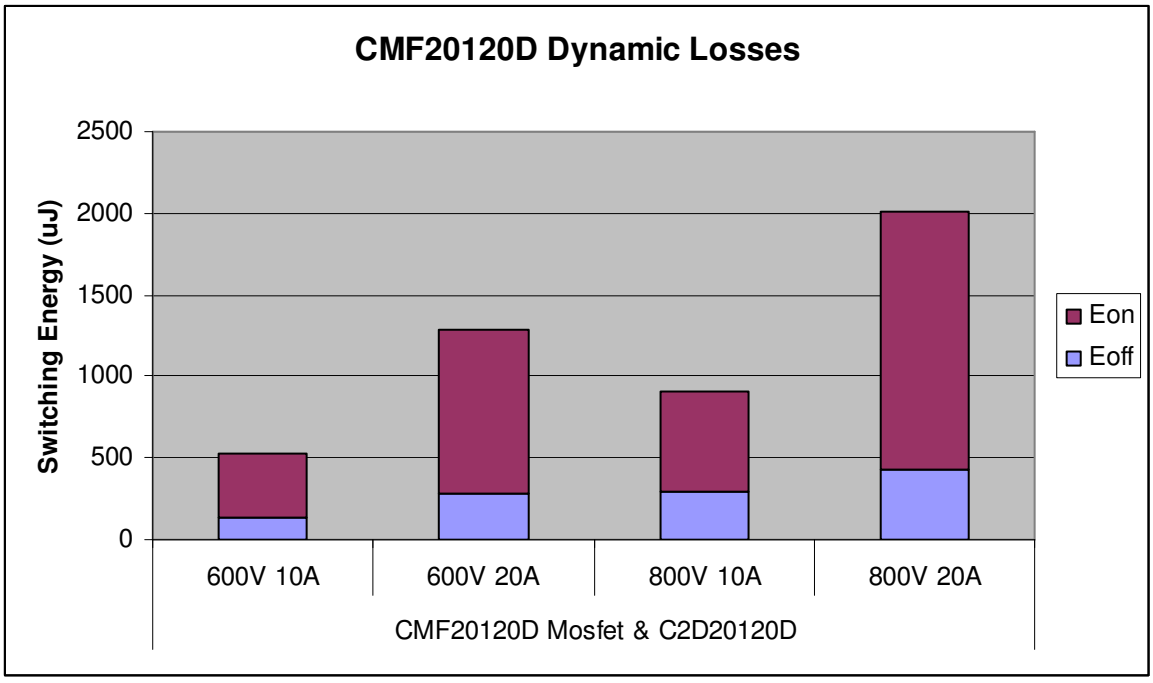

Figure 128: CMF20120D Dynamic Losses (Units are in uJ)

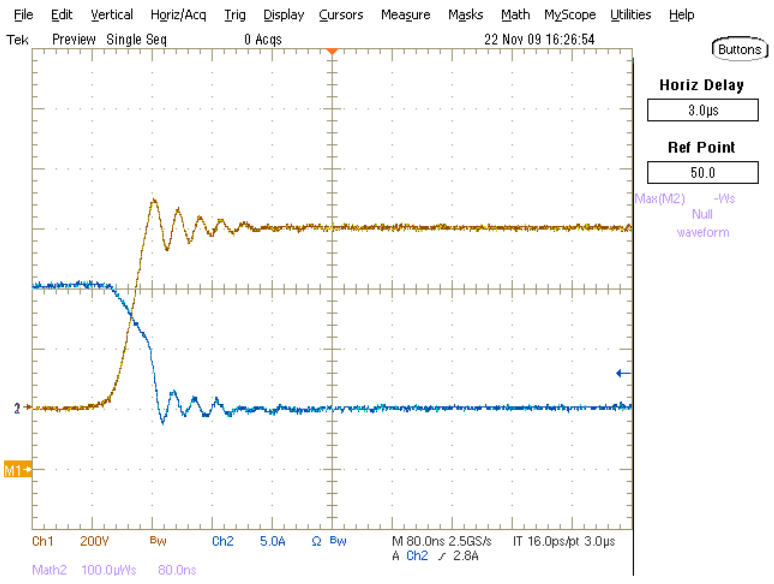

Figure 129: CMF20120D Turn Off Behavior at 600V, 10A
(blue = current, yellow = voltage)

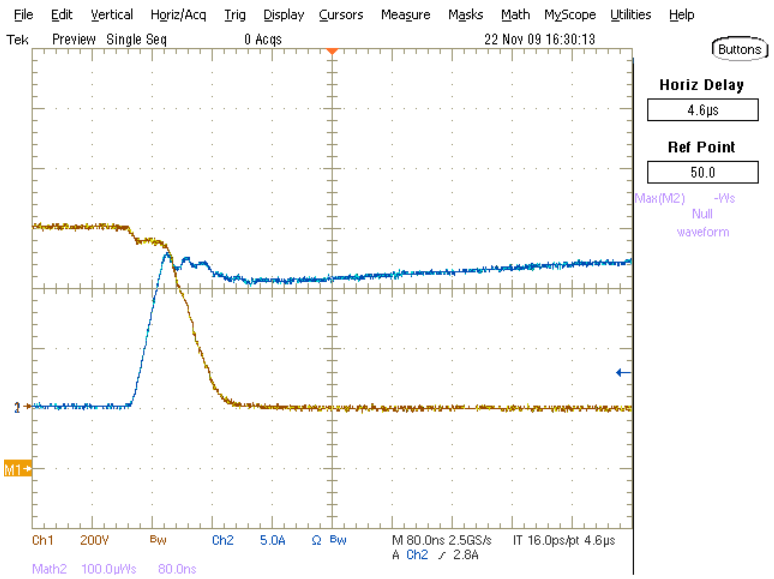

Figure 130: CMF20120D Turn On Behavior at 600V, 10A
(blue = current, yellow = voltage)

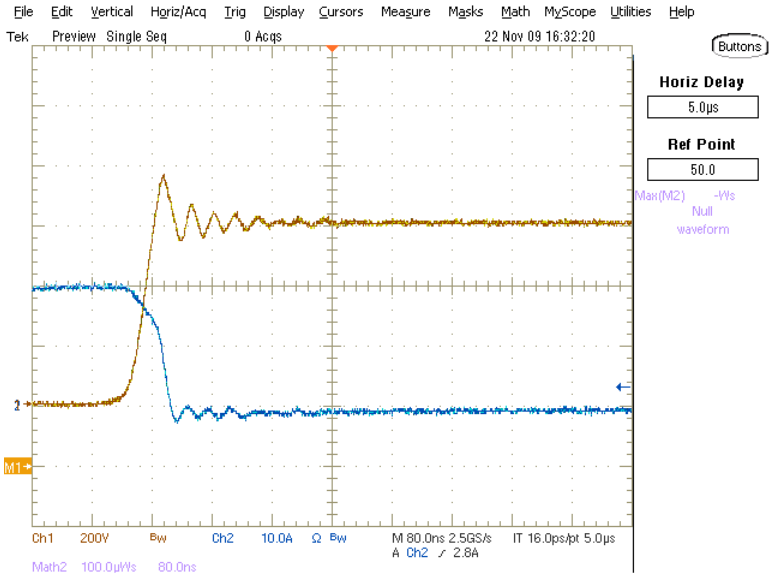

Figure 131: CMF20120D Turn Off Behavior at 600V, 20A
(blue = current, yellow = voltage)

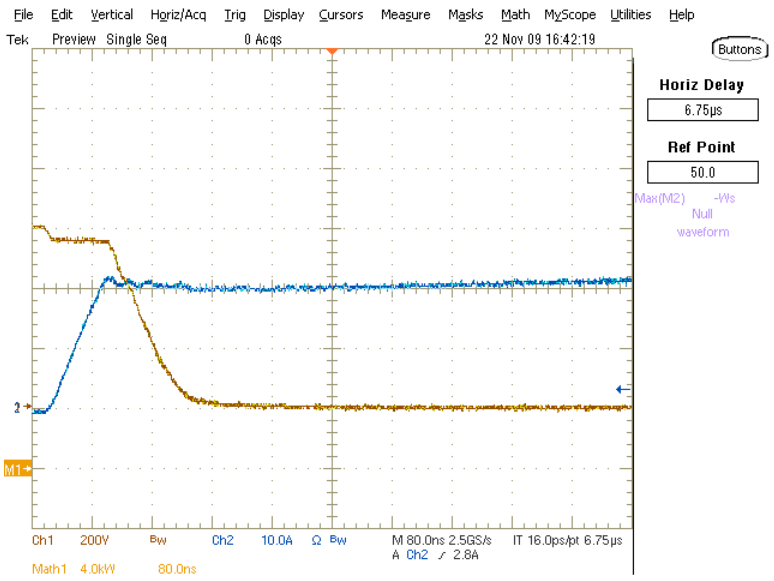

Figure 132: CMF20120D Turn On Behavior at 600V, 20A
(blue = current, yellow = voltage)

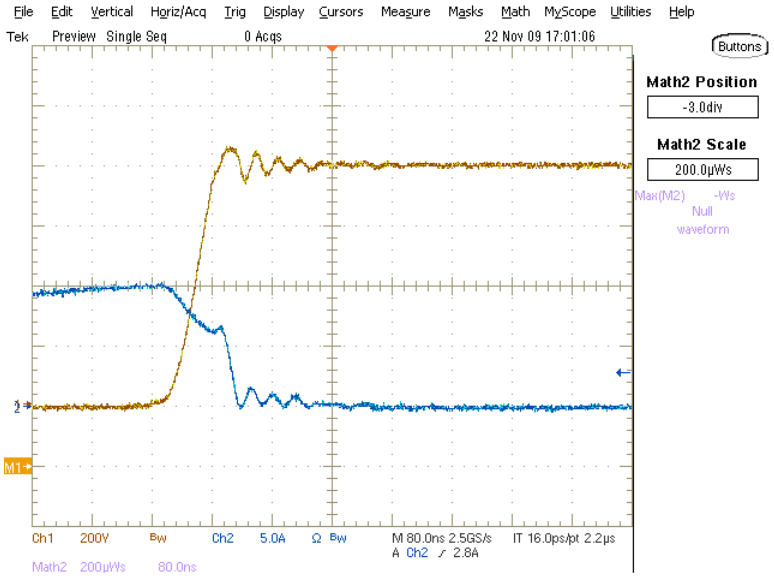

Figure 133: CMF20120D Turn Off Behavior at 800V, 10A
(blue = current, yellow = voltage)

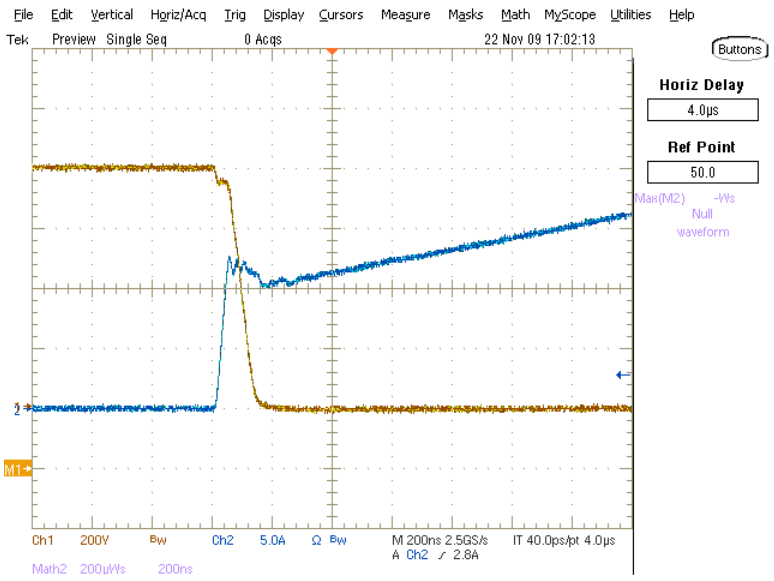

Figure 134: CMF20120D Turn On Behavior at 800V, 10A
(blue = current, yellow = voltage)

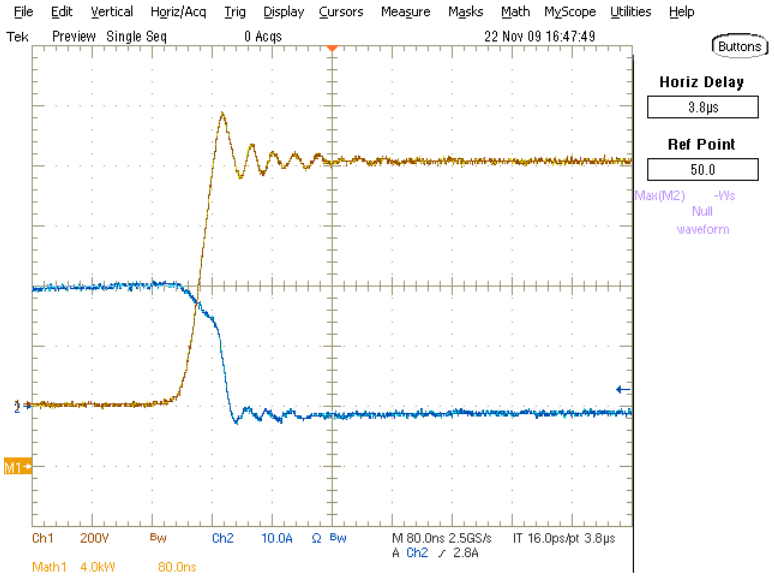

Figure 135: CMF20120D Turn Off Behavior at 800V, 20A
(blue = current, yellow = voltage)

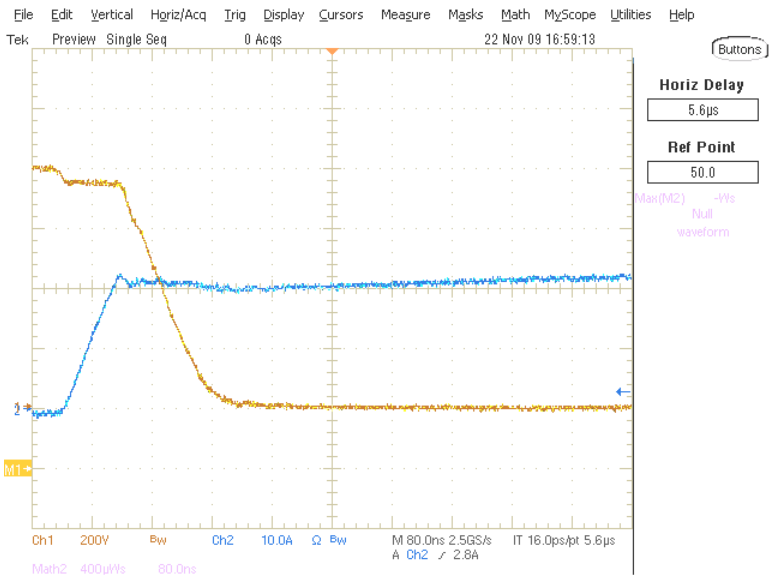

Figure 136: CMF20120D Turn On Behavior at 800V, 20A (blue = current, yellow = voltage)

5.15 Cree CMF20120D SiC MOSFET with Internal Body Diode

In this section the Cree CMF20120D SiC MOSFET was tested using only its internal body diode. This configuration is important to test because in any half bridge application such as motor drive inverters or UPS inverters will utilize the body diode of the device. As will be discussed in later sections, the SiC MOSFET has a benefit when compared to the CoolMOS MOSFET in that one can use a separate diode in parallel with the device due to the very high conduction characteristics of the body diode. The device was tested using the same baseline gate driver as all other devices in this chapter. The device used +15V unipolar gate driver with a 10Ohm gate resistor. The device performance is shown in Figures 138-145. A summary of the performance statistics is given in Table 18 below.

Table 18: CMF20120D with Body Diode Dynamic Losses (Units are in uJ)

10Ohm	CMF20120D Mosfet & Body Diode			
	600V 10A	600V 20A	800V 10A	800V 20A
Eoff	120	300	263	427
Eon	428	1220	706	1810
Etotal	**548**	**1520**	**969**	**2237**

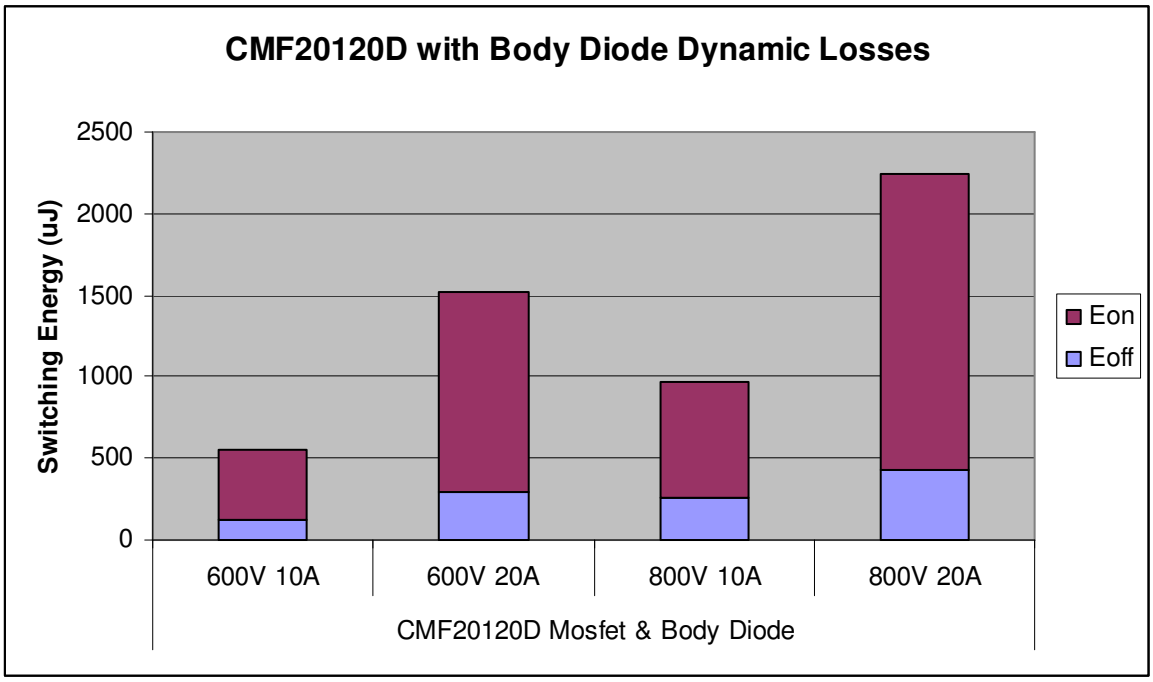

Figure 137: CMF20120D with Body Diode Dynamic Losses (Units are in uJ)

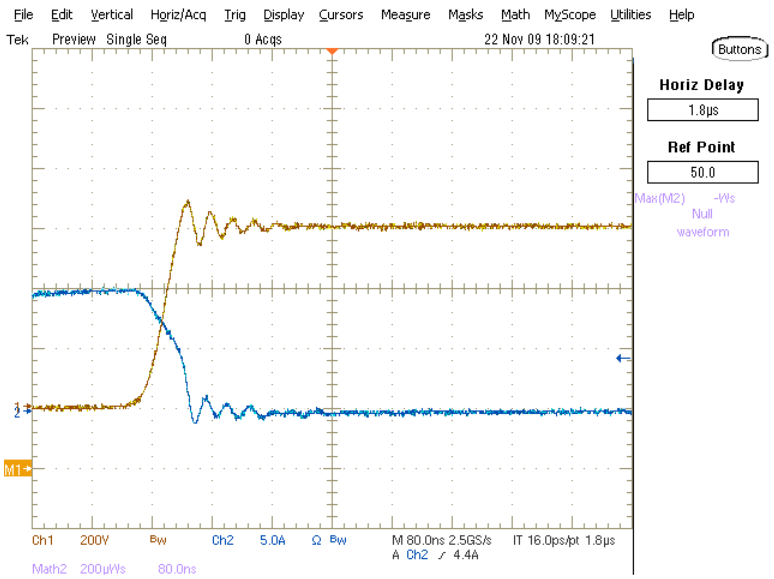

Figure 138: CMF20120D with Body Diode Turn Off Behavior at 600V, 10A (blue = current, yellow = voltage)

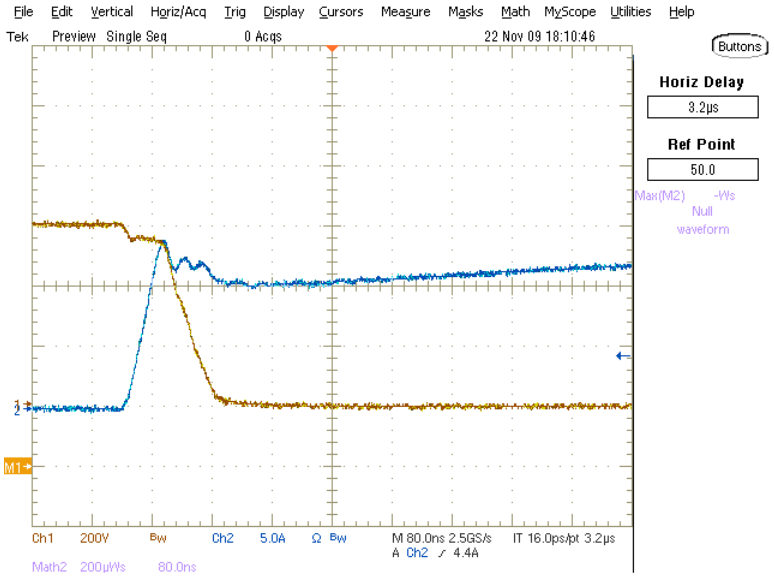

Figure 139: CMF20120D with Body Diode Turn On Behavior at 600V, 10A (blue = current, yellow = voltage)

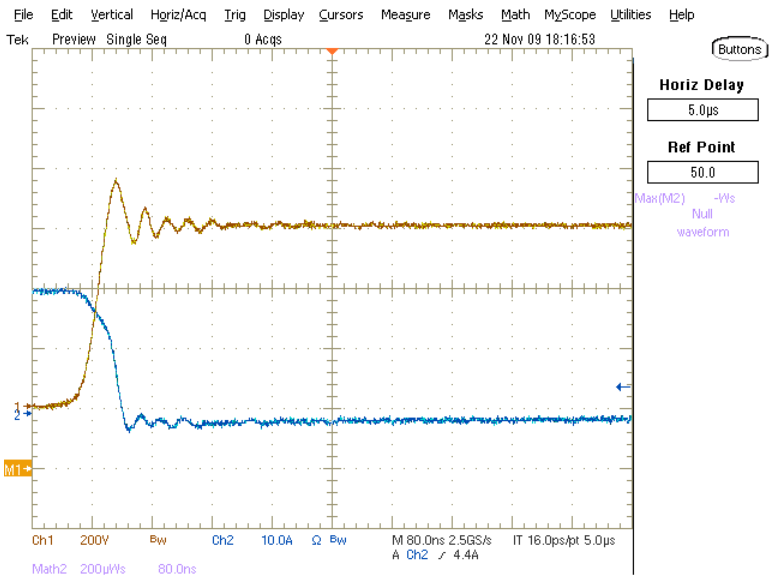

Figure 140: CMF20120D with Body Diode Turn Off Behavior at 600V, 20A (blue = current, yellow = voltage)

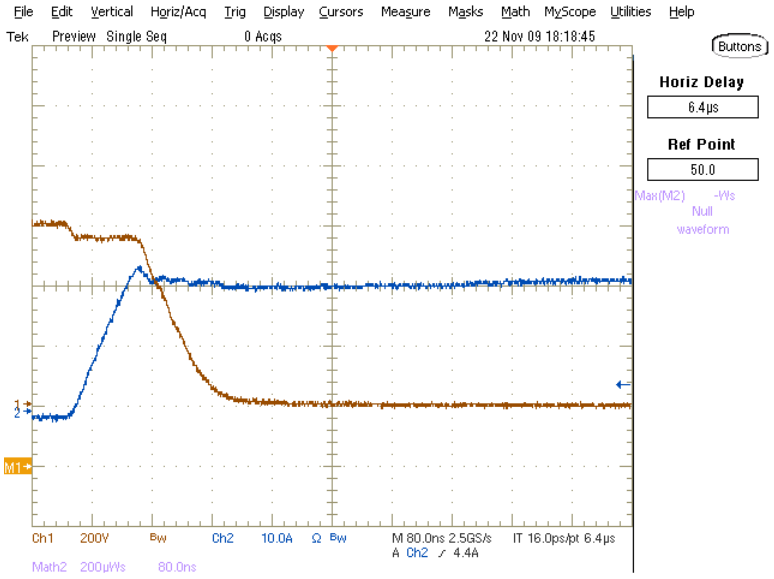

Figure 141: CMF20120D with Body Diode Turn On Behavior at 600V, 20A (blue = current, yellow = voltage)

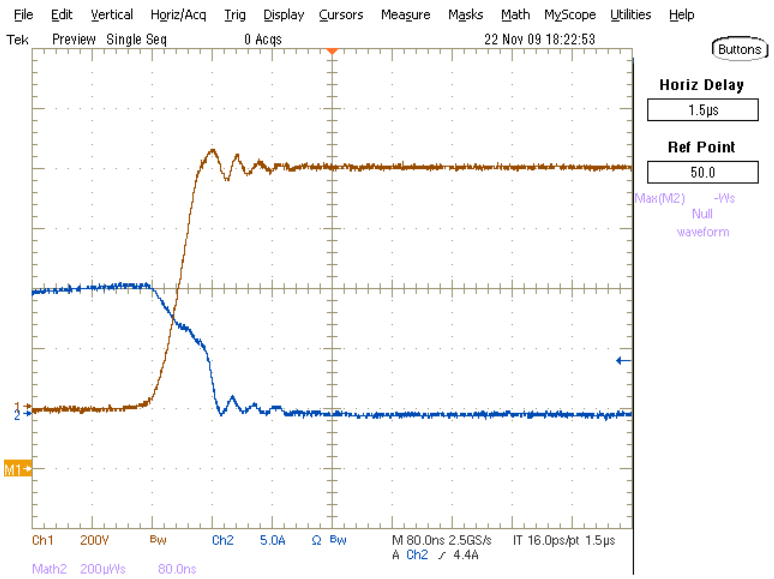

Figure 142: CMF20120D with Body Diode Turn Off Behavior at 800V, 10A (blue = current, yellow = voltage)

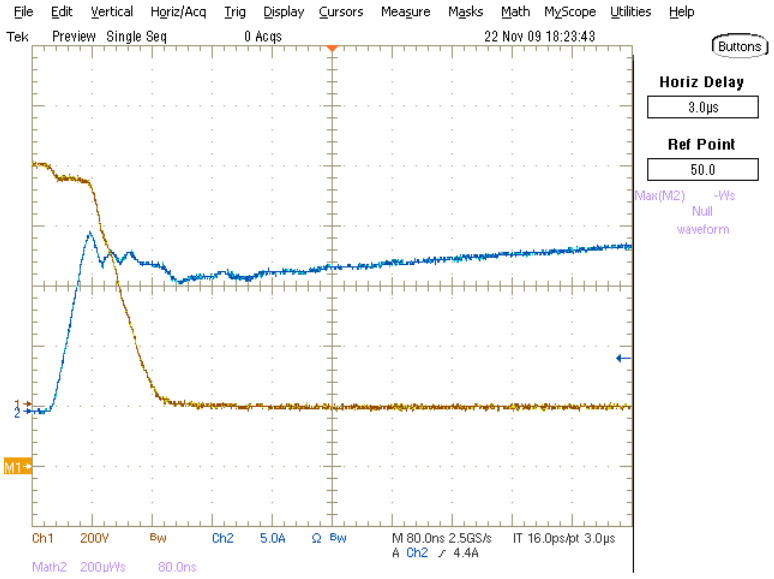

Figure 143: CMF20120D with Body Diode Turn On Behavior at 800V, 10A (blue = current, yellow = voltage)

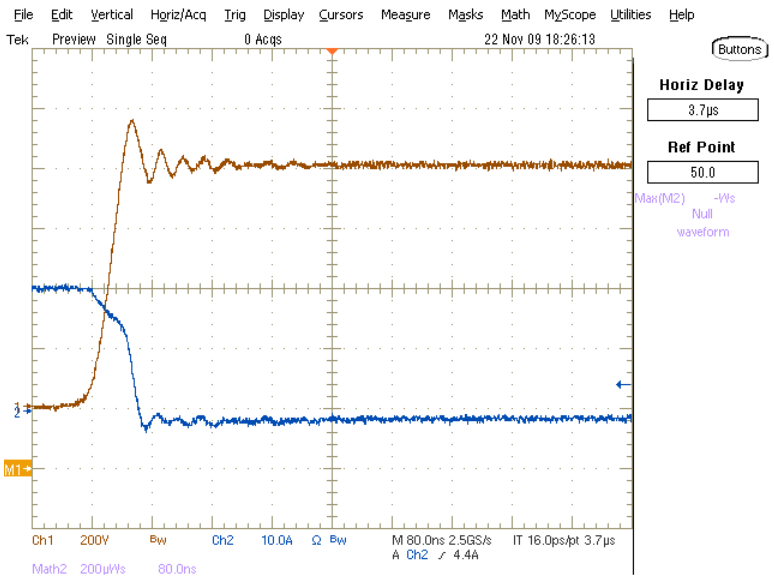

Figure 144: CMF20120D with Body Diode Turn Off Behavior at 800V, 20A (blue = current, yellow = voltage)

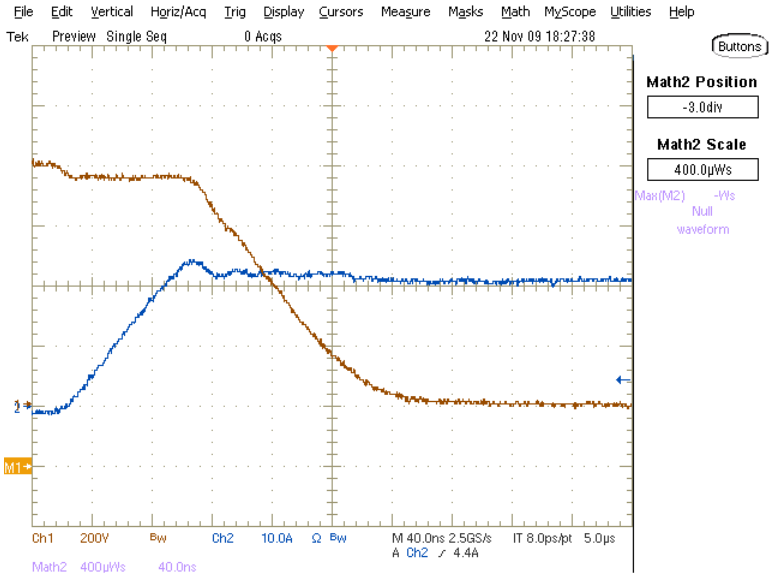

Figure 145: CMF20120D with Body Diode Turn On Behavior at 800V, 20A (blue = current, yellow = voltage)

CHAPTER 6

6 OPTIMIZATION OF GATE DRIVER FOR SIC DEVICES

The SiC JFETs developed by SemiSouth are unique devices and as such they have very particular gate drive requirements. The devices are voltage controlled devices like a MOSFET, however they do not have an insulating gate oxide like a MOSFET. The devices have a significant gate charge requirement that must be dealt with while turning the devices on and off. The tradeoff with these devices is that since they do not have an insulating gate oxide they will sync significant current into their gate. If a low impedance path is used to drive the gate capacitance of the device, the gate drive will drive current through the parasitic gate-source diode in the device during the conduction stage of the switching cycle. This wastes power and decreases the efficiency of the device.

The SiC MOSFET has also been optimized here in an attempt to match the test setup used for the results in the datasheet. For the SiC MOSFET, Cree used a +20V gate driver in order to drive the device. The +20V vs +15V gate driver allows the device to turn on much quicker because the driver can charge the gate capacitance 33% faster. The gate driver used by Cree when testing the SiC MOSFET also had a much lower gate resistance than the IR2213 device. Because of this, the gate resistance was also reduced in the test setup.

6.1 SiC JFET Gate Drive Optimization Method

Because of the above described drawback of using a JFET structure as a power switching device, SemiSouth recommends using a gate driver that can deliver a very large current until the gate capacitance is charged. After the gate capacitance is charged, the driver should lower the current it drives into the gate since current in excess of what it takes to keep the gate at a few volts will be wasting power and could decrease efficiency significantly. The easiest way to do this is by using an AC coupled driver that uses a large gate resistance in series with the driver output. A bypass capacitor is used to wrap around the resistor and allow a very low impedance path during the gate capacitance charge/discharge. The other benefit of this method is that it creates a negative gate voltage bias during turn off since the ac capacitor must discharge. This gives the gate drive the benefits of a bipolar driver while only using a single supply. A schematic of the original gate driver and the modified gate driver is shown in Figures 146 and 147 below.

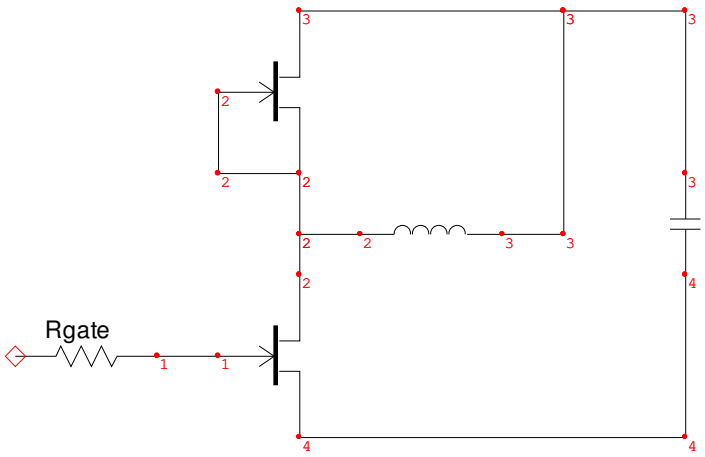

Figure 146: Original Gate Driver Schematic for Silicon IGBT Devices

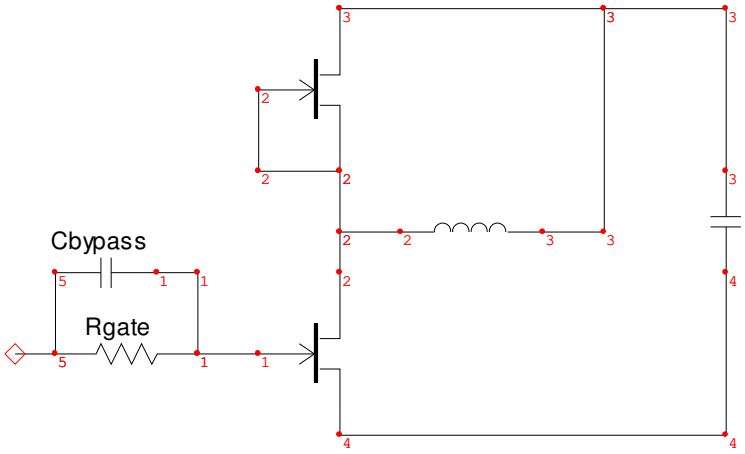

Figure 147: Modified Gate Driver Schematic for SiC JFET Devices

6.2 SJEP120R125 SiC JFET Gate Drive Optimization

For the 125mOhm SiC JFET, the resistor in series with the gate driver was chosen such that at 25C, 125mA of gate current was driven through the device during the conduction stage. This kept the Rds,on below the specified datasheet parameter value of 125mOhms at all times. In order for 125mA to be driven into the gate of the JFET, it must have a gate-source voltage of 3V based on the datasheet graphs. Given this information, the R used was 100Ohms based on the below Ohm's Law formula in (6.2.1-6.2.3).

$$R = (Vdd - Vgs)/I \tag{6.2.1}$$

$$R = (15V - 3V)/125mA \tag{6.2.2}$$

$$R = 100Ohms \tag{6.2.3}$$

The bypass capacitor was chosen so that it would store greater than the total gate charge of 30nC. This makes sure that the driver has low enough series impedance to fully charge the gate capacitance of the device before the bypass capacitor impedance can slow down the turn on process. The bypass capacitor was chosen using the following formulas in (6.2.4-6.2.6).

$$C > Qg/(Vdd - Vgs) \tag{6.2.1}$$

$$C > 30nC/(15V - 3V) \tag{6.2.2}$$

$$C > 2.5nF \tag{6.2.3}$$

The optimization of the bypass capacitor was done by taking the initial value of 2.5nF and increasing it in 0.5nF increments while measuring the total switching energy. This was done at 600V buss voltage and 10A drain current. This was repeated until the point where increasing the capacitor did not decrease total switching energy by more than 1%. At this point, increasing the capacitor any more would not give a significant increase in efficiency and the added gate capacitance would waste energy from the gate driver charging and discharging it every switching cycle. For the 125mOhm device, the optimization showed that a bypass capacitor of 6nF was the optimal value for efficiency with this device.

Once the gate drive optimization was complete for the 125mOhm SiC JFET device, the same test that was run in Section 5.10 was re-run in order to compare device with the other Chapter 5 devices. The device performance is shown in Figures 149-156. A summary

of the performance statistics is given in Table 19 below. It is easy to see while comparing Table 19 and table 13 that the switching energy when using the optimized gate driver is drastically lower. The total switching energy was reduced by a factor of 4-5. Most notably, the turn off energy was reduced by a factor of 8-10. This is the case because of the negative 15V bias that the charged capacitor applies to the gate of the device when the turn off event occurs. The turn on energy is not reduced by much, but the energy there is really controlled by the diode characteristics and not as much the device turn on speed. This is extremely high incentive to use the optimized gate driver, especially since it is essentially a single part addition to a bill of materials.

Table 19: Optimized SJEP120R125 Dynamic Losses (Units are in uJ)

100Ohm	SJEP120R125 & C2D20120D			
6nF	600V 10A	600V 20A	800V 10A	800V 20A
Eoff	74	210	241	371
Eon	137	279	235	492
Etotal	**211**	**489**	**476**	**863**

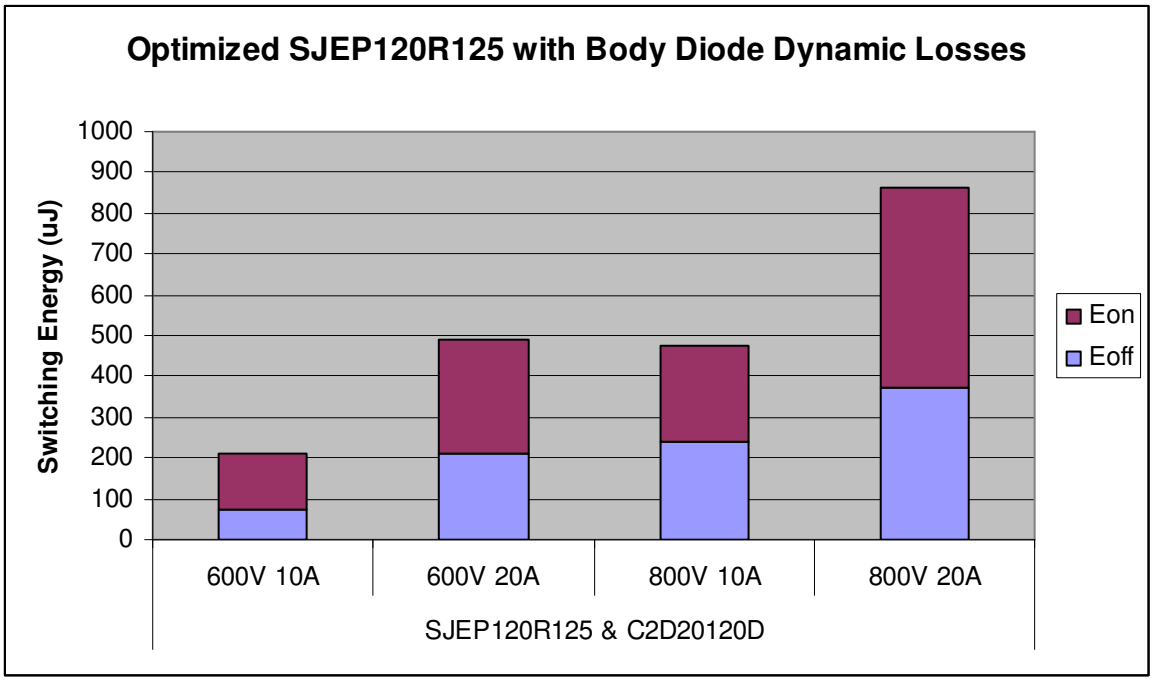

Figure 148: Optimized SJEP120R125 Dynamic Losses (Units are in uJ)

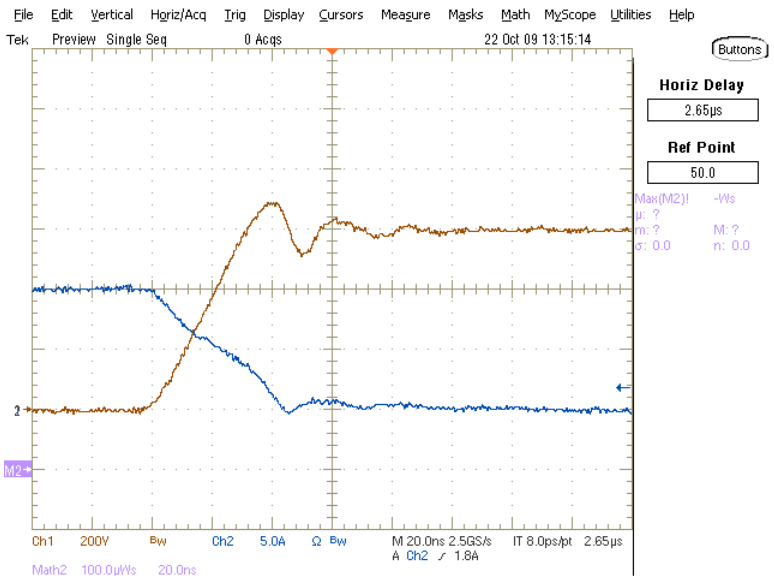

Figure 149: Optimized SJEP120R125 Turn Off Behavior at 600V, 10A (blue = current, yellow = voltage)

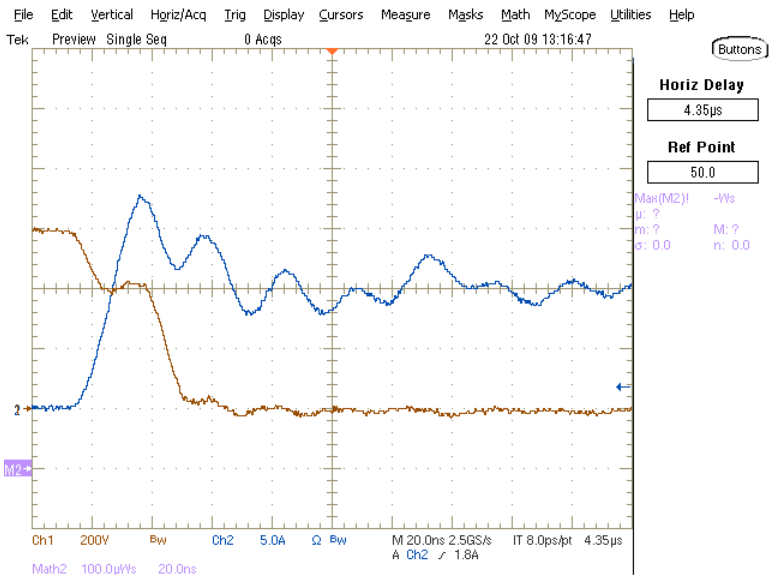

Figure 150: Optimized SJEP120R125 Turn On Behavior at 600V, 10A (blue = current, yellow = voltage)

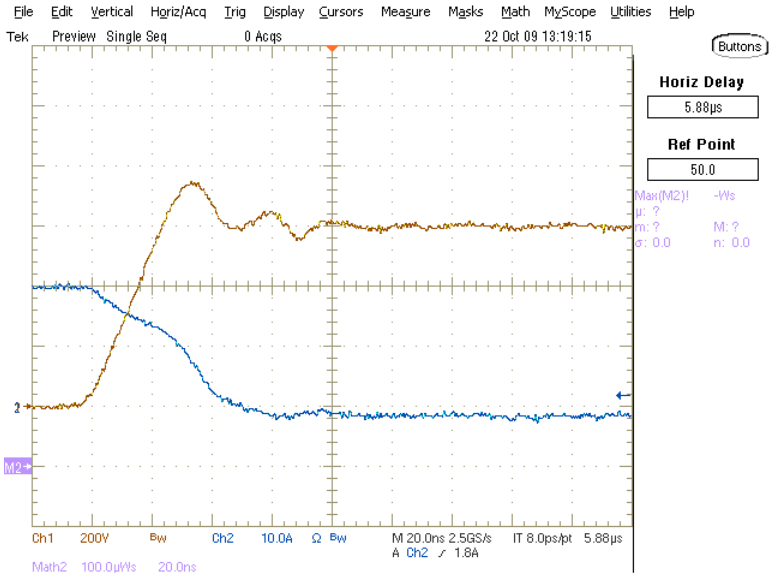

Figure 151: Optimized SJEP120R125 Turn Off Behavior at 600V, 20A (blue = current, yellow = voltage)

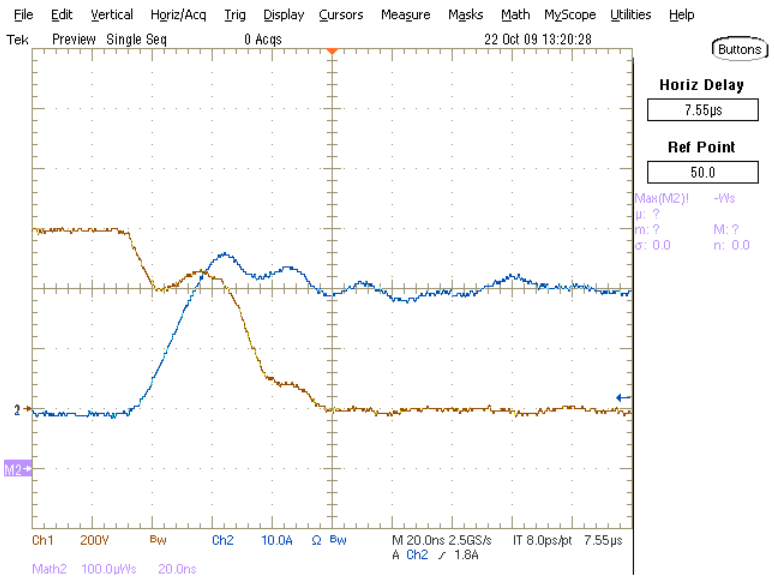

Figure 152: Optimized SJEP120R125 Turn On Behavior at 600V, 20A (blue = current, yellow = voltage)

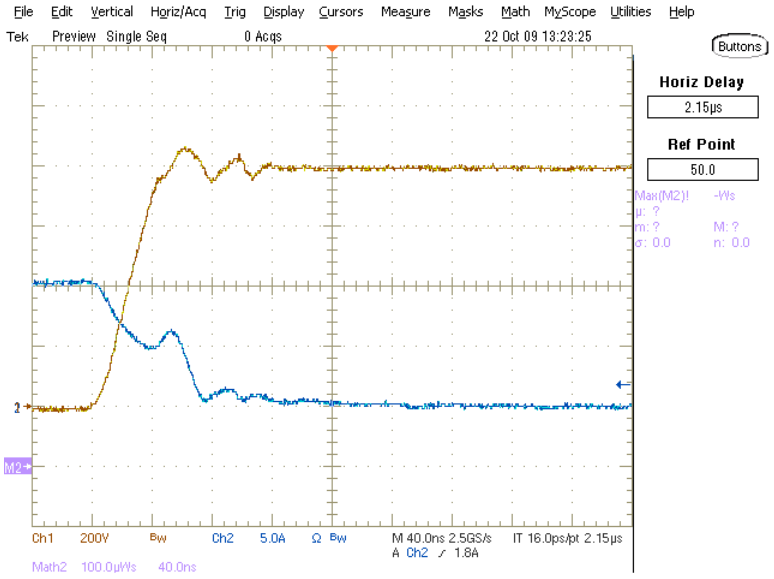

Figure 153: Optimized SJEP120R125 Turn Off Behavior at 800V, 10A (blue = current, yellow = voltage)

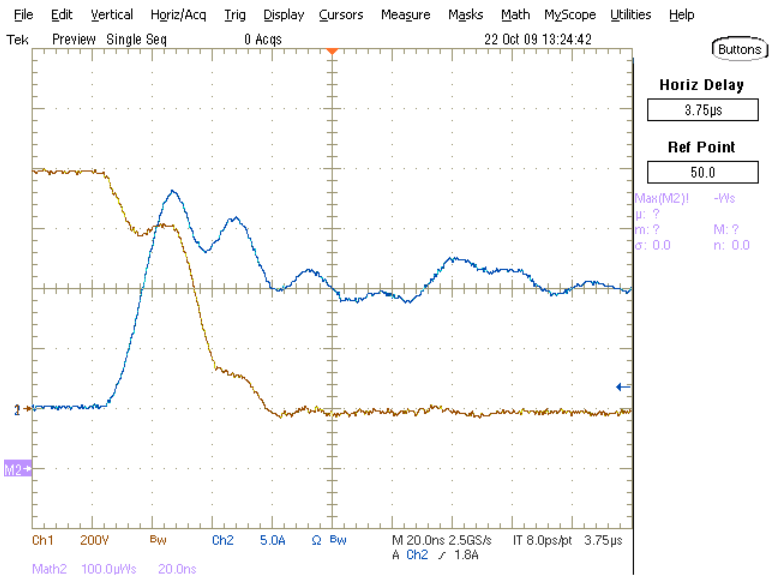

Figure 154: Optimized SJEP120R125 Turn On Behavior at 800V, 10A (blue = current, yellow = voltage)

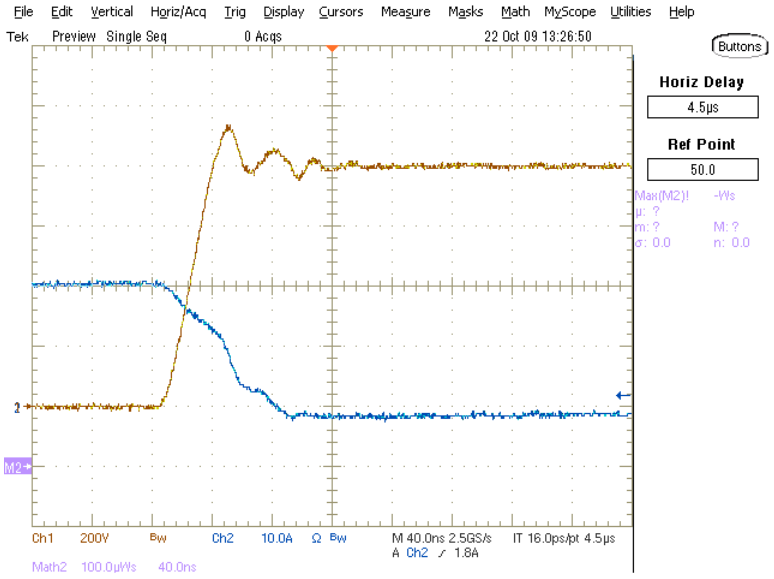

Figure 155: Optimized SJEP120R125 Turn Off Behavior at 800V, 20A (blue = current, yellow = voltage)

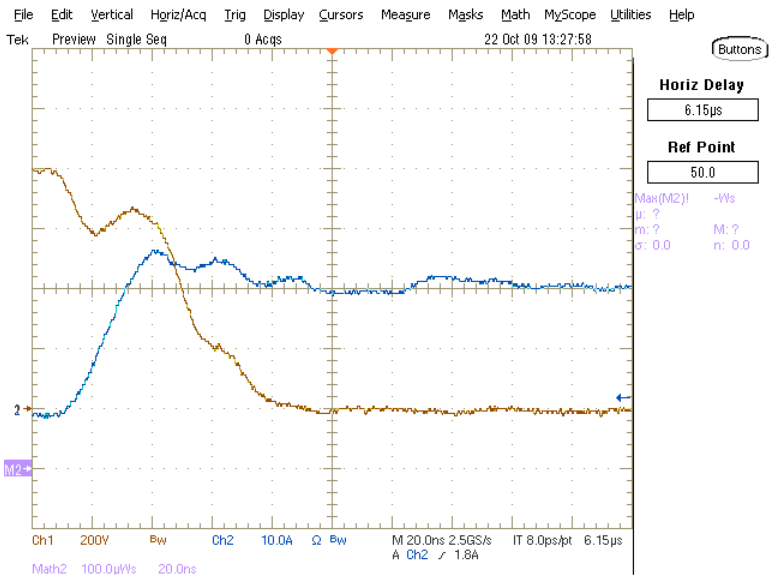

Figure 156: Optimized SJEP120R125 Turn On Behavior at 800V, 20A (blue = current, yellow = voltage)

6.3 SJEP120R063 SiC JFET Gate Drive Optimization

For the 63mOhm SiC JFET, the resistor in series with the gate driver was chosen such that at 25C, 125mA of gate current was driven through the device during the conduction stage. This kept the Rds,on below the specified datasheet parameter value of 63mOhms at all times. In order for 125mA to be driven into the gate of the JFET, it must have a gate-source voltage of 3V based on the datasheet graphs. Given this information, the R used was 100Ohms based on the below Ohm's Law formula in (6.3.1-6.3.3).

$$R = (Vdd - Vgs)/I \tag{6.3.1}$$

$$R = (15V - 3V)/125mA \tag{6.3.2}$$

$$R = 100Ohms \tag{6.3.3}$$

The bypass capacitor was chosen so that it would store greater than the total gate charge of 60nC. This makes sure that the driver has low enough series impedance to fully charge the gate capacitance of the device before the bypass capacitor impedance can slow down the turn on process. The bypass capacitor was chosen using the following formula in (6.3.4-6.3.6).

$$C > Qg/(Vdd - Vgs) \tag{6.3.4}$$

$$C > 60nC/(15V - 3V) \tag{6.3.5}$$

$$C > 5nF \tag{6.3.6}$$

The optimization of the bypass capacitor was done by taking the initial value of 5nF and increasing it in 0.5nF increments while measuring the total switching energy. This was done at 600V buss voltage and 10A drain current. This was repeated until the point where increasing the capacitor did not decrease total switching energy by more than 1%. At this point, increasing the capacitor any more would not give a significant increase in efficiency and the added gate capacitance would waste energy from the gate driver charging and discharging it every switching cycle. For the 63mOhm device, the optimization showed that a bypass capacitor of 12nF was the optimal value for efficiency with this device.

Once the gate drive optimization was complete for the 63mOhm SiC JFET device, the same test that was run in Section 5.11 was re-run in order to compare device with the other Chapter 5 devices. The device performance is shown in Figures 158-165. A summary of the

performance statistics is given in Table 20 below. It is easy to see while comparing Table 20 and table 14 that the switching energy when using the optimized gate driver is drastically lower. The total switching energy was reduced by a factor of 4-5. Most notably, the turn off energy was reduced by a factor of 8-10. This is the case because of the negative 15V bias that the charged capacitor applies to the gate of the device when the turn off event occurs. The turn on energy is not reduced by much, but the energy there is really controlled by the diode characteristics and not as much the device turn on speed. This is extremely high incentive to use the optimized gate driver, especially since it is essentially a single part addition to a bill of materials.

Table 20: Optimized SJEP120R063 Dynamic Losses (Units are in uJ)

100Ohm	SJEP120R063 & C2D20120D			
12nF	600V 10A	600V 20A	800V 10A	800V 20A
Eoff	107	278	277	458
Eon	167	316	269	518
Etotal	**274**	**594**	**546**	**976**

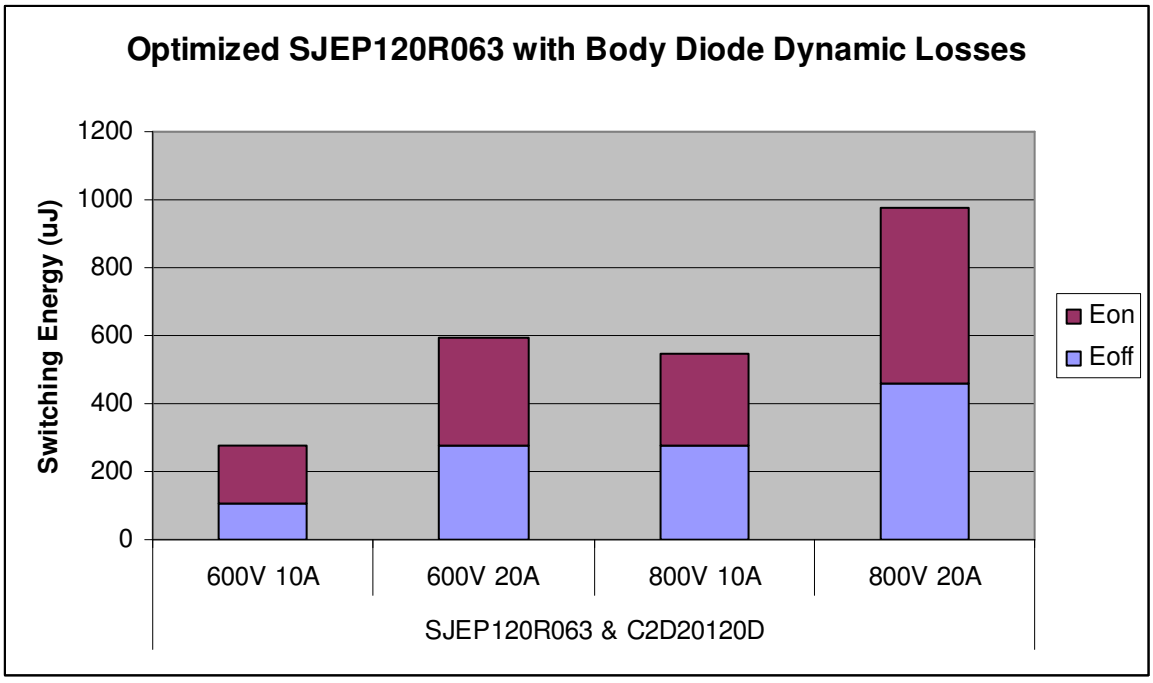

Figure 157: Optimized SJEP120R063 Dynamic Losses (Units are in uJ)

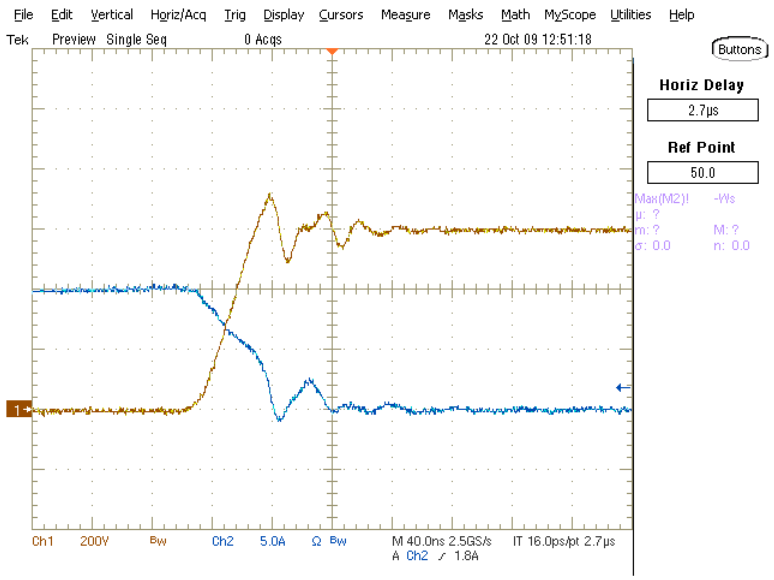

Figure 158: Optimized SJEP120R063 Turn Off Behavior at 600V, 10A (blue = current, yellow = voltage)

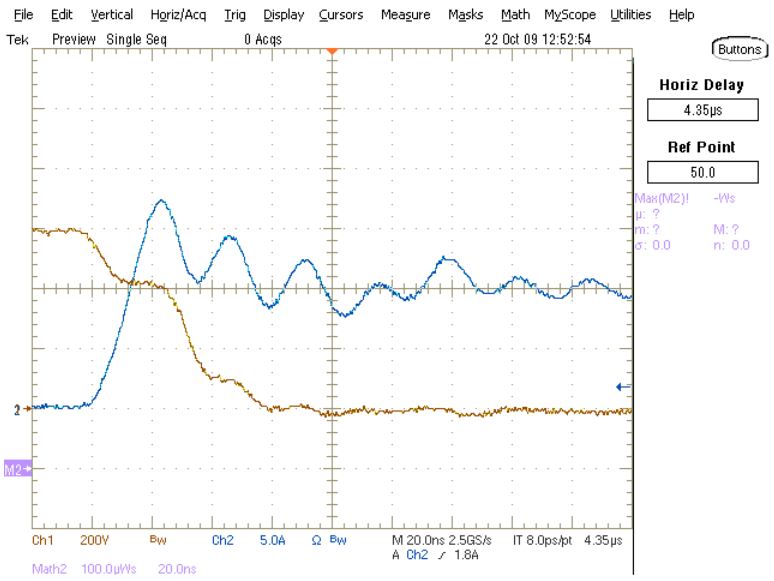

Figure 159: Optimized SJEP120R063 Turn On Behavior at 600V, 10A (blue = current, yellow = voltage)

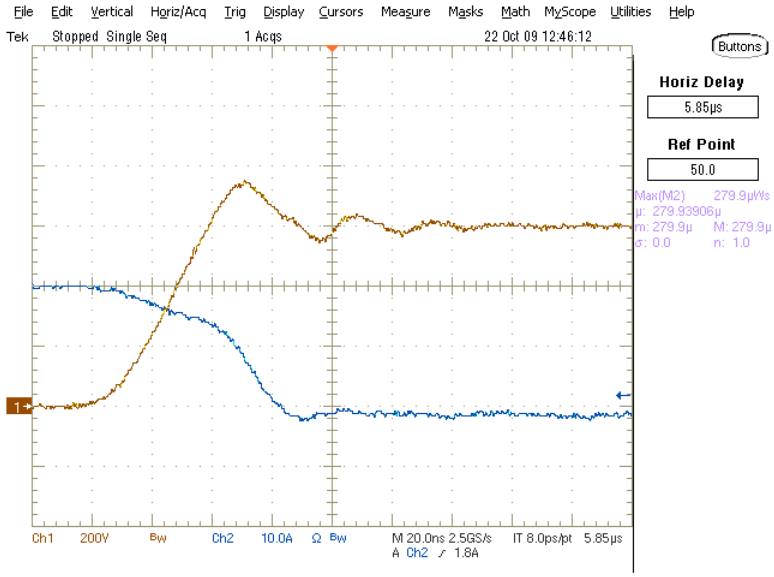

Figure 160: Optimized SJEP120R063 Turn Off Behavior at 600V, 20A (blue = current, yellow = voltage)

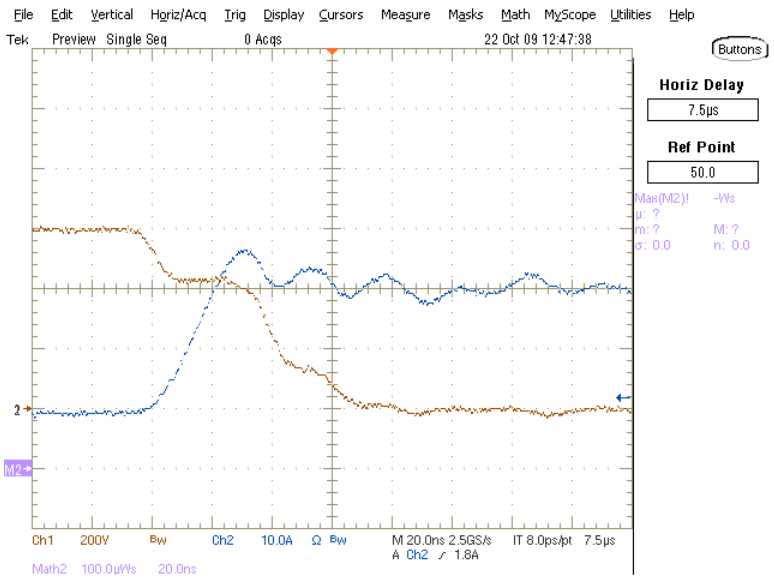

Figure 161: Optimized SJEP120R063 Turn On Behavior at 600V, 20A (blue = current, yellow = voltage)

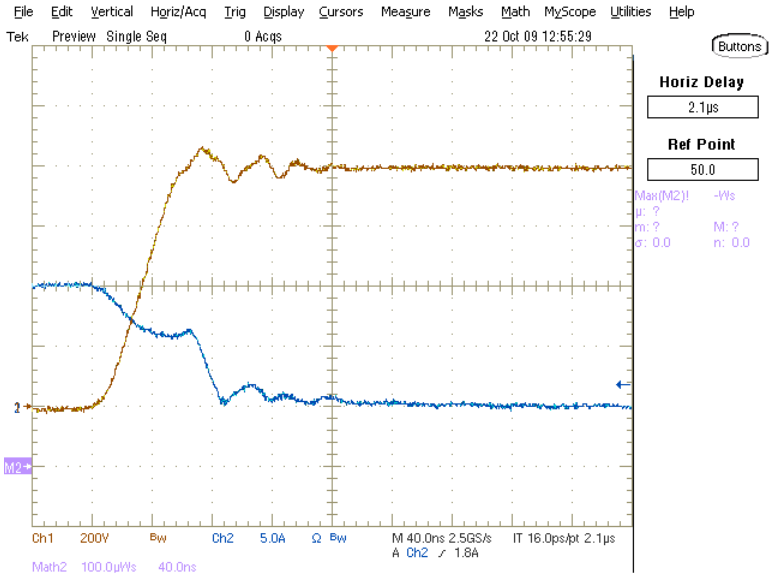

Figure 162: Optimized SJEP120R063 Turn Off Behavior at 800V, 10A (blue = current, yellow = voltage)

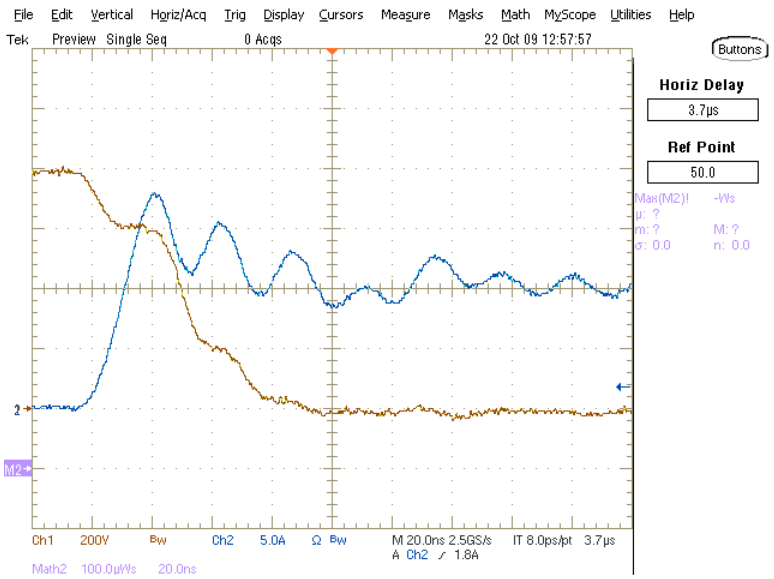

Figure 163: Optimized SJEP120R063 Turn On Behavior at 800V, 10A (blue = current, yellow = voltage)

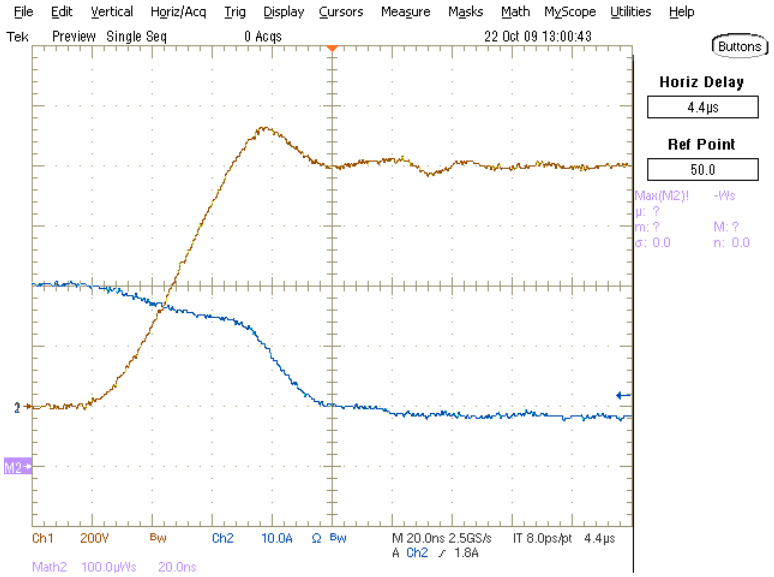

Figure 164: Optimized SJEP120R063 Turn Off Behavior at 800V, 20A (blue = current, yellow = voltage)

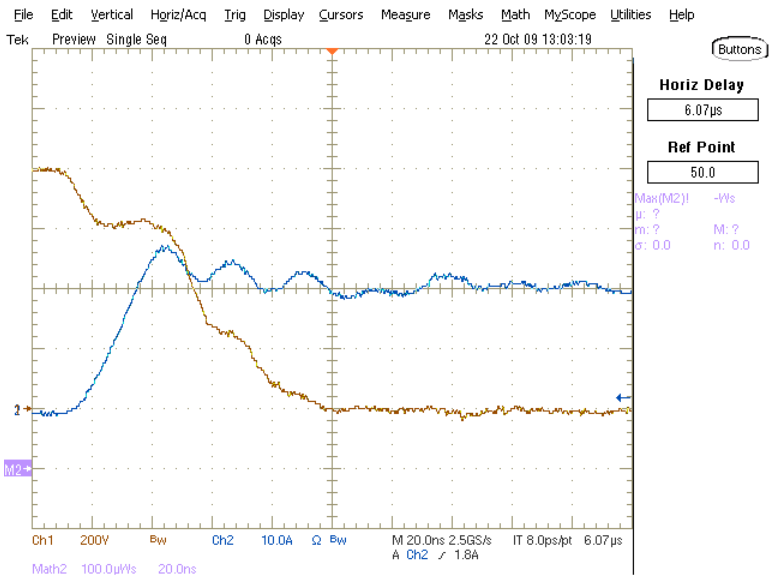

Figure 165: Optimized SJEP120R063 Turn On Behavior at 800V, 20A (blue = current, yellow = voltage)

6.4 CMF20120D SiC MOSFET Gate Drive Optimization

The IR2213 gate driver IC has an output impedance of roughly 18V/2A = 9Ohms. This was measured by looking at the output current driven by the device with the output shorted. All the International Rectifier and Fairchild devices used either the IR2213 gate driver or a similar output impedance driver for their datasheet benchmark testing. Cree, however, used a high current gate driver with insignificant output impedance. Because of this, in order to achieve the datasheet rated switching energies, a 1Ohm gate resistor had to be used. The total 10Ohm gate resistance in addition to the 20V gate drive voltage helped the SiC MOSFET switch with less than 30% the losses. The device performance is shown in Figures 167-174. A summary of the performance statistics is given in Table 21 below.

Table 21: Optimized CMF20120D Dynamic Losses (Units are in uJ)

1Ohm	CMF20120D Mosfet & C2D20120D			
20V	600V 10A	600V 20A	800V 10A	800V 20A
Eoff	127	205	261	294
Eon	132	330	254	475
Etotal	**259**	**535**	**515**	**769**

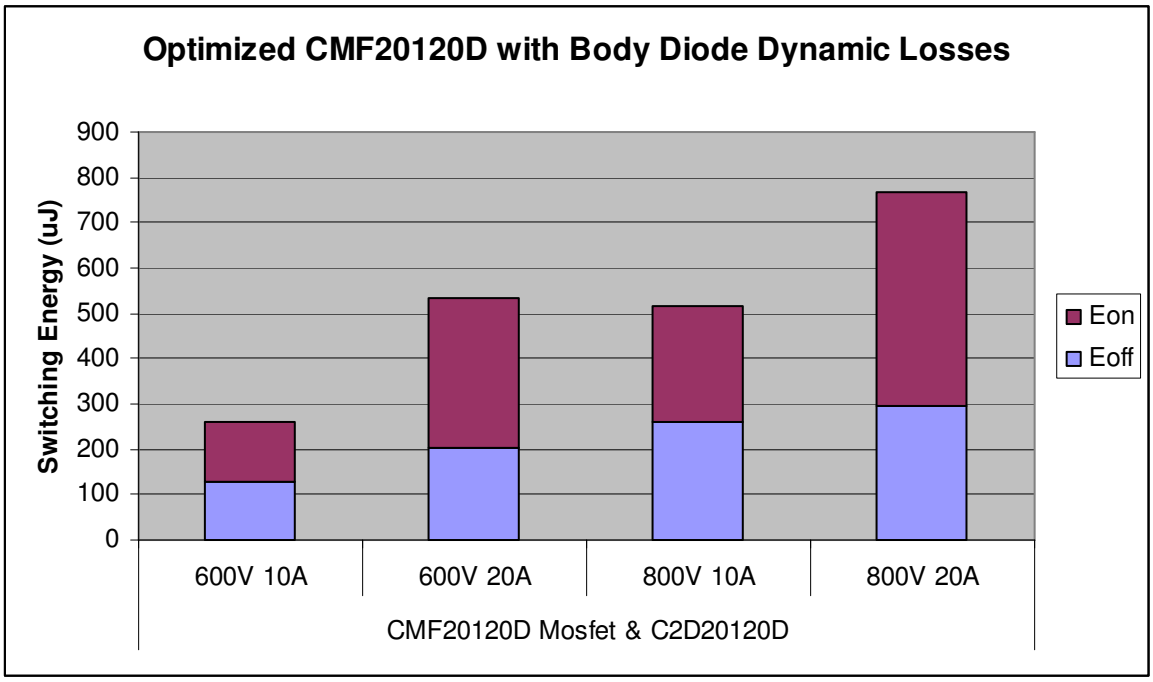

Figure 166: Optimized CMF20120D Dynamic Losses (Units are in uJ)

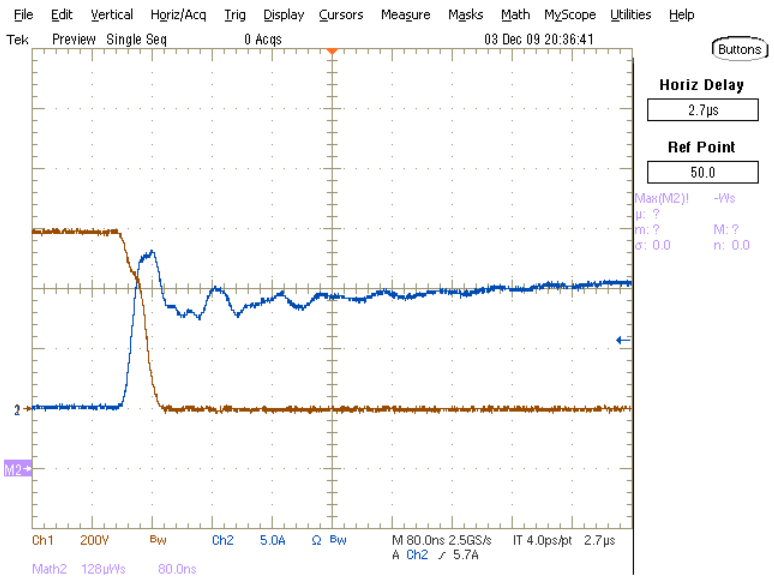

Figure 167: Optimized CMF20120D Turn Off Behavior at 600V, 10A (blue = current, yellow = voltage)

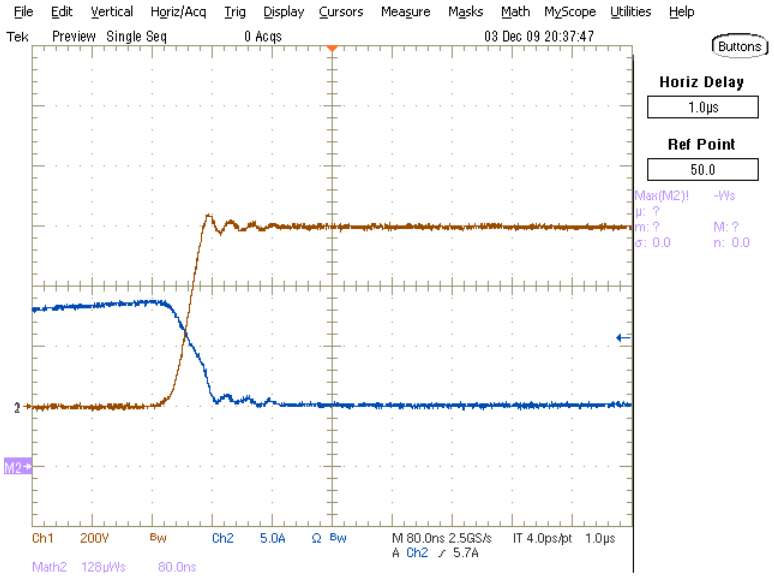

Figure 168: Optimized CMF20120D Turn On Behavior at 600V, 10A (blue = current, yellow = voltage)

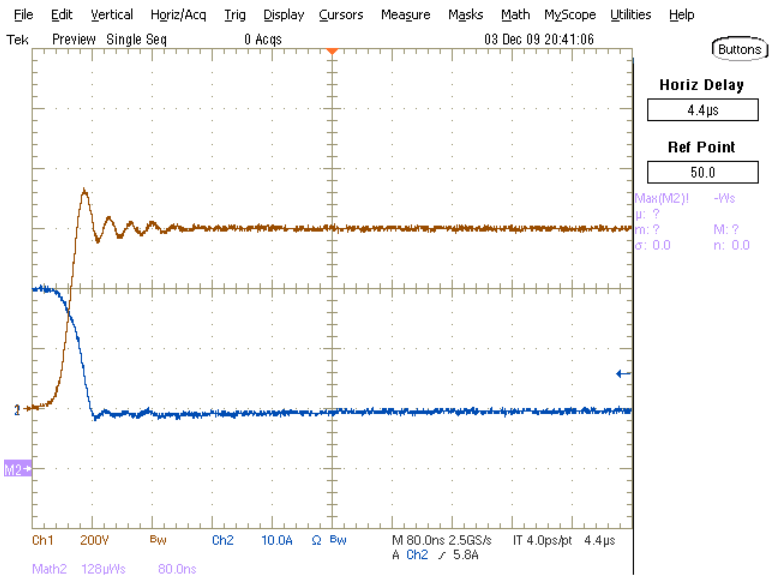

Figure 169: Optimized CMF20120D Turn Off Behavior at 600V, 20A (blue = current, yellow = voltage)

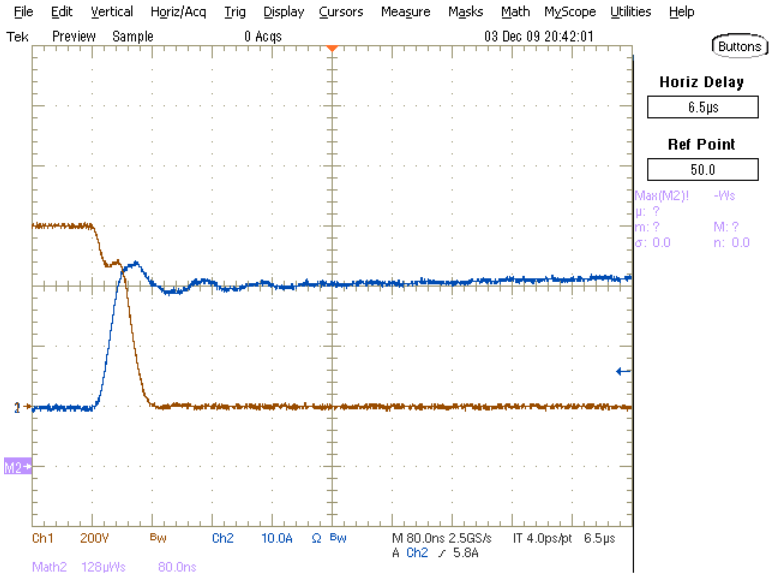

Figure 170: Optimized CMF20120D Turn On Behavior at 600V, 20A (blue = current, yellow = voltage)

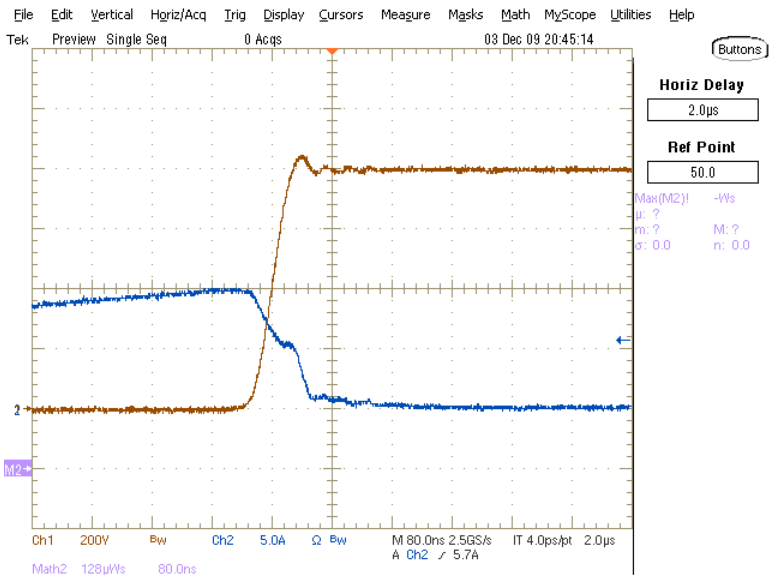

Figure 171: Optimized CMF20120D Turn Off Behavior at 800V, 10A (blue = current, yellow = voltage)

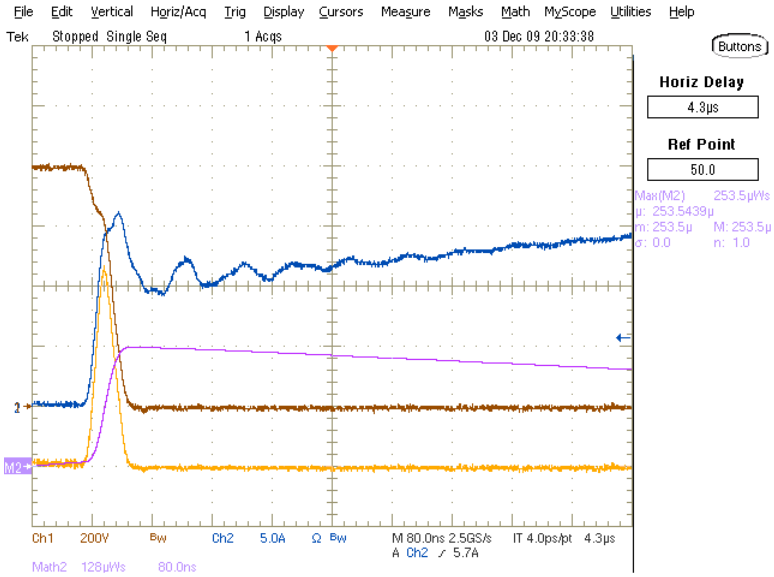

Figure 172: Optimized CMF20120D Turn On Behavior at 800V, 10A (blue = current, yellow = voltage)

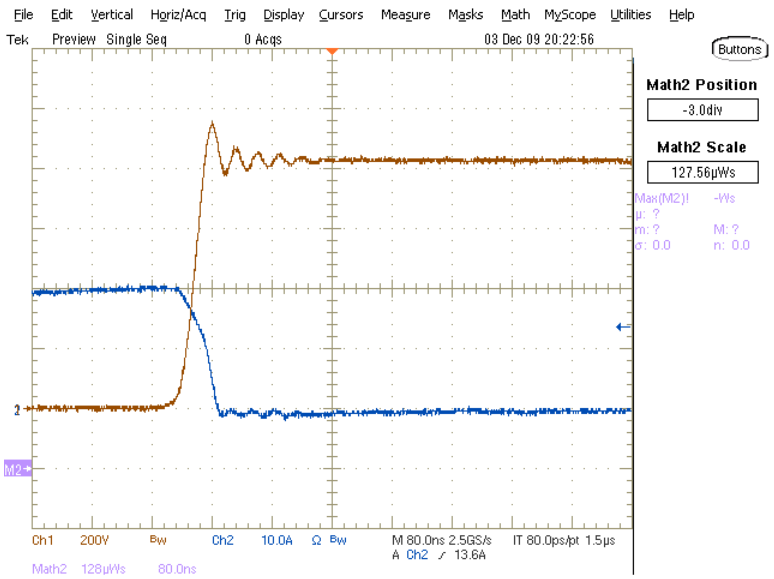

Figure 173: Optimized CMF20120D Turn Off Behavior at 800V, 20A (blue = current, yellow = voltage)

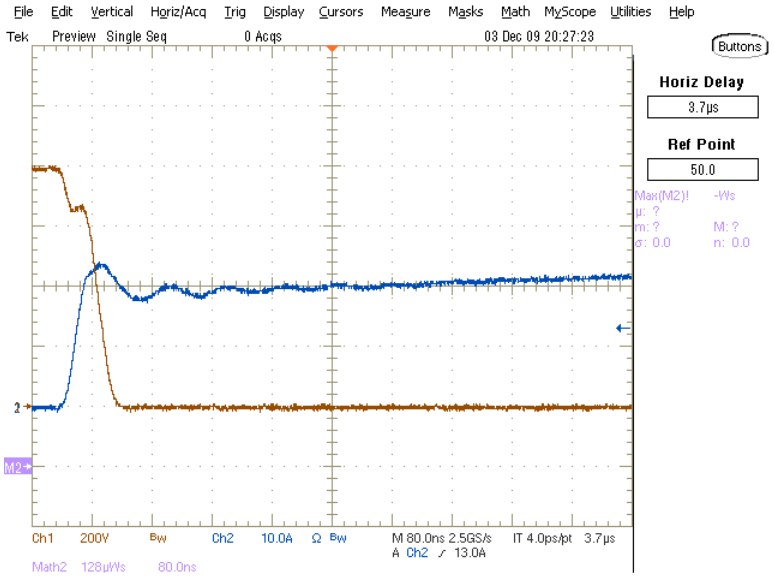

Figure 174: Optimized CMF20120D Turn On Behavior at 800V, 20A (blue = current, yellow = voltage)

CHAPTER 7

7 LAB SUMMARY AND COMPARISON OF SWITCHING DEVICES

A total of 14 switching device combinations were two-pulse tested in Chapters 5 and 6. The Silicon Carbide devices show a clear opportunity to reduce dynamic losses in hard switching applications where high blocking voltage is required. The higher breakdown field of SiC material allows the MOSFET and JFET devices to compete with Silicon IGBT's in terms of conduction characteristics. The devices far outperform comparable Silicon devices with respect to switching losses as can be seen in the tables listed below. FIgure 175 summarizes the switching energies for the traditional silicon devices evaluated. The most promising Silicon device with respect to switching energies was the Fairchild FGL40N120AND device with 2464uJ total switching energy at 800V, 20A. A summary of the switching energies for the same devices but using a Cree SiC diode is shown in Figure 176. The switching energy reduction was very impressive and has been summarized in Figure 177 below. The reduction in switching energy is in the range of 24-34%, which is very significant and could help a power electronics designer optimize other parts of the power circuit. Three such ways are:

1) Reduction of heatsink or use of lower airflow fans for cooling

2) The ability to use a smaller chip size for the IGBT

3) Switching frequency increase which would reduce inductor size

Each of the above examples gives the power circuit designer levels of flexibility in designing the architecture of the product. It must be stressed that the change described above included absolutely no changes to the power circuitry other than the diode change. The gate driver remained 100% the same. Even the exact same layout was used in order to have the same stray inductance values, etc.

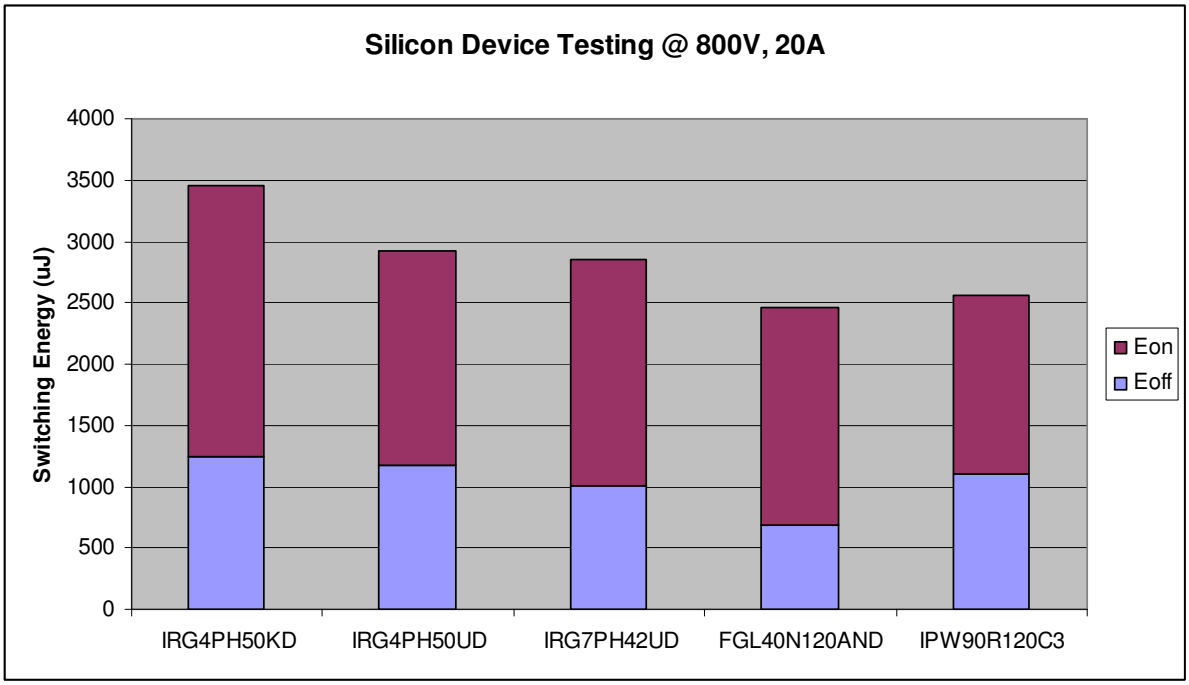

Figure 175: Switching Energy Summary for Silicon Devices

Table 22: Switching Energy Summary for Silicon Devices

	Silicon Device Testing @ 800V, 20A		
	Eoff	Eon	Etotal
IRG4PH50KD	1250	2210	**3460**
IRG4PH50UD	1178	1742	**2920**
IRG7PH42UD	1010	1850	**2860**
FGL40N120AND	684	1780	**2464**
IPW90R120C3	1110	1450	**2560**

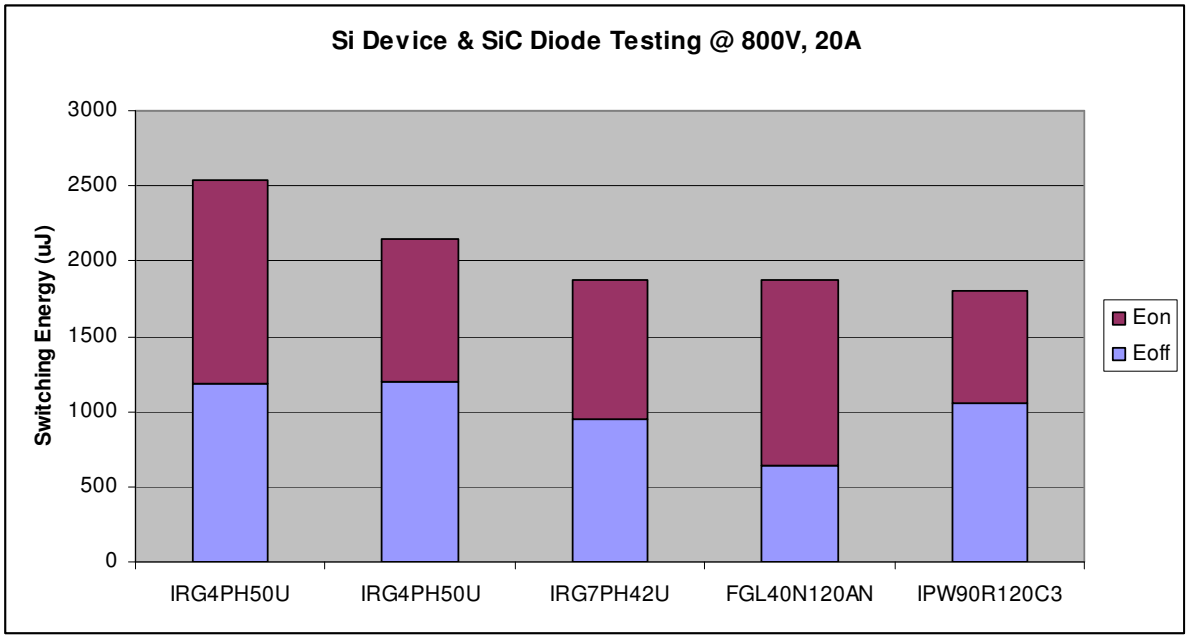

Figure 176: Switching Energy Summary for Silicon Switch with SiC Diode

Table 23: Switching Energy Summary for Silicon Switch with SiC Diode

	Si Device & SiC Diode Testing @ 800V, 20A		
	Eoff	Eon	Etotal
IRG4PH50U	1190	1350	**2540**
IRG4PH50U	1200	941	**2141**
IRG7PH42U	952	925	**1877**
FGL40N120AN	641	1230	**1871**
IPW90R120C3	1060	740	**1800**

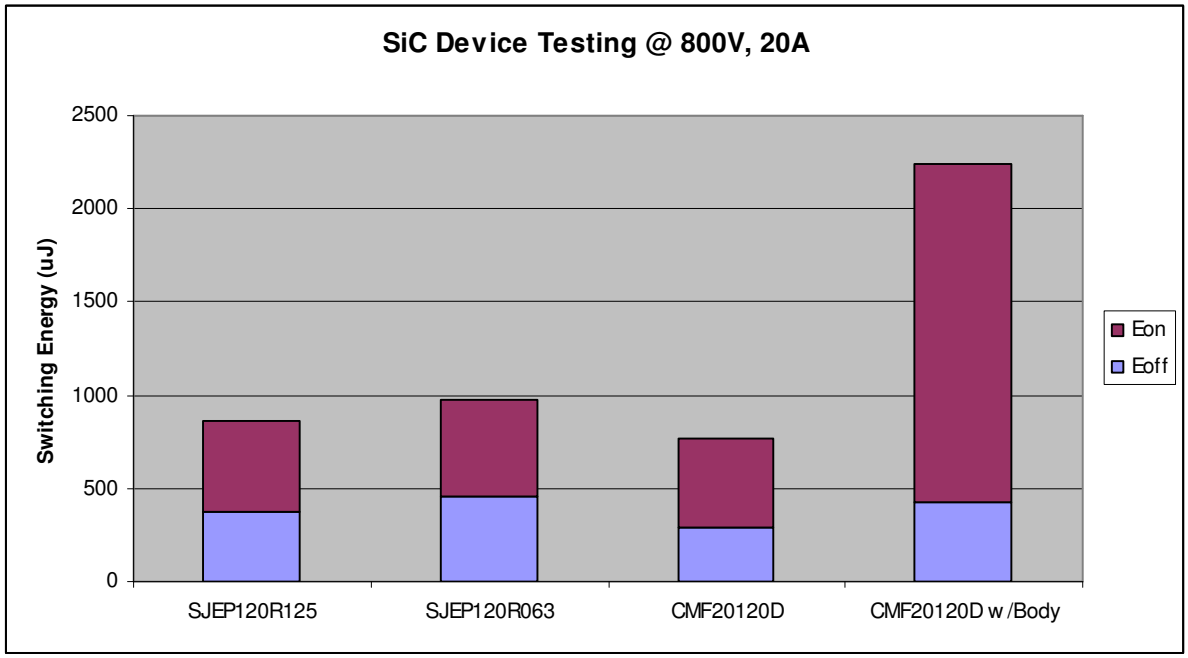

Figure 177: Reduction of Switching Energy by Using SiC Diode

Table 24: Reduction of Switching Energy by Using SiC Diode

	Reduction of Etotal with SiC Diode
IRG4PH50U	**26.59%**
IRG4PH50U	**26.68%**
IRG7PH42U	**34.37%**
FGL40N120AN	**24.07%**
IPW90R120C3	**29.69%**

The replacement of the Silicon switch with a SiC MOSFET or JFET proved to provide an even more compelling benefit. The key takeaway from this exercise is that the SemiSouth SiC JFET devices are not suitable for a direct replacement like the SiC Diodes are. With no changes to the gate drive circuitry the SemiSouth JFET devices do not see a significant benefit in dynamic performance when compared to the silicon switches. The benfit, however,

can be achieved by adding a very simple and cheap gate bypass capacitor to the circuit. It should be noted that this will not incur much added losses in gate drive circuitry because the bypass capacitor looks like an open circuit once charged. The only losses associated with this gate drive enhancement are the 1/2C*V^2 losses for the capacitor. However, the typical gate charge for the Silicon IGBT's tested was roughly 3-4 times higher than the SemiSouth JFET. Because of this, with the added bypass capacitor the SiC JFET devices dissipate very similar gate power as the comparable Silicon IGBT's.

The key to the Cree SiC MOSFET devices is the 20V gate voltage and high current gate drive they desire. When tested using the standard gate drive impedance, the devices do not perform better than the FGL40N120AN device did. The gate drive changes, however, were very minor and do not significantly change the gate drive power requirements. Once the gate driver for the SiC MOSFET was optimized, the device performed the best of any devices tested with only 769uJ of total switching energy at 800V, 20A.

Another key aspect of the SiC MOSFET is the dynamic performance of the devices body diode. The SiC MOSFET body diode performed very well compared to the Infineon CoolMOS body diode. The body diode does have some reverse recovery current, but is very low compared to even the Fairchild FGL40N120AND co-pack diode. The SiC MOSFET body diode is extremely soft compared to the FGL40N120AND diode in that it has a much lower peak reverse recovery current, but the recovery time is much longer. For reference, the SiC MOSFET body diode has a trr of 258ns and Irrm of 2.2A while the Silicon diode has a trr of 75ns and Irrm of 8A. What this means is that if a power electronics designer chose to

use the CMF20120D with its body diode they could very well do so. The sacrifice would be part of the reduction in losses achieved from using a separate SiC body diode. One very important characteristic of the SiC MOSFET is that the body diode has such a high forward drop of roughly double that of a comparable SiC Diode. Because of this, a SiC Diode can be paralleled easily causing the body diode of the MOSFET to never conduct.

A summary of the SiC JFET and MOSFET device dynamic results is shown in Figure 178 below. Also included in Figure 179 below is a summary of how much going from an FGL40N120AND device will reduce switching losses. In summary, using simply a SiC Diode yields roughly 24% reduction in dynamic losses while either of the three SiC switches and SiC diode yields roughly 60-70% reduction in dynamic losses. Using the CMF20120D with body diode is a 12% reduction.

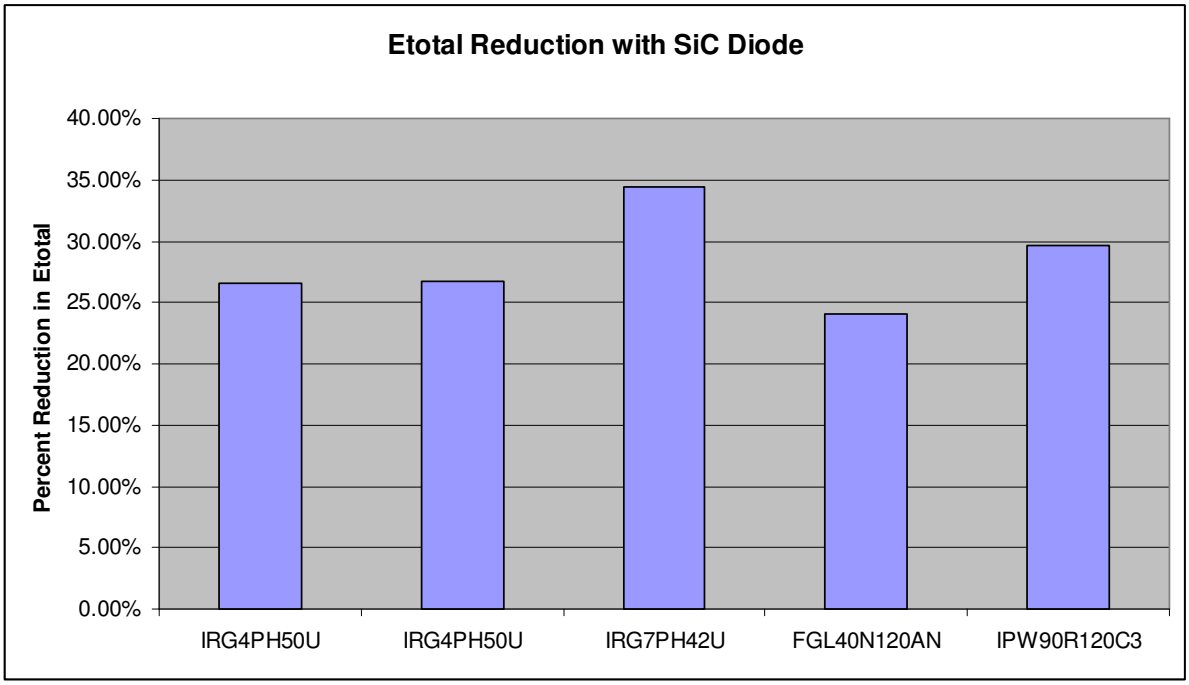

Figure 178: Switching Energy Summary for SiC Switches & Diode

Table 25: Switching Energy Summary for SiC Switches & Diode

	SiC Device Testing @ 800V, 20A		
	Eoff	Eon	Etotal
SJEP120R125	371	492	**863**
SJEP120R063	458	518	**976**
CMF20120D	294	475	**769**
CMF20120D w/Body	427	1810	**2237**

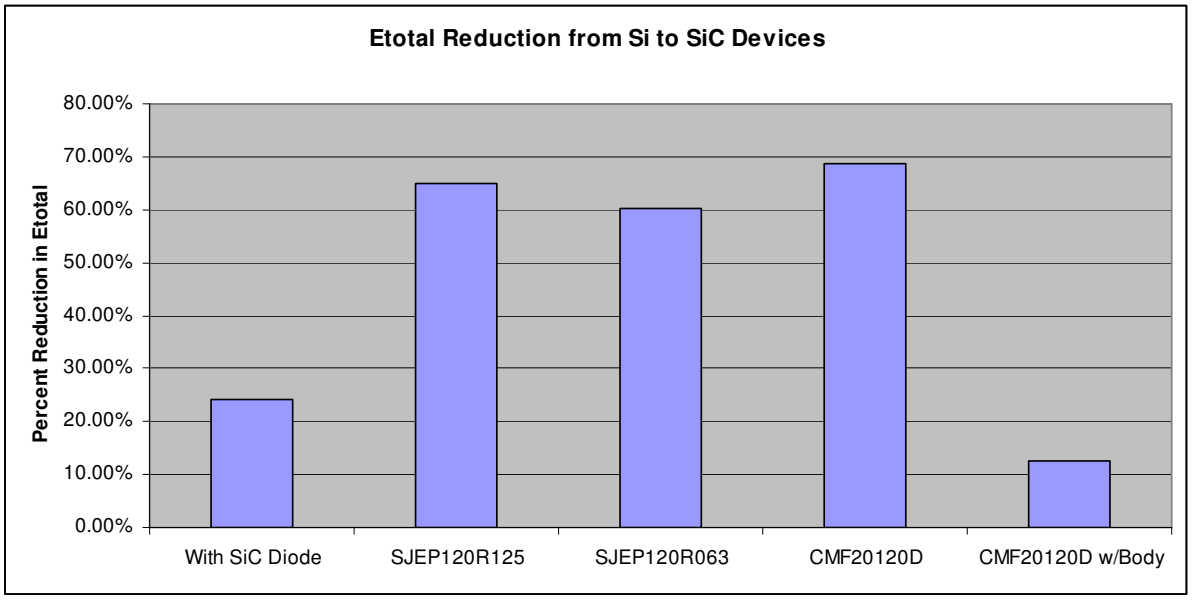

Figure 179: Reduction of Switching Energy from FGL40N120AND

Table 26: Reduction of Switching Energy from FGL40N120AND

	Reduction of Etotal from Si Devices
With SiC Diode	**24.07%**
SJEP120R125	**64.98%**
SJEP120R063	**60.39%**
CMF20120D	**68.79%**
CMF20120D w/Body	**12.62%**

CHAPTER 8

8 LABORATORY TESTING OF 300W FLYBACK POWER SUPPLY WITH SIC SWITCHING DEVICES

For this chapter, a 300W flyback power supply was evaluated to see how exchanging the main silicon switching devices for SiC MOSFET's could improve efficiency. The power supply is a two secondary flyback supply with one output rail at +48V nominal and the second output rail at +15V nominal. The +48V rail is directly regulated while the +15V rail is loosely regulated simply by the turns ratio of the flyback transformer. The flyback supply uses a two switch topology in order to clamp leakage inductance energy back to the input capacitors. Using the two switch topology also allows the flyback converter to see less voltage stress on the MOSFET devices since voltage spikes are clamped to the input rail. A schematic of the flyback converter is shown in Figure 180 below. A digital picture of the test setup and power board is shown in Figure 181 below as well.

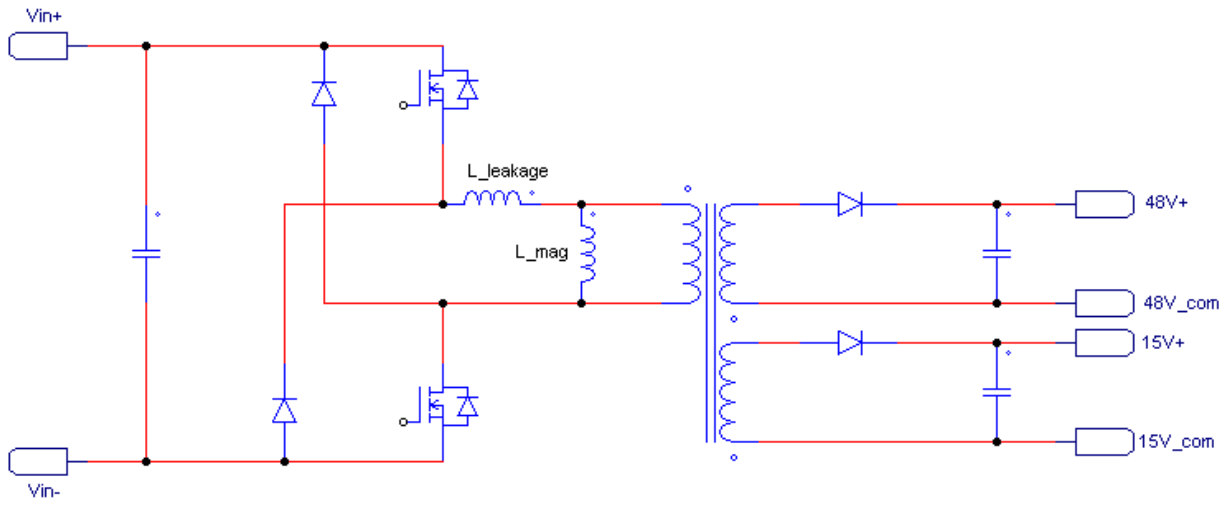

Figure 180: Schematic of 300W Flyback Supply

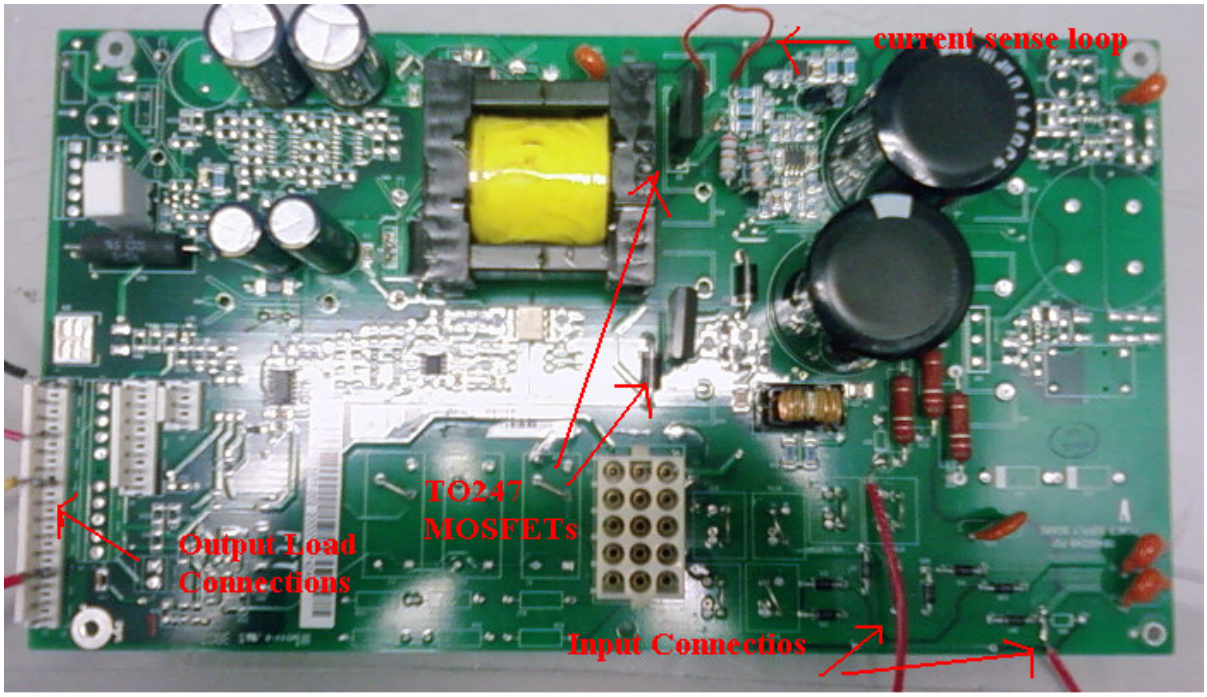

Figure 181: Picture of Test Setup and Power Board for 300W Flyback Supply

The original flyback power supply used ST Microelectronics 1000V STW8NB100 devices for both of the switches. The upper device used a pulse transformer to isolate the

gate driver circuitry while the lower device had the gate driver directly referenced to the negative input terminal. The converter switched the MOSFETs at a switching frequency of 75kHz. The primary side clamp diodes were On Semiconductor 1000V MUR4100E diodes and the secondary side rectifier diodes were On Semiconductor 400V MURH840CT diodes. The power supplies are specified to regulate the outputs to +/- 10% for the +15V supply since it was not directly regulated and +/- 5% for the 48V supply over all operating conditions. At the load used, the +15V and +48V supplies were regulated to +16.2V and +50.2V respectively.

During the test, the power supply was loaded using an 8 Ohm resistor for the +15V supply and a 10 Ohm resistor for the +48V supply. The output power was therefore calculated in equations (8.1-8.3) below.

$$(16.2V)\text{^}2/8Ohms = 32.8Watts \tag{8.1}$$

$$(50.2V)\text{^}2/10Ohms = 252Watts \tag{8.2}$$

$$32.8Watts + 252Watts = 284.8Watts \tag{8.3}$$

The power supply was loaded to a total of 284.8 Watts at the output. The test could have been done using only the +48V supply, however, the output diode of the +48V supply was not designed to handle the current. The supply was designed to handle up to roughly 250 Watts on the +48V supply and 50 Watts on the +15V supply. Using all the original hardware, the power supply was run with the previously stated loads and measured for

efficiency. The efficiency of the converter was measured to be 83.74% as shown in equations (8.4-8.7) below.

$$Vavg,in = 699.8V \tag{8.4}$$

$$Iavg,in = 486mA \tag{8.5}$$

$$Pin = 699.8V * 486mA = 340.1Watts \tag{8.6}$$

$$Efficiency = Pout / Pin = 284.8Watts / 340.1Watts = 83.74\% \tag{8.7}$$

Next, as in Chapters 5 and 6, switching energies for the MOSFET devices were measured. The current waveform showed a MOSFET minimum current of 1.6A and a maximum current of 2.8A with a 21.5% duty cycle. Using this information, the conduction power loss was calculated from the given Rds,on of 1.3Ohms. The conduction loss was calculated to be 0.62 Watts as in equation (8.8) below.

$$((2.8A - 1.6A)/2 + 1.6A) * 0.215 * 1.2Ohms = 0.62Watts \tag{8.8}$$

The power loss for each device is shown below in Table 27. It can be seen that the total device losses for the two MOSFETs was 11.17Watts. We can calculate that the 11.17Watts accounts for roughly 20% of the total losses in the converter. This is reasonable given that the rest of the losses likely were dissipated in the transformer windings and output rectifier diodes for each supply.

Table 27: Upper and Lower Device Switching Losses for Original Flyback Devices

	Upper Device:	Lower Device:
Eoff:	16.70uJ	38.30uJ
Eon:	26.30uJ	51.20uJ
Etotal:	43.00uJ	89.50uJ
Pcond:	0.62W	0.62W
Ptotal:	3.84W	7.33W

The next step in this testing was to replace both ST Microelectronics silicon MOSFETs with Cree CMF20120D SiC MOSFETs and see how the loss profile improved. The gate driver was modified as in section 6.4 of this report. The efficiency of the converter was again measured to be 85.7% as shown in equations (8.9-8.12) below. This showed an efficiency improvement of roughly 2% for the flyback converter.

$$Vavg,in = 699.6V \tag{8.9}$$

$$Iavg,in = 475mA \tag{8.10}$$

$$Pin = 699.6V * 475mA = 332.3Watts \tag{8.11}$$

$$Efficiency = Pout / Pin = 284.8Watts / 332.3Watts = 85.7\% \tag{8.12}$$

Next, the switching energies for the SiC MOSFETs were measured and again the conduction power loss was calculated from the given Rds,on of 110mOhms. The conduction loss was calculated to be 0.52Watts as in equation (8.13).

$$((2.8A - 1.6A)/2 + 1.6A) * 0.215 * 0.110Ohms = 0.52Watts \tag{8.13}$$

The power loss for each device is shown below in Table 28. It can be seen that the total device losses for the two MOSFETs was 3.76Watts. This lines up with the calculations made earlier. The total losses with the silicon devices were 340.1W-284.8W = 55.3W and the total losses with the SiC devices were 332.3W-284.8W = 47.5W. The decrease in losses when switching from silicon to SiC devices was roughly 7.8Watts according to system power calculations. This is close to what was calculated earlier in the device loss calculations. The device loss calculations show 11.17W-3.76W = 7.4W decrease in losses. It was noted earlier that the supply efficiency improved roughly 2% for this flyback converter. While this may not seem extremely impressive at first glance, when we look further we see that the losses in the switches decreased from 11.17Watts to 3.76Watts. This is a 66% reduction in switch loss, which is very considerable. This could mean a smaller heatsink or even that the user could run the converter at a higher frequency with the same device.

Table 28: Upper and Lower Device Switching Losses for Flyback with SiC Devices

	Upper Device:	Lower Device:
Eoff:	7.10uJ	15.20uJ
Eon:	9.20uJ	17.30uJ
Etotal:	16.30uJ	32.50uJ
Pcond:	0.05W	0.05W
Ptotal:	1.27W	2.49W

CHAPTER 9

9 LABORATORY TESTING OF 6KVA DOUBLE CONVERSION UPS WITH SIC SWITCHING DEVICES

For this chapter, an Eaton Powerware 6kVA true online double conversion Uninterruptible Power Supply (UPS) was tested for efficiency at various load levels. The purpose of the testing was to evaluate the Cree SiC devices in a UPS application to determine how they performed. Two criteria were evaluated:

1) Are the devices direct drop-in replacements for comparable IGBT's and Diodes in this application?
2) How much performance benefit (in terms of efficiency) can be achieved by direct replacement of Silicon IGBT's and Diodes with Cree SiC next-generation devices?

An Eaton Powerware model 9125 UPS was used as the test bed. The UPS is rated for 6kVA at a power factor of 0.7, which means the maximum resistive output power it can handle is 4.2kW as given in equation (9.1).

$$0.7 * 6000VA = 4200W = 4.2kW \quad (9.1)$$

The UPS is designed to run off a single phase 230V nominal input line. In practice, the UPS can be configured to run off 220-240V input. For the purposes of this test, the UPS

was set to the 220V output mode. The UPS consists of a rectifier half bridge stage followed by an inverter half bridge stage, each connected by a DC link. A battery converter and charger interface with the DC link when outages occur to keep the load up. For the purposes of this testing, the battery converter has been ignored since online efficiency was the only concern. Both the rectifier and inverter run at a switching frequency of 20kHz. The UPS does not have the ability to change the switching frequency since all hardware was designed to specifically run at 20kHz. Because of this, all tests were carried out at 20kHz. In the case of the SiC devices, this was a distinct disadvantage due to the fact that the devices suffer higher conduction losses but typically make up for it with their drastically lower switching losses. At 20kHz, however, the switching losses were likely not dominant which could erode the benefits of using a SiC device in the first place.

Four different cases were tested in this chapter. In section 9.1, the baseline efficiency was tested using all the original hardware that came with the UPS. The original gate drive resistance was used and the original Silicon IGBT/Diodes were used for both the rectifier and inverter sections. For section 9.2, only the inverter devices were replaced in order to see if there was an efficiency benefit by using SiC MOSFET/Diode co-packs as drop-in replacements. Section 9.3 further tested the SiC devices by attempting to decrease the switching time. The gate resistor was decreased since the datasheet for the Cree devices recommends a much smaller gate resistance than a typical Silicon IGBT. Finally, in section 9.4, the rectifier was modified by only replacing the anti-parallel diodes with SiC Diodes. The Silicon IGBT's were kept the same and the gate driver components were kept exactly the

same. Figure 182 below shows the UPS test setup and power board and Figure 183 below shoes a zoom in of the heatsink the devices were mounted to so that the reader can get a better appreciation of how difficult getting V-I measurements of the switching devices would be.

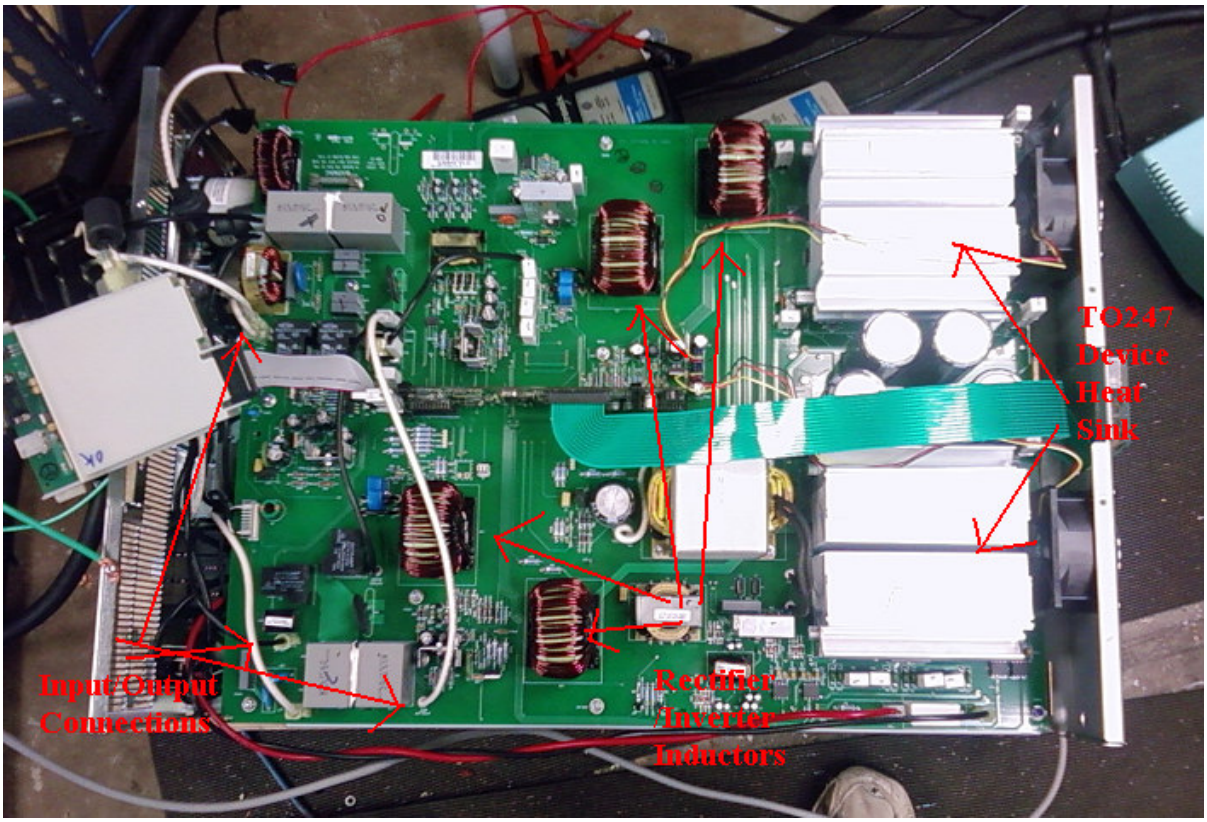

Figure 182: Picture of UPS Test Setup and Power Board

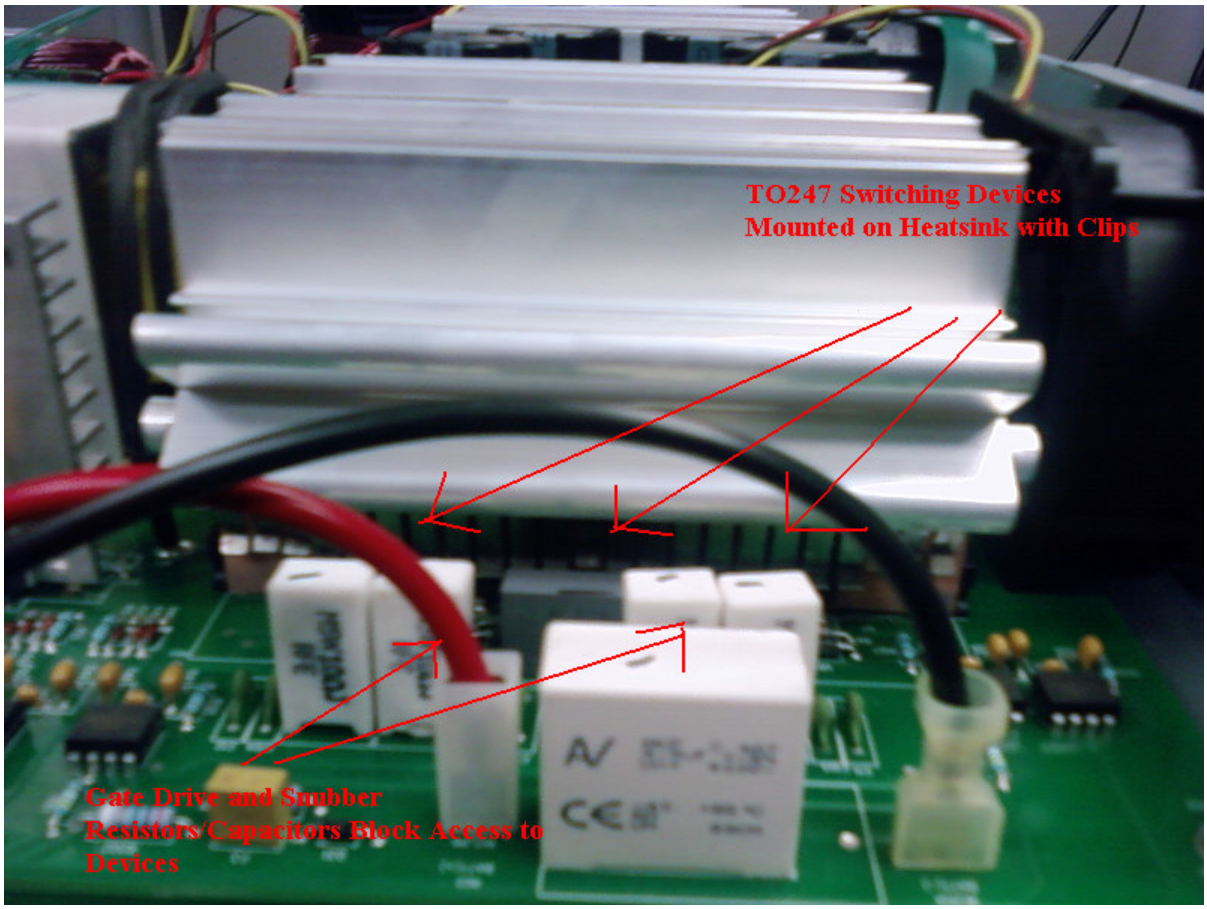

Figure 183: Zoom In Picture of Heatsink and Devices Mounting

9.1 Baseline Efficiency Measurement Using Original Silicon Devices

The first test in this chapter was meant to establish baseline efficiency for the double conversion power stage. The power stage consists of several pieces that contribute to losses in the UPS. The major sources of losses in the UPS are:

1) Rectifier Inductors
2) Rectifier Switching Devices
3) Switchmode Power Supply

a. Digital Logic Controls

b. Sensing Circuitry

c. Fan Power

4) Inverter Switching Devices

5) Inverter Inductors

The UPS utilizes toroidal inductors using powdered iron cores, which are very lossy compared to ferrite material. Switching at 20kHz, the ripple current losses are likely very substantial in these devices. The switchmode power supply for this UPS is another area for considerable losses. The switchmode power supply has to supply power to all logic circuitry, sensing circuitry, microcontrollers, and cooling fans for the system.

The only loss elements relating to this evaluation are the rectifier and inverter switching device losses. Because of this, all other elements were kept identical between tests in order to keep reliable data. For the baseline Silicon device testing, the test data is summarized in table 29 below. Note again that the testing was done at three different load levels in order to get a wide system understanding of the impact SiC devices can have. In Figures 184 through 189 the input voltage/current and output voltage/current waveforms are shown in two different zoom for the different load levels.

Table 29: Silicon Device 6kVA UPS Efficiency Testing

1kW: Silicon Devices							
Vin:	214.70V	Iin:	6.54A	Pin:	1404.57W		
Vout:	223.90V	Iout:	4.64A	Pout:	1038.90W	Efficiency:	**73.97%**

2kW: Silicon Devices							
Vin:	213.50V	Iin:	11.33A	Pin:	2418.96W		

Vout:	223.50V	Iout:	9.32A	Pout:	2083.02W	Efficiency:	**86.11%**

4kW: Silicon Devices							
Vin:	211.20V	Iin:	21.63A	Pin:	4568.26W		
Vout:	223.40V	Iout:	18.85A	Pout:	4211.09W	Efficiency:	**92.18%**

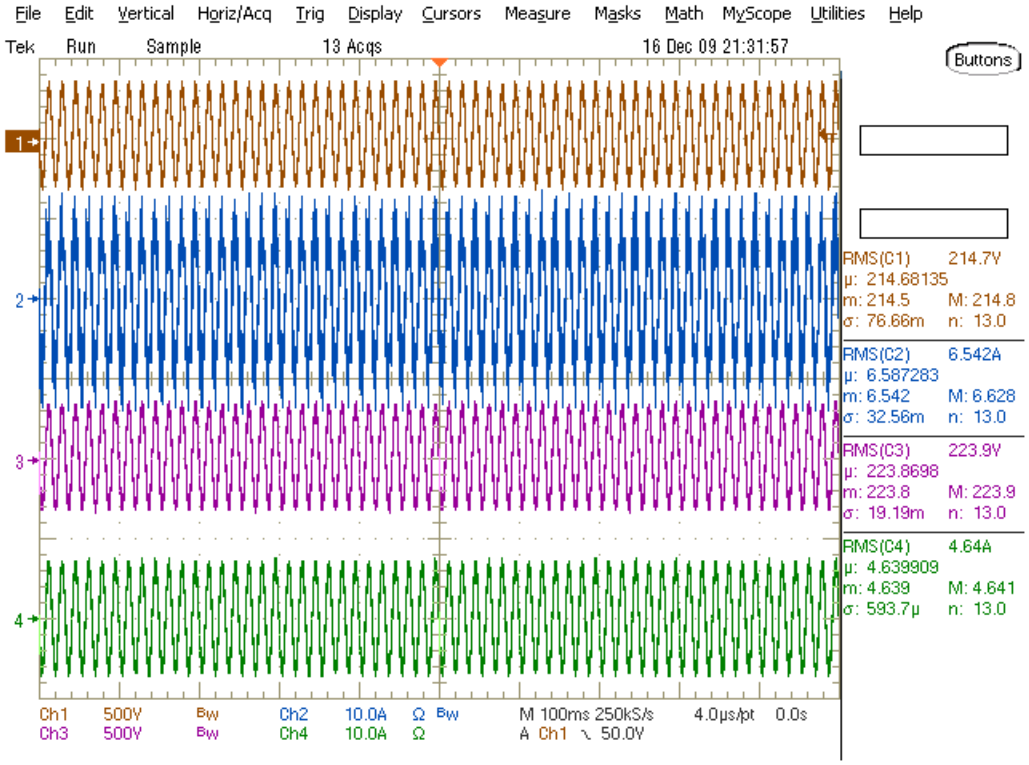

Figure 184: 1kW Efficiency Zoomed Out
(Channel 1 = Vin, Channel 2 = Iin, Channel 3 = Vout, Channel 4 = Iout)

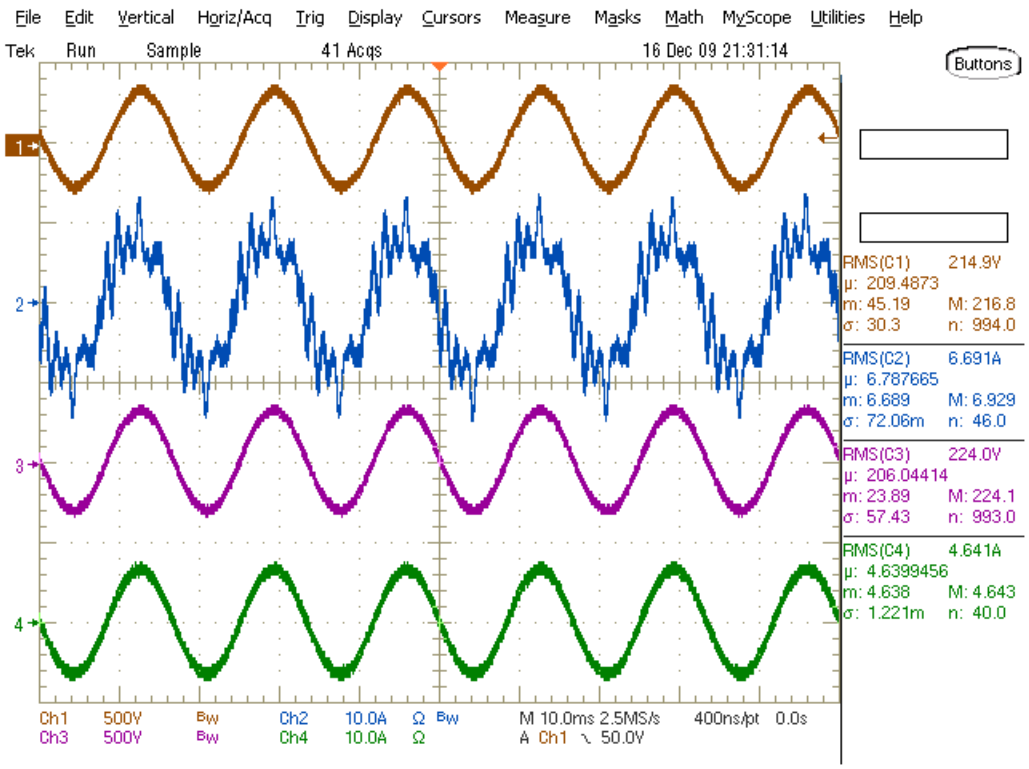

Figure 185: 1kW Efficiency Zoomed In
(Channel 1 = Vin, Channel 2 = Iin, Channel 3 = Vout, Channel 4 = Iout)

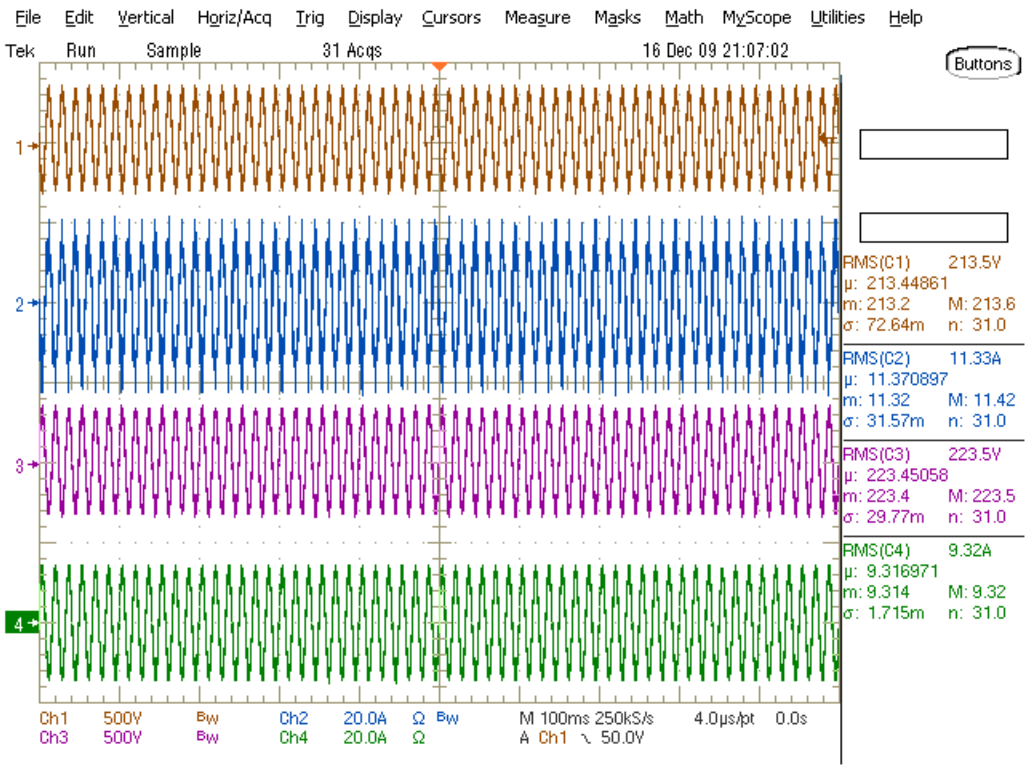

Figure 186: 2kW Efficiency Zoomed Out
(Channel 1 = Vin, Channel 2 = Iin, Channel 3 = Vout, Channel 4 = Iout)

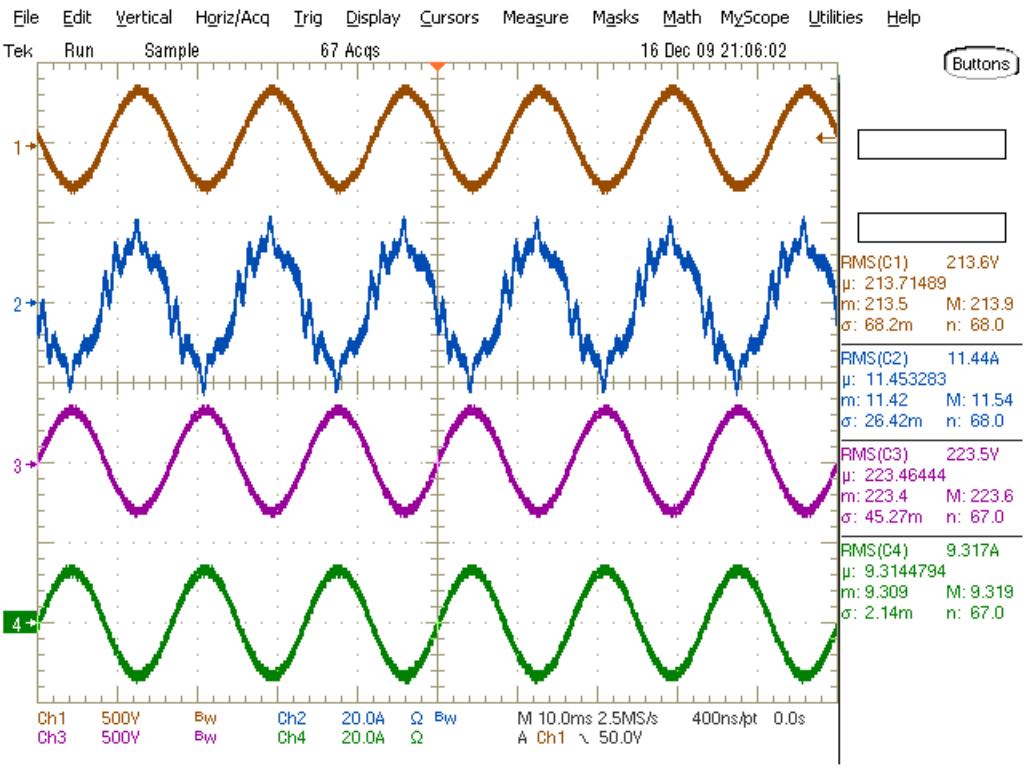

Figure 187: 2kW Efficiency Zoomed In
(Channel 1 = Vin, Channel 2 = Iin, Channel 3 = Vout, Channel 4 = Iout)

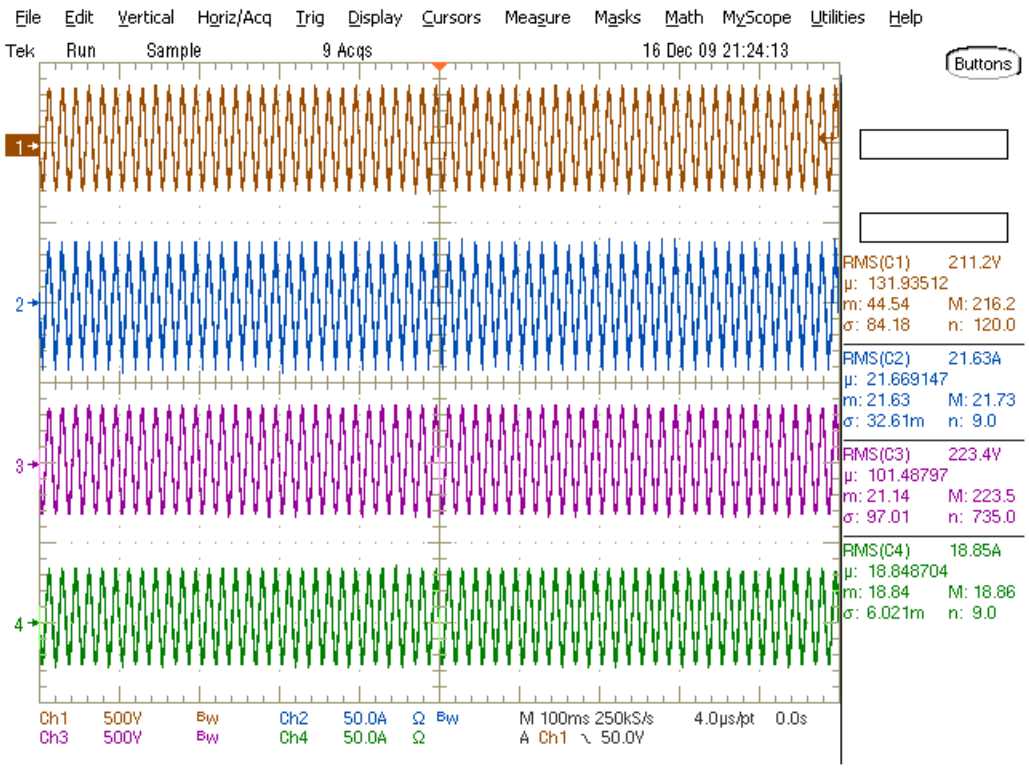

Figure 188: 4kW Efficiency Zoomed Out
(Channel 1 = Vin, Channel 2 = Iin, Channel 3 = Vout, Channel 4 = Iout)

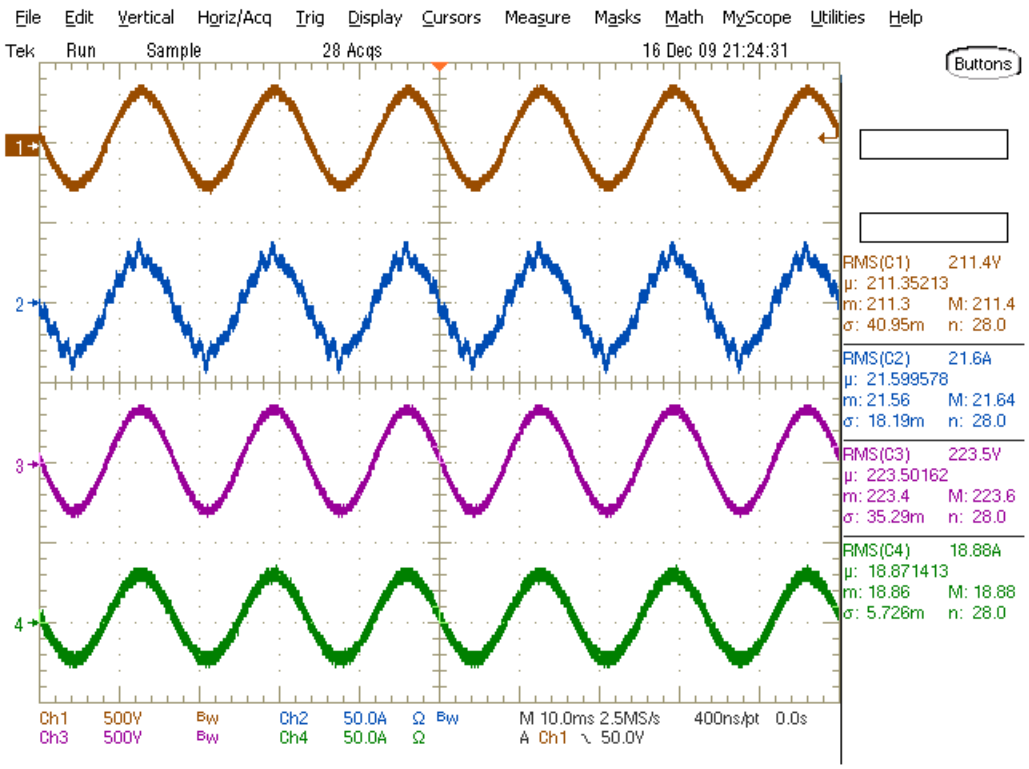

Figure 189: 4kW Efficiency Zoomed In
(Channel 1 = Vin, Channel 2 = Iin, Channel 3 = Vout, Channel 4 = Iout)

9.2 Replacement of Inverter Silicon IGBT/Diode Co-Packs with SiC MOSFET/Diode Co-Packs

For this section of the efficiency testing, all inverter switching devices were replaced with SiC devices. The inverter switches were replaced from 2 parallel HGTG27N120BN Fairchild 34A 1200V IGBT's to 2 parallel CMF20120 Cree 20A 1200V SiC MOSFET's. The inverter diodes were replaced from a single ISL9R30120G2 Fairchild 30A 1200V Diode to 2 parallel C2D10120 Cree 10A 1200V SiC Diodes. All gate drive parts were kept exactly the same as in Section 9.1 in keeping with the drop-in replacement theme of the tests. Rectifier devices were kept exactly the same as well using the original Silicon IGBT/Diodes.

The test data is summarized in table 30 below. Note again that the testing was done at three different load levels in order to get a wide system understanding of the impact SiC devices can have. In Figures 190 through 195 the input voltage/current and output voltage/current waveforms are shown in two different zoom for the different load levels.

Comparing the data in table 30 to the data in table 29, we can see how the efficiency was affected by converting the inverter switching devices to SiC. It is interesting to note that the efficiency increased significantly at 1kW (1.21%), at 2kW there was no practical change (-0.13%), and at 4kW the efficiency actually decreased significantly (-1.01%).

Table 30: SiC Inverter 6kVA UPS Efficiency Testing

1kW: SiC Inverter							
Vin:	217.00V	Iin:	6.30A	Pin:	1366.45W		
Vout:	222.30V	Iout:	4.62A	Pout:	1027.25W	Efficiency:	**75.18%**

2kW: SiC Inverter							
Vin:	214.90V	Iin:	11.09A	Pin:	2383.24W		
Vout:	221.40V	Iout:	9.26A	Pout:	2049.28W	Efficiency:	**85.99%**

4kW: SiC Inverter							
Vin:	211.50V	Iin:	21.33A	Pin:	4511.30W		
Vout:	220.90V	Iout:	18.62A	Pout:	4113.16W	Efficiency:	**91.17%**

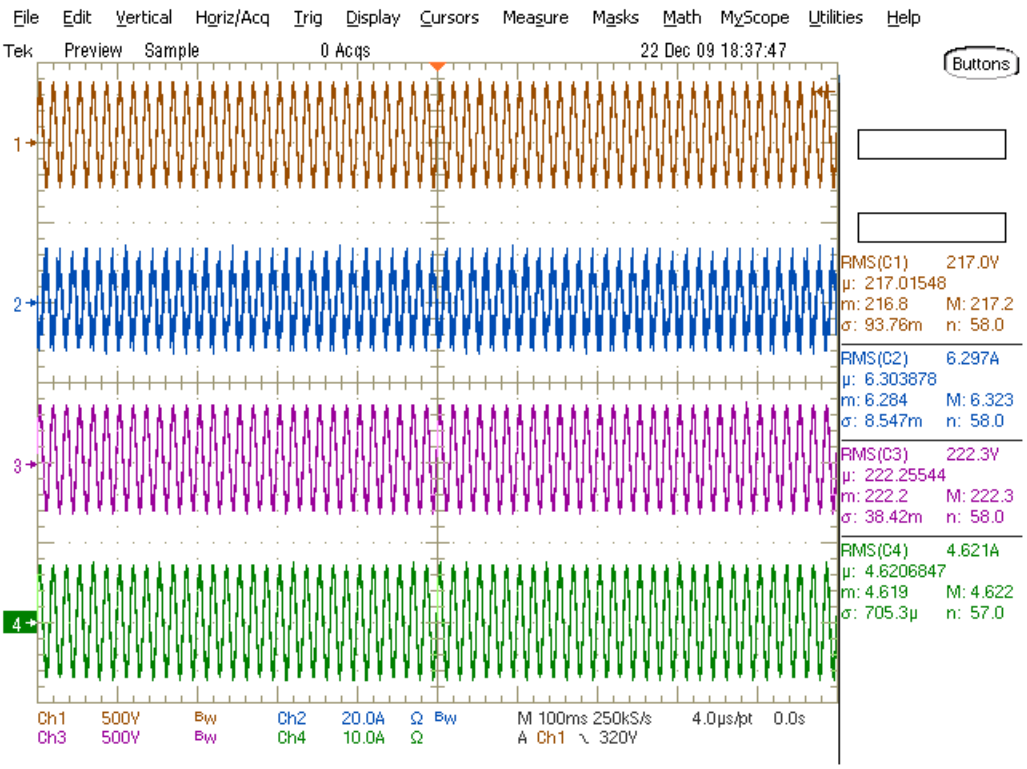

Figure 190: 1kW Efficiency Zoomed Out
(Channel 1 = Vin, Channel 2 = Iin, Channel 3 = Vout, Channel 4 = Iout)

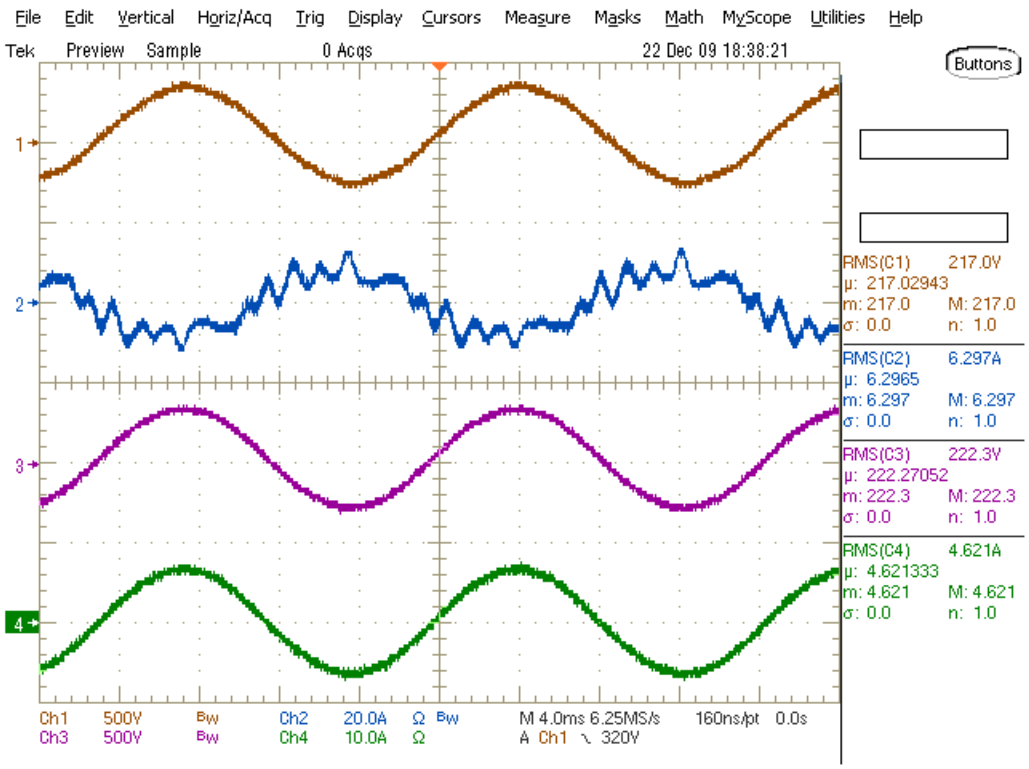

Figure 191: 1kW Efficiency Zoomed In
(Channel 1 = Vin, Channel 2 = Iin, Channel 3 = Vout, Channel 4 = Iout)

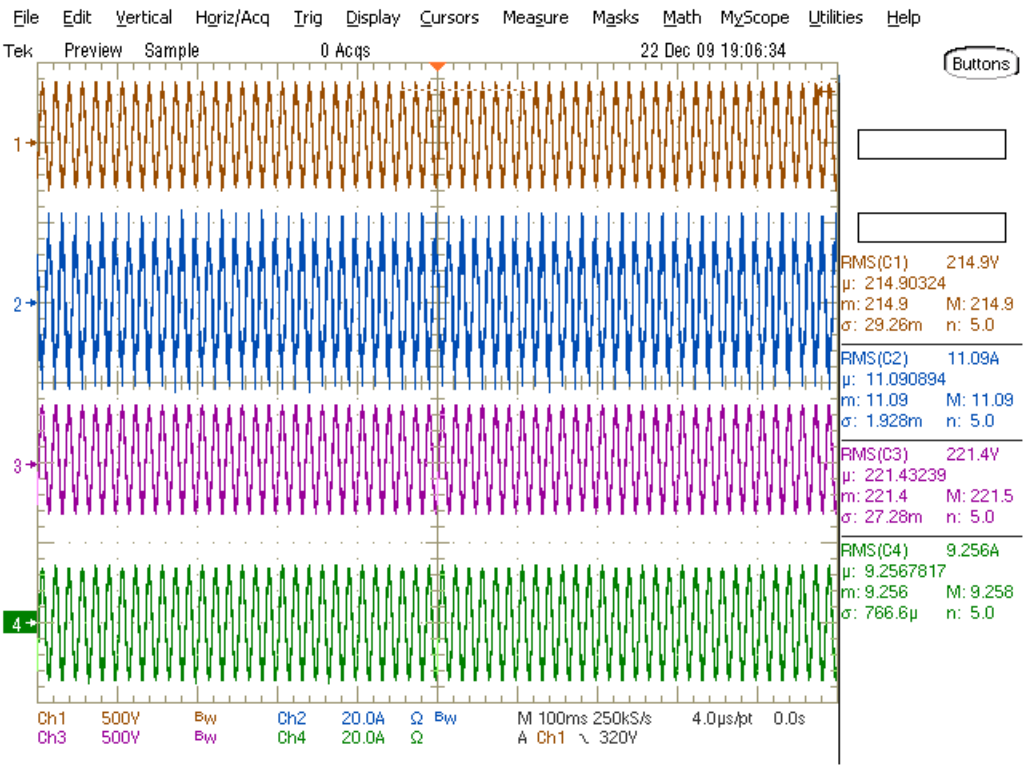

Figure 192: 2kW Efficiency Zoomed Out
(Channel 1 = Vin, Channel 2 = Iin, Channel 3 = Vout, Channel 4 = Iout)

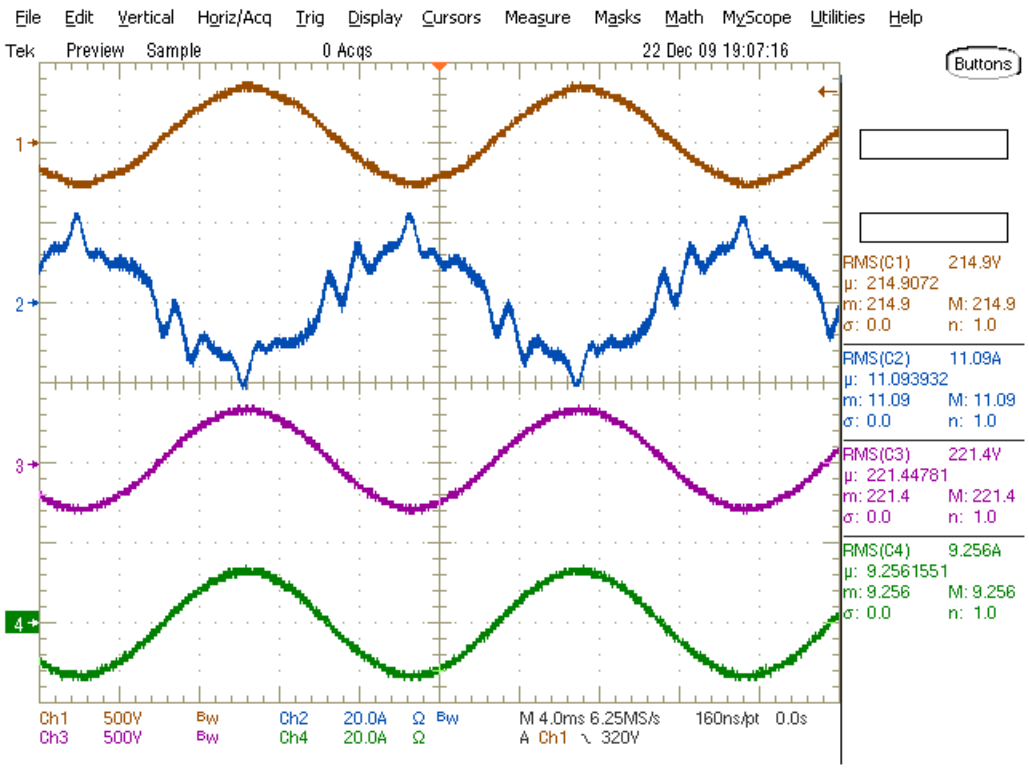

Figure 193: 2kW Efficiency Zoomed In
(Channel 1 = Vin, Channel 2 = Iin, Channel 3 = Vout, Channel 4 = Iout)

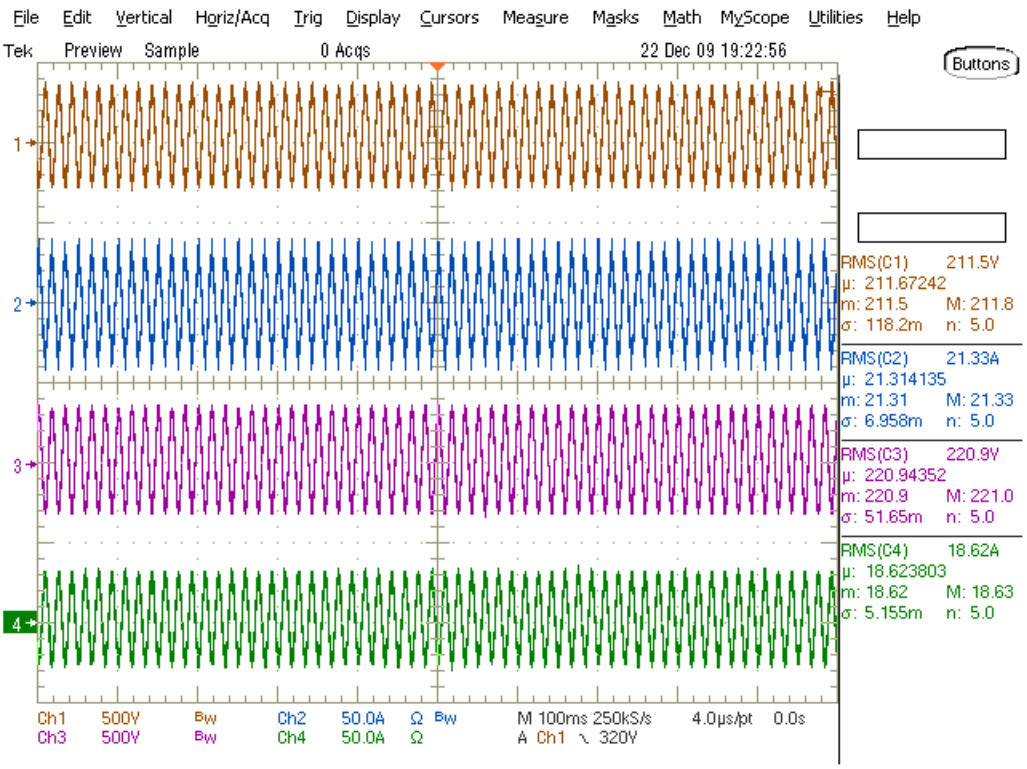

Figure 194: 4kW Efficiency Zoomed Out
(Channel 1 = Vin, Channel 2 = Iin, Channel 3 = Vout, Channel 4 = Iout)

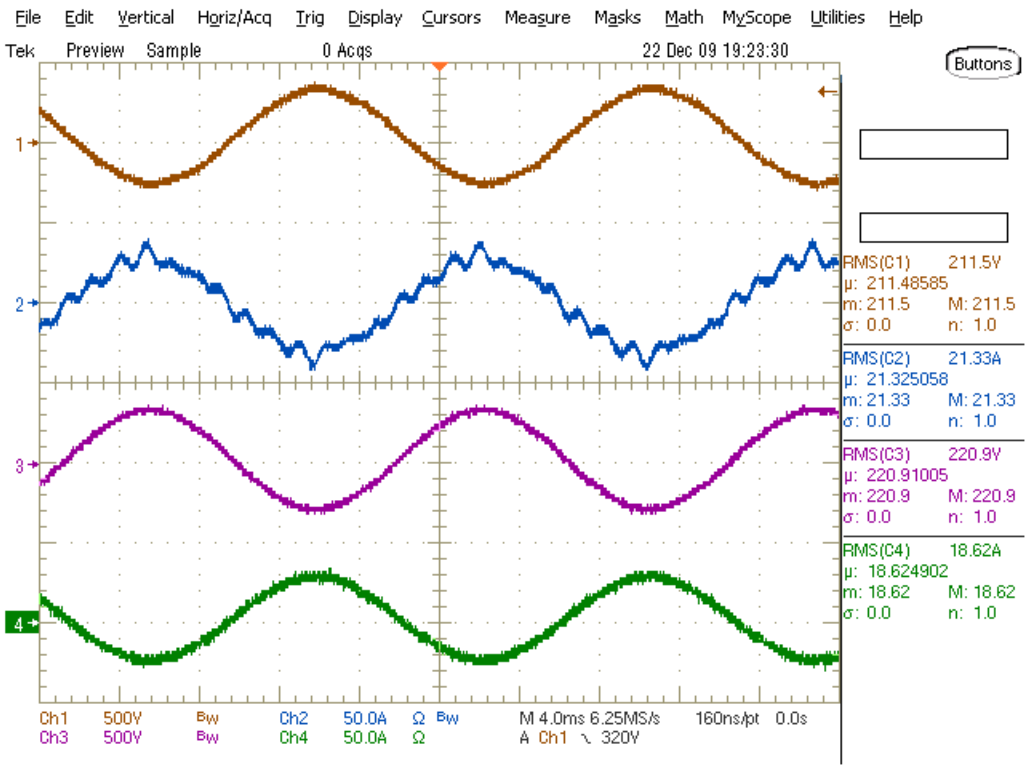

Figure 195: 4kW Efficiency Zoomed In
(Channel 1 = Vin, Channel 2 = Iin, Channel 3 = Vout, Channel 4 = Iout)

9.3 Reduction of Inverter SiC MOSFET Gate Drive Resistor

The next efficiency testing that was done was to take the same setup as in section 9.2 and lower the gate resistor for the inverter devices. All inverter switching devices were still SiC MOSFET/Diodes by Cree and all rectifier devices were still Silicon IGBT/Diodes by Fairchild. The inverter gate driver was originally 10 Ohms in series with 33 Ohms. The gate driver circuit utilizes an HCNW3120 isolated gate driver IC to drive the top and bottom switches. The circuit uses a 10 Ohm gate resistor from the IC and then two different 33 Ohm gate resistors for each device that is paralleled. A schematic of the original gate drive is shown in Figure 196 below. Cree recommends a 10 Ohm gate drive resistor when switching

their 20A SiC MOSFET devices. This is the gate resistor value they use for all specified parameters in the datasheet. This was the target resistor for this section, and the 33 Ohm gate resistor was replaced with a 1.8 Ohm resistor. This resistor created an 11.8 Ohm effective gate resistance for the driver. A schematic of the modified gate drive is shown in Figure 197 below. The gate driver signals from the left in these figures come from the HCNW3120 gate driver IC which is powered by a +18V/-8V isolated power supply.

The test data is summarized in table 31 below. Note again that the testing was done at three different load levels in order to get a wide system understanding of the impact SiC devices can have. In Figures 198 through 203 the input voltage/current and output voltage/current waveforms are shown in two different zoom for the different load levels. The testing was also attempted with even lower gate resistor values; however, lowering the gate resistor further did not cause a measurable change in efficiency of the converter.

Comparing the data in table 31 to the data in table 29, we can see how the efficiency was affected by converting the inverter switching devices to SiC and updating the gate drive resistance. It is interesting to note that the efficiency increased even more than in section 9.2 at 1kW (2.69%), at 2kW we now can see an improvement in efficiency (1.04%), and at 4kW the efficiency is basically a wash (-0.10%).

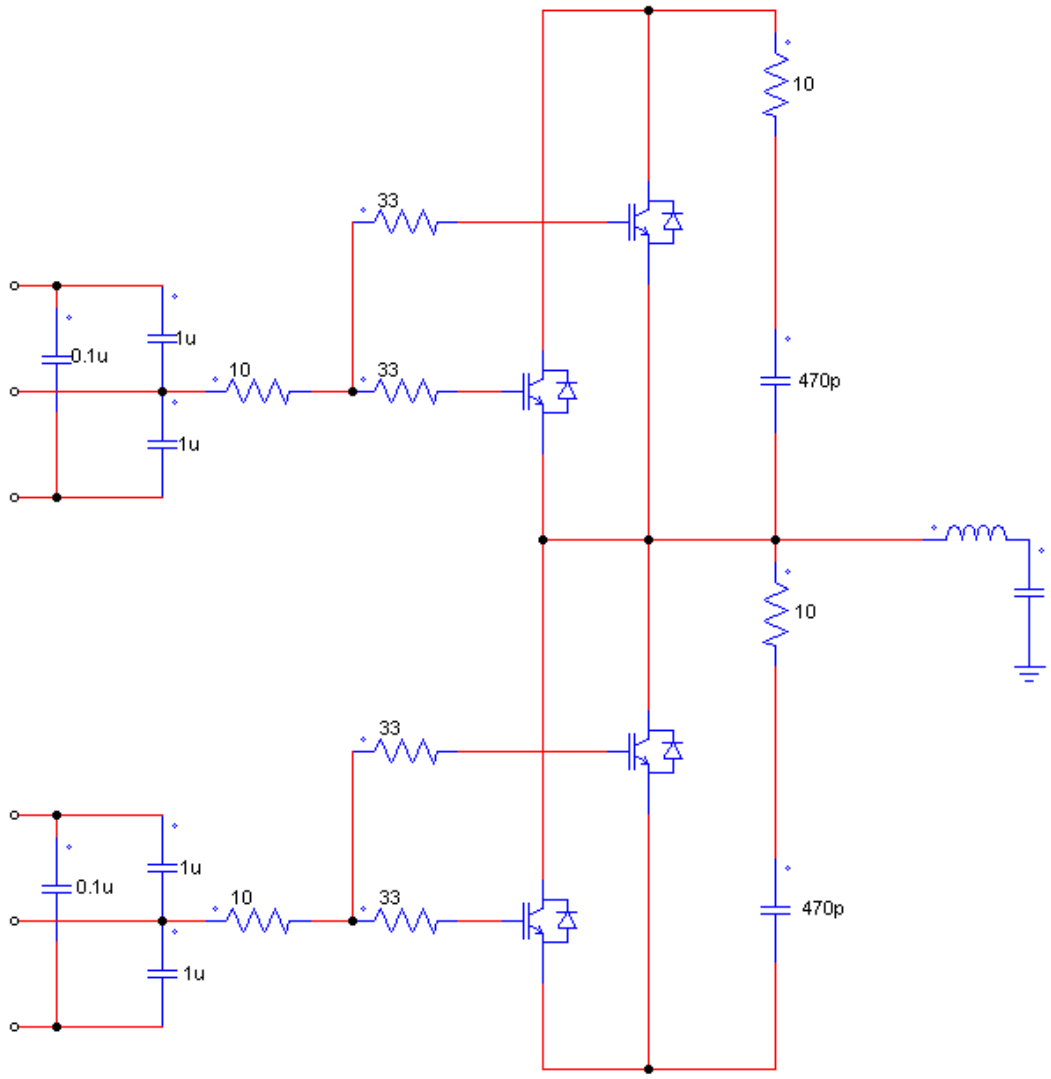

Figure 196: Schematic of Original Gate Drive Circuit

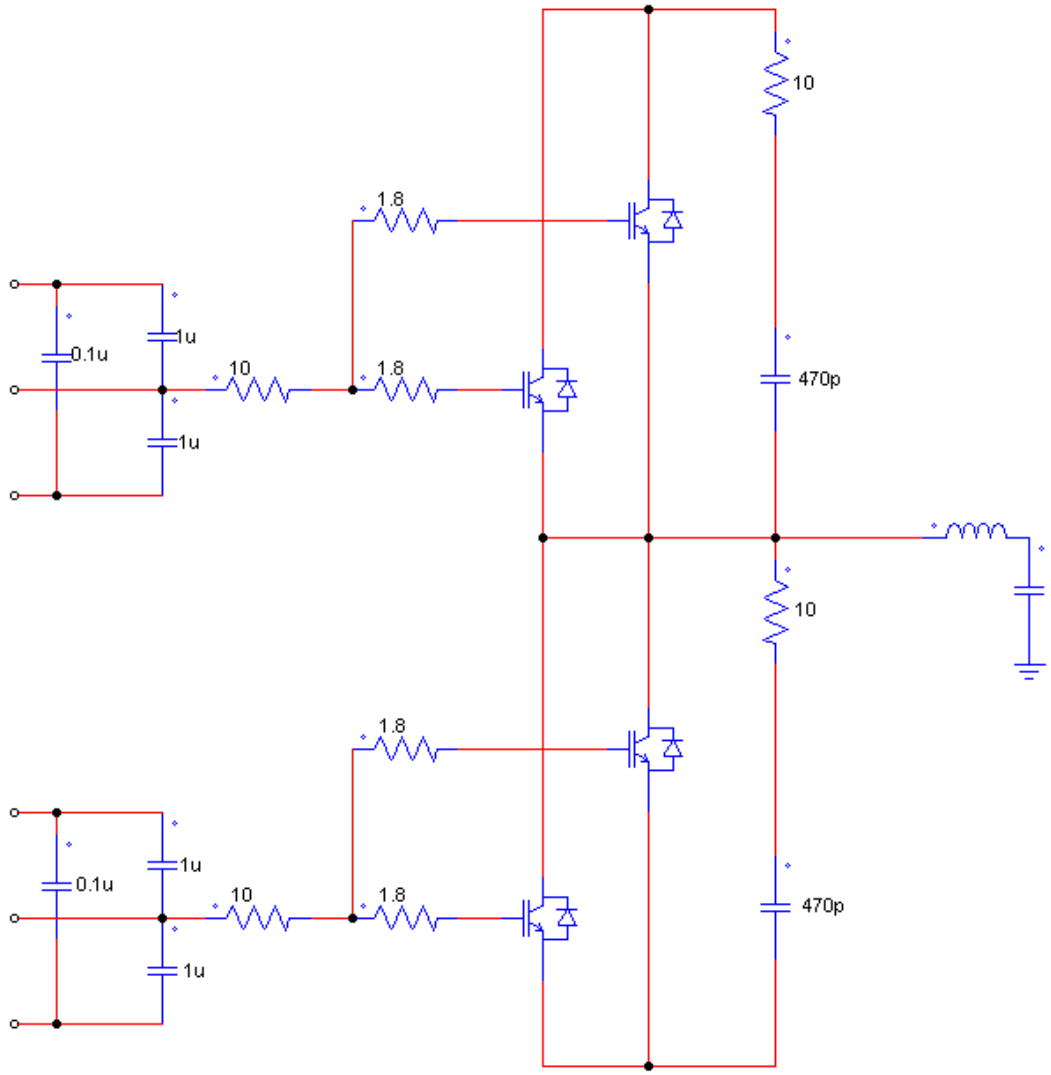

Figure 197: Schematic of Updated Gate Driver Circuit for Section 9.3

Table 31: SiC Inverter with Reduced Rg 6kVA UPS Efficiency Testing

1kW: SiC Inverter with 11.8Ohm Rg							
Vin:	215.20V	Iin:	6.20A	Pin:	1334.67W		
Vout:	221.70V	Iout:	4.62A	Pout:	1023.15W	Efficiency:	**76.66%**

2kW: SiC Inverter with 11.8Ohm Rg							
Vin:	216.30V	Iin:	10.97A	Pin:	2372.81W		
Vout:	222.60V	Iout:	9.29A	Pout:	2067.95W	Efficiency:	**87.15%**

4kW: SiC Inverter with 11.8Ohm Rg							
Vin:	211.80V	Iin:	21.21A	Pin:	4492.28W		
Vout:	221.10V	Iout:	18.71A	Pout:	4136.78W	Efficiency:	**92.09%**

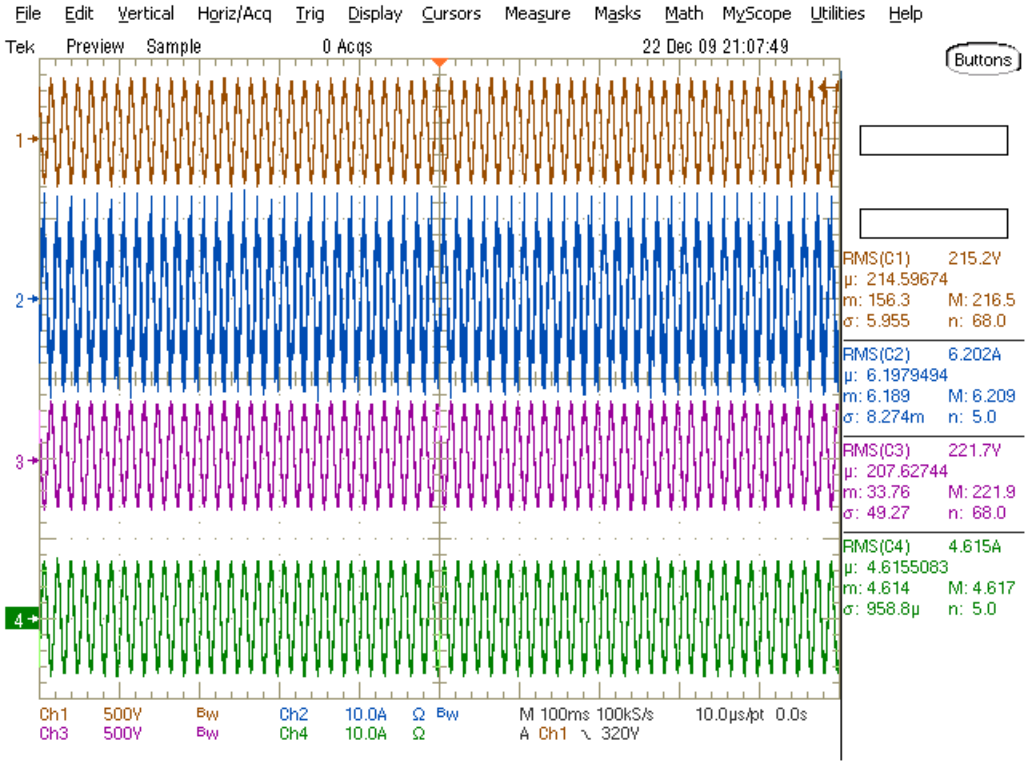

Figure 198: 1kW Efficiency Zoomed Out
(Channel 1 = Vin, Channel 2 = Iin, Channel 3 = Vout, Channel 4 = Iout)

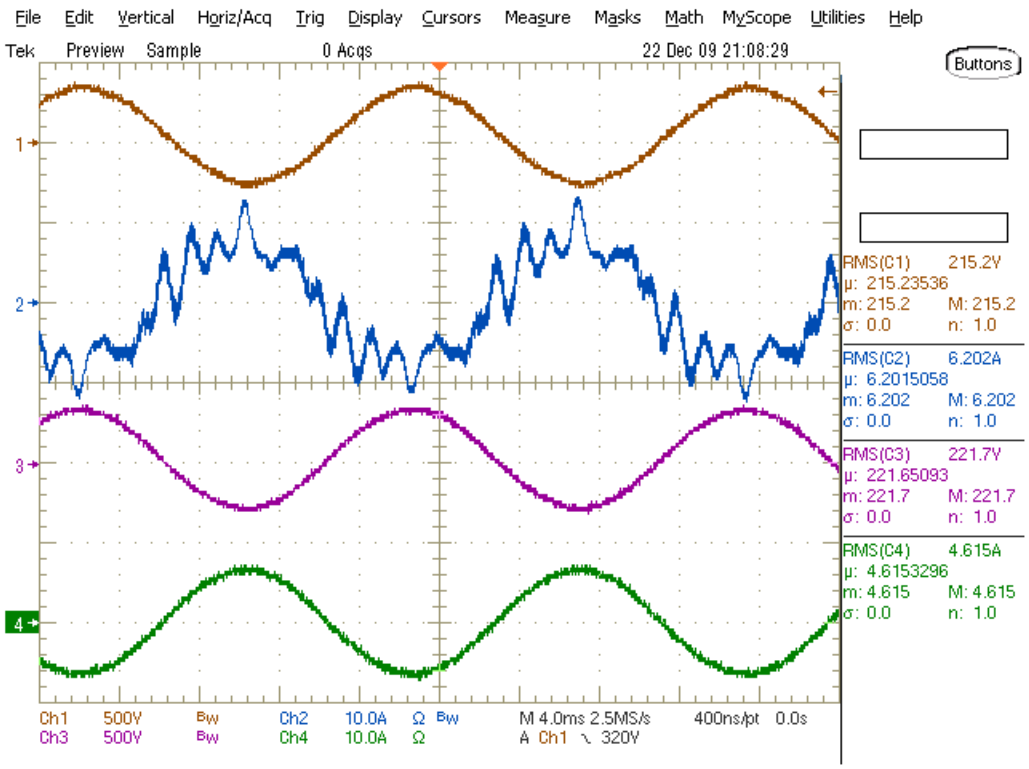

Figure 199: 1kW Efficiency Zoomed In
(Channel 1 = Vin, Channel 2 = Iin, Channel 3 = Vout, Channel 4 = Iout)

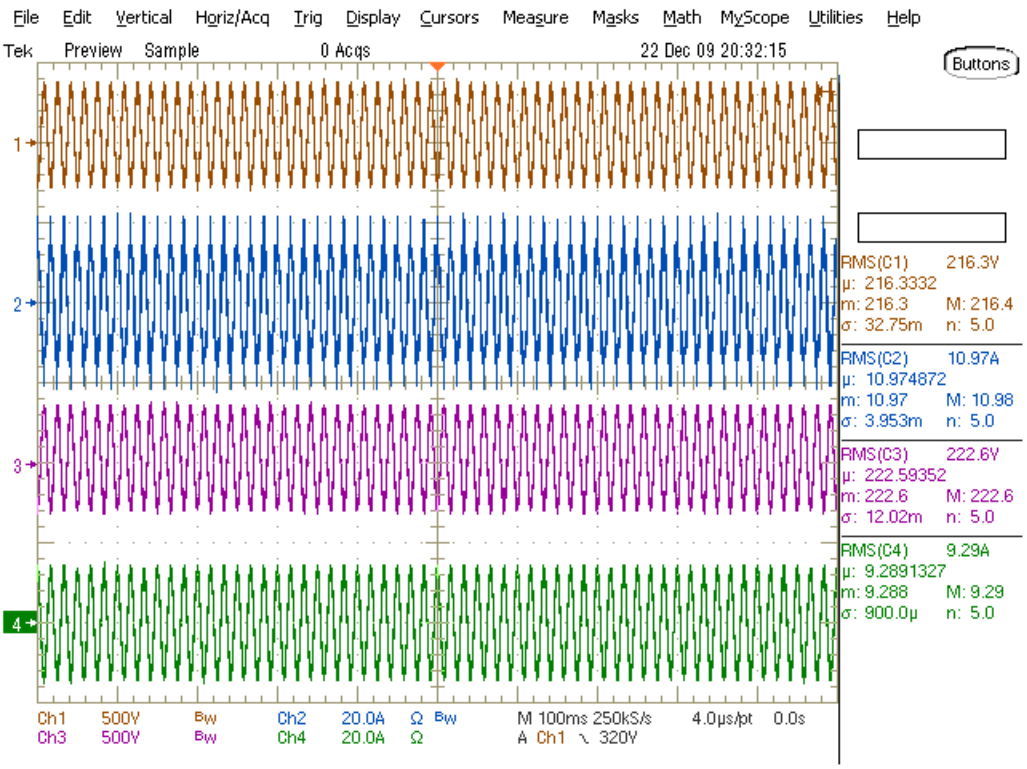

Figure 200: 2kW Efficiency Zoomed Out
(Channel 1 = Vin, Channel 2 = Iin, Channel 3 = Vout, Channel 4 = Iout)

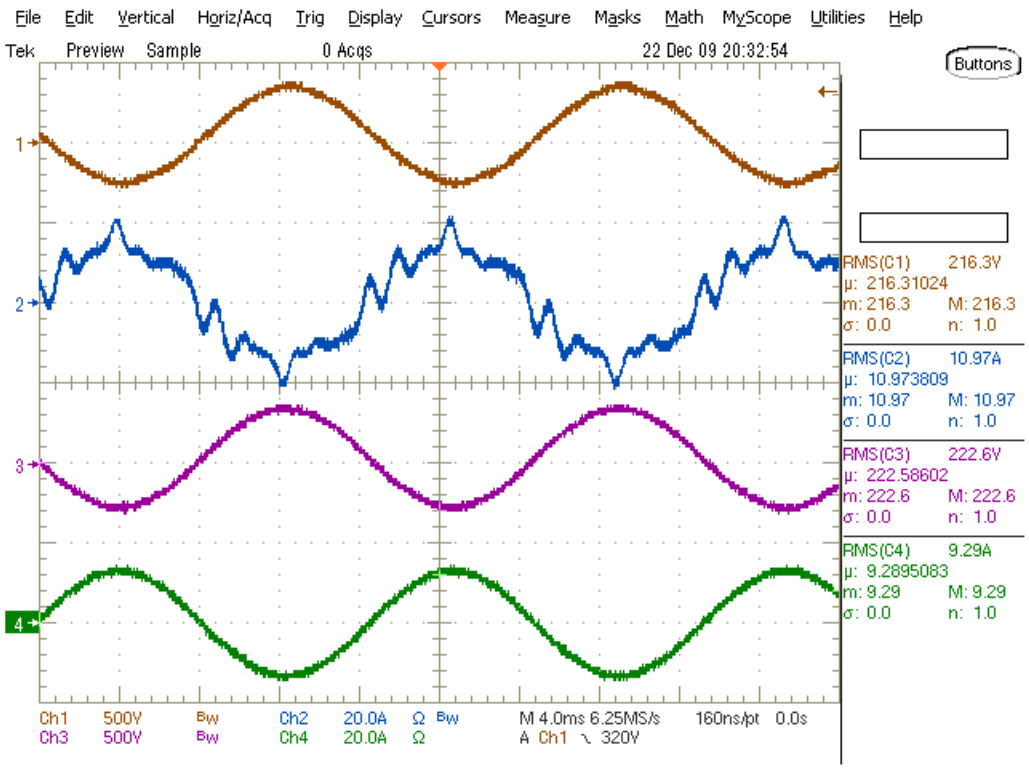

Figure 201: 2kW Efficiency Zoomed In
(Channel 1 = Vin, Channel 2 = Iin, Channel 3 = Vout, Channel 4 = Iout)

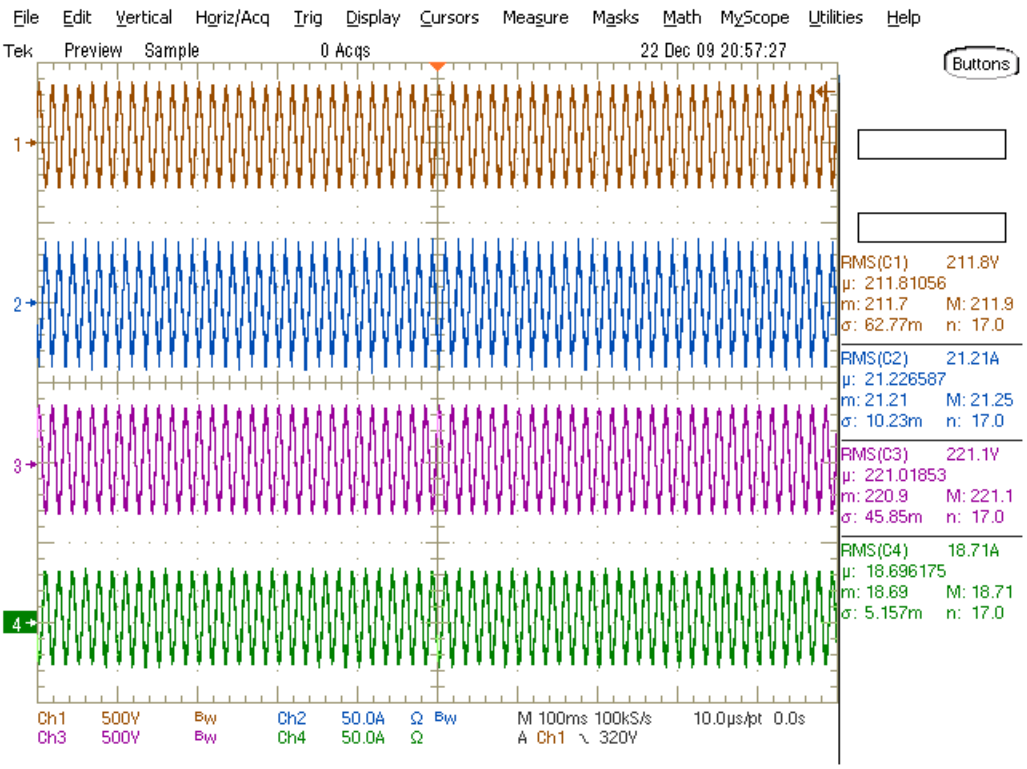

Figure 202: 4kW Efficiency Zoomed Out
(Channel 1 = Vin, Channel 2 = Iin, Channel 3 = Vout, Channel 4 = Iout)

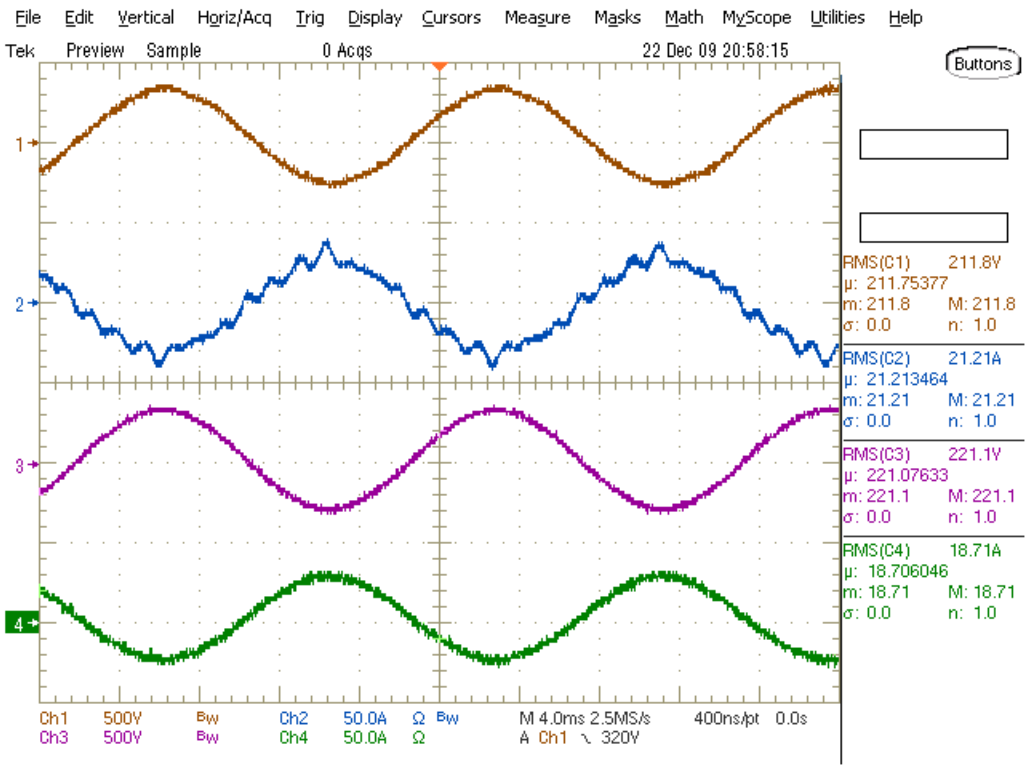

Figure 203: 4kW Efficiency Zoomed In
(Channel 1 = Vin, Channel 2 = Iin, Channel 3 = Vout, Channel 4 = Iout)

9.4 Replacement of Rectifier Diodes

The final efficiency testing that was done was to take the same setup as in section 9.3 and modify the rectifier instead. As explained in the previous sections, the testing up to this point was done with only modifications to the inverter. The rectifier circuitry was completely intact, and is used here as a test bed for a final test. The results here can be compared to the results in section 9.3, since the inverter here will be exactly the same as that section. The rectifier modification that was made was to remove only the diode devices and replace them with Cree SiC 2x10A dual diode packs. The IGBT devices and all associated gate drive circuitry were kept original for the rectifier switches.

The test data is summarized in table 32 below. Note again that the testing was done at three different load levels in order to get a wide system understanding of the impact SiC devices can have. In Figures 204 through 209 the input voltage/current and output voltage/current waveforms are shown in two different zoom for the different load levels.

Comparing the data in table 32 to the data in table 31, we can see how the efficiency was affected by converting the inverter switching devices to SiC. It is interesting to note that the efficiency decreased significantly at 1kW (-1.34%), at 2kW there was a slight decrease in efficiency (-0.26%), and at 4kW the efficiency actually increased significantly (0.96%).

Table 32: SiC Inverter and SiC Rectifier Diodes 6kVA UPS Efficiency Testing

1kW: SiC Inverter with 11.8Ohm Rg & Rectifier Diodes							
Vin:	216.80V	Iin:	6.31A	Pin:	1368.44W		
Vout:	222.70V	Iout:	4.63A	Pout:	1030.66W	Efficiency:	**75.32%**

2kW: SiC Inverter with 11.8Ohm Rg & Rectifier Diodes							
Vin:	215.50V	Iin:	11.02A	Pin:	2374.81W		
Vout:	222.40V	Iout:	9.28A	Pout:	2063.43W	Efficiency:	**86.89%**

4kW: SiC Inverter with 11.8Ohm Rg & Rectifier Diodes							
Vin:	213.50V	Iin:	21.09A	Pin:	4502.72W		
Vout:	222.50V	Iout:	18.83A	Pout:	4189.68W	Efficiency:	**93.05%**

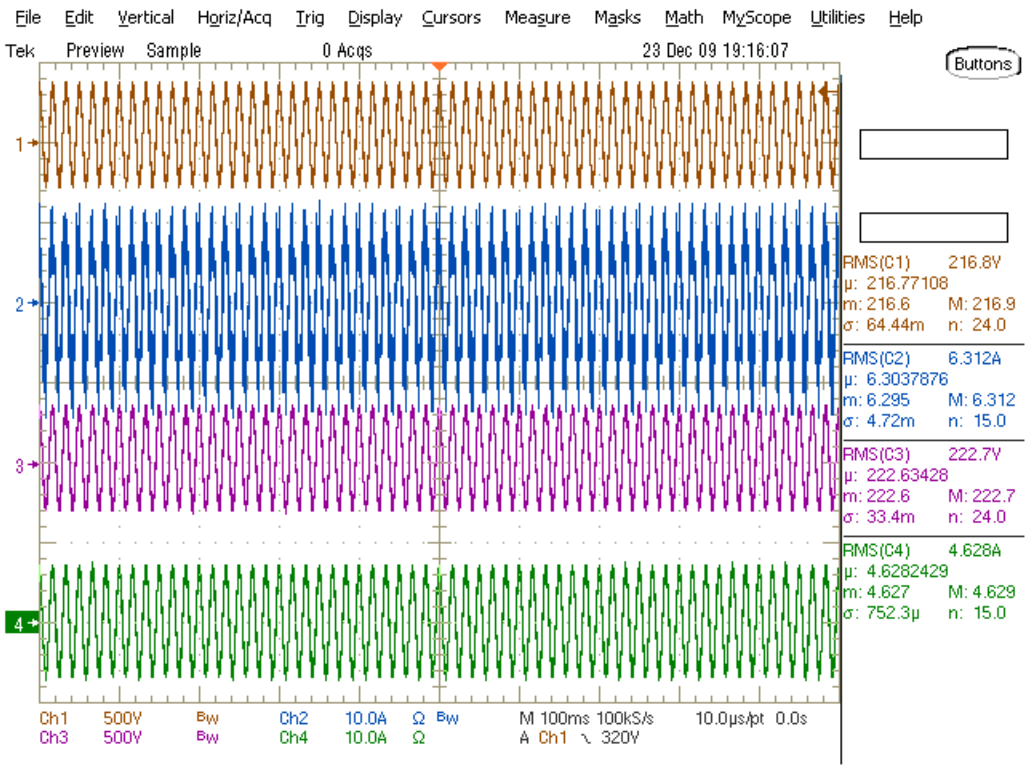

Figure 204: 1kW Efficiency Zoomed Out
(Channel 1 = Vin, Channel 2 = Iin, Channel 3 = Vout, Channel 4 = Iout)

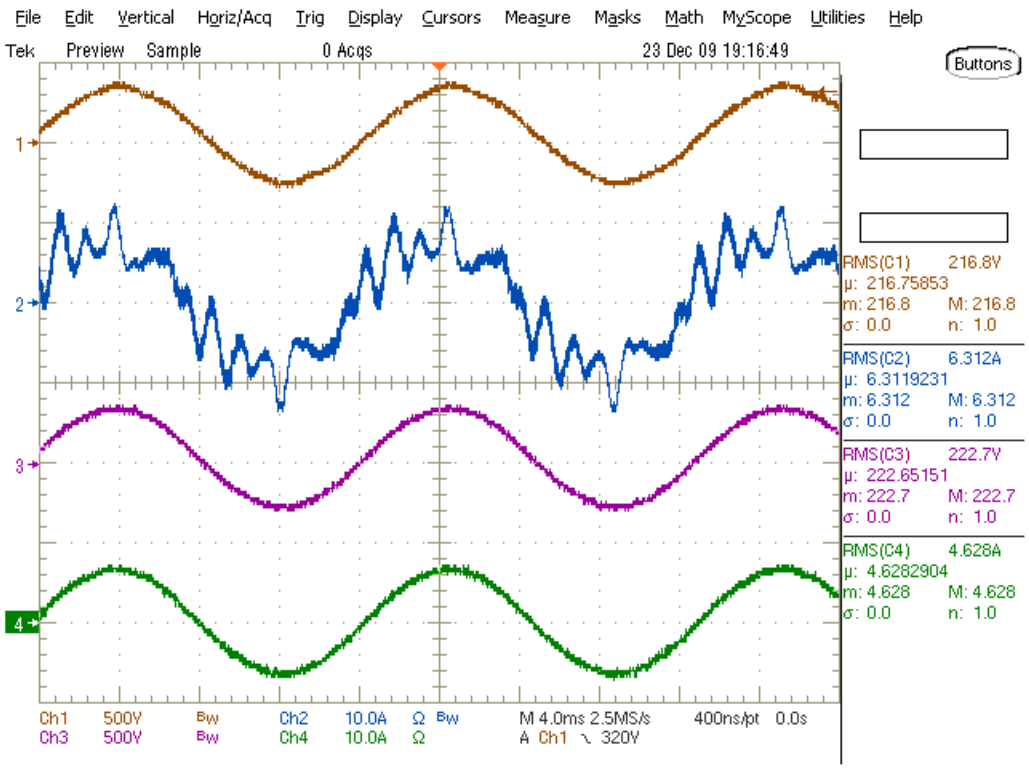

Figure 205: 1kW Efficiency Zoomed In
(Channel 1 = Vin, Channel 2 = Iin, Channel 3 = Vout, Channel 4 = Iout)

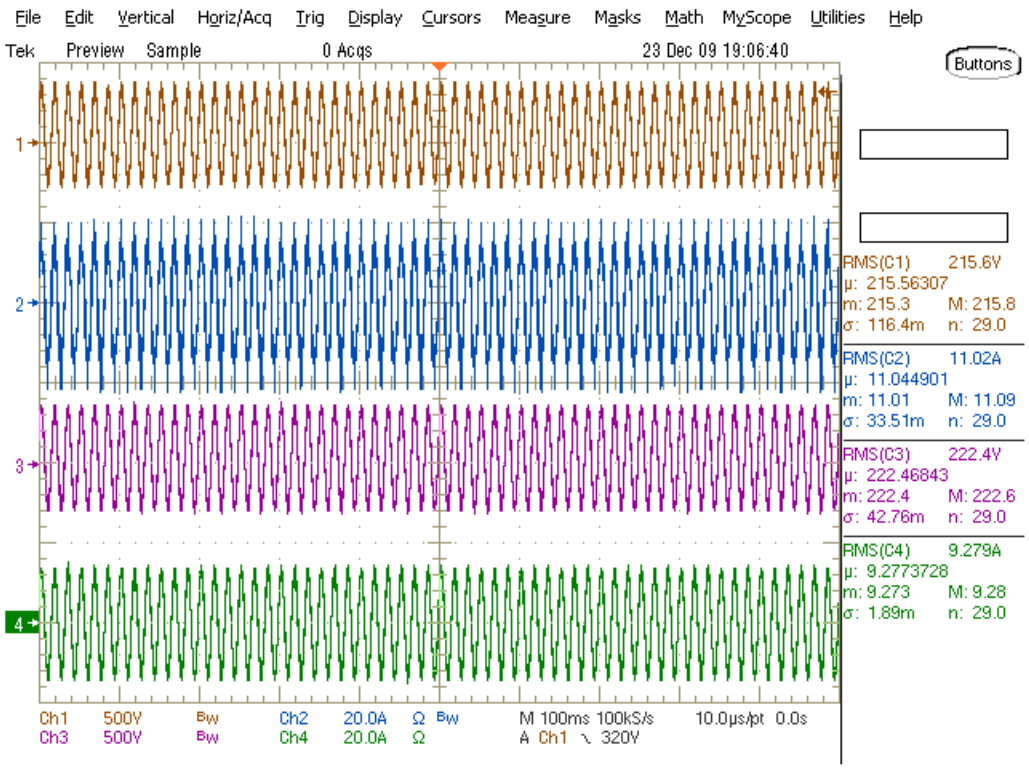

Figure 206: 2kW Efficiency Zoomed Out
(Channel 1 = Vin, Channel 2 = Iin, Channel 3 = Vout, Channel 4 = Iout)

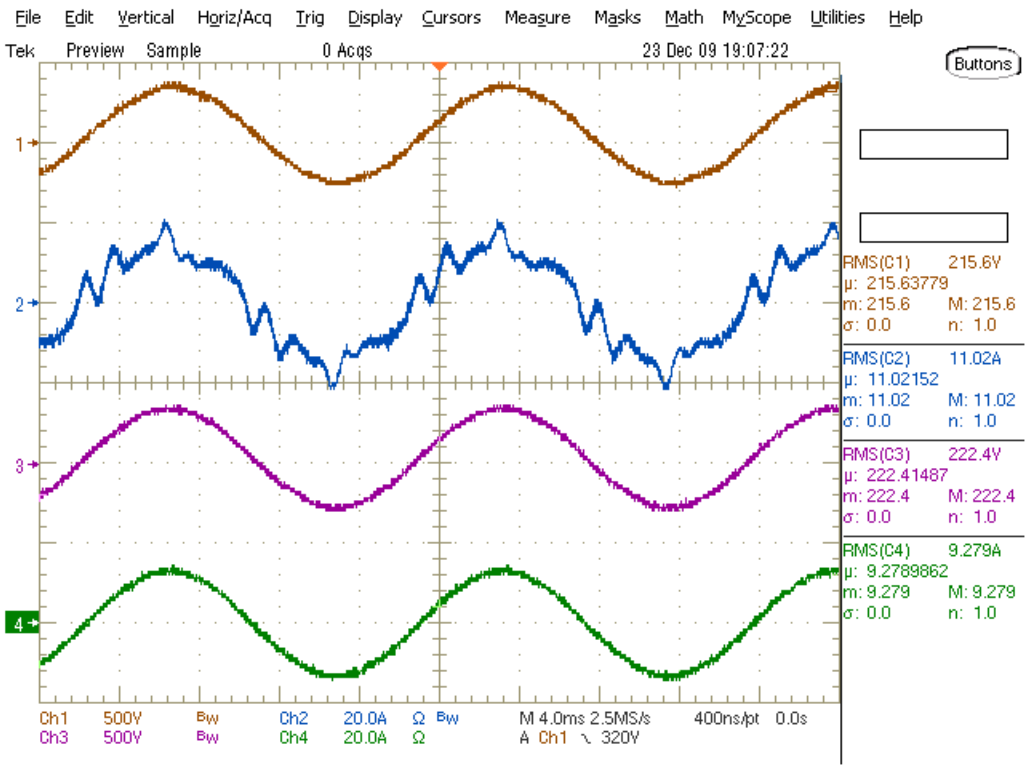

Figure 207: 2kW Efficiency Zoomed In
(Channel 1 = Vin, Channel 2 = Iin, Channel 3 = Vout, Channel 4 = Iout)

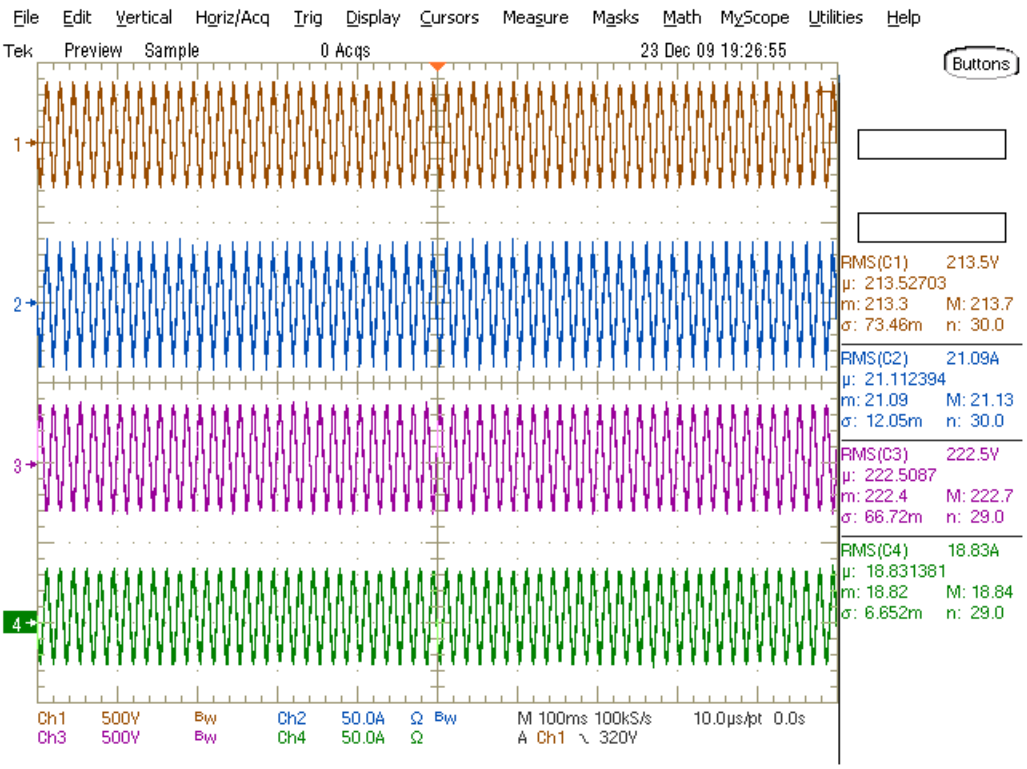

Figure 208: 4kW Efficiency Zoomed Out
(Channel 1 = Vin, Channel 2 = Iin, Channel 3 = Vout, Channel 4 = Iout)

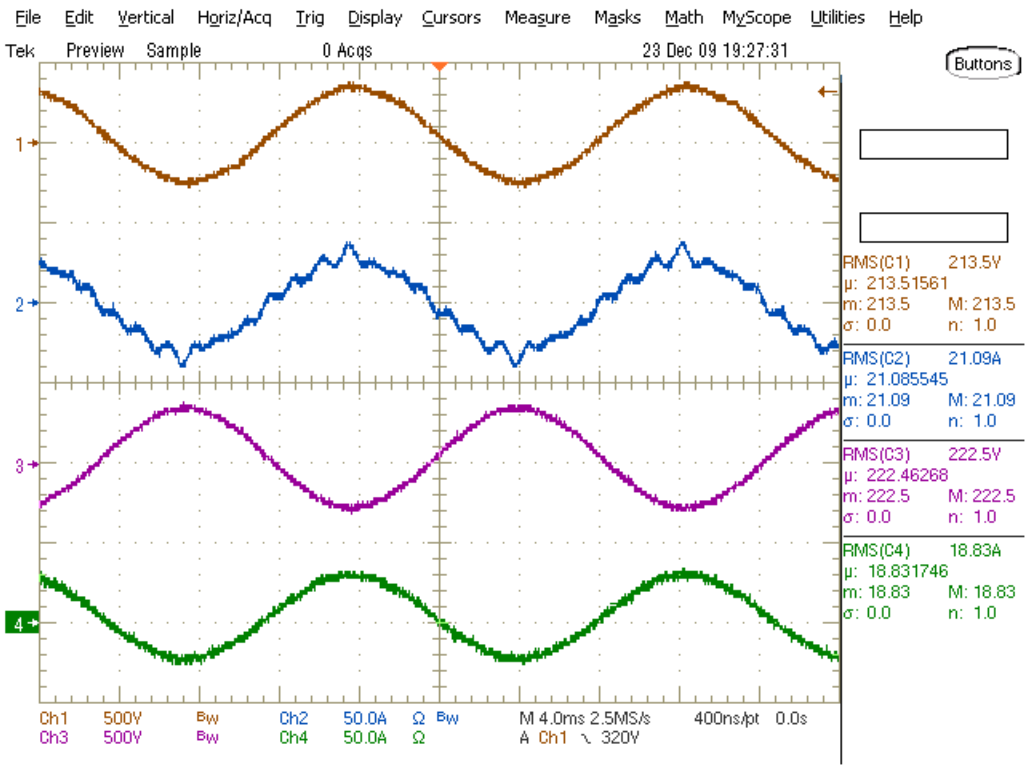

Figure 209: 4kW Efficiency Zoomed In
(Channel 1 = Vin, Channel 2 = Iin, Channel 3 = Vout, Channel 4 = Iout)

9.5 Summary and Conclusions

One key takeaway from this exercise is that the Cree SiC MOSFET devices should not be treated as a drop-in replacement for any IGBT device unless careful consideration of the gate drive circuitry has been made. An important characteristic of the SiC MOSFET device is its very smooth transition from the linear region of operation to the saturated constant-current region of operation on the I-V curve. In order to show this comparison, the I-V curve for the CMF20120D SiC MOSFET is shown below in Figure 210 and the I-V curve for a typical MOSFET is shown below in Figure 211. The MOSFET used

is a 900V Infineon CoolMOS IPW90R120C3 device. The figure is used merely as a comparison of the shape of the I-V curve and not to compare the actual values of conduction losses. Both I-V curves are for the devices at 25C junction temperature, and both devices are rated for roughly 20Amps at elevated junction temperature.

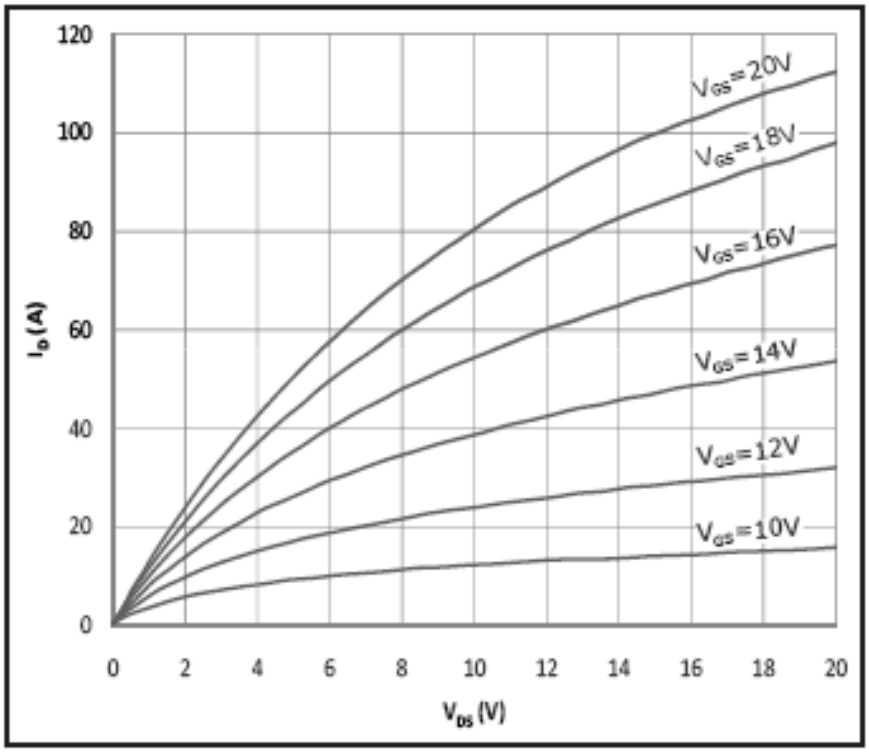

Figure 210: I-V curve for CMF20120D SiC MOSFET at 25C

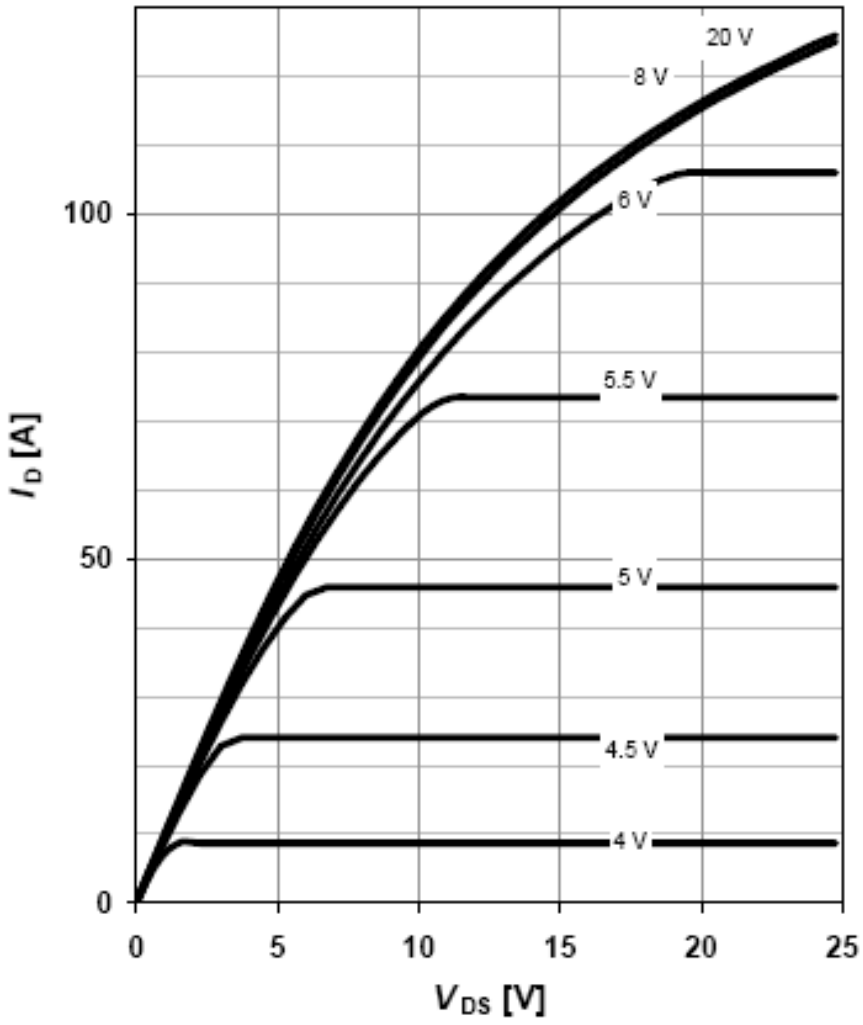

Figure 211: I-V curve for IPW90R120C3 MOSFET at 25C

What we see from the second figure is that the standard silicon MOSFET exhibits a very distinct transition from the linear region in which the device has a relatively constant Rds,on to the constant current region where the device essentially will not allow anymore current to flow through the D-S terminals. For example, at 5Vgs, the Rds,on is almost exactly 120mOhms all the way up to roughly 45Amps of current after which it will

not allow anymore than about 45Amps of current. Additionally, the Rds,on is not significantly affected by the gate-source voltage provided that the device is still in the linear region. The SiC MOSFET, on the other hand, shows a very "soft" transition. Lets take the case where Vgs = 18V, as in our testing for this chapter. We can see that at 20Amps, the voltage drop is roughly 2Volts and the Rds,on is relatively constant at 2V/20A = 100mOhms. As the device conducts currents higher than 20Amps, however, the Rds,on actually increases as the device slowly transitions into the constant current region over the course of 20-100Amps. This means that the 100mOhm Rds,on that was expected is not necessarily valid for the peak currents of the sine wave that the device will see. The main takeaway here is that the SiC devices should have a gate driver that can deliver 20Vgs in order to fully take advantage of the device conduction characteristics. The 20A rating for the device is even listed on the datasheet specifically for a 20V Vgs rating.

The other way the gate driver can affect the performance of the SiC MOSFET devices is the switching losses. It was not possible to obtain any dynamic switching waveforms for this UPS application due to the extremely tight proximity of the devices to gate drive components, controls components, the heatsink, and other parts. This was attempted early on in the testing and ended up damaging the power board of the UPS. Once the power board was repaired, it was deemed too risky to try again due to the scheduling of the project and availability of more parts to fix the power board should another failure occur. We can, however, use the knowledge gained from earlier chapters of this report to help understand how the gate driver affects the SiC MOSFET devices. Testing on the Cree SiC MOSFET

was done in sections 5.14 and 6.4 of this report. The initial test was done using a standard IGBT gate driver that utilized +15V gate voltage and a driver IC that was setup to deliver less than 1 Amp of current to the gate. This caused the device to perform very poorly, as can be seen below in Table 33. We can see from the table that the turn on loss doubles by simply using a 20V gate driver instead of 15V. Furthermore, when dropping the gate resistor to the one specified in the datasheet both losses are reduced significantly. Although the driver for this UPS uses a switchmode power supply that tries to regulate 18V, the actual loaded voltage is closer to 17V in practice as measured during testing. Because of this, we can assume the losses are slightly lower than what is shown in column 1. We did reduce the gate resistor in section 9.3, but that did not help as much as hoped because this forced the gate voltage to drop even further when more current was drawn.

Table 33: SiC MOSFET Dynamic Results (Units are in uJ)

	CMF20120D Losses at 800V 20A		
	19Ohm, 15V	19Ohm, 20V	10Ohm, 20V
Eoff	430	455	294
Eon	1580	731	475
Etotal	**2010**	**1186**	**769**

A summary of the efficiency data from the previous sections is combined below in Table 34. Comparing columns 1 and 2, we see that the efficiency improved when changing the inverter devices to all SiC only at 1kW load. At 2kW load, the efficiency actually decreased very slightly and at 4kW load the efficiency decreased very significantly. What this tells us is that the device losses in this system are heavily dominated by conduction losses, especially at the higher end of load levels. At the lower loads, the silicon devices

have much worse conduction loss characteristics. This is due to the fact that the IGBT has a bipolar knee voltage that must be overcome when conducting. This creates a lower limit for the amount of Vce,sat that can be achieved at lower loads. The I-V characteristics for the HGTG27N120BN IGBT is shown below in Figure 212 for reference. You can see that even at very light loads, a knee voltage is present. The SiC MOSFET, on the other hand, simply has an Rds,on while in the triode region. As the load increases, the IGBT has a much smaller equivalent series resistance compared to the MOSFET's Rds,on. As such, and in addition to the soft transition between the linear and saturation region discussed earlier causes the MOSFET to increase conduction voltage faster than the IGBT.

Table 34: Summary of Efficiency Performance

	Si Devices	SiC Inverter	SiC Inverter Lower Rg	SiC Inverter Lower Rg Rectifier Diode
1kW	73.97%	75.18%	76.66%	75.32%
2kW	86.11%	85.99%	87.15%	86.89%
4kW	92.18%	91.17%	92.09%	93.05%

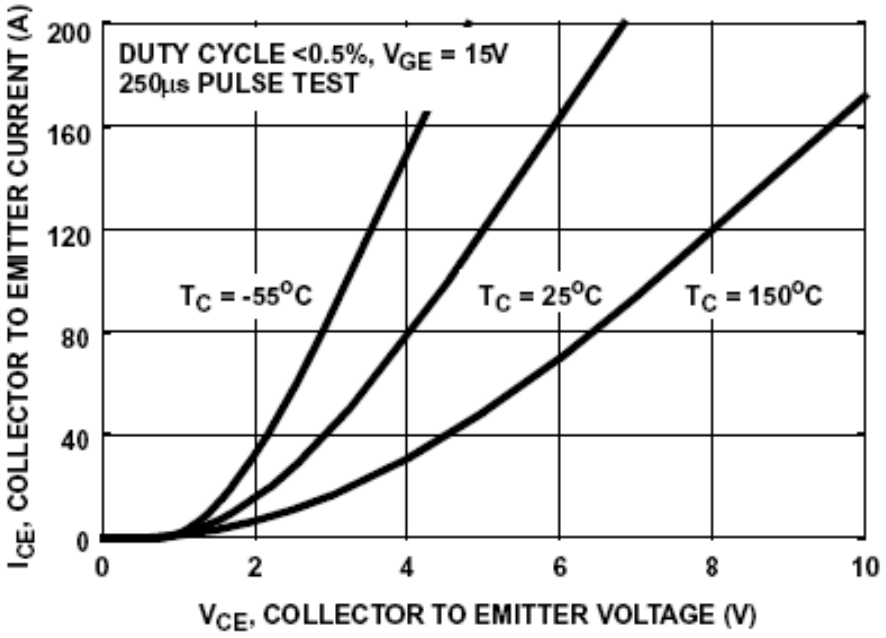

Figure 212: I-V Characteristics for HGTG27N120BN IGBT

The main benefit of the SiC MOSFET devices is their incredibly quick switching speed. This speed, however, is limited in our case by the driver IC's ability to quickly charge and discharge the gate capacitance. The driver IC used in this UPS (the HCNW3120) has a maximum output current limited to 2 Amperes. Since there are two devices in parallel, the driver capability is limited to only 1 Amp per device. Because of this, we were able to reduce the switching losses slightly by reducing the gate resistance in the circuit, but only a slight efficiency improvement was possible. In table 9.5.2 above, we can compare columns 1 and 3 to see the best possible efficiency gain we could achieve for the inverter after modifying the gate driver resistor values. We see that the efficiency benefit is a very substantial 2.67% improvement at 1kW and is even substantial at just over 1% for 2kW. At 4kW, however, the efficiency does not see a significant benefit when using the SiC devices

(actually 0.10% worse efficiency). It is very important to note that the SiC devices used were much lower rating than the Silicon devices compared to. What was done here is to replace 70Amps worth of IGBT's with 40Amps worth of SiC MOSFET current rating. The diodes were converted from 30Amps worth of Silicon Diode current rating to 20Amps worth of SiC Diode current rating. On top of this, the efficiency improved very significantly at lower loads and is a wash at full load. This shows a clear benefit from using SiC devices in a UPS inverter especially keeping in mind that the devices were only partially optimized and could get much better if gate driver circuitry was designed specifically for the SiC needs of the MOSFETs tested. A plot of the efficiency curves from 1kW to 4kW has been shown in Figure 213 below.

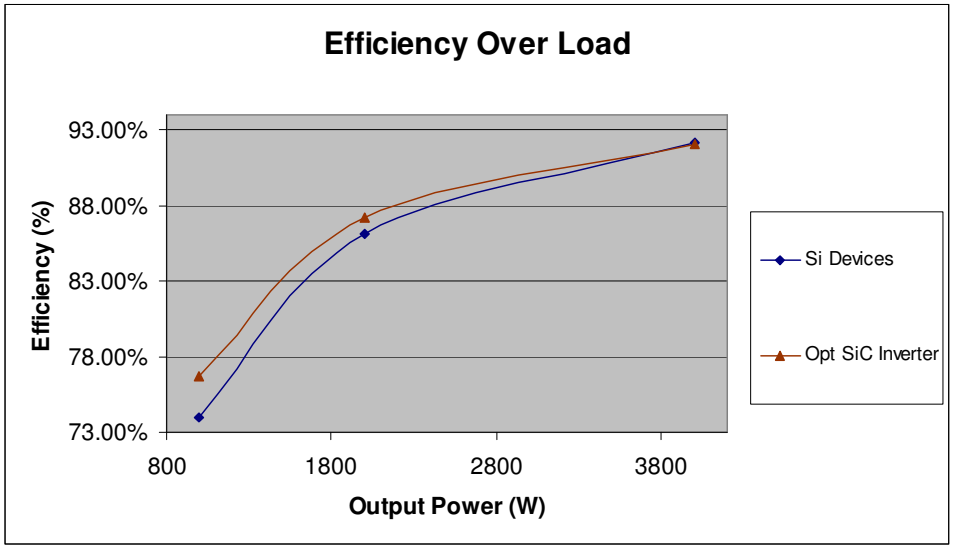

Figure 213: Efficiency Curves for Original Testing and Optimized SiC Inverter
(Silicon IGBTs are 2x34A = 68A current rating, SiC MOSFETs are 2x20A = 40A current rating)

The rectifier testing in this chapter set out to measure how much efficiency gain could be gained by simply replacing the diodes in the power circuit with SiC Diodes and keeping the silicon IGBT's in tact. Also, no modifications were made to gate drive circuitry. The SiC diodes exhibit no reverse recovery and therefore improve the turn on behavior in the silicon IGBTs as seen in Chapter 5 of this report. The comparison from Table 34 must be made between columns 3 and 4, since the inverter was kept identical between the two. The only change made between the two columns was that each 30A Fairchild ISL9R30120G2 diode was replaced by a 20A Cree C2D20120D SiC double diode. The TO-247 package actually contains two paralleled 10A SiC diodes internally. Again, we replaced 30Amps worth of silicon current rated devices with 20Amps worth of SiC current rated devices. For this experiment, we can see from Table 34 that the efficiency results were actually opposite from the previous exercise. The efficiency actually got worse at 1kW and 2kW loads (-1.34% and -0.26% reduction in efficiency respectively) and improved substantially at 4kW load (0.96% improvement). A plot of efficiency curves from 1kW to 4kW for these two experiments has been shown in Figure 214 below. The data results tell us that at low loads, the higher conduction characteristics of the SiC devices and the fact that only 20A rating of SiC diode was used instead of 30A rating of silicon diode caused the conduction losses to dominate and actually hurt the converter efficiency more than the benefit from not having reverse recovery energy. During the higher load levels, however, the high peak currents that are switched on and off cause very high reverse recovery losses with the Silicon diodes. At the higher current levels, the improvement in dynamic switching characteristics of the SiC

diodes outweighs the worse conduction characteristics of the SiC devices and the lower current rating of the devices.

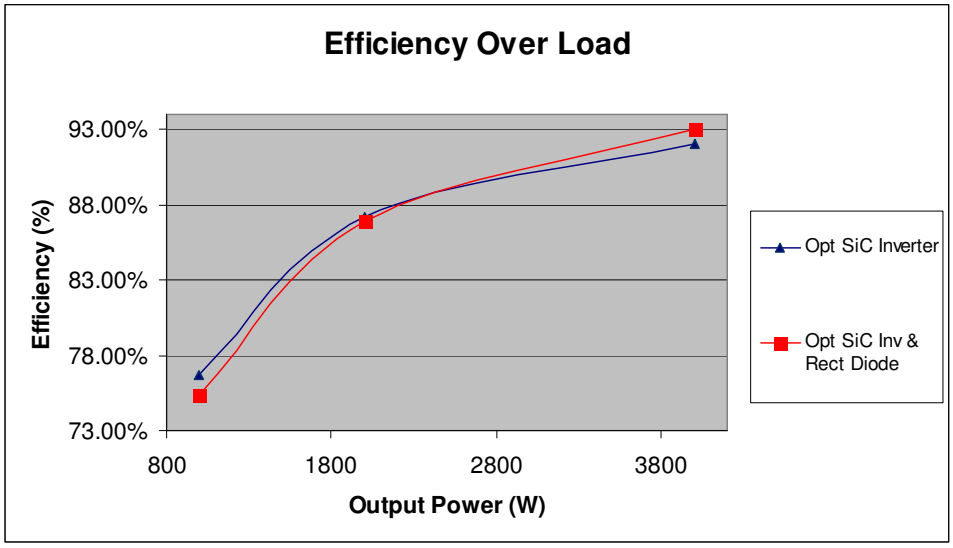

Figure 214: Efficiency Curves for Rectifier Diode Testing
(Silicon Diodes are 1x30A = 30A current rating, SiC Diodes are 2x10A = 20A current rating)

CHAPTER 10

10 CONCLUSION

This project consisted of three major sections, each building upon the other. In the first section consisting of Chapters 2-4, a loss computation tool was developed, evaluated and used to understand efficiency characteristics of various devices. The motivation of this section was the need for a standardized and flexible tool for use at the authors company. Since the beginning of this project work, the tool has been used in UPS design projects already in a global design project and has proven to meet all expectations for the project. Further, the tool was used in an evaluation by the company to determine the benefits of using a 3-level NPC inverter topology in a next generation UPS design.

In the second section of this project consisting of Chapters 5-7, switching devices from several design generations, manufacturers, and semiconductor material were bench tested for dynamic switching performance. The purpose of this section was to get an understanding of how different devices operated in a controlled environment where each device could be tested on exact apples to apples basis with the same conditions all around. The testing showed clear benefits in dynamic performance of post-silicon devices such as SiC JFET and MOSFET devices. The devices have either recently hit the market or are soon to hit the market and an analysis of how they perform compared to their silicon counterparts is very useful to a power electronics designer. The testing gives an understanding of how generations of IGBTs have improved as well as how different manufacturers' tradeoff turn

on vs. turn off performance. Also, a survey of how different diodes affect the turn on waveforms for a specific switch was studied.

The third section of this report details testing done on two real world power designs. The first is a two switch two output winding 300W flyback power supply and the second is a double conversion true online 6kVA UPS. The two power systems were evaluated first from an efficiency standpoint using their original silicon switching devices and next using up-and-coming SiC switching devices. The same devices were used in this section as were tested in the second section of this report. This section of the report shows how SiC devices can significantly help the efficiency of a power electronic system, but also brings up very important concerns about the ability to use SiC MOSFETs as a drop in replacement for traditional Silicon IGBT devices. Gate driver current drive capability and voltage level off the drive were the two issues identified as needing to be increased in order to utilize the SiC MOSFET devices. The gate drive modifications are minor, but are definitely substantial enough that they should be addressed at the beginning of a design and not used as a patch up. What this means to the designer is that SiC switching devices could be used in new designs, but likely not for an old design where gate drive circuitry is difficult to change.

REFERENCES

[1] Agarwal, Anant et al. "Advanced HF SiC MOS Devices". EPE 2009 – Barcelona, 2009.

[2] Bell, Bob. "Two-Switch Topology Benefits Forward and Flyback Power Converters". EDN Magazine. Sept 2000: 107-111.

[3] B.J. Baliga, *Fundamentals of Modern Switching Devices*, Springer-Verlag, 2008, New York.

[4] "CoolMOS C3 900V Product Brief". Infineon Application Note. 2008

[5] Covi, Kevin, "IGBTs Challenge MOSFETs in Switching Power Supplies". IBM Technical Paper, 2006.

[6] Erickson, Robert and Dragan Maksimovic. *Fundamentals of Power Electronics*. Norwell, MA: Kluwer Academic Publishers, 2001.

[7] "Examination of Reverse Recovery Losses in a Synchronous Buck Converter Circuit". Silicon Semiconductor Application Note, 2003.

[8] Graovac, Dusan and Marco Purschel, "IGBT Power Losses Calculation Using the Data-Sheet Parameters". Infineon Application Note. Jan 2009

[9] Jang, Yungtaek et al, “Performance Evaluation of Silicon-Carbide MOSFET in Three-Phase High-Power-Factor Rectifier”. Delta Products Corporation Power Electronics Laboratory.

[10] Lebron-Velilla, Ramon and Gene Schwarze, “Silicon Carbide Diodes Performance Characterization and Comparison With Silicon Devices”. NASA Glenn Research Center, Aug 2003.

[11] McNutt, Ty et al, “Silicon Carbide JFET Cascode Switch for Power Conditioning Applications”. Northrop Grumman Advanced Technology Laboratory.

[12] Melkonyan, Ashot. “High Efficiency Power Supply Using New SiC Devices”. Kassel University Press, 2006.

[13] Mohan, Ned, Tore Undeland and William Robbins. *Power Electronics - Converters, Applications, and Design*. New York, NY: John Wiley & Sons, 2003.

[14] O’Neill, Michael, “Silicon Carbide”. Power Electronics Technology Jan 2005: 14-22

[15] O’Neill, Michael, “Silicon Carbide MOSFETs Challenge IGBTs”. Power Electronics Technology Sep 2008.

[16] Pierobon et al, “Characterization of Schottky SiC Diodes for Power Applications”. Department of Electronics and Informatics – University of Padova Italy.

[17] Rajapakse, A.D., A.M. Gole, and P.L. Wilson, “Approximate Loss Formulae for Estimation of IGBT Switching Losses through EMTP-type Simulations”. IEEE paper.

[18] Richmond, Jim et al, “An Overview of Cree Silicon Carbide Power Devices”. Cree Application Note, 2004.

[19] Sannuti, P et al, “Channel Electron Mobility in 4H-SiC Lateral Junction Field Effect Transistors”. Solid-State Electronics 2005: 1900-1904.

[20] Shenai et al, “Optimum Semiconductors for High-Power Electronics”. IEEE Paper, 1989.

[21] “Silicon Carbide Enhanced-Mode Junction Field Effect Transistor and Recommendations for Use”. SemiSouth Application Note AN-SS1. Aug 2009.

[22] Skibinski, et al, “Developments in Hybrid Si-SiC Power Modules”. Rockwell Automation Paper, Nov 2006.

[23] Um, K.J. “Application Note 9020: IGBT Basic II”. Fairchild Application Note. Apr 2002

[24] Zhang, Hui and Leon Tolbert, “Efficiency of SiC JFET-Based Inverters”. Department of Electrical Engineering, The University of Tennessee.

APPENDICES

APPENDIX A:

IR Datasheet for IRG4PH50KD

International
IOR Rectifier

PD- 91575B

IRG4PH50KD

INSULATED GATE BIPOLAR TRANSISTOR WITH ULTRAFAST SOFT RECOVERY DIODE

Short Circuit Rated
UltraFast IGBT

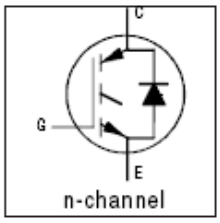

V_{CES} = 1200V

$V_{CE(on)\ typ.}$ = 2.77V

@V_{GE} = 15V, I_C = 24A

Features

- High short circuit rating optimized for motor control, t_{sc} =10µs, V_{CC} = 720V , T_J = 125°C, V_{GE} = 15V
- Combines low conduction losses with high switching speed
- Tighter parameter distribution and higher efficiency than previous generations
- IGBT co-packaged with HEXFRED™ ultrafast, ultrasoft recovery antiparallel diodes

Benefits

- Latest generation 4 IGBT's offer highest power density motor controls possible
- HEXFRED™ diodes optimized for performance with IGBTs. Minimized recovery characteristics reduce noise, EMI and switching losses
- This part replaces the IRGPH50KD2 and IRGPH50MD2 products
- For hints see design tip 97003

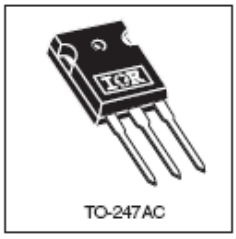

TO-247AC

Absolute Maximum Ratings

	Parameter	Max.	Units
V_{CES}	Collector-to-Emitter Voltage	1200	V
I_C @ T_C = 25°C	Continuous Collector Current	45	A
I_C @ T_C = 100°C	Continuous Collector Current	24	
I_{CM}	Pulsed Collector Current ①	90	
I_{LM}	Clamped Inductive Load Current ②	90	
I_F @ T_C = 100°C	Diode Continuous Forward Current	16	
I_{FM}	Diode Maximum Forward Current	90	
t_{sc}	Short Circuit Withstand Time	10	µs
V_{GE}	Gate-to-Emitter Voltage	± 20	V
P_D @ T_C = 25°C	Maximum Power Dissipation	200	W
P_D @ T_C = 100°C	Maximum Power Dissipation	78	
T_J	Operating Junction and	-55 to +150	°C
T_{STG}	Storage Temperature Range		
	Soldering Temperature, for 10 sec.	300 (0.063 in. (1.6mm) from case)	
	Mounting Torque, 6-32 or M3 Screw.	10 lbf•in (1.1 N•m)	

Thermal Resistance

	Parameter	Min.	Typ.	Max.	Units
$R_{\theta JC}$	Junction-to-Case - IGBT	—	—	0.64	°C/W
$R_{\theta JC}$	Junction-to-Case - Diode	—	—	0.83	
$R_{\theta CS}$	Case-to-Sink, flat, greased surface	—	0.24	—	
$R_{\theta JA}$	Junction-to-Ambient, typical socket mount	—	—	40	
Wt	Weight	—	6 (0.21)	—	g (oz)

Electrical Characteristics @ T_J = 25°C (unless otherwise specified)

	Parameter	Min.	Typ.	Max.	Units	Conditions
$V_{(BR)CES}$	Collector-to-Emitter Breakdown Voltage③	1200	—	—	V	V_{GE} = 0V, I_C = 250µA
$\Delta V_{(BR)CES}/\Delta T_J$	Temperature Coeff. of Breakdown Voltage	—	0.91	—	V/°C	V_{GE} = 0V, I_C = 1.0mA
$V_{CE(on)}$	Collector-to-Emitter Saturation Voltage	—	2.77	3.5	V	I_C = 24A V_{GE} = 15V
		—	3.28	—		I_C = 45A See Fig. 2, 5
		—	2.54	—		I_C = 24A, T_J = 150°C
$V_{GE(th)}$	Gate Threshold Voltage	3.0	—	6.0	V	V_{CE} = V_{GE}, I_C = 250µA
$\Delta V_{GE(th)}/\Delta T_J$	Temperature Coeff. of Threshold Voltage	—	-10	—	mV/°C	V_{CE} = V_{GE}, I_C = 250µA
g_{fe}	Forward Transconductance ④	13	19	—	S	V_{CE} = 100V, I_C = 24A
I_{CES}	Zero Gate Voltage Collector Current	—	—	250	µA	V_{GE} = 0V, V_{CE} = 1200V
		—	—	6500		V_{GE} = 0V, V_{CE} = 1200V, T_J = 150°C
V_{FM}	Diode Forward Voltage Drop	—	2.5	3.5	V	I_C = 16A See Fig. 13
		—	2.1	3.0		I_C = 16A, T_J = 150°C
I_{GES}	Gate-to-Emitter Leakage Current	—	—	±100	nA	V_{GE} = ±20V

Switching Characteristics @ T_J = 25°C (unless otherwise specified)

	Parameter	Min.	Typ.	Max.	Units	Conditions
Q_g	Total Gate Charge (turn-on)	—	180	270	nC	I_C = 24A
Q_{ge}	Gate - Emitter Charge (turn-on)	—	25	38		V_{CC} = 400V See Fig.8
Q_{gc}	Gate - Collector Charge (turn-on)	—	70	110		V_{GE} = 15V
$t_{d(on)}$	Turn-On Delay Time	—	87	—	ns	
t_r	Rise Time	—	100	—		T_J = 25°C
$t_{d(off)}$	Turn-Off Delay Time	—	140	300		I_C = 24A, V_{CC} = 800V
t_f	Fall Time	—	200	300		V_{GE} = 15V, R_G = 5.0Ω
E_{on}	Turn-On Switching Loss	—	3.83	—	mJ	Energy losses include "tail"
E_{off}	Turn-Off Switching Loss	—	1.90	—		and diode reverse recovery
E_{ts}	Total Switching Loss	—	5.73	7.9		See Fig. 9,10,18
t_{sc}	Short Circuit Withstand Time	10	—	—	µs	V_{CC} = 720V, T_J = 125°C
						V_{GE} = 15V, R_G = 5.0Ω
$t_{d(on)}$	Turn-On Delay Time	—	67	—	ns	T_J = 150°C, See Fig. 10,11,18
t_r	Rise Time	—	72	—		I_C = 24A, V_{CC} = 800V
$t_{d(off)}$	Turn-Off Delay Time	—	310	—		V_{GE} = 15V, R_G = 5.0Ω,
t_f	Fall Time	—	390	—		Energy losses include "tail"
E_{ts}	Total Switching Loss	—	8.36	—	mJ	and diode reverse recovery
L_E	Internal Emitter Inductance	—	13	—	nH	Measured 5mm from package
C_{ies}	Input Capacitance	—	2800	—	pF	V_{GE} = 0V
C_{oes}	Output Capacitance	—	140	—		V_{CC} = 30V See Fig. 7
C_{res}	Reverse Transfer Capacitance	—	53	—		f = 1.0MHz
t_{rr}	Diode Reverse Recovery Time	—	90	135	ns	T_J = 25°C See Fig.
		—	164	245		T_J = 125°C 14 I_F = 16A
I_{rr}	Diode Peak Reverse Recovery Current	—	5.8	10	A	T_J = 25°C See Fig.
		—	8.3	15		T_J = 125°C 15 V_R = 200V
Q_{rr}	Diode Reverse Recovery Charge	—	260	675	nC	T_J = 25°C See Fig.
		—	680	1838		T_J = 125°C 16 di/dt = 200A/µs
$di_{(rec)M}/dt$	Diode Peak Rate of Fall of Recovery	—	120	—	A/µs	T_J = 25°C See Fig.
	During t_b	—	76	—		T_J = 125°C 17

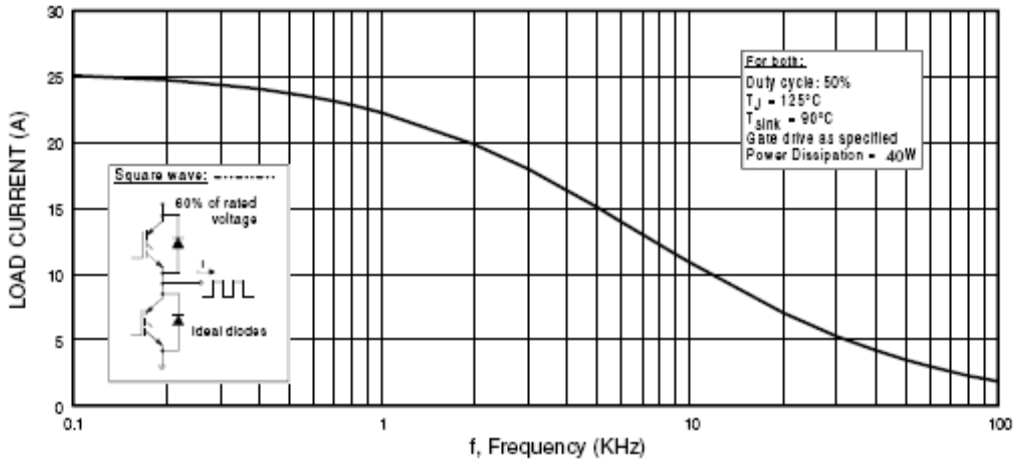

Fig. 1 - Typical Load Current vs. Frequency
(Load Current = I_{RMS} of fundamental)

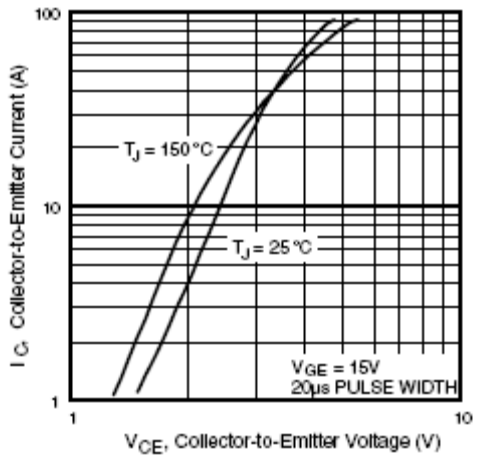

Fig. 2 - Typical Output Characteristics

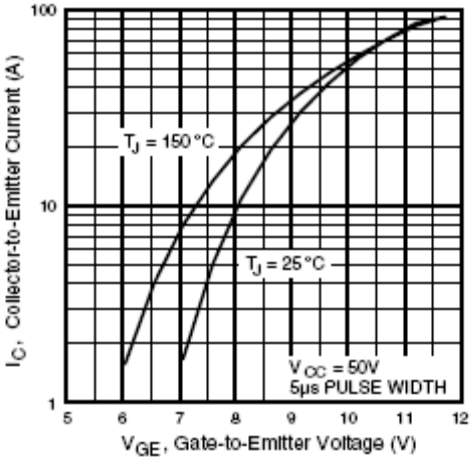

Fig. 3 - Typical Transfer Characteristics

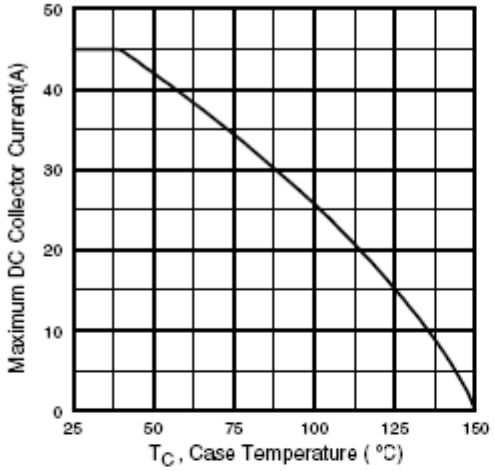

Fig. 4 - Maximum Collector Current vs. Case Temperature

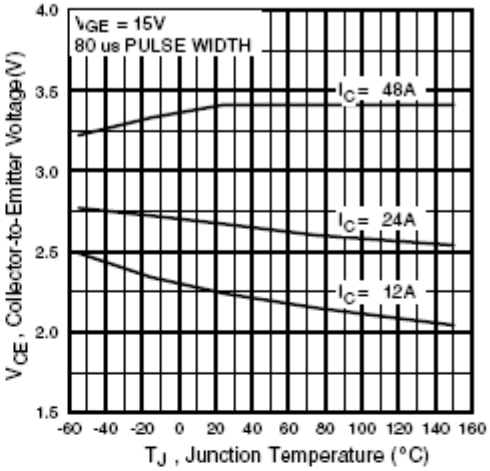

Fig. 5 - Typical Collector-to-Emitter Voltage vs. Junction Temperature

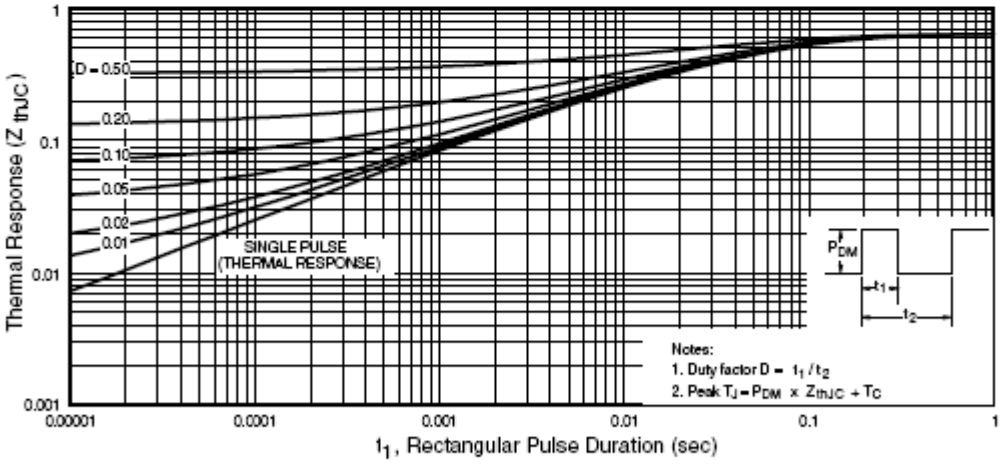

Fig. 6 - Maximum Effective Transient Thermal Impedance, Junction-to-Case

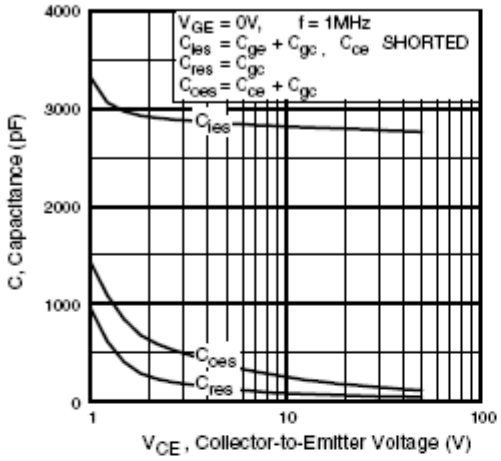

Fig. 7 - Typical Capacitance vs. Collector-to-Emitter Voltage

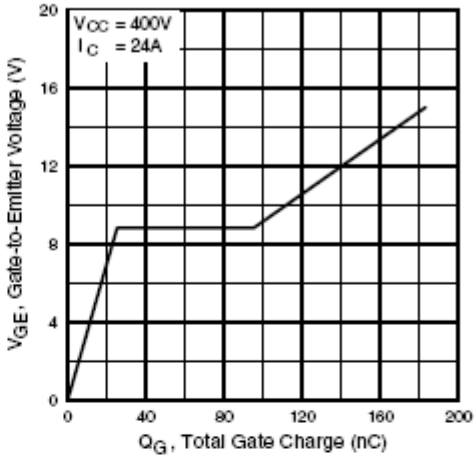

Fig. 8 - Typical Gate Charge vs. Gate-to-Emitter Voltage

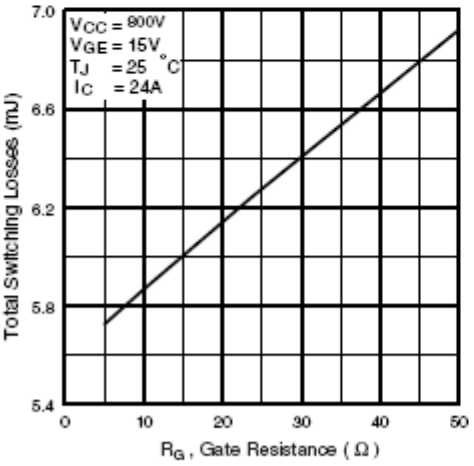

Fig. 9 - Typical Switching Losses vs. Gate Resistance

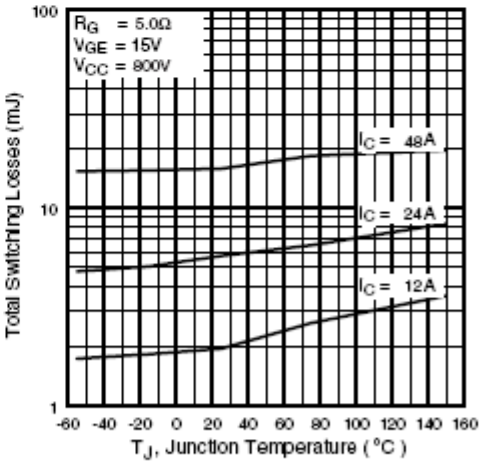

Fig. 10 - Typical Switching Losses vs. Junction Temperature

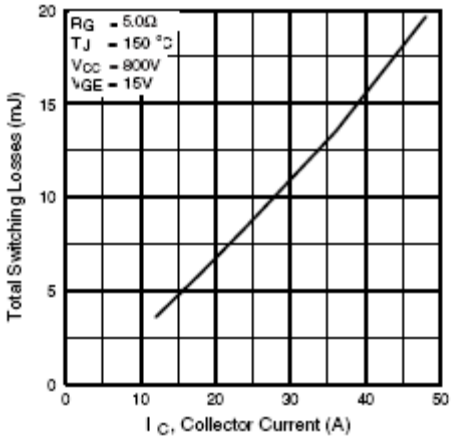

Fig. 11 - Typical Switching Losses vs. Collector Current

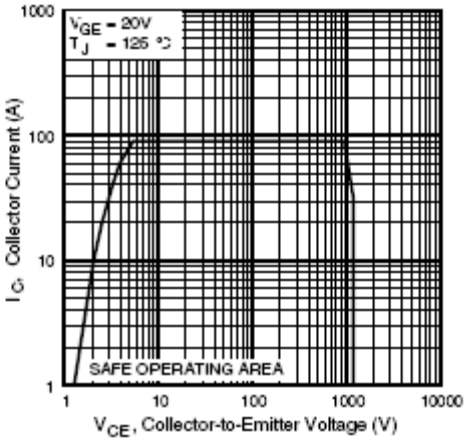

Fig. 12 - Turn-Off SOA

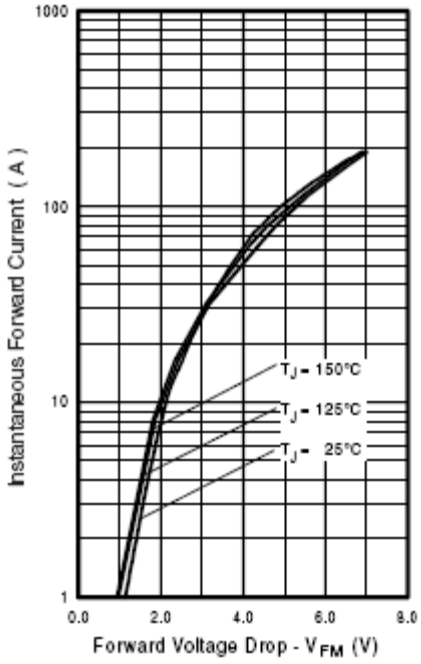

Fig. 13 - Typical Forward Voltage Drop vs. Instantaneous Forward Current

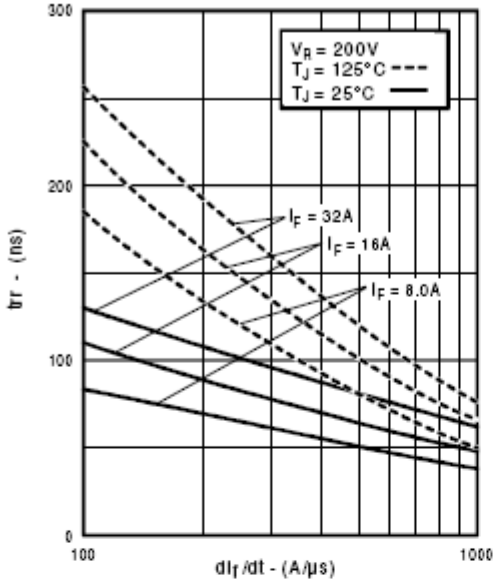

Fig. 14 - Typical Reverse Recovery vs. di_f/dt

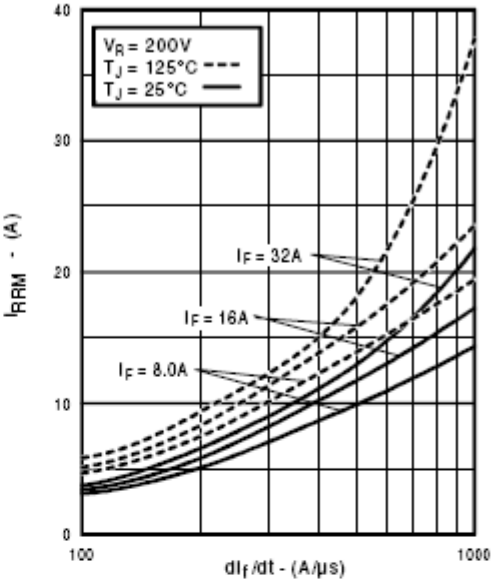

Fig. 15 - Typical Recovery Current vs. di_f/dt

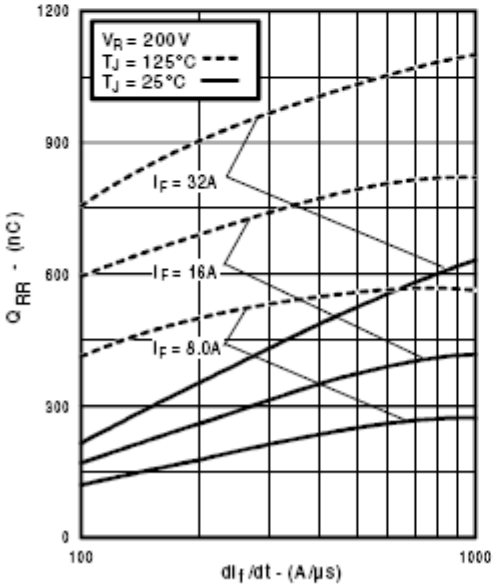

Fig. 16 - Typical Stored Charge vs. di_f/dt

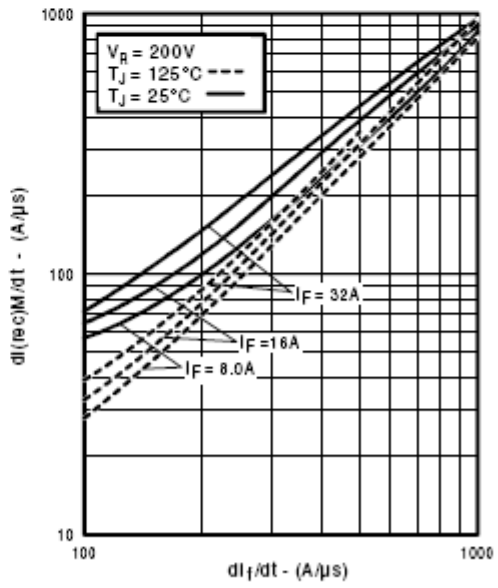

Fig. 17 - Typical $di_{(rec)M}/dt$ vs. di_f/dt

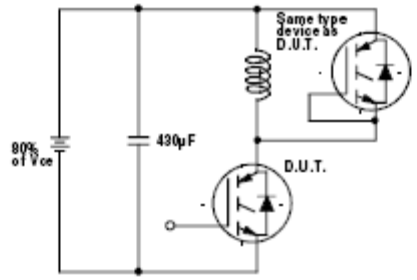

Fig. 18a - Test Circuit for Measurement of I_{LM}, E_{on}, $E_{off(diode)}$, t_{rr}, Q_{rr}, I_{rr}, $t_{d(on)}$, t_r, $t_{d(off)}$, t_f

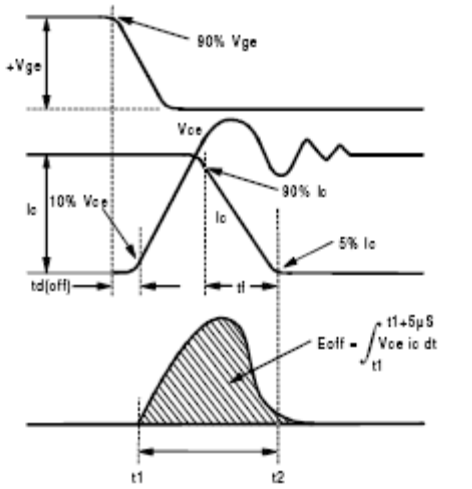

Fig. 18b - Test Waveforms for Circuit of Fig. 18a, Defining E_{off}, $t_{d(off)}$, t_f

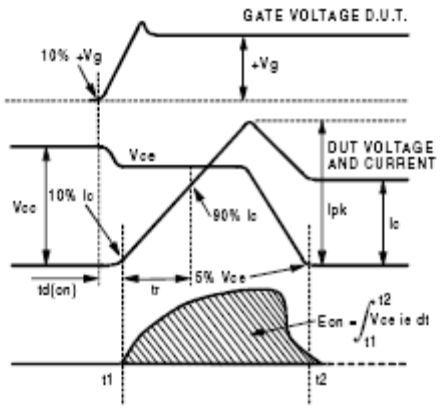

Fig. 18c - Test Waveforms for Circuit of Fig. 18a, Defining E_{on}, $t_{d(on)}$, t_r

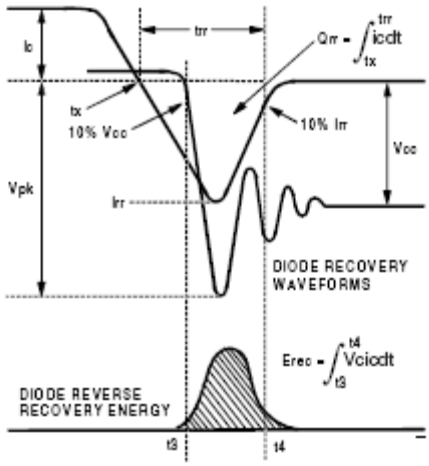

Fig. 18d - Test Waveforms for Circuit of Fig. 18a, Defining E_{rec}, t_{rr}, Q_{rr}, I_{rr}

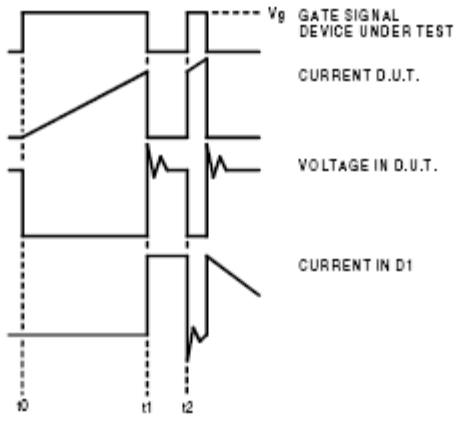

Figure 18e. Macro Waveforms for Figure 18a's Test Circuit

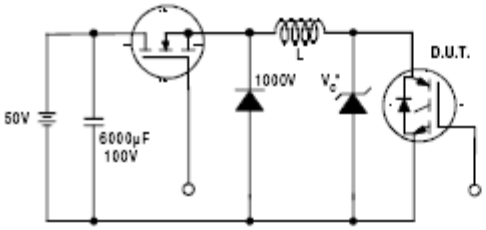

Figure 19. Clamped Inductive Load Test Circuit

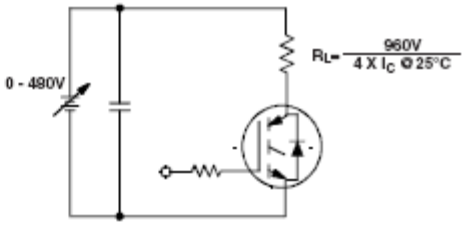

Figure 20. Pulsed Collector Current Test Circuit

Notes:

① Repetitive rating: V_{GE}=20V; pulse width limited by maximum junction temperature (figure 20)

② V_{CC}=80%(V_{CES}), V_{GE}=20V, L=10µH, R_G=5.0Ω (figure 19)

③ Pulse width ≤ 80µs; duty factor ≤ 0.1%.

④ Pulse width 5.0µs, single shot.

Case Outline — TO-247AC

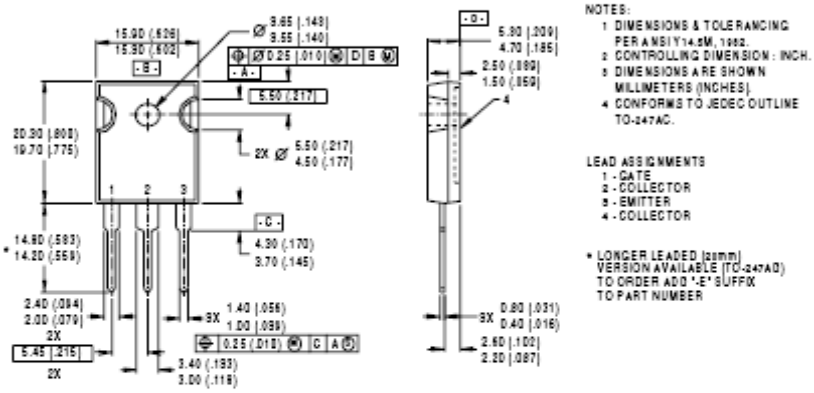

CONFORMS TO JEDEC OUTLINE TO-247AC (TO-3P)
Dimensions in Millimeters and (Inches)

International
IOR Rectifier

IR WORLD HEADQUARTERS: 233 Kansas St., El Segundo, California 90245, USA Tel: (310) 252-7105
IR EUROPEAN REGIONAL CENTRE: 439/445 Godstone Rd, Whyteleafe, Surrey CR3 OBL, UK Tel: ++ 44 (0)20 8645 8000
IR CANADA: 15 Lincoln Court, Brampton, Ontario L6T3Z2, Tel: (905) 453 2200
IR GERMANY: Saalburgstrasse 157, 61350 Bad Homburg Tel: ++ 49 (0) 6172 96590
IR ITALY: Via Liguria 49, 10071 Borgaro, Torino Tel: ++ 39 011 451 0111
IR JAPAN: K&H Bldg., 2F, 30-4 Nishi-Ikebukuro 3-Chome, Toshima-Ku, Tokyo 171 Tel: 81 (0)3 3983 0086
IR SOUTHEAST ASIA: 1 Kim Seng Promenade, Great World City West Tower, 13-11, Singapore 237994 Tel ++ 65 (0)838 4630
IR TAIWAN:16 Fl. Suite D. 207, Sec. 2, Tun Haw South Road, Taipei, 10673 Tel: 886-(0)2 2377 9936

APPENDIX B:

Matlab Script for Example Exercise in Chapter 2.2

Appendix B - Matlab Loss Calculations using IRG4PH50KD

```
clear all; close all; clc;

%%Inputs Needed Are As Follows
IGBT_Vt = 1.3;
IGBT_R = 80e-3;
Diode_Vt = 1.6;
Diode_R = 40e-3;
IGBT_Eon_int = 0;
IGBT_Eon_sl = 0.1785;
IGBT_Eoff_int = 0;
IGBT_Eoff_sl = 0.1785;
Diode_Err_int = 0;
Diode_Err_sl = 0;


%%Design Constants
n = 2;
f = 50;
fs = 20000;
L = 1000e-6;
R = 12.8;
VDC = 410;
mod_index = 0.95;


%%Simulation Constants
IL(1)=0;
IL2(1)=0;
w = 2*pi*f;
ws = 2*pi*fs;
carrier_direction = 1;
i = 1;
Vtri(1)=-1;
IGBT_Cond(1)=0;
Diode_Cond(1)=0;
IGBT_on(1)=0;
IGBT_off(1)=0;
Diode_rr(1)=0;
simulation_step = 0.5e-6;


for t_simulation = 0:simulation_step:20e-3

    %%Vref is the reference sine wave for the output
    Vref(i) = mod_index*sin(w*t_simulation);


    %%This code creates the triangle wave Vtri
    if i>1
        Vtri(i) = Vtri(i-1)+carrier_direction*(4*fs*simulation_step);
    end
    if Vtri(i)>=1
        carrier_direction=-1;
    end
    if Vtri(i)<=-1
        carrier_direction=1;
    end



    %%Calculate PWM Signals
    if Vtri(i)<=Vref(i)
        PWM(i)=1;
```

```
else
    PWM(i)=0;
end


%%Calculate Inductor Current
if i>1
    Vo = IL(i-1)*R;
    %Vo = Vref(i)*VDC;
    if PWM(i)==1
        didt = (VDC-Vo)/L;
        IL(i)=IL(i-1)+didt*simulation_step;
    end
    if PWM(i)==0
        didt = (-VDC-Vo)/L;
        IL(i)=IL(i-1)+didt*simulation_step;
    end
end

IL2(i) = IL(i)/n;

%%Calculate IGBT Conduction Losses
if (IL2(i)>0 && PWM(i)==1)
    IGBT_Cond(i) = (IL2(i))^2*IGBT_R + abs(IL2(i))*IGBT_Vt;
elseif (IL2(i)<0 && PWM(i)==0)
    IGBT_Cond(i) = (IL2(i))^2*IGBT_R + abs(IL2(i))*IGBT_Vt;
else
    IGBT_Cond(i) = 0;
end

%%Calculate Diode Conduction Losses
if (IL2(i)>0 && PWM(i)==0)
    Diode_Cond(i) = (IL2(i))^2*Diode_R + abs(IL2(i))*Diode_Vt;
elseif (IL2(i)<0 && PWM(i)==1)
    Diode_Cond(i) = (IL2(i))^2*Diode_R + abs(IL2(i))*Diode_Vt;
else
    Diode_Cond(i) = 0;
end

%%Calculate Switching Losses & RR Losses
if (i>1 & IL2(i)>0)
    if (PWM(i-1)==1 & PWM(i)==0)
        IGBT_off(i)=IGBT_Eoff_int+IGBT_Eoff_sl*abs(IL2(i));
        IGBT_on(i)=0;
        Diode_rr(i)=0;
    elseif (PWM(i-1)==0 & PWM(i)==1)
        IGBT_on(i)=IGBT_Eon_int+IGBT_Eon_sl*abs(IL2(i));
        IGBT_off(i)=0;
        Diode_rr(i)=Diode_Err_int+Diode_Err_sl*abs(IL2(i));
    else
        IGBT_off(i)=0;
        IGBT_on(i)=0;
        Diode_rr(i)=0;
    end
elseif (i>1 & IL2(i)<=0)
    if (PWM(i-1)==0 & PWM(i)==1)
        IGBT_off(i)=IGBT_Eoff_int+IGBT_Eoff_sl*abs(IL2(i));
        IGBT_on(i)=0;
        Diode_rr(i)=0;
    elseif (PWM(i-1)==1 & PWM(i)==0)
        IGBT_on(i)=IGBT_Eon_int+IGBT_Eon_sl*abs(IL2(i));
        IGBT_off(i)=0;
        Diode_rr(i)=Diode_Err_int+Diode_Err_sl*abs(IL2(i));
```

```
        else
            IGBT_off(i)=0;
            IGBT_on(i)=0;
            Diode_rr(i)=0;
        end
    end
    if IGBT_off(i)<0
        IGBT_off(i)=0;
    end
    if IGBT_on(i)<0
        IGBT_on(i)=0;
    end
    if Diode_rr(i)<0
        Diode_rr(i)=0;
    end

    i=i+1;

end
```

```
t_simulation_ext = 0:simulation_step:20e-3;


plot(t_simulation_ext, Vref);
hold on;
plot(t_simulation_ext, Vtri, 'm');
title('Reference Signal and Carrier Signal')
axis([0 0.02 -1.1 1.1])
hold off;

figure()
plot(t_simulation_ext,PWM);
title('PWM Signals')

figure()
plot(t_simulation_ext, IL);
title('Inductor Current')

figure()
plot(t_simulation_ext, IGBT_Cond);
title('IGBT Conduction Losses (Watts)')

figure()
plot(t_simulation_ext, Diode_Cond);
title('Diode Conduction Losses (Watts)')

figure()
plot(t_simulation_ext, IGBT_off);
title('IGBT Turn Off Losses (mJ)')

figure()
plot(t_simulation_ext, IGBT_on);
title('IGBT Turn On Losses (mJ)')

figure()
plot(t_simulation_ext, Diode_rr);
```

```
title('Diode Reverse Recovery Losses (mJ)')

IGBT_Cond_Total = n*mean(IGBT_Cond)
Diode_Cond_Total = n*mean(Diode_Cond)
IGBT_Sw_Total = (n*820/600)*[(sum(IGBT_on)/1000)/20e-3 + (sum(IGBT_off)/1000)/20e-3]
Diode_Recov_Total = (n*820/600)*[(sum(Diode_rr)/1000)/20e-3]
```

APPENDIX C:

IR Datasheet for IRG4PC30KD

PD -91587A

International
IOR Rectifier

IRG4PC30KD

INSULATED GATE BIPOLAR TRANSISTOR WITH ULTRAFAST SOFT RECOVERY DIODE

Short Circuit Rated
UltraFast IGBT

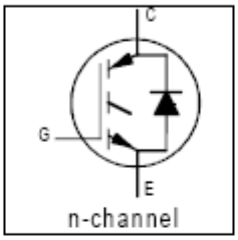

V_{CES} = 600V

$V_{CE(on)\ typ.}$ = 2.21V

@V_{GE} = 15V, I_C = 16A

Features

- High short circuit rating optimized for motor control, t_{sc} =10µs, @360V V_{CE} (start), T_J = 125°C, V_{GE} = 15V
- Combines low conduction losses with high switching speed
- Tighter parameter distribution and higher efficiency than previous generations
- IGBT co-packaged with HEXFRED™ ultrafast, ultrasoft recovery antiparallel diodes

Benefits

- Latest generation 4 IGBTs offer highest power density motor controls possible
- HEXFRED™ diodes optimized for performance with IGBTs. Minimized recovery characteristics reduce noise, EMI and switching losses
- This part replaces the IRGBC30KD2 and IRGBC30MD2 products
- For hints see design tip 97003

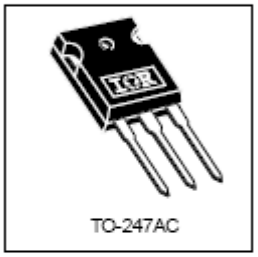

TO-247AC

Absolute Maximum Ratings

	Parameter	Max.	Units
V_{CES}	Collector-to-Emitter Voltage	600	V
I_C @ T_C = 25°C	Continuous Collector Current	28	A
I_C @ T_C = 100°C	Continuous Collector Current	16	
I_{CM}	Pulsed Collector Current ①	58	
I_{LM}	Clamped Inductive Load Current ②	58	
I_F @ T_C = 100°C	Diode Continuous Forward Current	12	
I_{FM}	Diode Maximum Forward Current	58	
t_{sc}	Short Circuit Withstand Time	10	µs
V_{GE}	Gate-to-Emitter Voltage	± 20	V
P_D @ T_C = 25°C	Maximum Power Dissipation	100	W
P_D @ T_C = 100°C	Maximum Power Dissipation	42	
T_J T_{STG}	Operating Junction and Storage Temperature Range	-55 to +150	°C
	Soldering Temperature, for 10 sec.	300 (0.063 in. (1.6mm) from case)	
	Mounting Torque, 6-32 or M3 Screw.	10 lbf•in (1.1 N•m)	

Thermal Resistance

	Parameter	Min.	Typ.	Max.	Units
$R_{\theta JC}$	Junction-to-Case - IGBT	—	—	1.2	°C/W
$R_{\theta JC}$	Junction-to-Case - Diode	—	—	2.5	
$R_{\theta CS}$	Case-to-Sink, flat, greased surface	—	0.24	—	
$R_{\theta JA}$	Junction-to-Ambient, typical socket mount	—	—	40	
Wt	Weight	—	6 (0.21)	—	g (oz)

Electrical Characteristics @ T_J = 25°C (unless otherwise specified)

	Parameter	Min.	Typ.	Max.	Units	Conditions
$V_{(BR)CES}$	Collector-to-Emitter Breakdown Voltage③	600	—	—	V	V_{GE} = 0V, I_C = 250µA
$\Delta V_{(BR)CES}/\Delta T_J$	Temperature Coeff. of Breakdown Voltage	—	0.54	—	V/°C	V_{GE} = 0V, I_C = 1.0mA
$V_{CE(on)}$	Collector-to-Emitter Saturation Voltage	—	2.21	2.7	V	I_C = 16A, V_{GE} = 15V
		—	2.88	—		I_C = 28A, See Fig. 2, 5
		—	2.36	—		I_C = 16A, T_J = 150°C
$V_{GE(th)}$	Gate Threshold Voltage	3.0	—	6.0		V_{CE} = V_{GE}, I_C = 250µA
$\Delta V_{GE(th)}/\Delta T_J$	Temperature Coeff. of Threshold Voltage	—	-12	—	mV/°C	V_{CE} = V_{GE}, I_C = 250µA
g_{fe}	Forward Transconductance ④	5.4	8.1	—	S	V_{CE} = 100V, I_C = 16A
I_{CES}	Zero Gate Voltage Collector Current	—	—	250	µA	V_{GE} = 0V, V_{CE} = 600V
		—	—	2500		V_{GE} = 0V, V_{CE} = 600V, T_J = 150°C
V_{FM}	Diode Forward Voltage Drop	—	1.4	1.7	V	I_C = 12A, See Fig. 13
		—	1.3	1.6		I_C = 12A, T_J = 150°C
I_{GES}	Gate-to-Emitter Leakage Current	—	—	±100	nA	V_{GE} = ±20V

Switching Characteristics @ T_J = 25°C (unless otherwise specified)

	Parameter	Min.	Typ.	Max.	Units	Conditions
Q_g	Total Gate Charge (turn-on)	—	67	100	nC	I_C = 16A
Q_{ge}	Gate - Emitter Charge (turn-on)	—	11	16		V_{CC} = 400V See Fig.8
Q_{gc}	Gate - Collector Charge (turn-on)	—	25	37		V_{GE} = 15V
$t_{d(on)}$	Turn-On Delay Time	—	60	—	ns	
t_r	Rise Time	—	42	—		T_J = 25°C
$t_{d(off)}$	Turn-Off Delay Time	—	160	250		I_C = 16A, V_{CC} = 480V
t_f	Fall Time	—	80	120		V_{GE} = 15V, R_G = 23Ω
E_{on}	Turn-On Switching Loss	—	0.60	—	mJ	Energy losses include "tail"
E_{off}	Turn-Off Switching Loss	—	0.58	—		and diode reverse recovery
E_{ts}	Total Switching Loss	—	1.18	1.6		See Fig. 9,10,14
t_{sc}	Short Circuit Withstand Time	10	—	—	µs	V_{CC} = 360V, T_J = 125°C
						V_{GE} = 15V, R_G = 10Ω , V_{CPK} < 500V
$t_{d(on)}$	Turn-On Delay Time	—	58	—	ns	T_J = 150°C, See Fig. 11,14
t_r	Rise Time	—	42	—		I_C = 16A, V_{CC} = 480V
$t_{d(off)}$	Turn-Off Delay Time	—	210	—		V_{GE} = 15V, R_G = 23Ω,
t_f	Fall Time	—	160	—		Energy losses include "tail"
E_{ts}	Total Switching Loss	—	1.69	—	mJ	and diode reverse recovery
L_E	Internal Emitter Inductance	—	13	—	nH	Measured 5mm from package
C_{ies}	Input Capacitance	—	920	—	pF	V_{GE} = 0V
C_{oes}	Output Capacitance	—	110	—		V_{CC} = 30V See Fig. 7
C_{res}	Reverse Transfer Capacitance	—	27	—		f = 1.0MHz
t_{rr}	Diode Reverse Recovery Time	—	42	60	ns	T_J = 25°C See Fig. 14, I_F = 12A
		—	80	120		T_J = 125°C
I_{rr}	Diode Peak Reverse Recovery Current	—	3.5	6.0	A	T_J = 25°C See Fig. 15, V_R = 200V
		—	5.6	10		T_J = 125°C
Q_{rr}	Diode Reverse Recovery Charge	—	80	180	nC	T_J = 25°C See Fig. 16, di/dt = 200Aµs
		—	220	600		T_J = 125°C
$di_{(rec)M}/dt$	Diode Peak Rate of Fall of Recovery During t_b	—	180	—	A/µs	T_J = 25°C See Fig. 17
		—	160	—		T_J = 125°C

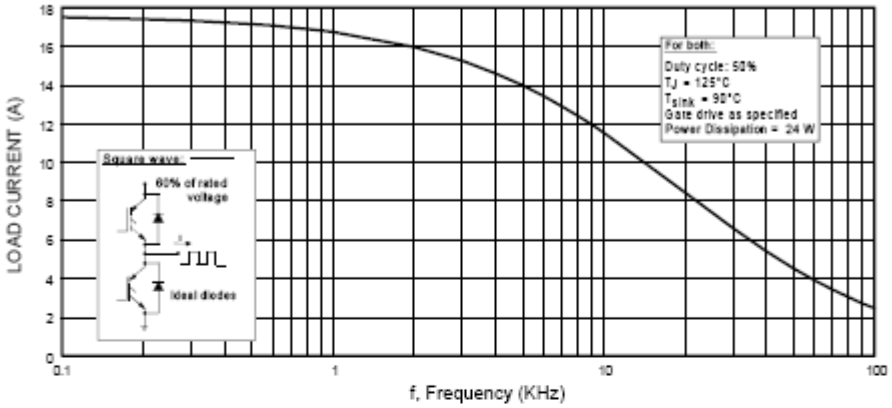

Fig. 1 - Typical Load Current vs. Frequency
(Load Current = I_{RMS} of fundamental)

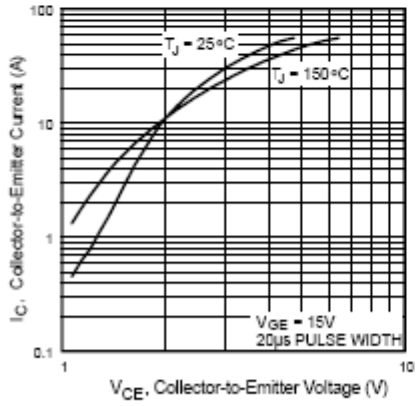

Fig. 2 - Typical Output Characteristics

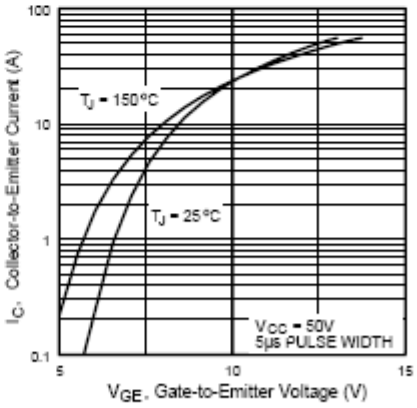

Fig. 3 - Typical Transfer Characteristics

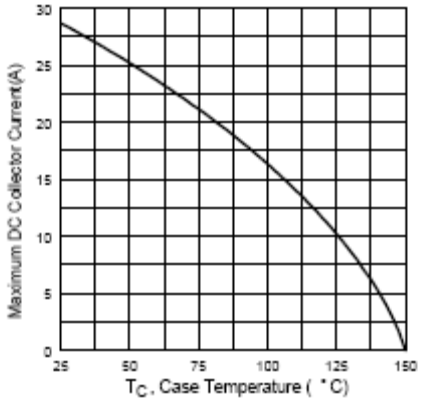

Fig. 4 - Maximum Collector Current vs. Case Temperature

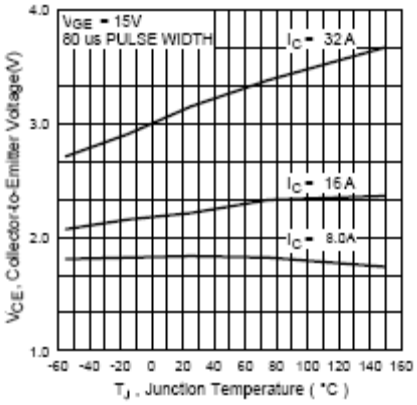

Fig. 5 - Typical Collector-to-Emitter Voltage vs. Junction Temperature

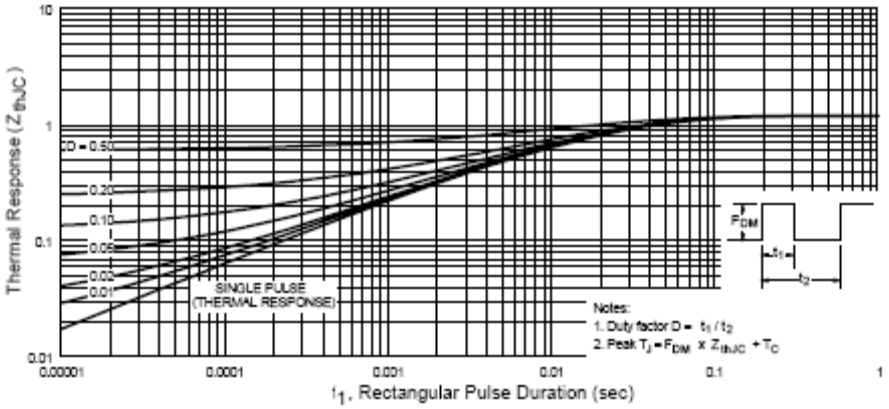

Fig. 6 - Maximum Effective Transient Thermal Impedance, Junction-to-Case

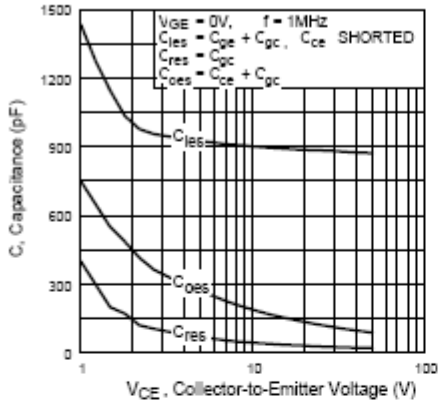

Fig. 7 - Typical Capacitance vs. Collector-to-Emitter Voltage

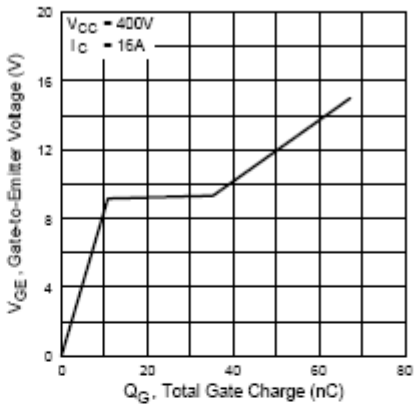

Fig. 8 - Typical Gate Charge vs. Gate-to-Emitter Voltage

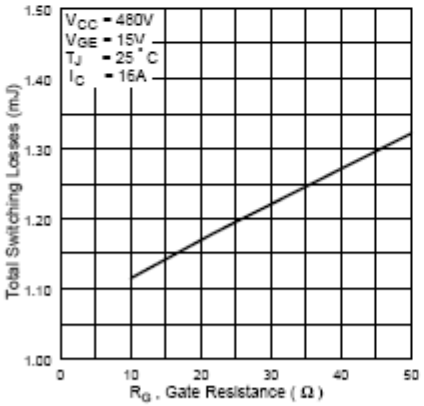

Fig. 9 - Typical Switching Losses vs. Gate Resistance

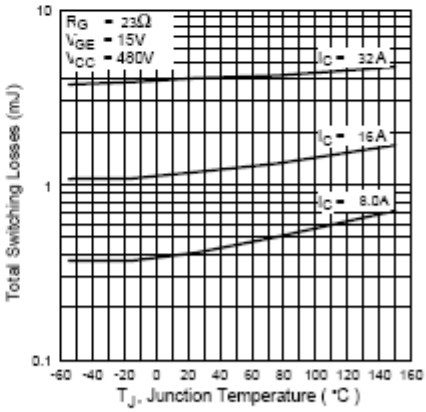

Fig. 10 - Typical Switching Losses vs. Junction Temperature

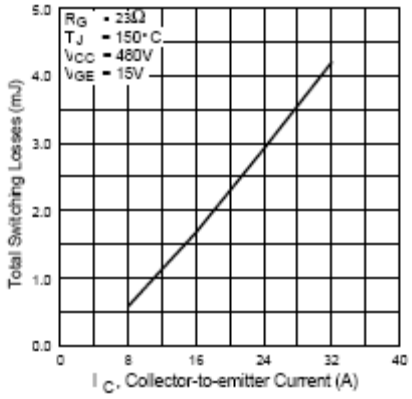

Fig. 11 - Typical Switching Losses vs. Collector-to-Emitter Current

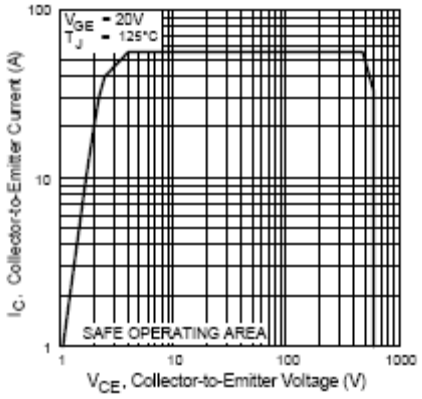

Fig. 12 - Turn-Off SOA

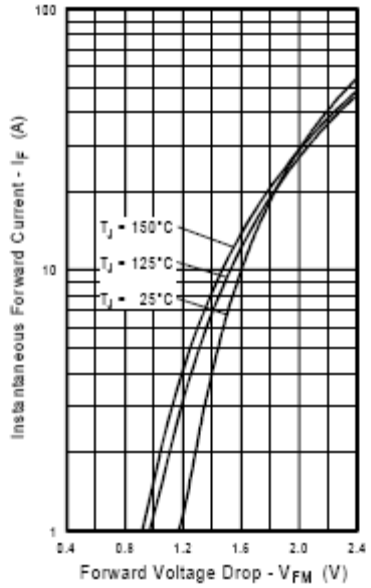

Fig. 13 - Maximum Forward Voltage Drop vs. Instantaneous Forward Current

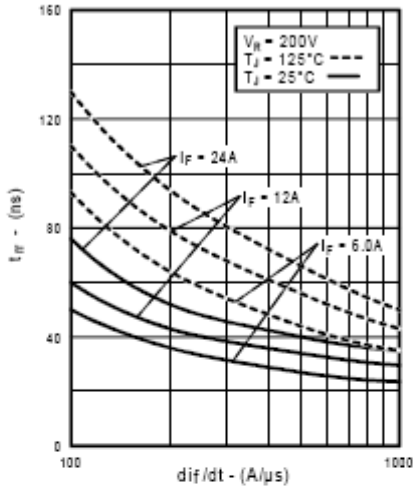

Fig. 14 - Typical Reverse Recovery vs. di_f/dt

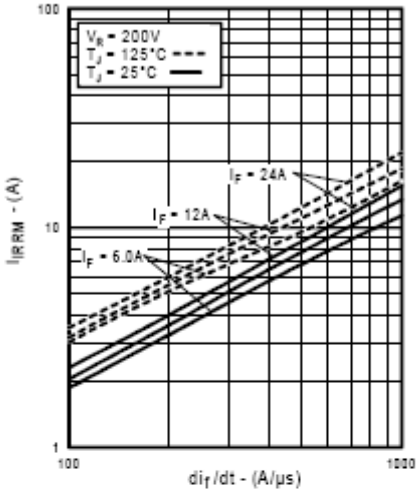

Fig. 15 - Typical Recovery Current vs. di_f/dt

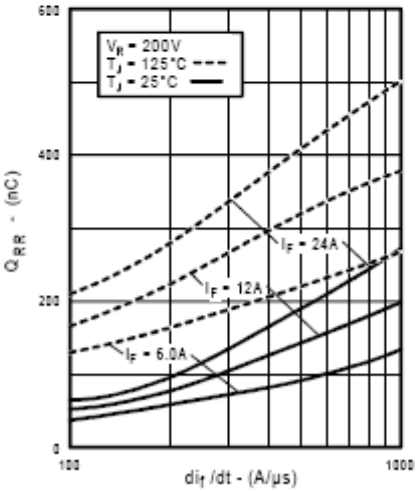

Fig. 16 - Typical Stored Charge vs. di_f/dt

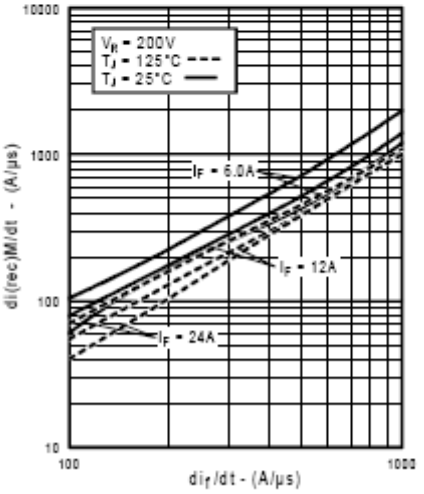

Fig. 17 - Typical $di_{(rec)M}/dt$ vs. di_f/dt

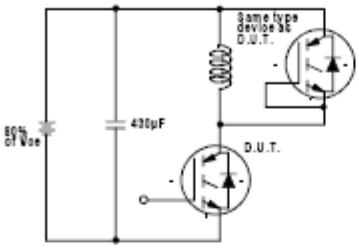

Fig. 18a - Test Circuit for Measurement of I_{LM}, E_{on}, $E_{off(diode)}$, t_{rr}, Q_{rr}, I_{rr}, $t_{d(on)}$, t_r, $t_{d(off)}$, t_f

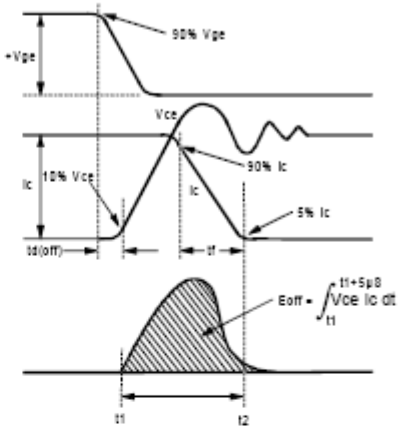

Fig. 18b - Test Waveforms for Circuit of Fig. 18a, Defining E_{off}, $t_{d(off)}$, t_f

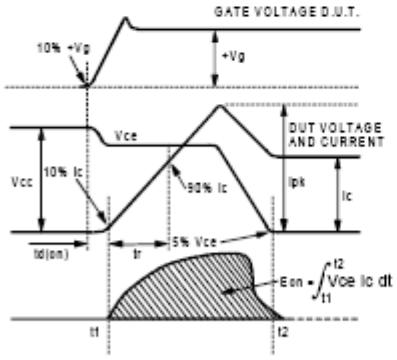

Fig. 18c - Test Waveforms for Circuit of Fig. 18a, Defining E_{on}, $t_{d(on)}$, t_r

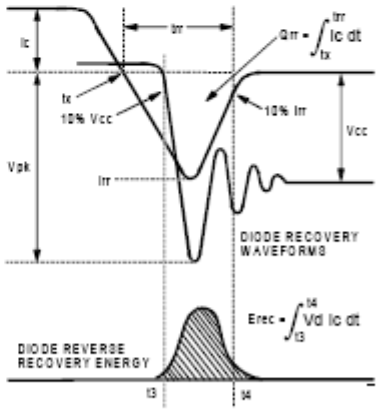

Fig. 18d - Test Waveforms for Circuit of Fig. 18a, Defining E_{rec}, t_{rr}, Q_{rr}, I_{rr}

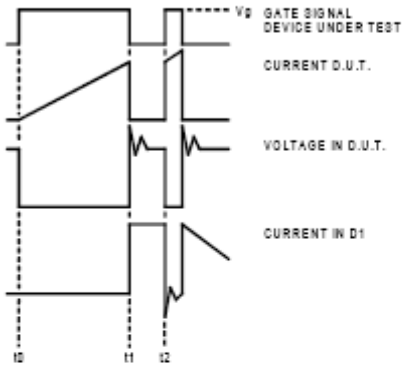

Figure 18e. Macro Waveforms for Figure 18a's Test Circuit

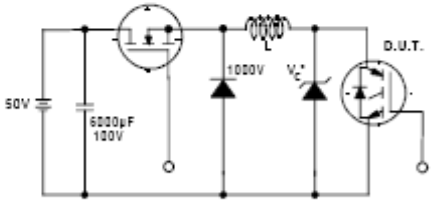

Figure 19. Clamped Inductive Load Test Circuit

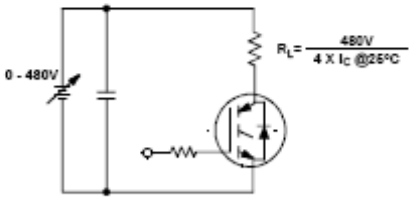

Figure 20. Pulsed Collector Current Test Circuit

Notes:

① Repetitive rating: V_{GE}=20V; pulse width limited by maximum junction temperature (figure 20)

② V_{CC}=80%(V_{CES}), V_{GE}=20V, L=10µH, R_G= 23Ω (figure 19)

③ Pulse width ≤ 80µs; duty factor ≤ 0.1%.

④ Pulse width 5.0µs, single shot.

Case Outline — TO-247AC

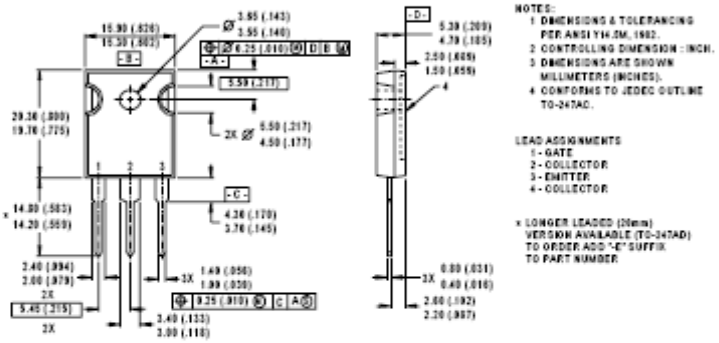

CONFORMS TO JEDEC OUTLINE TO-247AC (TO-3P)
Dimensions in Millimeters and (Inches)

International
IOR Rectifier

IR WORLD HEADQUARTERS: 233 Kansas St., El Segundo, California 90245, USA Tel: (310) 252-7105
IR EUROPEAN REGIONAL CENTRE: 439/445 Godstone Rd, Whyteleafe, Surrey CR3 0BL, UK Tel: ++ 44 (0)20 8645 8000
IR CANADA: 15 Lincoln Court, Brampton, Ontario L6T3Z2, Tel: (905) 453 2200
IR GERMANY: Saalburgstrasse 157, 61350 Bad Homburg Tel: ++ 49 (0) 6172 96590
IR ITALY: Via Liguria 49, 10071 Borgaro, Torino Tel: ++ 39 011 451 0111
IR JAPAN: K&H Bldg., 2F, 30-4 Nishi-Ikebukuro 3-Chome, Toshima-Ku, Tokyo 171 Tel: 81 (0)3 3983 0086
IR SOUTHEAST ASIA: 1 Kim Seng Promenade, Great World City West Tower, 13-11, Singapore 237994 Tel: ++ 65 (0)838 4630
IR TAIWAN: 16 Fl. Suite D. 207, Sec. 2, Tun Haw South Road, Taipei, 10673 Tel: 886-(0)2 2377 9936

Data and specifications subject to change without notice. 4/00

APPENDIX D:

Matlab Script for Example Exercise in Chapter 2.3

Appendix D - Matlab Loss Calculations using IRG4PC30KD

```
clear all; close all; clc;

%%Inputs Needed Are As Follows
IGBT_Vt = 1.1;
IGBT_R = 85e-3;
Diode_Vt = 1;
Diode_R = 42e-3;
IGBT_Eon_int = 0;
IGBT_Eon_sl = 0.0451;
IGBT_Eoff_int = 0;
IGBT_Eoff_sl = 0.0451;
Diode_Err_int = 0;
Diode_Err_sl = 0;


%%Design Constants
n = 2;
f = 50;
fs = 20000;
L = 250e-6;
R = 12.8;
VDC = 410;
mod_index = 0.95;


%%Simulation Constants
IL(1)=0;
w = 2*pi*f;
ws = 2*pi*fs;
carrier_direction = 1;
i = 1;
Vtri(1)=0;
Vtri2(1)=0;
IGBT_Cond(1)=0;
Diode_Cond(1)=0;
IGBT_on(1)=0;
IGBT_off(1)=0;
Diode_rr(1)=0;
simulation_step = 0.5e-6;


for t_simulation = 0:simulation_step:20e-3

    %%Vref is the reference sine wave for the output
    Vref(i) = mod_index*sin(w*t_simulation);


    %%This code creates the triangle wave Vtri
    if i>1
        Vtri(i) = Vtri(i-1)+carrier_direction*(2*fs*simulation_step);
        if Vref(i)>=0
            Vtri2(i)=Vtri(i);
        elseif Vref(i)<=0
            Vtri2(i)=-Vtri(i);
        end

    end


    if Vtri(i)>=1
        carrier_direction=-1;
    end
    if Vtri(i)<0
```

```
    carrier_direction=1;
end



%%Calculate PWM Signals
if Vref(i)>=0
    PWM2(i)=1;
    if Vtri2(i)<=Vref(i)
        PWM(i)=1;
    else
        PWM(i)=0;
    end
elseif Vref(i)<0
    PWM(i)=0;
    if Vtri2(i)<=Vref(i)
        PWM2(i)=1;
    else
        PWM2(i)=0;
    end
end


%%Calculate Inductor Current
if i>1
    Vo = IL(i-1)*R;
    %Vo = Vref(i)*VDC;
    if (PWM(i)==1 && PWM2(i)==1)
        didt = (VDC-Vo)/L;
        IL(i)=IL(i-1)+didt*simulation_step;
    end
    if (PWM(i)==0 && PWM2(i)==0)
        didt = (-VDC-Vo)/L;
        IL(i)=IL(i-1)+didt*simulation_step;
    end
    if (PWM(i)==0 && PWM2(i)==1)
        didt = (0-Vo)/L;
        IL(i)=IL(i-1)+didt*simulation_step;
    end
    if (PWM(i)==1 && PWM2(i)==0)
        ERROR=1
    end
end

IL2(i)=IL(i)/n;

%%Calculate IGBT Conduction Losses
if (IL2(i)>0 && PWM(i)==1)   %PWM2 is always 1 when IL>0
    IGBT_Cond(i) = 2 * [(IL2(i))^2*IGBT_R + abs(IL2(i))*IGBT_Vt];
elseif (IL2(i)>0 && PWM(i)==0)   %PWM2 is always 1 when IL>0
    IGBT_Cond(i) = (IL2(i))^2*IGBT_R + abs(IL2(i))*IGBT_Vt;
elseif (IL2(i)<0 && PWM2(i)==0)   %PWM is always 0 when IL<0
    IGBT_Cond(i) = 2 * [(IL2(i))^2*IGBT_R + abs(IL2(i))*IGBT_Vt];
elseif (IL2(i)<0 && PWM2(i)==1)  %PWM is always 0 when IL<0
    IGBT_Cond(i) = (IL2(i))^2*IGBT_R + abs(IL2(i))*IGBT_Vt;
else
    IGBT_Cond(i) = 0;
end

%%Calculate Diode Conduction Losses
if (IL2(i)>0 && PWM(i)==1)   %PWM2 is always 1 when IL>0
    Diode_Cond(i) = 0;
```

```
    elseif (IL2(i)>0 && PWM(i)==0)   %PWM2 is always 1 when IL>0
        Diode_Cond(i) = (IL2(i))^2*Diode_R + abs(IL2(i))*Diode_Vt;
    elseif (IL2(i)<0 && PWM2(i)==0)   %PWM is always 0 when IL<0
        Diode_Cond(i) = 0;
    elseif (IL2(i)<0 && PWM2(i)==1)  %PWM is always 0 when IL<0
        Diode_Cond(i) = (IL2(i))^2*Diode_R + abs(IL2(i))*Diode_Vt;
    else
        Diode_Cond(i) = 0;
    end


    %%Calculate Switching Losses & RR Losses
    if (i>1 & IL2(i)>0)  %PWM2 is always 1 when IL>0
        if (PWM(i-1)==1 & PWM(i)==0)
            IGBT_off(i)=IGBT_Eoff_int+IGBT_Eoff_sl*abs(IL2(i));
            IGBT_on(i)=0;
            Diode_rr(i)=0;
        elseif (PWM(i-1)==0 & PWM(i)==1)
            IGBT_on(i)=IGBT_Eon_int+IGBT_Eon_sl*abs(IL2(i));
            IGBT_off(i)=0;
            Diode_rr(i)=Diode_Err_int+Diode_Err_sl*abs(IL2(i));
        else
            IGBT_off(i)=0;
            IGBT_on(i)=0;
            Diode_rr(i)=0;
        end
    end
    if (i>1 & IL2(i)<=0) %PWM is always 0 when IL<0
        if (PWM2(i-1)==0 & PWM2(i)==1)
            IGBT_off(i)=IGBT_Eoff_int+IGBT_Eoff_sl*abs(IL2(i));
            IGBT_on(i)=0;
            Diode_rr(i)=0;
        elseif (PWM2(i-1)==1 & PWM2(i)==0)
            IGBT_on(i)=IGBT_Eon_int+IGBT_Eon_sl*abs(IL2(i));
            IGBT_off(i)=0;
            Diode_rr(i)=Diode_Err_int+Diode_Err_sl*abs(IL2(i));
        else
            IGBT_off(i)=0;
            IGBT_on(i)=0;
            Diode_rr(i)=0;
        end
    end
    if IGBT_off(i)<0
        IGBT_off(i)=0;
    end
    if IGBT_on(i)<0
        IGBT_on(i)=0;
    end
    if Diode_rr(i)<0
        Diode_rr(i)=0;
    end

    i=i+1;

end




t_simulation_ext = 0:simulation_step:20e-3;
```

```
% plot(t_simulation_ext, Vref);
% hold on;
% plot(t_simulation_ext, Vtri2, 'm');
% title('Reference Signal and Carrier Signal')
% hold off;
%
% figure()
% plot(t_simulation_ext,PWM);
% axis([0 0.02 -0.1 1.1])
% title('PWM Signals')
%
% figure()
% plot(t_simulation_ext, PWM2);
% axis([0 0.02 -0.1 1.1])
% title('PWM2 Signals')



%  figure()
%  plot(t_simulation_ext, IL);
%  title('Inductor Current')
%
% figure()
% plot(t_simulation_ext, IGBT_Cond);
% title('IGBT Conduction Losses (Watts)')
%
% figure()
% plot(t_simulation_ext, Diode_Cond);
% title('Diode Conduction Losses (Watts)')
%
% figure()
% plot(t_simulation_ext, IGBT_off);
% title('IGBT Turn Off Losses (mJ)')
%
% figure()
% plot(t_simulation_ext, IGBT_on);
% title('IGBT Turn On Losses (mJ)')
%
% figure()
% plot(t_simulation_ext, Diode_rr);
% title('Diode Reverse Recovery Losses (mJ)')

IGBT_Cond_Total = n*mean(IGBT_Cond)
Diode_Cond_Total = n*mean(Diode_Cond)
IGBT_Sw_Total = (n*410/300)*[(sum(IGBT_on)/1000)/20e-3 + (sum(IGBT_off)/1000)/20e-3]
Diode_Recov_Total = (n*410/300)*[(sum(Diode_rr)/1000)/20e-3]
```

APPENDIX E:

Infineon Datasheet for FF100R12YT3

IGBT-Wechselrichter / IGBT-inverter — Vorläufige Daten / preliminary data

Höchstzulässige Werte / maximum rated values

Kollektor-Emitter-Sperrspannung collector-emitter voltage	T_{vj} = 25°C	V_{CES}	1200	V
Kollektor-Dauergleichstrom DC-collector current	T_C = 80°C, T_{vj} = 150°C T_C = 25°C, T_{vj} = 150°C	$I_{C\,nom}$ I_C	100 140	A A
Periodischer Kollektor Spitzenstrom repetitive peak collector current	t_P = 1 ms	I_{CRM}	200	A
Gesamt-Verlustleistung total power dissipation	T_C = 25°C, T_{vj} = 150°C	P_{tot}	445	W
Gate-Emitter-Spitzenspannung gate-emitter peak voltage		V_{GES}	+/-20	V

Charakteristische Werte / characteristic values

			min.	typ.	max.	
Kollektor-Emitter Sättigungsspannung collector-emitter saturation voltage	I_C = 100 A, V_{GE} = 15 V I_C = 100 A, V_{GE} = 15 V	T_{vj} = 25°C T_{vj} = 125°C	$V_{CE\,sat}$		1,70 1,90	2,15	V V
Gate-Schwellenspannung gate threshold voltage	I_C = 4,00 mA, V_{CE} = V_{GE}, T_{vj} = 25°C		V_{GEth}	5,0	5,8	6,5	V
Gateladung gate charge	V_{GE} = -15 V ... +15 V		Q_G		0,95		µC
Interner Gatewiderstand internal gate resistor	T_{vj} = 25°C		R_{Gint}		2,0		Ω
Eingangskapazität input capacitance	f = 1 MHz, T_{vj} = 25°C, V_{CE} = 25 V, V_{GE} = 0 V		C_{ies}		7,10		nF
Rückwirkungskapazität reverse transfer capacitance	f = 1 MHz, T_{vj} = 25°C, V_{CE} = 25 V, V_{GE} = 0 V		C_{res}		0,26		nF
Kollektor-Emitter Reststrom collector-emitter cut-off current	V_{CE} = 1200 V, V_{GE} = 0 V, T_{vj} = 25°C		I_{CES}			1,0	mA
Gate-Emitter Reststrom gate-emitter leakage current	V_{CE} = 0 V, V_{GE} = 20 V, T_{vj} = 25°C		I_{GES}			400	nA
Einschaltverzögerungszeit (ind. Last) turn-on delay time (inductive load)	I_C = 100 A, V_{CE} = 600 V V_{GE} = ±15 V R_{Gon} = 6,8 Ω	T_{vj} = 25°C T_{vj} = 125°C	$t_{d\,on}$		0,14 0,15		µs µs
Anstiegszeit (induktive Last) rise time (inductive load)	I_C = 100 A, V_{CE} = 600 V V_{GE} = ±15 V R_{Gon} = 6,8 Ω	T_{vj} = 25°C T_{vj} = 125°C	t_r		0,027 0,037		µs µs
Abschaltverzögerungszeit (ind. Last) turn-off delay time (inductive load)	I_C = 100 A, V_{CE} = 600 V V_{GE} = ±15 V R_{Goff} = 6,8 Ω	T_{vj} = 25°C T_{vj} = 125°C	$t_{d\,off}$		0,43 0,52		µs µs
Fallzeit (induktive Last) fall time (inductive load)	I_C = 100 A, V_{CE} = 600 V V_{GE} = ±15 V R_{Goff} = 6,8 Ω	T_{vj} = 25°C T_{vj} = 125°C	t_f		0,10 0,16		µs µs
Einschaltverlustenergie pro Puls turn-on energy loss per pulse	I_C = 100 A, V_{CE} = 600 V, L_S = 40 nH V_{GE} = ±15 V, di/dt = 2600 A/µs (T_{vj}=125°C) R_{Gon} = 6,8 Ω	T_{vj} = 25°C T_{vj} = 125°C	E_{on}		6,90 9,70		mJ mJ
Abschaltverlustenergie pro Puls turn-off energy loss per pulse	I_C = 100 A, V_{CE} = 600 V, L_S = 40 nH V_{GE} = ±15 V, du/dt = 3500 V/µs (T_{vj}=125°C) R_{Goff} = 6,8 Ω	T_{vj} = 25°C T_{vj} = 125°C	E_{off}		7,90 12,0		mJ mJ
Kurzschlussverhalten SC data	V_{GE} ≤ 15 V, V_{CC} = 900 V V_{CEmax} = V_{CES} -L_{sCE} ·di/dt	t_P ≤ 10 µs, T_{vj} = 125°C	I_{SC}		400		A
Innerer Wärmewiderstand thermal resistance, junction to case	pro IGBT per IGBT		R_{thJC}		0,25	0,28	K/W
Übergangs-Wärmewiderstand thermal resistance, case to heatsink	pro IGBT / per IGBT λ_{Paste} = 1 W/(m·K) / λ_{grease} = 1 W/(m·K)		R_{thCH}		0,16		K/W

prepared by: Christoph Messelke	date of publication: 2006-11-28
approved by: Marc Buschkühle	revision: 2.1

Vorläufige Daten
preliminary data

Diode-Wechselrichter / diode-inverter

Höchstzulässige Werte / maximum rated values

Periodische Spitzensperrspannung repetitive peak reverse voltage	T_{vj} = 25°C	V_{RRM}	1200		V
Dauergleichstrom DC forward current		I_F	100		A
Periodischer Spitzenstrom repetitive peak forward current	t_P = 1 ms	I_{FRM}	200		A
Grenzlastintegral I²t - value	V_R = 0 V, t_P = 10 ms, T_{vj} = 125°C	I²t	1950		A²s

Charakteristische Werte / characteristic values

			min.	typ.	max.	
Durchlassspannung forward voltage	I_F = 100 A, V_{GE} = 0 V I_F = 100 A, V_{GE} = 0 V	T_{vj} = 25°C T_{vj} = 125°C	V_F	1,65 1,65	2,15	V V
Rückstromspitze peak reverse recovery current	I_F = 100 A, - di_F/dt = 2600 A/µs (T_{vj}=125°C) V_R = 600 V V_{GE} = -15 V	T_{vj} = 25°C T_{vj} = 125°C	I_{RM}	155 160		A A
Sperrverzögerungsladung recovered charge	I_F = 100 A, - di_F/dt = 2600 A/µs (T_{vj}=125°C) V_R = 600 V V_{GE} = -15 V	T_{vj} = 25°C T_{vj} = 125°C	Q_r	12,0 20,5		µC µC
Abschaltenergie pro Puls reverse recovery energy	I_F = 100 A, - di_F/dt = 2600 A/µs (T_{vj}=125°C) V_R = 600 V V_{GE} = -15 V	T_{vj} = 25°C T_{vj} = 125°C	E_{rec}	4,80 8,60		mJ mJ
Innerer Wärmewiderstand thermal resistance, junction to case	pro Diode per diode		R_{thJC}		0,43	0,48	K/W
Übergangs-Wärmewiderstand thermal resistance, case to heatsink	pro Diode / per diode λ_{Paste} = 1 W/(m·K) / λ_{grease} = 1 W/(m·K)		R_{thCH}		0,23		K/W

NTC-Widerstand / NTC-thermistor

Charakteristische Werte / characteristic values

			min.	typ.	max.	
Nennwiderstand rated resistance	T_C = 25°C		R_{25}		5,00		kΩ
Abweichung von R_{100} deviation of R_{100}	T_C = 100°C, R_{100} = 493 Ω		ΔR/R	-5		5	%
Verlustleistung power dissipation	T_C = 25°C		P_{25}			20,0	mW
B-Wert B-value	$R_2 = R_{25} \exp[B_{25/50}(1/T_2 - 1/(298{,}15\ K))]$		$B_{25/50}$		3375		K

prepared by: Christoph Messelke	date of publication: 2006-11-28
approved by: Marc Buschkühle	revision: 2.1

Vorläufige Daten
preliminary data

Modul / module

Isolations-Prüfspannung insulation test voltage	RMS, f = 50 Hz, t = 1 min	V_{ISOL}		2,5		kV
Material für innere Isolation material for internal insulation				Al_2O_3		
Kriechstrecke creepage distance	Kontakt - Kühlkörper / terminal to heatsink Kontakt - Kontakt / terminal to terminal			13,5 7,5		mm
Luftstrecke clearance distance	Kontakt - Kühlkörper / terminal to heatsink Kontakt - Kontakt / terminal to terminal			12,0 7,5		mm
Vergleichszahl der Kriechwegbildung comparative tracking index		CTI		> 225		
			min.	typ.	max.	
Modulinduktivität stray inductance module		L_{sCE}		17		nH
Modulleitungswiderstand, Anschlüsse - Chip module lead resistance, terminals - chip	T_C = 25°C, pro Schalter / per switch	$R_{CC'+EE'}$		1,80		mΩ
Höchstzulässige Sperrschichttemperatur maximum junction temperature	Wechselrichter, Brems-Chopper / Inverter, Brake-Chopper	$T_{vj\ max}$			150	°C
Temperatur im Schaltbetrieb temperature under switching conditions	Wechselrichter, Brems-Chopper / Inverter, Brake-Chopper	$T_{vj\ op}$	-40		125	°C
Lagertemperatur storage temperature		T_{stg}	-40		125	°C
Anpresskraft für mech. Bef. pro Feder mountig force per clamp		F	40	-	80	N
Gewicht weight		G		36		g

Der Strom im Dauerbetrieb ist auf 25 A eff pro Anschlusspin begrenzt.
The current under continuous operation is limited to 25 A rms per connector pin

Vorläufige Daten
preliminary data

Ausgangskennlinie IGBT-Wechselr. (typisch)
output characteristic IGBT-inverter (typical)
$I_C = f(V_{CE})$
V_{GE} = 15 V

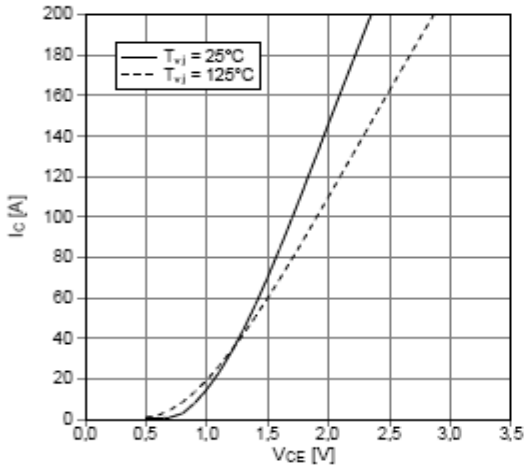

Ausgangskennlinienfeld IGBT-Wechselr. (typisch)
output characteristic IGBT-inverter (typical)
$I_C = f(V_{CE})$
T_{vj} = 125°C

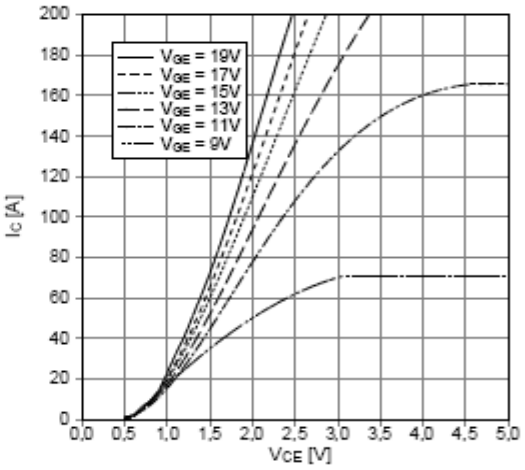

Übertragungscharakteristik IGBT-Wechselr. (typisch)
transfer characteristic IGBT-inverter (typical)
$I_C = f(V_{GE})$
V_{CE} = 20 V

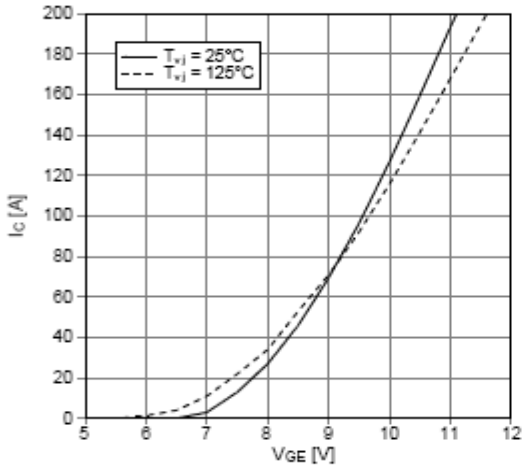

Schaltverluste IGBT-Wechselr. (typisch)
switching losses IGBT-inverter (typical)
$E_{on} = f(I_C)$, $E_{off} = f(I_C)$
V_{GE} = ±15 V, R_{Gon} = 6,8 Ω, R_{Goff} = 6,8 Ω, V_{CE} = 600 V

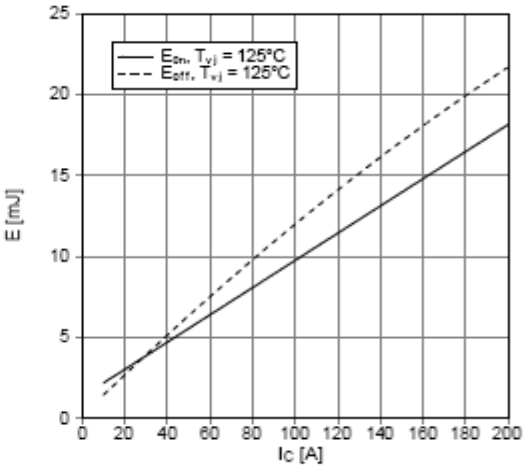

prepared by: Christoph Messelke	date of publication: 2006-11-28
approved by: Marc Buschkühle	revision: 2.1

Schaltverluste IGBT-Wechselr. (typisch)
switching losses IGBT-Inverter (typical)
$E_{on} = f(R_G)$, $E_{off} = f(R_G)$
V_{GE} = ±15 V, I_C = 100 A, V_{CE} = 600 V

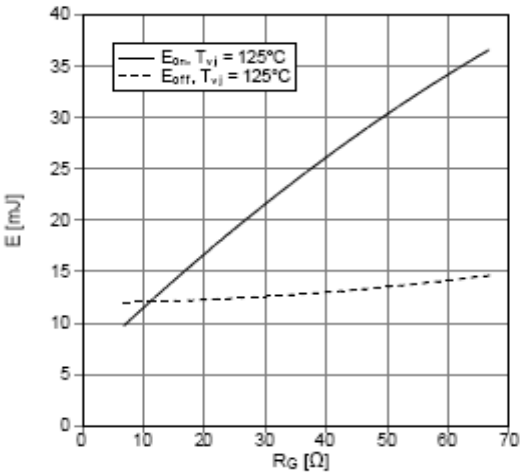

Transienter Wärmewiderstand IGBT-Wechselr.
transient thermal impedance IGBT-inverter
$Z_{thJH} = f(t)$

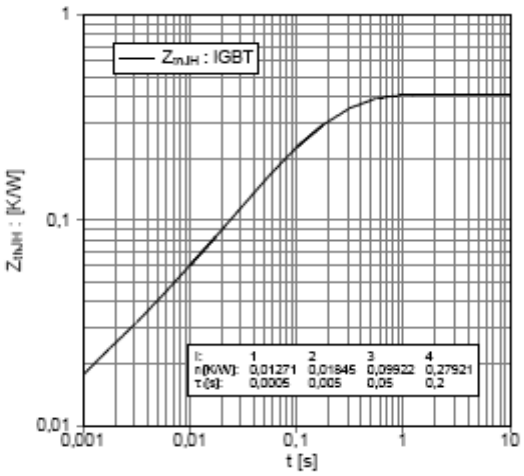

Sicherer Rückwärts-Arbeitsbereich IGBT-Wr. (RBSOA)
reverse bias safe operating area IGBT-inv. (RBSOA)
$I_C = f(V_{CE})$
V_{GE} = ±15 V, R_{Goff} = 6,8 Ω, T_{vj} = 125°C

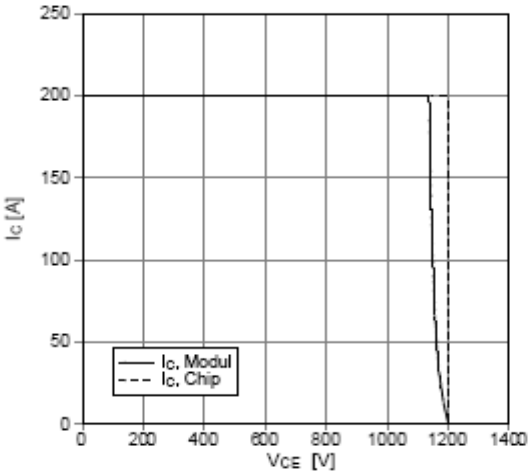

Durchlasskennlinie der Diode-Wechselr. (typisch)
forward characteristic of diode-inverter (typical)
$I_F = f(V_F)$

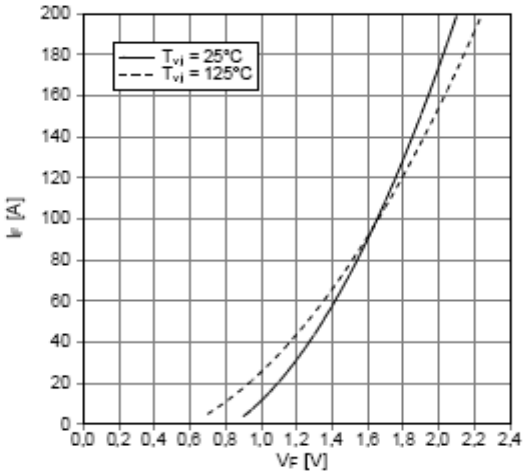

prepared by: Christoph Messelke	date of publication: 2006-11-28
approved by: Marc Buschkühle	revision: 2.1

Vorläufige Daten
preliminary data

Schaltverluste Diode-Wechselr. (typisch)
switching losses diode-inverter (typical)
$E_{rec} = f(I_F)$
$R_{Gon} = 6{,}8\ \Omega$, $V_{CE} = 600$ V

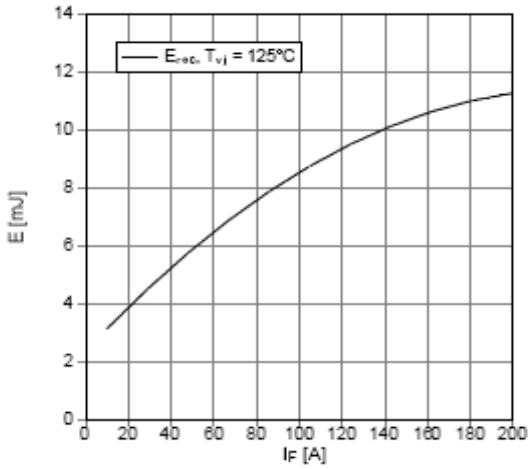

Schaltverluste Diode-Wechselr. (typisch)
switching losses diode-inverter (typical)
$E_{rec} = f(R_G)$
$I_F = 100$ A, $V_{CE} = 600$ V

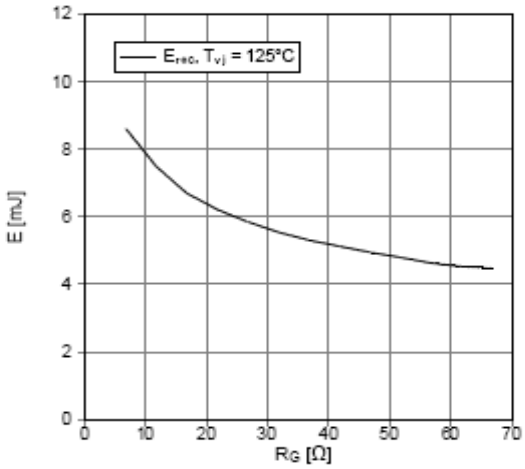

Transienter Wärmewiderstand Diode-Wechselr.
transient thermal impedance diode-inverter
$Z_{thJH} = f(t)$

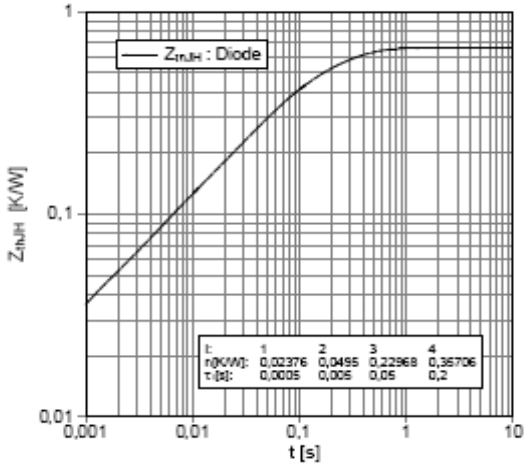

NTC-Temperaturkennlinie (typisch)
NTC-temperature characteristic (typical)
R = f (T)

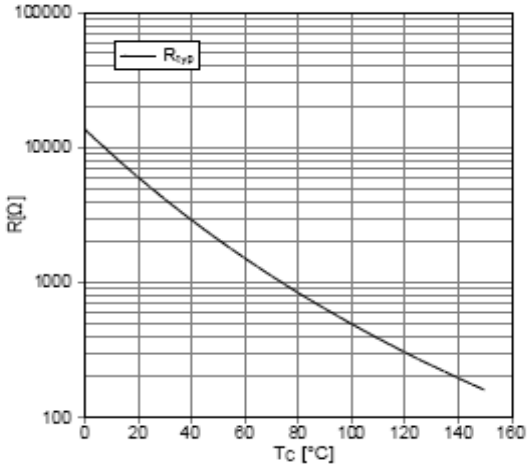

prepared by: Christoph Messelke	date of publication: 2006-11-28
approved by: Marc Buschkühle	revision: 2.1

Vorläufige Daten
preliminary data

Schaltplan / circuit diagram

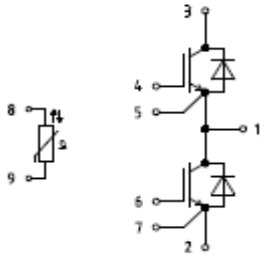

Gehäuseabmessungen / package outlines

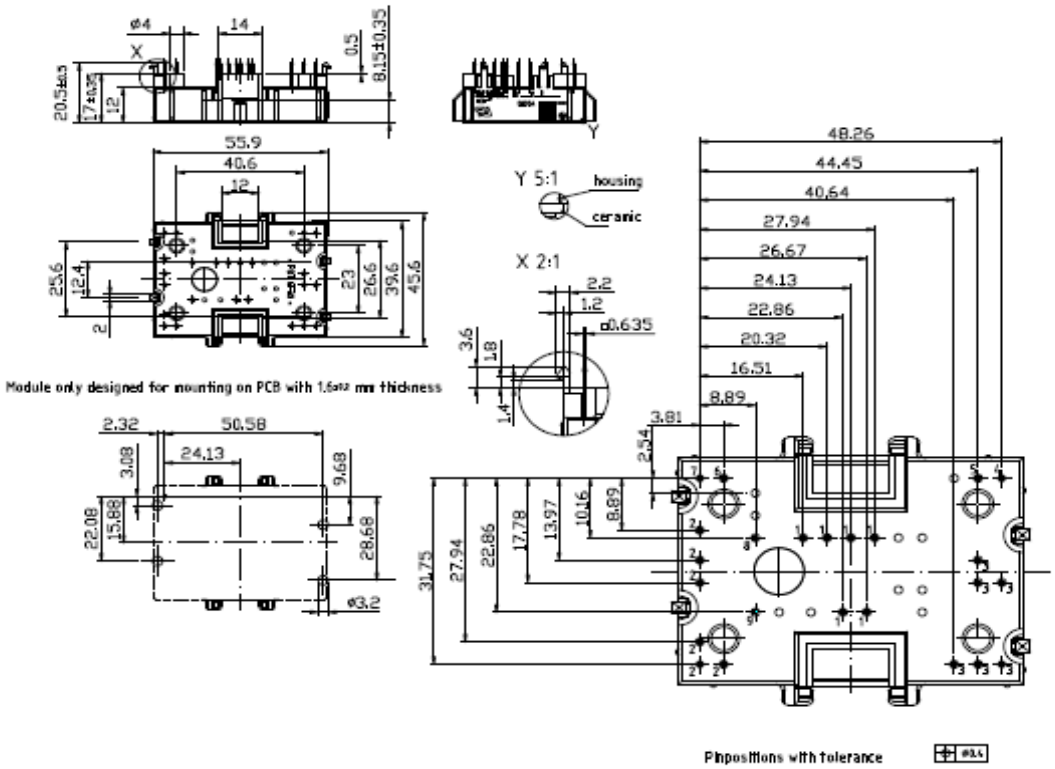

prepared by: Christoph Messelke	date of publication: 2006-11-28
approved by: Marc Buschkühle	revision: 2.1

Vorläufige Daten
preliminary data

Nutzungsbedingungen

Die in diesem Produktdatenblatt enthaltenen Daten sind ausschließlich für technisch geschultes Fachpersonal bestimmt. Die Beurteilung der Eignung dieses Produktes für Ihre Anwendung sowie die Beurteilung der Vollständigkeit der bereitgestellten Produktdaten für diese Anwendung obliegt Ihnen bzw. Ihren technischen Abteilungen.

In diesem Produktdatenblatt werden diejenigen Merkmale beschrieben, für die wir eine liefervertragliche Gewährleistung übernehmen. Eine solche Gewährleistung richtet sich ausschließlich nach Maßgabe der im jeweiligen Liefervertrag enthaltenen Bestimmungen. Garantien jeglicher Art werden für das Produkt und dessen Eigenschaften keinesfalls übernommen.

Sollten Sie von uns Produktinformationen benötigen, die über den Inhalt dieses Produktdatenblatts hinausgehen und insbesondere eine spezifische Verwendung und den Einsatz dieses Produktes betreffen, setzen Sie sich bitte mit dem für Sie zuständigen Vertriebsbüro in Verbindung (siehe www.eupec.com, Vertrieb&Kontakt). Für Interessenten halten wir Application Notes bereit.

Aufgrund der technischen Anforderungen könnte unser Produkt gesundheitsgefährdende Substanzen enthalten. Bei Rückfragen zu den in diesem Produkt jeweils enthaltenen Substanzen setzen Sie sich bitte ebenfalls mit dem für Sie zuständigen Vertriebsbüro in Verbindung.

Sollten Sie beabsichtigen, das Produkt in Anwendungen der Luftfahrt, in gesundheits- oder lebensgefährdenden oder lebenserhaltenden Anwendungsbereichen einzusetzen, bitten wir um Mitteilung. Wir weisen darauf hin, dass wir für diese Fälle
- die gemeinsame Durchführung eines Risiko- und Qualitätsassessments;
- den Abschluss von speziellen Qualitätssicherungsvereinbarungen;
- die gemeinsame Einführung von Maßnahmen zu einer laufenden Produktbeobachtung dringend empfehlen und gegebenenfalls die Belieferung von der Umsetzung solcher Maßnahmen abhängig machen.

Soweit erforderlich, bitten wir Sie, entsprechende Hinweise an Ihre Kunden zu geben.

Inhaltliche Änderungen dieses Produktdatenblatts bleiben vorbehalten.

Terms & Conditions of usage

The data contained in this product data sheet is exclusively intended for technically trained staff. You and your technical departments will have to evaluate the suitability of the product for the intended application and the completeness of the product data with respect to such application.

This product data sheet is describing the characteristics of this product for which a warranty is granted. Any such warranty is granted exclusively pursuant the terms and conditions of the supply agreement. There will be no guarantee of any kind for the product and its characteristics.

Should you require product information in excess of the data given in this product data sheet or which concerns the specific application of our product, please contact the sales office, which is responsible for you (see www.eupec.com, sales&contact). For those that are specifically interested we may provide application notes.

Due to technical requirements our product may contain dangerous substances. For information on the types in question please contact the sales office, which is responsible for you.

Should you intend to use the Product in aviation applications, in health or live endangering or life support applications, please notify. Please note, that for any such applications we urgently recommend
- to perform joint Risk and Quality Assessments;
- the conclusion of Quality Agreements;
- to establish joint measures of an ongoing product survey,

and that we may make delivery depended on the realization of any such measures.

If and to the extent necessary, please forward equivalent notices to your customers.

Changes of this product data sheet are reserved.

prepared by: Christoph Messelke	date of publication: 2006-11-28
approved by: Marc Buschkühle	revision: 2.1

APPENDIX F:

Infineon Iposim Loss Calculation Results

Never stop thinking

Created For: DC/AC | Three Phase - 2 Level | Sine-Triangle
Created By: James McBryde
Created On: 9/12/2009 2:18:17 PM

IPOSIM
Infineon Power Module Selector and Simulator

Input Requirements

Control Algorithm	Sine-Triangle	
DC Link Voltage	800	V
Blocking Voltage	1200	V
Output Frequency	50	Hz
Output Current RMS	24	A
Modulation Index	0.95	
Current Phase Shift	0	°
Switching Frequency	20000	Hz

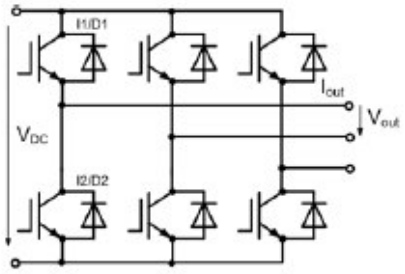

Modules

FF100R12YT3

Igbt Parameters

$V_{CEsat,25°C}$	1.70	V
$E_{on}+E_{off,125°C}$	21.80	mWs
$R_{G,on}$	6.800	Ω
$R_{G,off}$	6.800	Ω
R_{thJC}	0.280	K/W
R_{thCH}	0.160	K/W

Diode Parameters

$V_{F,25°C}$	1.65	V
$E_{rec,125°C}$	8.60	mWs
R_{thJC}	0.480	K/W
R_{thCH}	0.230	K/W

Application Data

$R_{G,on}$	6.800	Ω
$R_{G,off}$	6.800	Ω

Fixed Heat Sink

Case Temperature	82	°C

Junction Temperatures

✓ IGBT	123.4	°C
✓ Diode	122.7	°C

Switching Losses

IGBT	80.435	W
Diode	50.039	W

Conduction Losses

IGBT	9.030	W
Diode	2.428	W

✓ Calculated junction temperature is within range.

✗ Calculated junction temperature is greater than maximum junction temperature.

APPENDIX G:

Semikron Datasheet for SK100GB12T4T

SK100GB12T4T

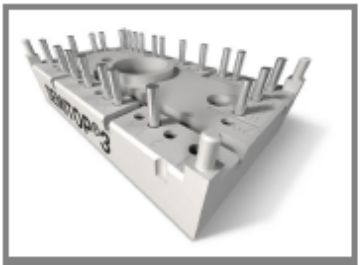

SEMITOP® 3

IGBT Module

SK100GB12T4 T

Target Data

Features

- One screw mounting module
- Trench4 IGBT technology
- CAL4 technology FWD
- Integrated NTC temperature sensor

Typical Applications

Remarks

- $V_{CE,sat}$, V_F = chip level value

GB-T

Absolute Maximum Ratings			T_s = 25 °C, unless otherwise specified	
Symbol	Conditions		Values	Units
IGBT				
V_{CES}	T_j = 25 °C		1200	V
I_C	T_j = 175 °C	T_s = 25 °C	100	A
		T_s = 70 °C	80	A
I_{CRM}	I_{CRM} = 3 x I_{Cnom}		300	A
V_{GES}			± 20	V
t_{psc}	V_{CC} = 800 V; $V_{GE} \leq$ 15 V; V_{CES} < 1200 V	T_j = 150 °C	10	µs
Inverse Diode				
I_F	T_j = 175 °C	T_s = 25 °C	85	A
		T_s = 70 °C	65	A
I_{FRM}	I_{FRM} = 3 x I_{Fnom}		300	A
I_{FSM}	t_p = 10 ms; half sine wave	T_j = 150 °C	715	A
Module				
$I_{t(RMS)}$				A
T_{vj}			-40 ... +175	°C
T_{stg}			-40 ... +125	°C
V_{isol}	AC, 1 min.		2500	V

Characteristics			T_s = 25 °C, unless otherwise specified			
Symbol	Conditions		min.	typ.	max.	Units
IGBT						
$V_{GE(th)}$	V_{GE} = V_{CE}, I_C = 3,4 mA		5	5,8	6,5	V
I_{CES}	V_{GE} = 0 V, V_{CE} = V_{CES}	T_j = 25 °C			0,02	mA
		T_j = 125 °C				mA
I_{GES}	V_{CE} = 0 V, V_{GE} = 20 V	T_j = 25 °C			1200	nA
		T_j = 125 °C				nA
V_{CE0}		T_j = 25 °C		1,1	1,3	V
		T_j = 150 °C		1	1,2	V
r_{CE}	V_{GE} = 15 V	T_j = 25°C		7,5		mΩ
		T_j = 150°C		12,5		mΩ
$V_{CE(sat)}$	I_{Cnom} = 100 A, V_{GE} = 15 V	T_j = 25°C$_{chiplev.}$		1,85	2,05	V
		T_j = 150°C$_{chiplev.}$		2,25	2,45	V
C_{ies}				5,54		nF
C_{oes}	V_{CE} = 25, V_{GE} = 0 V	f = 1 MHz		0,41		nF
C_{res}				0,32		nF
Q_G	V_{GE}=-7V...+15V			750		nC
R_{Gint}	T_j = 25 °C			2		Ω
$t_{d(on)}$				63		ns
t_r	R_{Gon} = 16 Ω	V_{CC} = 600V		65		ns
E_{on}	di/dt = 1800 A/µs	I_C = 100A		16,6		mJ
$t_{d(off)}$	R_{Goff} = 16 Ω	T_j = 150 °C		521		ns
t_f	di/dt = 1800 A/µs	V_{GE} = ±15 V		80		ns
E_{off}				10		mJ
$R_{th(j-s)}$	per IGBT			0,6		K/W

SK100GB12T4T

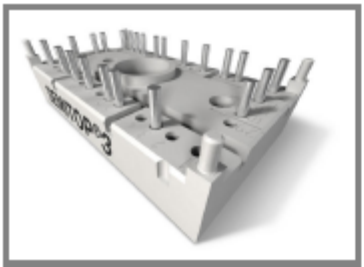

SEMITOP® 3

IGBT Module

SK100GB12T4 T

Target Data

Features

- One screw mounting module
- Trench4 IGBT technology
- CAL4 technology FWD
- Integrated NTC temperature sensor

Typical Applications

Remarks

- $V_{CE,sat}$, V_F = chip level value

GB-T

Characteristics						
Symbol	Conditions		min.	typ.	max.	Units
Inverse Diode						
$V_F = V_{EC}$	I_{Fnom} = 100 A; V_{GE} = 0 V	T_j = 25 °$C_{chiplev.}$		2,25	2,55	V
		T_j = 150 °$C_{chiplev.}$		2,2	2,5	V
V_{F0}		T_j = 25 °C		1,3	1,5	V
		T_j = 150 °C		0,9	1,1	V
r_F		T_j = 25 °C		9,5	10,5	mΩ
		T_j = 150 °C		13	14	mΩ
I_{RRM}	I_F = 100 A	T_j = 150 °C		52		A
Q_{rr}	di/dt = 1800 A/µs			14		µC
E_{rr}	V_{CC} = 600V			5,2		mJ
$R_{th(j-s)D}$	per diode			0,87		K/W
M_s	to heat sink				2,5	Nm
w				30		g
Temperature sensor						
R_{100}	T_s=100°C (R_{25}=5kΩ)			493±5%		Ω

This is an electrostatic discharge sensitive device (ESDS), international standard IEC 60747-1, Chapter IX.

This technical information specifies semiconductor devices but promises no characteristics. No warranty or guarantee expressed or implied is made regarding delivery, performance or suitability.

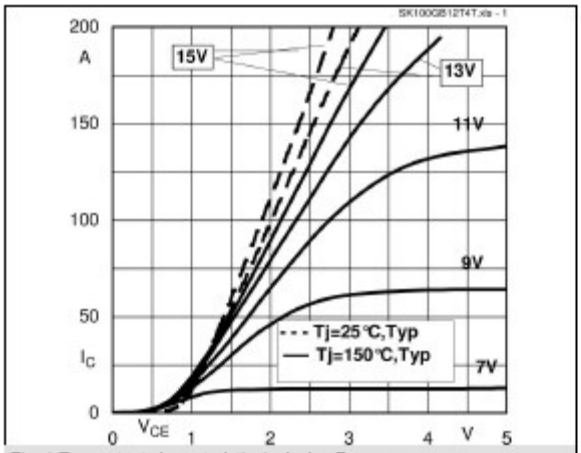

Fig. 1 Typ. output characteristic, inclusive $R_{CC'+EE'}$

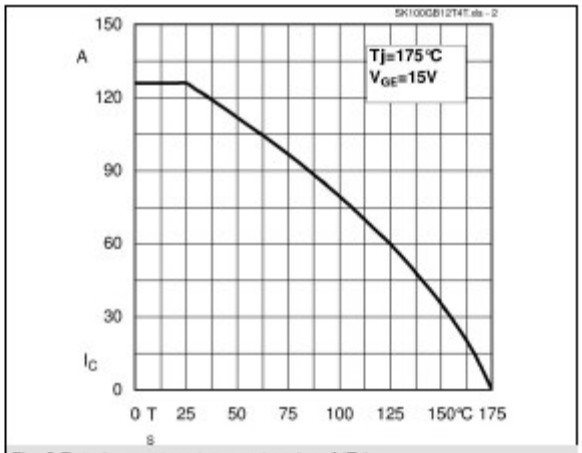

Fig. 2 Rated current vs. temperature $I_C = f(T_s)$

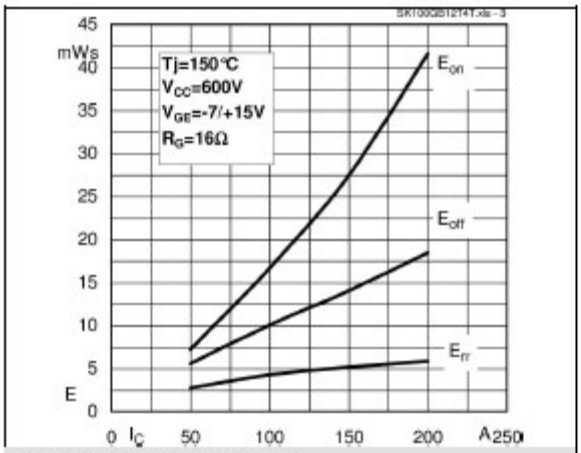

Fig. 3 Typ. turn-on /-off energy = f (I_C)

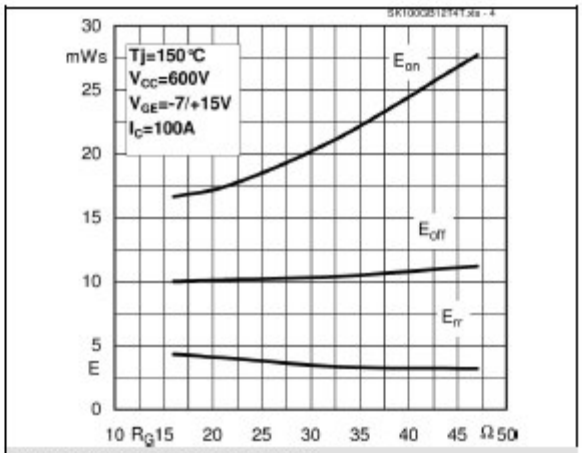

Fig. 4 Typ. turn-on /-off energy = f (R_G)

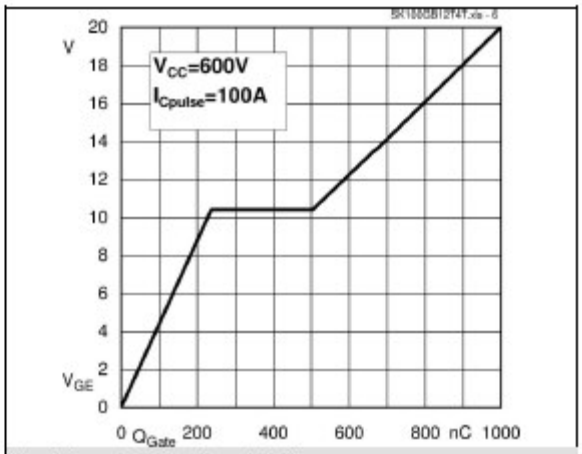

Fig. 6 Typ. gate charge characteristic

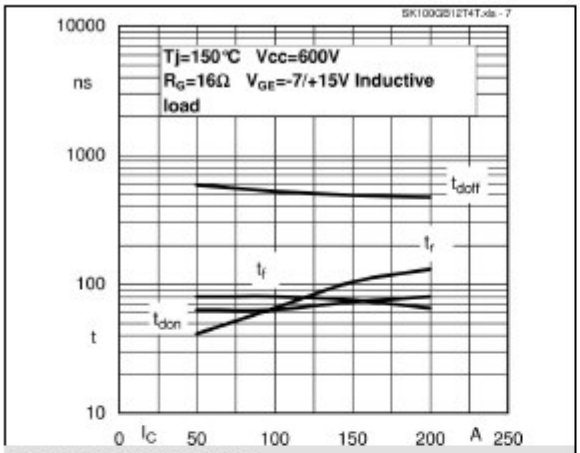

Fig. 7 Typ. switching times vs. I_C

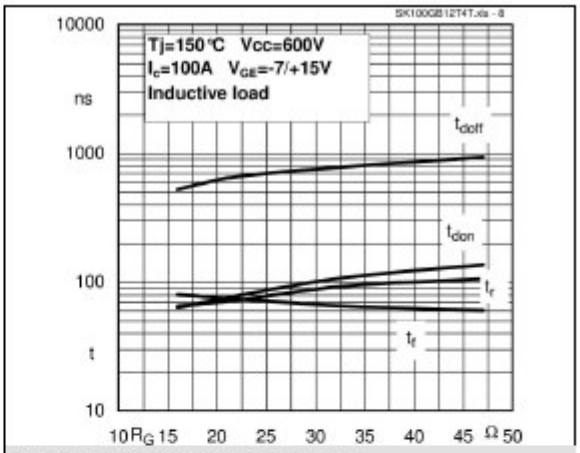

Fig. 8 Typ. switching times vs. gate resistor R_G

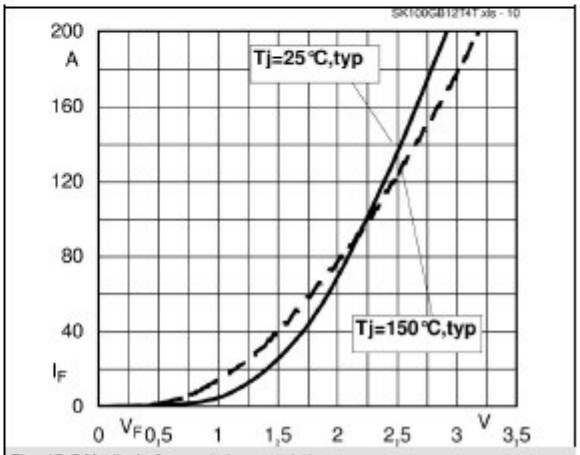

Fig. 10 CAL diode forward characteristic

SK100GB12T4T

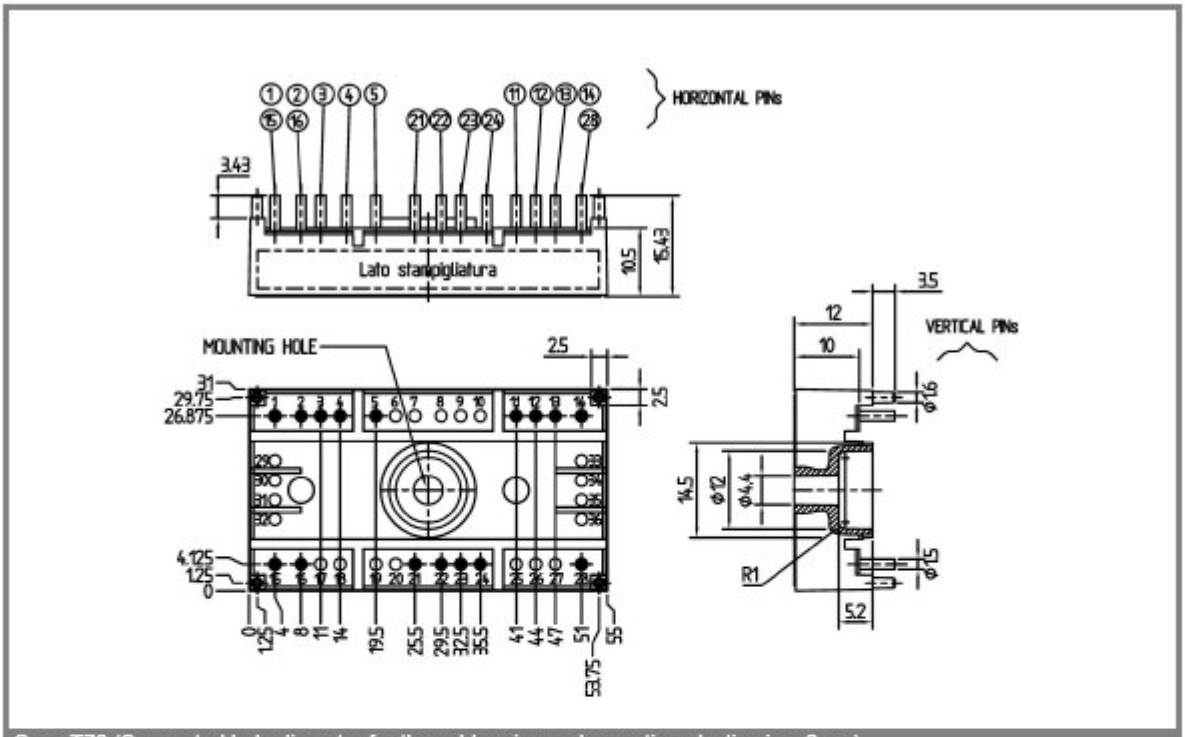

Case T73 (Suggested hole diameter for the solder pins and mounting plastic pins: 2mm)

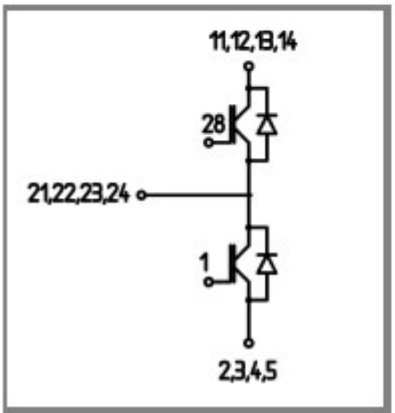

Case T73 GB-T

APPENDIX H:

Semikron Semisel Loss Calculation Results

SEMISEL™

SEMIKRON
innovation+service

Project:

Topology	DC/AC
Circuit	Inverter 3 Phases
E-Mail	jamesmcb@mail.com
Application	UPS

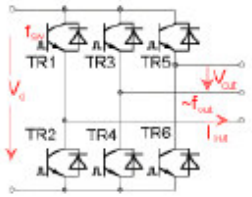

Circuit:

V_d	800 V
V_{out}	480 V
I_{out}	24 A
P_{out}	20 kW
f_{out}	60 Hz
Cos_{phi}	1
f_{sw}	20 kHz
$V_{min\ out}$	480 V
$f_{min\ out}$	60 Hz
Overload Factor	1
Overload Duration	1 sec

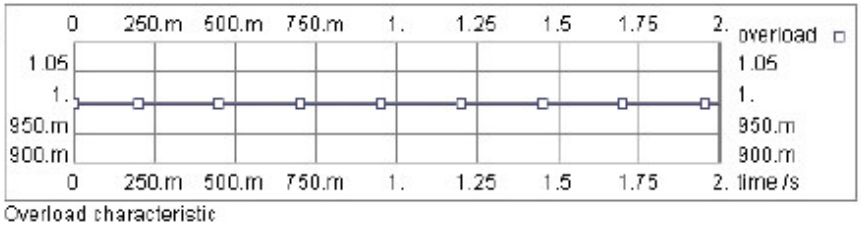

Overload characteristic

Device :

Product Line	**SEMITOP**
Device	**SK100GB12T4T***
Use Maximum Values	No
Max. Junction Temperature	175 °C

Transistor	**Diode**
E_{tr} = 26.6 mJ (@ 600V)	E_d = 5.2 mJ
$V_{CE0.150}$ = 1 V	$V_{T0.150}$ = 0.9 V
$r_{C.150}$ = 12.5 mOhm	$r_{T.150}$ = 13 mOhm
$V_{CE.sat}$ = 2.25 V	V_f = 2.20 V
I_c = 100.00 A	I_f = 100.00 A
$R_{th(j-c)}$ = 0.6 K/W	$R_{th(j-c)}$ = 0.87 K/W
$R_{th(c-s)}$ = 0 K/W	

* - Target data

Data set from 2009/06/24

Cooling:

Ambient temperature	40 °C
Number of switches per heat sink	6
Number of parallel devices on the same heat sink	1

Additional power source at this heat sink	0
Maximum Heat Sink Temperature	82 °C

Calculated losses and temperatures with rated current, at overload and at $f_{min\ out}$:

	Rated Current	Overload	f_{min} and Overload
$P_{cond\ tr}$	13 W	13 W	13 W
$P_{sw\ tr}$	83 W	83 W	86 W
P_{tr}	96 W	96 W	99 W
$P_{cond\ d}$	1.61 W	1.61 W	1.60 W
$P_{sw\ d}$	15 W	15 W	16 W
P_d	17 W	17 W	17 W
P_{tot}	677 W	677 W	701 W
	Average Values	Average Values	Maximum Values
T_h	82 °C	82 °C	82 °C
T_c	82 °C	82 °C	82 °C
T_{tr}	139 °C	139 °C	154 °C
T_d	97 °C	97 °C	100 °C

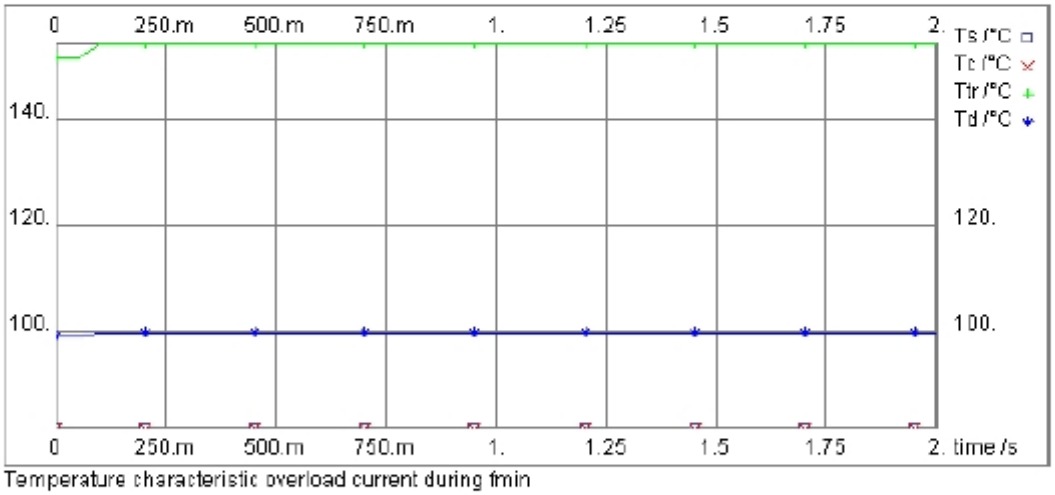

Temperature characteristic overload current during fmin

Evaluation:

Recommendation by SEMIKRON: Do not use SEMIKRON devices over 150 °C

Device driver suggestion

Name	Iout (av) /mA	Îout /A	Visol /kV	Vce max /V	Rgmin / Ohm	Channels
3x SKHI23/12 R	50	8	2.5	1200	2.7	2
1x SKHI61 R	20	2	2.5	900	10.0	6
3x SKYPER 32 R or SKYPER 32PRO R	50	15	4.0	1200	1.5	2

Additional Characteristics at given nominal operation conditions with one free parameter - X:

None selected

APPENDIX I:

Double Pulse Generator Schematic

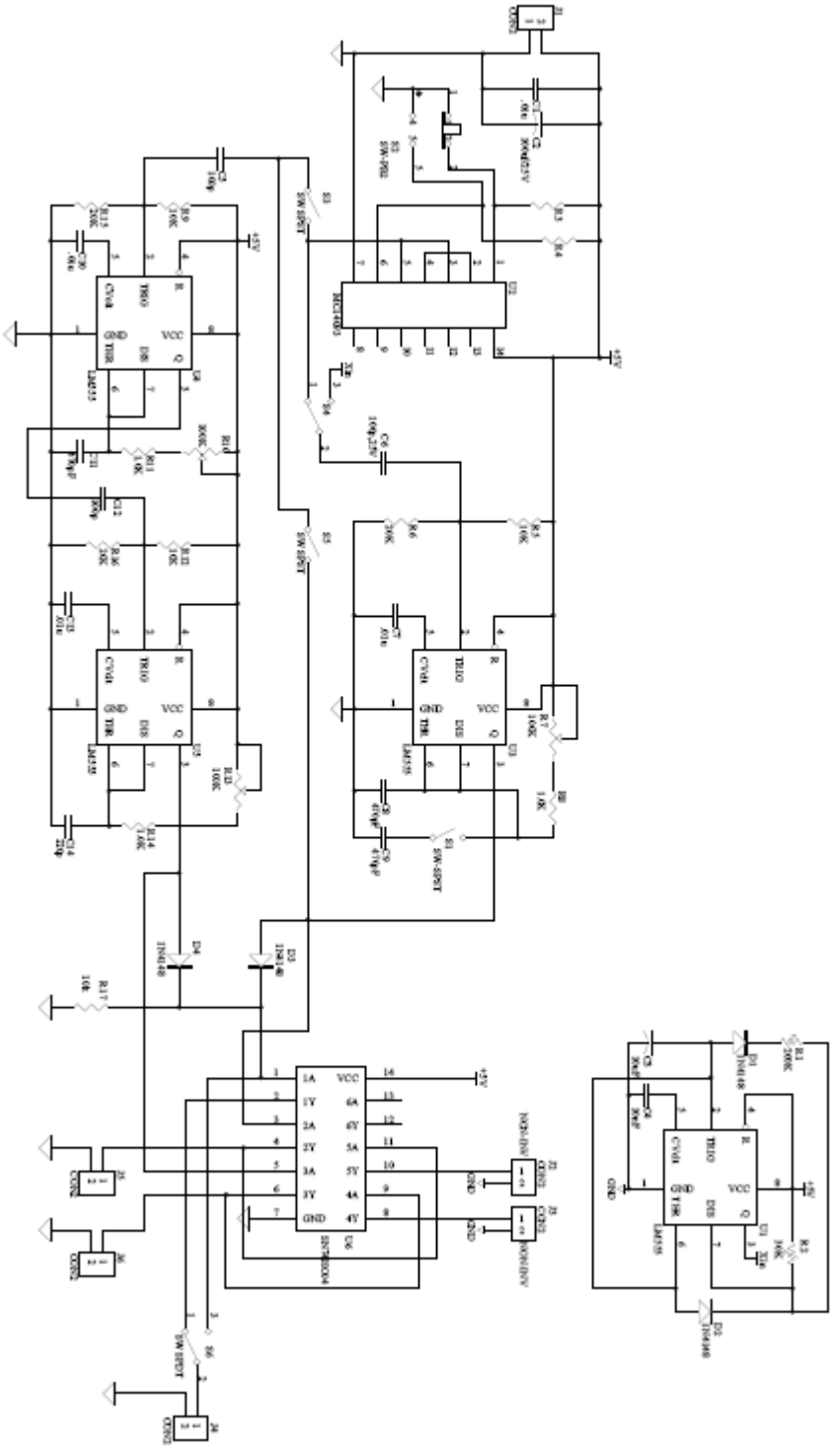

APPENDIX J:

Switching Tester Schematic

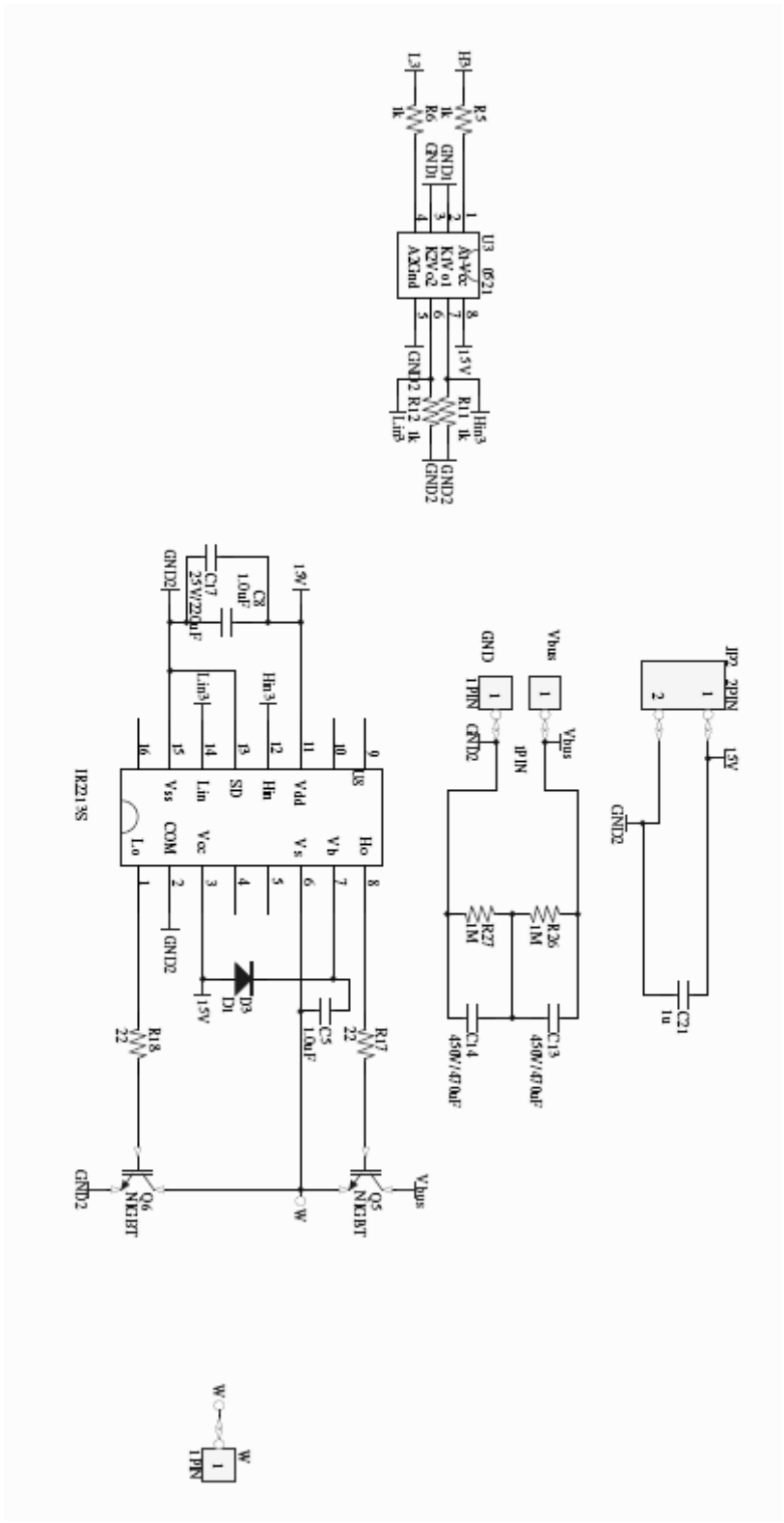
JP2 2PIN
15V
GND2
C21
1u
Vbus
GND
1PIN
GND2
iPIN
Vbus
R27
1M
R26
1M
C14
450V/47.0uF
C13
450V/47.0uF
U3 6021
Ain-Vcc
K1Vo1
K2Vo2
AGnd
R5
1k
R6
1k
R11 1k
R12 1k
Hin3
Lin3
GND1
GND2
15V
C8
1.0uF
C17
25V/220uF
Lin3
Hin3
IR2136S
Vss
COM
Lin
Vcc
SD
Hin
Vdd
Vs
Vb
Ho
Lo
D3
D1
C5
1.0uF
R18
22
R17
22
Q6
NIGBT
Q5
NIGBT
W
W
1PIN

APPENDIX K:

Cree CMF20120D SiC MOSFET Datasheet

CMF20120D

Silicon Carbide Power MOSFET

N-Channel Enhancement Mode

V_{DS}	= 1200 V
$R_{DS(on)}$	= 75 mΩ
I_D@V_{GS}=20V	= 20 A

Features

- Industry Leading $R_{DS(on)}$
- High Speed Switching
- Low Capacitances
- Fast Body Diode
- Easy to Parallel
- Simple to Drive

Benefits

- Higher System Efficiency
- Reduced Cooling Requirements
- Avalanche Ruggedness
- Increase System Switching Frequency

Applications

- Solar Inverters
- Downhole Drilling Equipment
- Motor Drives

Package

TO-247-3

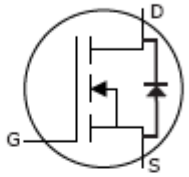

Part Number	Package
CMF20120D	TO-247-3

Maximum Ratings

Symbol	Parameter	Value	Unit	Test Conditions	Note
I_D	Continuous Drain Current	20	A	V_{GS}@20V, T_C = 150°C	
I_{Dpulse}	Pulsed Drain Current	50	A	t_D limited by T_{jmax}	
E_{AS}	Single Pulse Avalanche Energy	1	J	I_D = 26A, V_{DD} = 50 V, L = 3 mH	
E_{AR}	Repetitive Avalanche Energy	500	mJ	t_{AR} limited by T_{jmax}	
I_{AR}	Repetitive Avalanche Current	20	A	I_D = 20A, V_{DD} = 50 V, L = 3 mH t_{AR} limited by T_{jmax}	
V_{GS}	Gate Source Voltage	-5/+20	V		
P_{tot}	Power Dissipation	300	W	T_C=25°C	
T_J , T_{stg}	Operating Junction and Storage Temperature	-55 to +175	°C		
T_L	Solder Temperature	300	°C	1.6mm (0.063") from case for 10s	

CREE

Electrical Characteristics

Symbol	Parameter	Min.	Typ.	Max.	Unit	Test Conditions	Note
$V_{(BR)DSS}$	Drain-Source Breakdown Voltage	1200			V	V_{GS} = 0V, I_D = 10μA	
$V_{GS(th)}$	Gate Threshold Voltage	1.7	2.3 1.5	3	V	V_{DS} = V_{GS}, I_D = 1mA, T_J = 25ºC V_{DS} = V_{GS}, I_D = 1mA, T_J = 175ºC	
I_{DSS}	Zero Gate Voltage Drain Current		0.1 1	10 10	μA	V_{DS} = 1200V, V_{GS} = 0V, T_J = 25ºC V_{DS} = 1200V, V_{GS} = 0V, T_J = 175ºC	
I_{GSS}	Gate-Source Leakage Current			100	nA	V_{GS} = 20V, V_{DS} = 0V	
$R_{DS(on)}$	Drain-Source On-State Resistance		75 110	110 160	mΩ	V_{GS} = 20V, I_D = 20A, T_J = 25ºC V_{GS} = 20V, I_D = 20A, T_J = 175ºC	
g_{fs}	Transconductance		6.2 7.7		S	V_{DS}= 20V, V_{GS}= 10V, T_J = 25ºC V_{DS}= 20V, V_{GS}= 10V, T_J = 175ºC	fig. 3
C_{iss}	Input Capacitance		1806		pF	V_{GS} = 0V V_{DS} = 800V f = 1MHz V_{AC} = 20mV	fig. 5B
C_{oss}	Output Capacitance		190				
C_{rss}	Reverse Transfer Capacitance		18				
$t_{d(on)}$	Turn-On Delay Time		14		ns	T= 25ºC (unless otherwise noted) V_{DD} = 800V V_{GS} = 0/20V I_D = 20A R_G = 10Ω L = 856μH Per JEDEC24 Page 27	fig. 11
t_r	Rise Time		24				
$t_{d(off)}$	Turn-Off Delay Time		53				
t_f	Fall Time		46				
E_{ON}	Turn-On Switching Loss (25ºC) (175ºC)		0.45 0.38		mJ		
E_{OFF}	Turn-Off Switching Loss (25ºC) (175ºC)		0.30 0.45				

Reverse Diode Characteristics

Symbol	Parameter	Typ.	Max.	Unit	Test Conditions	Note
V_{sd}	Diode Forward Voltage	3.6		V	V_{GS} = -5V, I_F=20A, T_J = 25ºC	
t_{rr}	Reverse Recovery Time	258		ns	V_{GS} = -5V, I_F=20A, T_J = 25ºC V_R = 800V, I_F=I_s di_F/dt= 100A/μs	fig. 12,13
Q_{rr}	Reverse Recovery Charge	207		nC		
I_{rrm}	Peak Reverse Recovery Current	2.2		A		

Thermal Characteristics

Symbol	Parameter	Typ.	Max.	Unit	Test Conditions	Note
$R_{\theta JC}$	Thermal Resistance from Junction to Case		0.5	°C/W		fig. 6
$R_{\theta CS}$	Case to Sink, w/ Thermal Compound	0.25				
$R_{\theta JA}$	Thermal Resistance From Junction to Ambient		40			

Gate Charge Characteristics

Symbol	Parameter	Typ.	Max.	Unit	Test Conditions	Note
Q_{gs}	Gate to Source Charge	27.1		nC	V_{DD} = 800V I_D =20A	fig.9
Q_{gd}	Gate to Drain Charge	30.8				
Q_g	Gate Charge Total	91			V_{DD} = 800V V_{ID} =20A V_{GS} = -5/20V Per JEDEC24-2	

Typical Performance

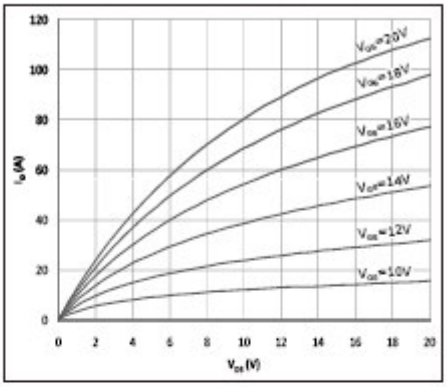

Fig 1. Typical Output Characteristics T_J = 25ºC

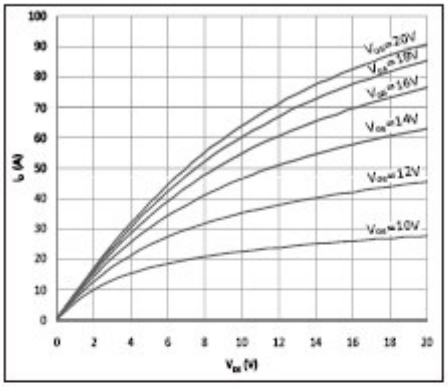

Fig 2. Typical Output Characteristics T_J = 175ºC

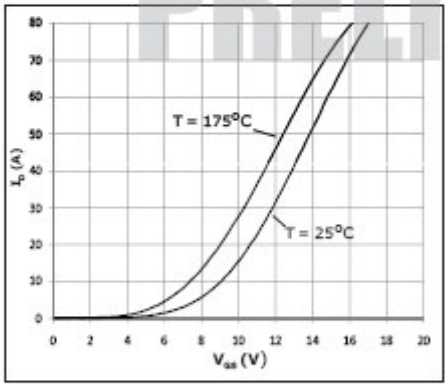

Figure 3. Typical Transfer Characteristics

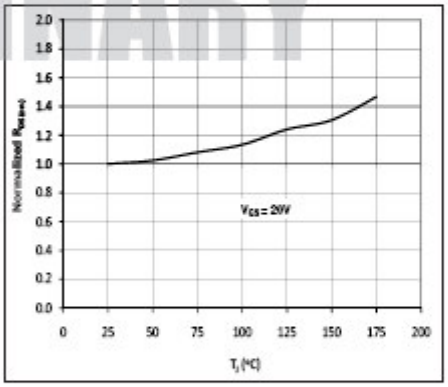

Fig 4. Normalized On-Resistance vs. Temperature

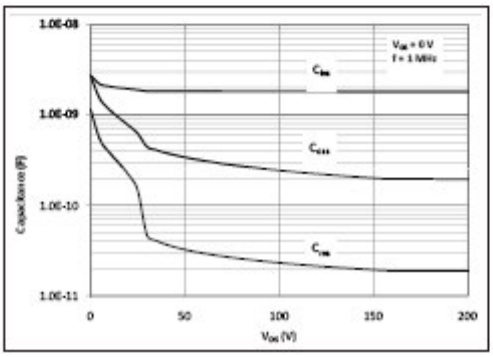

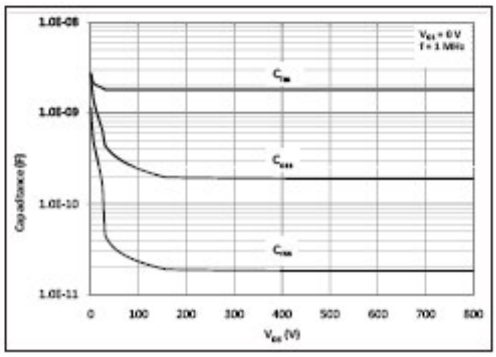

Fig 5A and 5B. Typical Capacitance vs. Drain – Source Voltage

Typical Performance

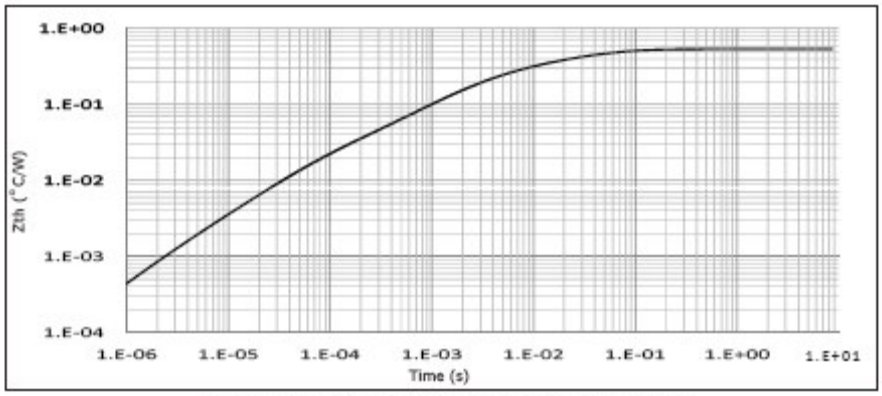

Fig 6. Transient Thermal Impedence, Junction - Case

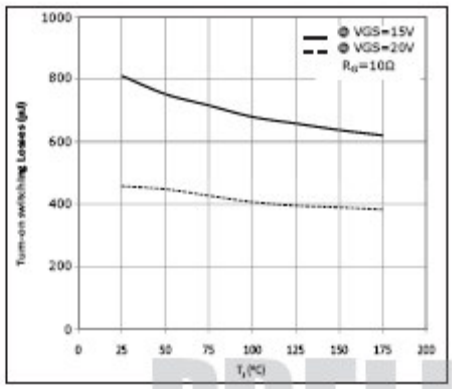

Fig 7. Inductive Switching Energy(Turn-on) vs. T

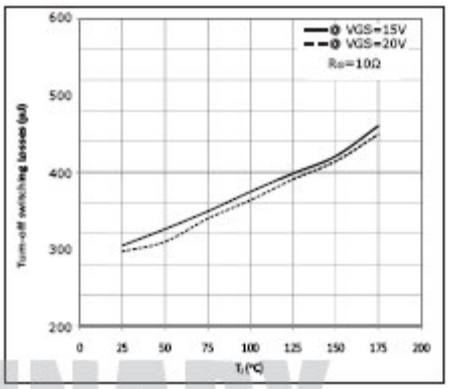

Fig 8. Inductive Switching Energy(Turn-off) vs. T

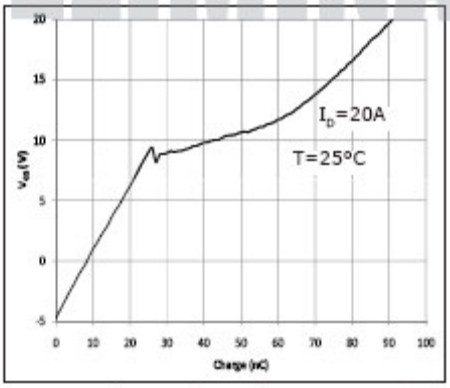

Fig 9. Typical Gate Charge Characteristics @ 25°C

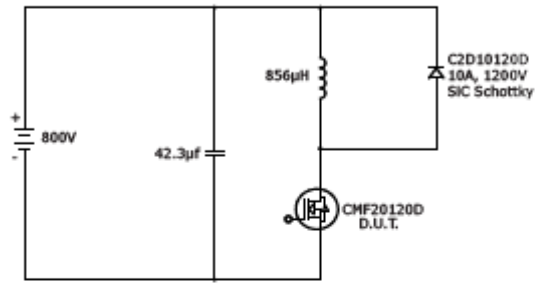

Fig 10. Switching Waveform Test Circuit

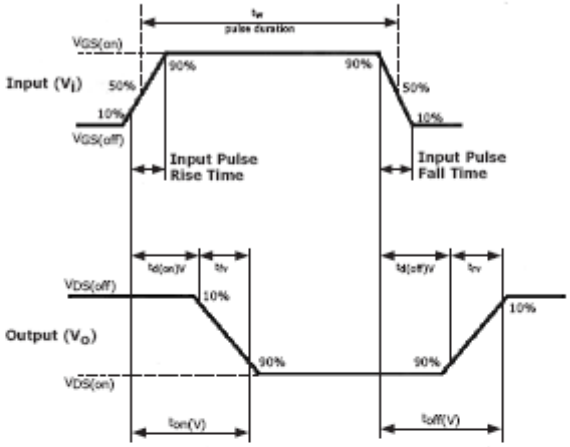

Fig 11. Switching Test Waveform Times

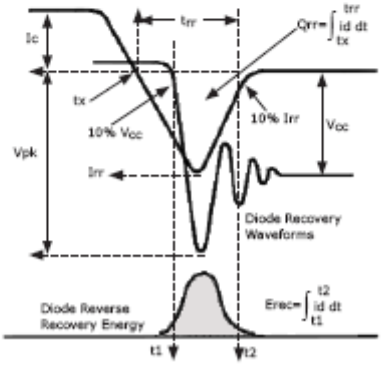

Fig 12. Body Diode Recovery Waveform

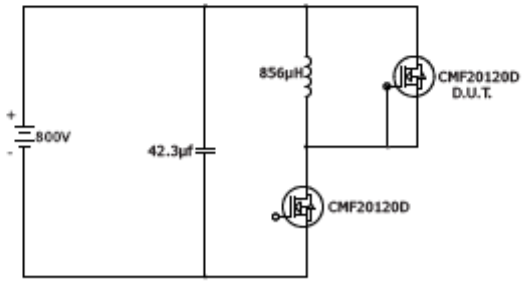

Fig 13. Body Diode Recovery Test

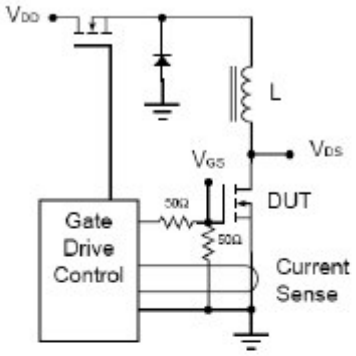

Fig 14. Avalanche Test Circuit

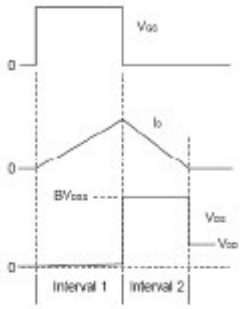

$$E_A = 1/2L \times I_D^2$$

Fig 15. Avalanche Waveform

Package Dimensions

Package TO-247-3

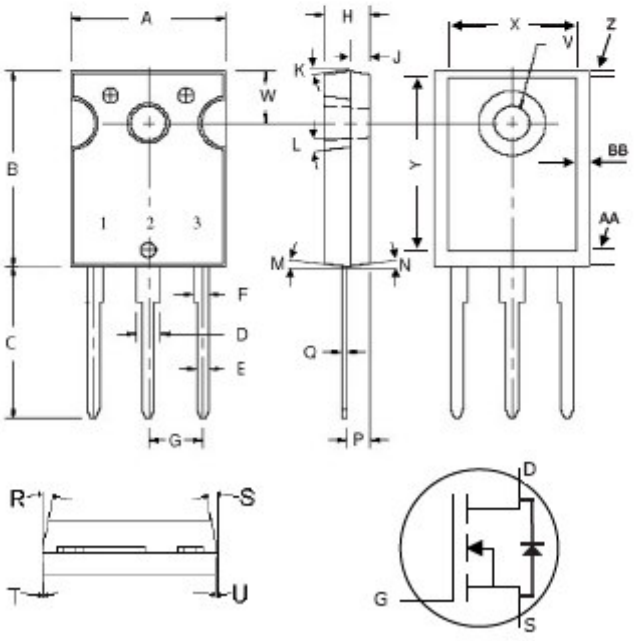

POS	Inches		Millimeters	
	Min	Max	Min	Max
A	.605	.631	15.367	16.027
B	.800	.830	20.320	21.082
C	.789	.800	20.05	20.31
D	.095	.126	2.413	3.200
E	.046	.052	1.168	1.321
F	.060	.084	1.524	2.134
G	.215 TYP		.215 TYP	
H	.180	.203	4.572	5.156
J	.078	.081	1.982	2.057
K	6°	21°	6°	21°
L	4°	6°	4°	6°
M	2°	4°	2°	4°
N	2°	4°	2°	4°
P	.090	.097	2.286	2.464
Q	.020	.030	.508	.762
R	9°	11°	9°	11°
S	9°	11°	9°	11°
T	2°	8°	2°	8°
U	2°	8°	2°	8°
V	.138	.144	3.505	3.658
W	.210	.220	5.334	5.588
X	.502	.557	12.751	14.148
Y	.637	.695	16.180	17.653
Z	.040	.052	1.016	1.321
AA	.032	.046	.813	1.168
BB	.110	.140	2.794	3.556

Recommended Solder Pad Layout

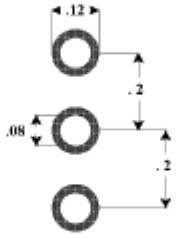

TO-247-3

Part Number	Package
CMF20120D	TO-247-3

APPENDIX L:

Fairchild HGTG27N120BN IGBT Datasheet

FAIRCHILD SEMICONDUCTOR®

HGTG27N120BN / HGT5A27N120BN

Data Sheet **October 2004**

72A, 1200V, NPT Series N-Channel IGBT

The HGTG27N120BN and HGT5A27N120BN are Non-Punch Through (NPT) IGBT design. This is a new member of the MOS gated high voltage switching IGBT family. IGBTs combine the best features of MOSFETs and bipolar transistors. This device has the high input impedance of a MOSFET and the low on-state conduction loss of a bipolar transistor.

The IGBT is ideal for many high voltage switching applications operating at moderate frequencies where low conduction losses are essential, such as: AC and DC motor controls, power supplies and drivers for solenoids, relays and contactors.

Formerly Developmental Type TA49280.

Ordering Information

PART NUMBER	PACKAGE	BRAND
HGTG27N120BN	TO-247	G27N120BN
HGT5A27N120BN	TO-247-ST	27N120BN

NOTE: When ordering, use the entire part number.

Symbol

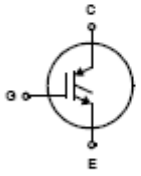

Features

- 72A, 1200V, $T_C = 25^oC$
- 1200V Switching SOA Capability
- Typical Fall Time. . . . . 140ns at $T_J = 150^oC$
- Short Circuit Rating
- Low Conduction Loss
- *Thermal Impedance* SPICE Model
  Temperature Compensating SABER™ Model
  www.fairchildsemi.com
- Avalanche Rated

Packaging

JEDEC STYLE TO-247

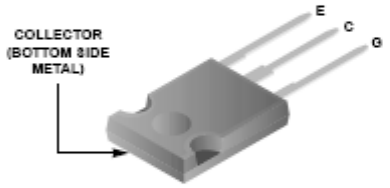

JEDEC STYLE TO-247-ST

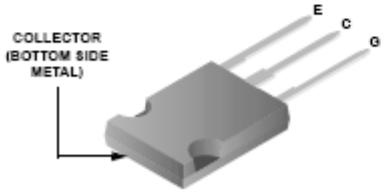

FAIRCHILD SEMICONDUCTOR IGBT PRODUCT IS COVERED BY ONE OR MORE OF THE FOLLOWING U.S. PATENTS

4,364,073	4,417,385	4,430,792	4,443,931	4,466,176	4,516,143	4,532,534	4,587,713
4,598,461	4,605,948	4,620,211	4,631,564	4,639,754	4,639,762	4,641,162	4,644,637
4,682,195	4,684,413	4,694,313	4,717,679	4,743,952	4,783,690	4,794,432	4,801,986
4,803,533	4,809,045	4,809,047	4,810,665	4,823,176	4,837,606	4,860,080	4,883,767
4,888,627	4,890,143	4,901,127	4,904,609	4,933,740	4,963,951	4,969,027	

Absolute Maximum Ratings $T_C = 25^oC$, Unless Otherwise Specified

		HGTG27N120BN	UNITS
Collector to Emitter Voltage	BV_{CES}	1200	V
Collector Current Continuous			
At $T_C = 25^oC$	I_{C25}	72	A
At $T_C = 110^oC$	I_{C110}	34	A
Collector Current Pulsed (Note 1)	I_{CM}	216	A
Gate to Emitter Voltage Continuous	V_{GES}	±20	V
Gate to Emitter Voltage Pulsed	V_{GEM}	±30	V
Switching Safe Operating Area at $T_J = 150^oC$ (Figure 2)	SSOA	150A at 1200V	
Power Dissipation Total at $T_C = 25^oC$	P_D	500	W
Power Dissipation Derating $T_C > 25^oC$		4.0	$W/^oC$
Forward Voltage Avalanche Energy (Note 2)	E_{AV}	135	mJ
Operating and Storage Junction Temperature Range	T_J, T_{STG}	-55 to 150	^oC
Maximum Lead Temperature for Soldering	T_L	260	^oC
Short Circuit Withstand Time (Note 3) at $V_{GE} = 15V$	t_{SC}	8	µs
Short Circuit Withstand Time (Note 3) at $V_{GE} = 12V$	t_{SC}	15	µs

CAUTION: Stresses above those listed in "Absolute Maximum Ratings" may cause permanent damage to the device. This is a stress only rating and operation of the device at these or any other conditions above those indicated in the operational sections of this specification is not implied.

NOTES:

1. Pulse width limited by Max junction temperature.
2. $I_{CE} = 30A$, $L = 400\mu H$, $T_J = 125^oC$
3. $V_{CE(PK)} = 960V$, $T_J = 125^oC$, $R_G = 3\Omega$

Electrical Specifications $T_C = 25^oC$, Unless Otherwise Specified

PARAMETER	SYMBOL	TEST CONDITIONS		MIN	TYP	MAX	UNITS
Collector to Emitter Breakdown Voltage	BV_{CES}	$I_C = 250\mu A$, $V_{GE} = 0V$		1200	-	-	V
Emitter to Collector Breakdown Voltage	BV_{ECS}	$I_C = 10mA$, $V_{GE} = 0V$		15	-	-	V
Collector to Emitter Leakage Current	I_{CES}	$V_{CE} = 1200V$	$T_C = 25^oC$	-	-	250	µA
			$T_C = 125^oC$	-	300	-	µA
			$T_C = 150^oC$	-	-	4	mA
Collector to Emitter Saturation Voltage	$V_{CE(SAT)}$	$I_C = 27A$, $V_{GE} = 15V$	$T_C = 25^oC$	-	2.45	2.7	V
			$T_C = 150^oC$	-	3.8	4.2	V
Gate to Emitter Threshold Voltage	$V_{GE(TH)}$	$I_C = 250\mu A$, $V_{CE} = V_{GE}$		6	6.6	-	V
Gate to Emitter Leakage Current	I_{GES}	$V_{GE} = \pm 20V$		-	-	±250	nA
Switching SOA	SSOA	$T_J = 150^oC$, $R_G = 3\Omega$, $V_{GE} = 15V$, $L = 200\mu H$, $V_{CE(PK)} = 1200V$		150	-	-	A
Gate to Emitter Plateau Voltage	V_{GEP}	$I_C = I_{C110}$, $V_{CE} = 0.5\ BV_{CES}$		-	9.2	-	V
On-State Gate Charge	$Q_{G(ON)}$	$I_C = 27A$, $V_{CE} = 600V$	$V_{GE} = 15V$	-	270	325	nC
			$V_{GE} = 20V$	-	350	420	nC
Current Turn-On Delay Time	$t_{d(ON)I}$	IGBT and Diode at $T_J = 25^oC$, $I_{CE} = 27A$, $V_{CE} = 960V$, $V_{GE} = 15V$, $R_G = 3\Omega$, $L = 1mH$, Test Circuit (Figure 18)		-	24	30	ns
Current Rise Time	t_{rI}			-	20	25	ns
Current Turn-Off Delay Time	$t_{d(OFF)I}$			-	195	240	ns
Current Fall Time	t_{fI}			-	80	120	ns
Turn-On Energy (Note 5)	E_{ON1}			-	2.2	-	mJ
Turn-On Energy (Note 5)	E_{ON2}			-	2.7	3.3	mJ
Turn-Off Energy (Note 4)	E_{OFF}			-	2.3	2.8	mJ

Electrical Specifications T_C = 25°C, Unless Otherwise Specified **(Continued)**

PARAMETER	SYMBOL	TEST CONDITIONS	MIN	TYP	MAX	UNITS
Current Turn-On Delay Time	$t_{d(ON)I}$	IGBT and Diode at T_J = 150°C, I_{CE} = 27A, V_{CE} = 960V, V_{GE} = 15V, R_G = 3Ω, L = 1mH, Test Circuit (Figure 18)	-	22	28	ns
Current Rise Time	t_{rI}		-	20	25	ns
Current Turn-Off Delay Time	$t_{d(OFF)I}$		-	220	280	ns
Current Fall Time	t_{fI}		-	140	200	ns
Turn-On Energy (Note 5)	E_{ON1}		-	2.7	-	mJ
Turn-On Energy (Note 5)	E_{ON2}		-	5.1	6.5	mJ
Turn-Off Energy (Note 4)	E_{OFF}		-	3.4	4.2	mJ
Thermal Resistance Junction To Case	$R_{\theta JC}$		-	-	0.25	°C/W

NOTES:

4. Turn-Off Energy Loss (E_{OFF}) is defined as the integral of the instantaneous power loss starting at the trailing edge of the input pulse and ending at the point where the collector current equals zero (I_{CE} = 0A). All devices were tested per JEDEC Standard No. 24-1 Method for Measurement of Power Device Turn-Off Switching Loss. This test method produces the true total Turn-Off Energy Loss.
5. Values for two Turn-On loss conditions are shown for the convenience of the circuit designer. E_{ON1} is the turn-on loss of the IGBT only. E_{ON2} is the turn-on loss when a typical diode is used in the test circuit and the diode is at the same T_J as the IGBT. The diode type is specified in Figure 18.

Typical Performance Curves Unless Otherwise Specified

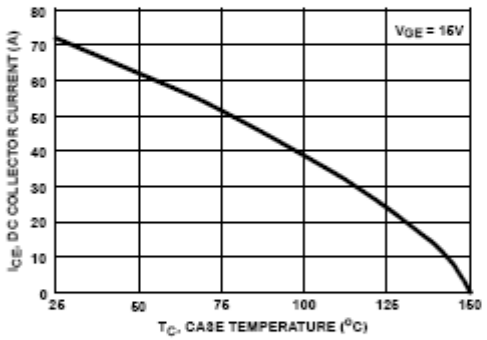

FIGURE 1. DC COLLECTOR CURRENT vs CASE TEMPERATURE

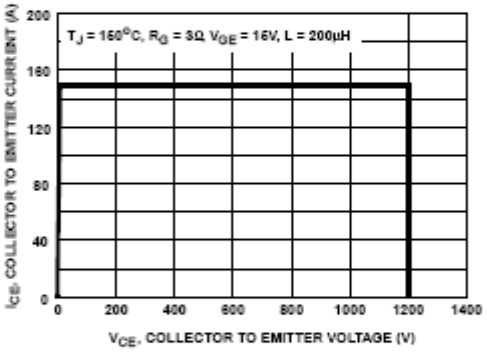

FIGURE 2. MINIMUM SWITCHING SAFE OPERATING AREA

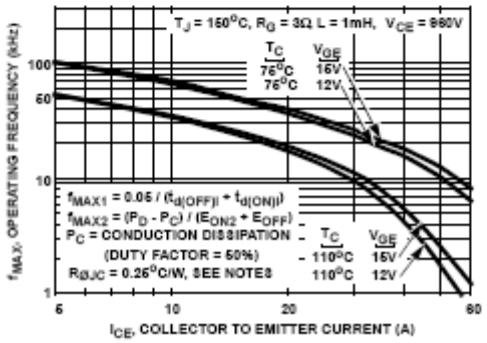

FIGURE 3. OPERATING FREQUENCY vs COLLECTOR TO EMITTER CURRENT

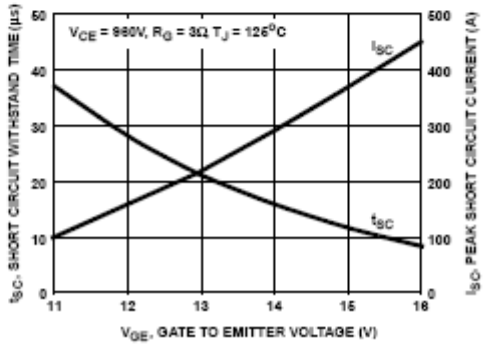

FIGURE 4. SHORT CIRCUIT WITHSTAND TIME

Typical Performance Curves Unless Otherwise Specified (Continued)

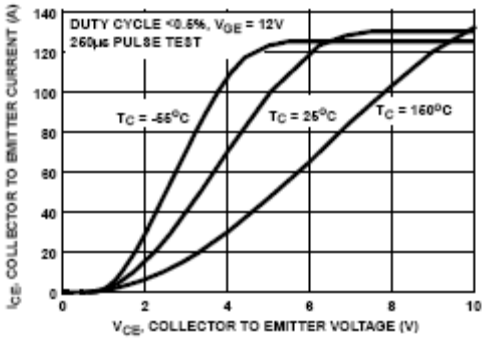

FIGURE 5. COLLECTOR TO EMITTER ON-STATE VOLTAGE

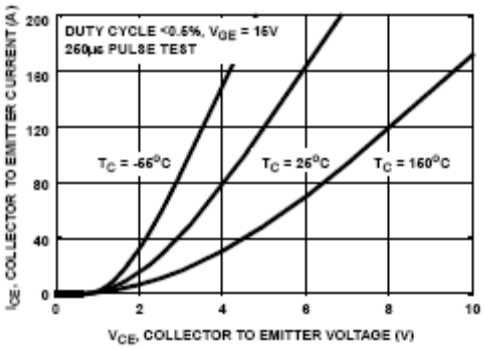

FIGURE 6. COLLECTOR TO EMITTER ON-STATE VOLTAGE

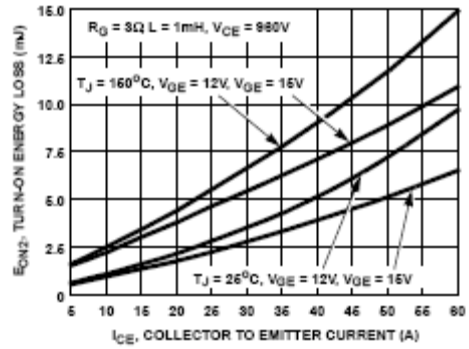

FIGURE 7. TURN-ON ENERGY LOSS vs COLLECTOR TO EMITTER CURRENT

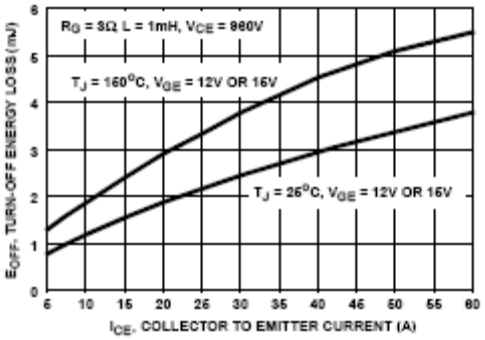

FIGURE 8. TURN-OFF ENERGY LOSS vs COLLECTOR TO EMITTER CURRENT

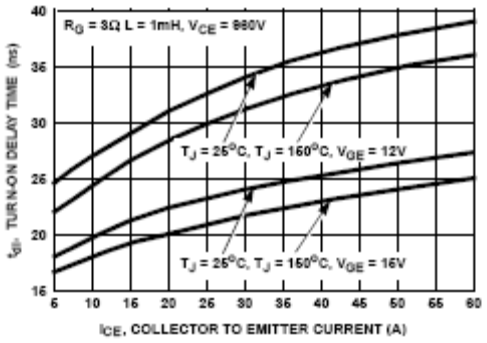

FIGURE 9. TURN-ON DELAY TIME vs COLLECTOR TO EMITTER CURRENT

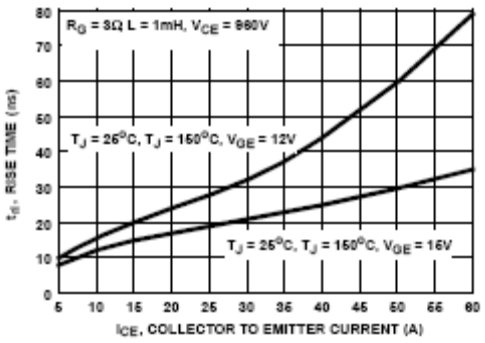

FIGURE 10. TURN-ON RISE TIME vs COLLECTOR TO EMITTER CURRENT

Typical Performance Curves Unless Otherwise Specified (Continued)

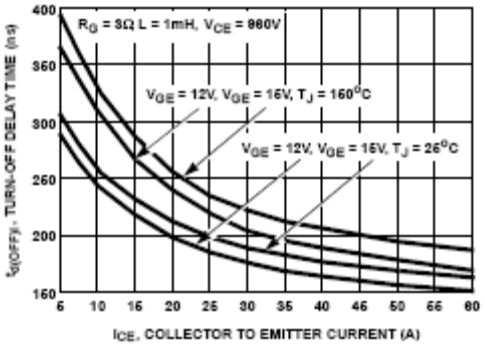

FIGURE 11. TURN-OFF DELAY TIME vs COLLECTOR TO EMITTER CURRENT

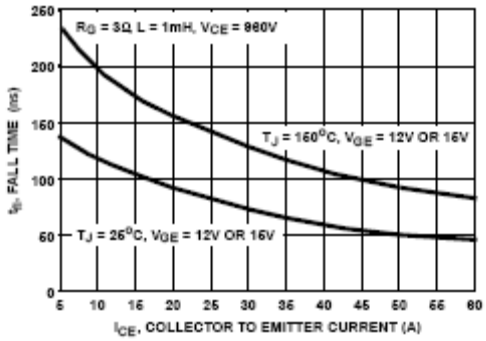

FIGURE 12. FALL TIME vs COLLECTOR TO EMITTER CURRENT

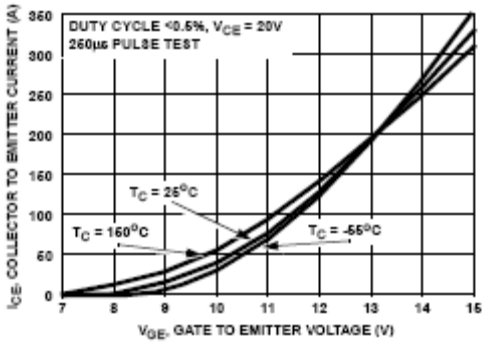

FIGURE 13. TRANSFER CHARACTERISTIC

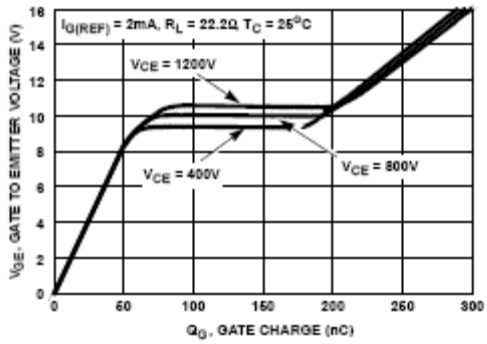

FIGURE 14. GATE CHARGE WAVEFORMS

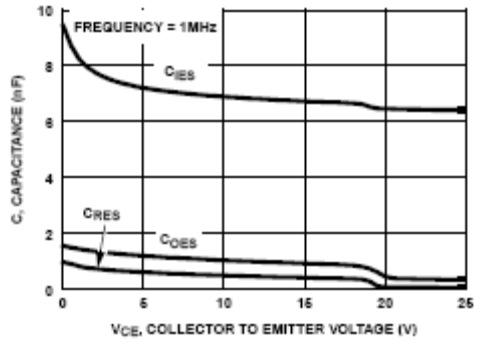

FIGURE 15. CAPACITANCE vs COLLECTOR TO EMITTER VOLTAGE

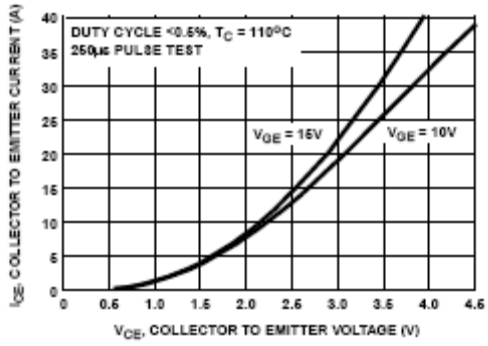

FIGURE 16. COLLECTOR TO EMITTER ON-STATE VOLTAGE

Typical Performance Curves Unless Otherwise Specified (Continued)

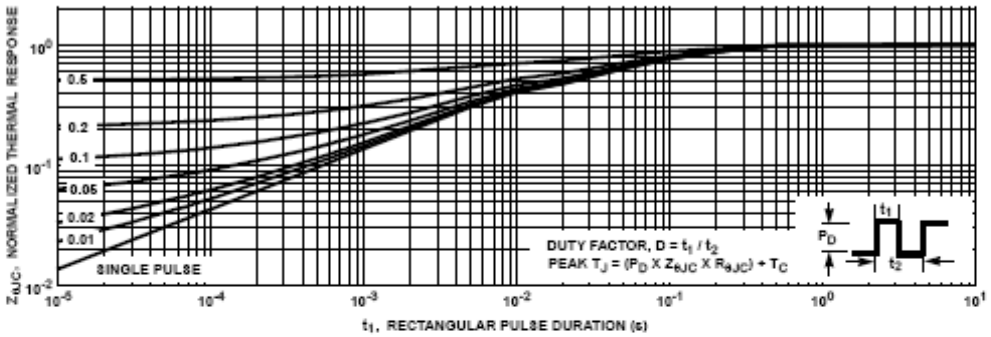

FIGURE 17. NORMALIZED TRANSIENT THERMAL RESPONSE, JUNCTION TO CASE

Test Circuit and Waveforms

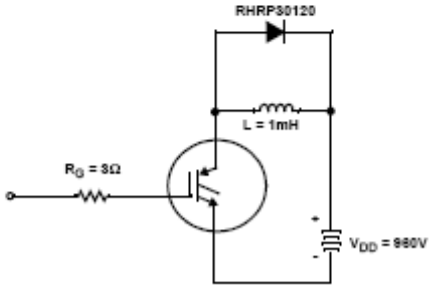

FIGURE 18. INDUCTIVE SWITCHING TEST CIRCUIT

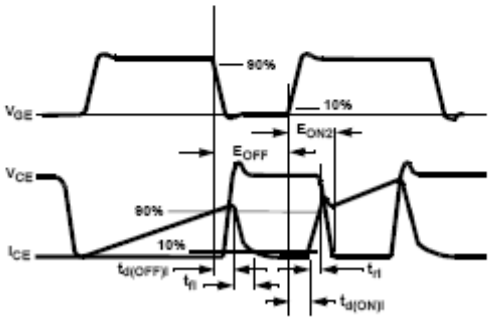

FIGURE 19. SWITCHING TEST WAVEFORMS

APPENDIX M:

Cree C2D20120D Diode Datasheet

C2D20120D–Silicon Carbide Schottky Diode

Zero Recovery® Rectifier

V_{RRM}	= 1200 V
I_F	= 20 A
Q_c	=122 nC

Features

- 1200-Volt Schottky Rectifier
- Zero Reverse Recovery
- Zero Forward Recovery
- High-Frequency Operation
- Temperature-Independent Switching Behavior
- Extremely Fast Swtitching
- Positive Temperature Coefficient on V_F

Package

TO-247-3

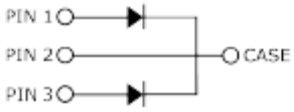

Benefits

- Replace Bipolar with Unipolar Rectifiers
- Essentially No Switching Losses
- Higher Efficiency
- Reduction of Heat Sink Requirements
- Parallel Devices Without Thermal Runaway

Applications

- Switch Mode Power Supplies
- Power Factor Correction
- Motor Drives

Part Number	Package	Marking
C2D20120D	TO-247-3	C2D20120

Maximum Ratings

Symbol	Parameter	Value	Unit	Test Conditions	Note
V_{RRM}	Repetitive Peak Reverse Voltage	1200	V		
V_{RSM}	Surge Peak Reverse Voltage	1200	V		
V_{DC}	DC Blocking Voltage	1200	V		
$I_{F(AVG)}$	Average Forward Current (Per Leg/Device)	10/20 22/44	A	T_C=150°C T_C=125°C	
$I_{F(PEAK)}$	Peak Forward Current (Per Leg/Device)	25/50	A	T_C=125°C, T_{REP}<1 mS, Duty=0.5	
I_{FRM}	Repetitive Peak Forward Surge Current	50*	A	T_C=25°C, t_P=8.3 ms, Half Sine Wave	
I_{FSM}	Non-Repetitive Peak Forward Surge Current	250*	A	T_C=25°C, t_P=10 µs, Pulse	
P_{tot}	Power Dissipation (Per Leg)	312* 104*	W	T_C=25°C T_C=125°C	
T_J , T_{stg}	Operating Junction and Storage Temperature	-55 to +175	°C		
	TO-247 Mounting Torque	1 8.8	Nm lbf-in	M3 Screw 6-32 Screw	

** Per Device, * Per Leg

Electrical Characteristics (Per Leg)

Symbol	Parameter	Typ.	Max.	Unit	Test Conditions	Note
V_F	Forward Voltage	1.6 2.5	1.8 3.0	V	I_F = 10 A T_J=25°C I_F = 10 A T_J=175°C	
I_R	Reverse Current	10 20	200 1000	µA	V_R = 1200 V T_J=25°C V_R = 1200 V T_J=175°C	
Q_C	Total Capacitive Charge	61		nC	V_R = 1200 V, I_F = 10A di/dt = 500 A/µs T_J = 25°C	
C	Total Capacitance	1000 80 59		pF	V_R = 0 V, T_J = 25°C, f = 1 MHz V_R = 200 V, T_J = 25°C, f = 1 MHz V_R = 400 V, T_J = 25°C, f = 1 MHz	

Note:
1. This is a majority carrier diode, so there is no reverse recovery charge.

Thermal Characteristics

Symbol	Parameter	Typ.	Max.	Unit	Test Conditions	Note
$R_{\theta JC}$	Thermal Resistance from Junction to Case	0.48** 0.24*		°C/W		

** Per Leg, * Both Legs

Typical Performance (Per Leg)

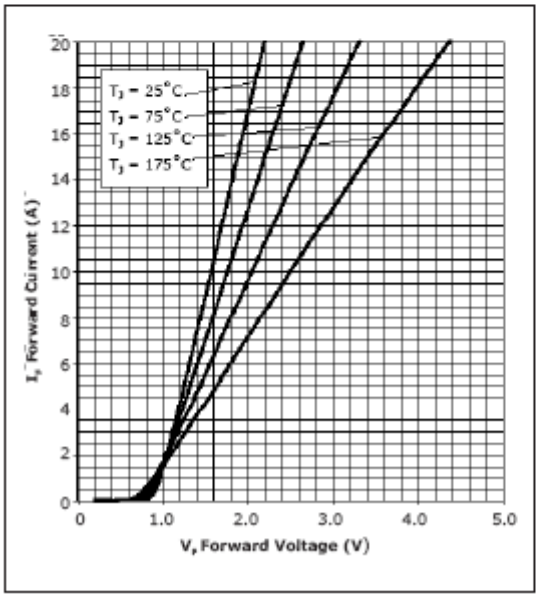

Figure 1. Forward Characteristics

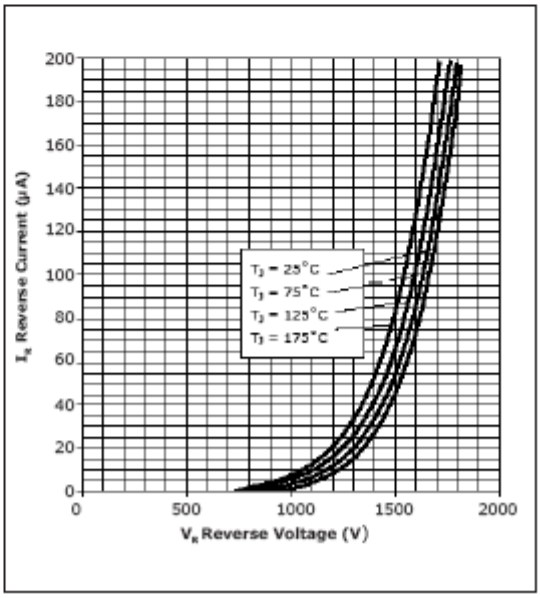

Figure 2. Reverse Characteristics

Typical Performance (Per Leg)

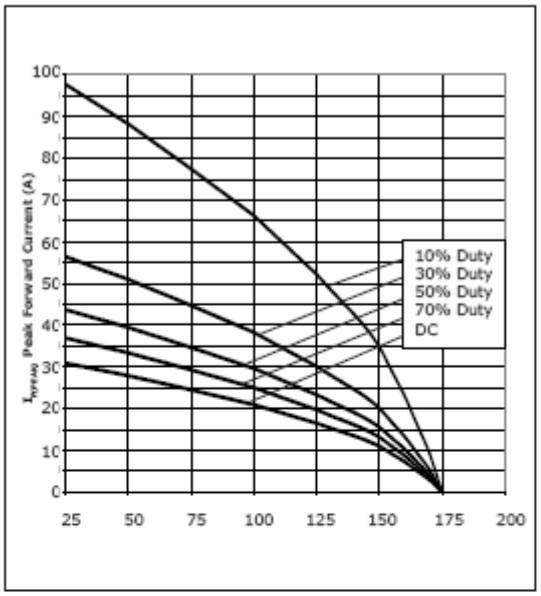

Figure 3. Current Derating

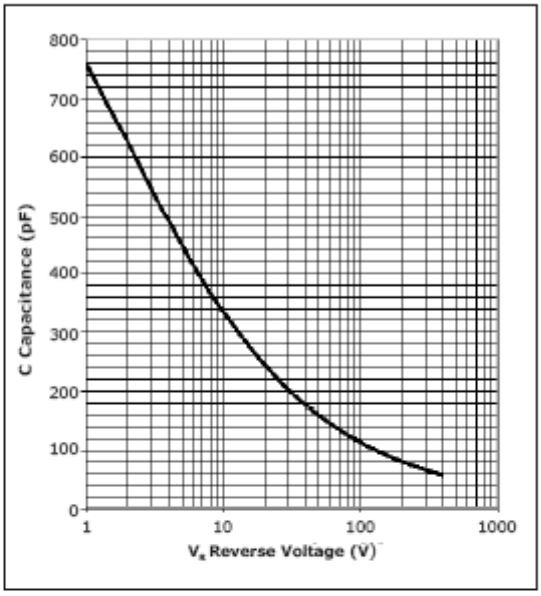

Figure 4. Capacitance vs. Reverse Voltage

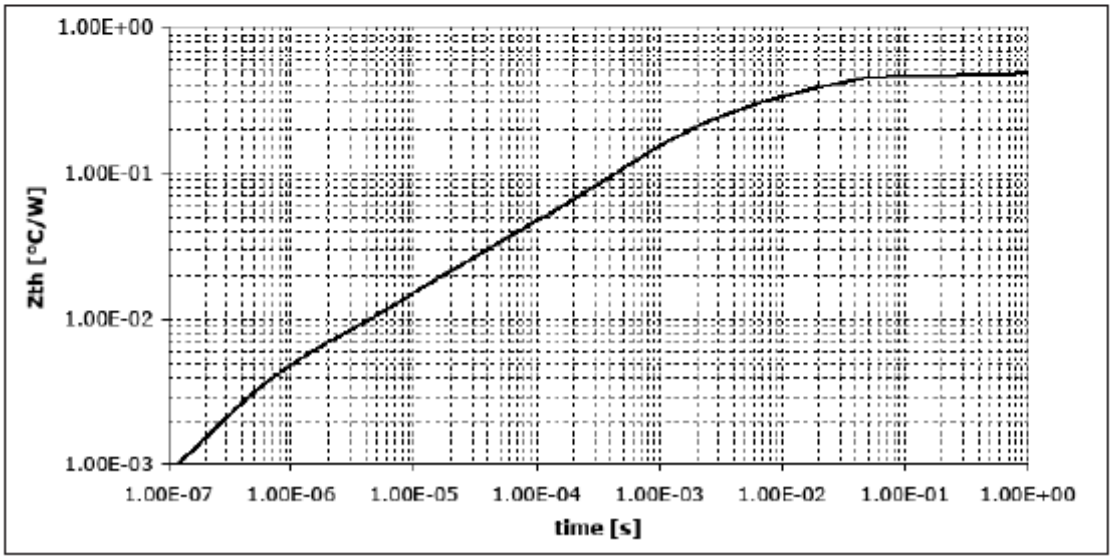

Figure 5. Transient Thermal Impedance

Package Dimensions

Package TO-247-3

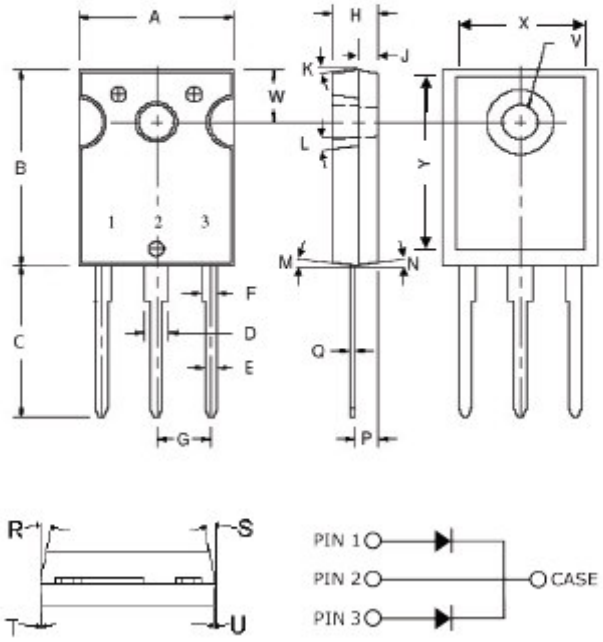

POS	Inches		Millimeters	
	Min	Max	Min	Max
A	.605	.631	15.367	16.027
B	.800	.830	20.320	21.082
C	.789	.800	20.05	20.31
D	.095	.126	2.413	3.200
E	.046	.052	1.168	1.321
F	.060	.084	1.524	2.134
G	.215 TYP		.215 TYP	
H	.180	.203	4.572	5.156
J	.078	.081	1.982	2.057
K	6°	21°	6°	21°
L	4°	6°	4°	6°
M	2°	4°	2°	4°
N	2°	4°	2°	4°
P	.090	.097	2.286	2.464
Q	.020	.030	.508	.762
R	9°	11°	9°	11°
S	9°	11°	9°	11°
T	2°	8°	2°	8°
U	2°	8°	2°	8°
V	.138	.144	3.505	3.658
W	.210	.220	5.334	5.588
X	.502	.557	12.751	14.148
Y	.637	.695	16.180	17.653

Recommended Solder Pad Layout

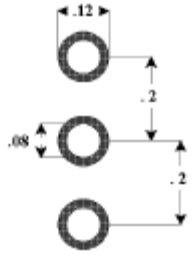

TO-247-3

Part Number	Package	Marking
C2D20120D	TO-247-3	C2D20120

APPENDIX N:

Fairchild ISL9R30120G2 Diode Datasheet

FAIRCHILD SEMICONDUCTOR®

May 2002

ISL9R30120G2

30A, 1200V Stealth™ Diode

General Description

The ISL9R30120G2 is a Stealth™ diode optimized for low loss performance in high frequency hard switched applications. The Stealth™ family exhibits low reverse recovery current ($I_{RM(REC)}$) and exceptionally soft recovery under typical operating conditions.

This device is intended for use as a free wheeling or boost diode in power supplies and other power switching applications. The low $I_{RM(REC)}$ and short t_a phase reduce loss in switching transistors. The soft recovery minimizes ringing, expanding the range of conditions under which the diode may be operated without the use of additional snubber circuitry. Consider using the Stealth™ diode with a 1200V NPT IGBT to provide the most efficient and highest power density design at lower cost.

Formerly developmental type TA49415.

Features

- Soft Recovery ..... $t_b / t_a > 4.5$
- Fast Recovery ..... $t_{rr} < 56ns$
- Operating Temperature ..... 150°C
- Reverse Voltage 1200V
- Avalanche Energy Rated

Applications

- Switch Mode Power Supplies
- Hard Switched PFC Boost Diode
- UPS Free Wheeling Diode
- Motor Drive FWD
- SMPS FWD
- Snubber Diode

Package

JEDEC STYLE 2 LEAD TO-247

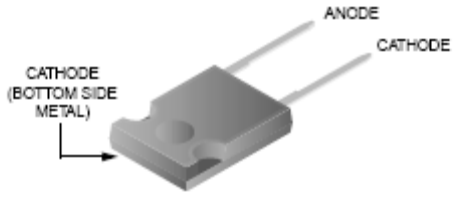

Symbol

Device Maximum Ratings T_C = 25°C unless otherwise noted

Symbol	Parameter	Ratings	Units
V_{RRM}	Repetitive Peak Reverse Voltage	1200	V
V_{RWM}	Working Peak Reverse Voltage	1200	V
V_R	DC Blocking Voltage	1200	V
$I_{F(AV)}$	Average Rectified Forward Current (T_C = 80°C)	30	A
I_{FRM}	Repetitive Peak Surge Current (20kHz Square Wave)	70	A
I_{FSM}	Nonrepetitive Peak Surge Current (Halfwave 1 Phase 60Hz)	325	A
P_D	Power Dissipation	166	W
E_{AVL}	Avalanche Energy (1A, 40mH)	20	mJ
T_J, T_{STG}	Operating and Storage Temperature Range	-55 to 150	°C
T_L T_{PKG}	Maximum Temperature for Soldering Leads at 0.063in (1.6mm) from Case for 10s Package Body for 10s, See Application Note AN-7528	 300 260	 °C °C

CAUTION: Stresses above those listed in "Absolute Maximum Ratings" may cause permanent damage to the device. This is a stress only rating and operation of the device at these or any other conditions above those indicated in the operational sections of this specification is not implied.

Package Marking and Ordering Information

Device Marking	Device	Package	Tape Width	Quantity
R30120G2	ISL9R30120G2	TO-247	N/A	30

Electrical Characteristics T_C = 25°C unless otherwise noted

Symbol	Parameter	Test Conditions		Min	Typ	Max	Units
Off State Characteristics							
I_R	Instantaneous Reverse Current	V_R = 1200V	T_C = 25°C	-	-	100	µA
			T_C = 125°C	-	-	1.0	mA
On State Characteristics							
V_F	Instantaneous Forward Voltage	I_F = 30A	T_C = 25°C	-	2.8	3.3	V
			T_C = 125°C	-	2.6	3.1	V
Dynamic Characteristics							
C_J	Junction Capacitance	V_R = 10V, I_F = 0A		-	115	-	pF
Switching Characteristics							
t_{rr}	Reverse Recovery Time	I_F = 1A, dI_F/dt = 100A/µs, V_R = 15V		-	45	55	ns
		I_F = 30A, dI_F/dt = 100A/µs, V_R = 15V		-	80	100	ns
t_{rr}	Reverse Recovery Time	I_F = 30A, dI_F/dt = 200A/µs, V_R = 780V, T_C = 25°C		-	269	-	ns
$I_{RM(REC)}$	Maximum Reverse Recovery Current			-	7.5	-	A
Q_{RR}	Reverse Recovered Charge			-	930	-	nC
t_{rr}	Reverse Recovery Time	I_F = 30A, dI_F/dt = 200A/µs, V_R = 780V, T_C = 125°C		-	529	-	ns
S	Softness Factor (t_b/t_a)			-	6.2	-	-
$I_{RM(REC)}$	Maximum Reverse Recovery Current			-	11	-	A
Q_{RR}	Reverse Recovered Charge			-	3.0	-	µC
t_{rr}	Reverse Recovery Time	I_F = 30A, dI_F/dt = 1000A/µs, V_R = 780V, T_C = 125°C		-	260	-	ns
S	Softness Factor (t_b/t_a)			-	4.8	-	-
$I_{RM(REC)}$	Maximum Reverse Recovery Current			-	30	-	A
Q_{RR}	Reverse Recovered Charge			-	3.4	-	µC
dI_M/dt	Maximum dI/dt during t_b			-	520	-	A/µs
Thermal Characteristics							
$R_{\theta JC}$	Thermal Resistance Junction to Case	TO-247		-	-	0.75	°C/W
$R_{\theta JA}$	Thermal Resistance Junction to Ambient	TO-247		-	-	30	°C/W

Typical Performance Curves

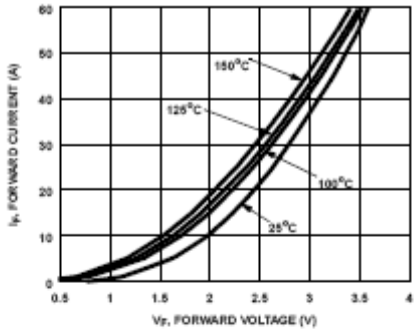

Figure 1. Forward Current vs Forward Voltage

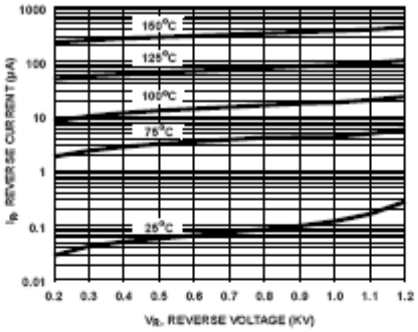

Figure 2. Reverse Current vs Reverse Voltage

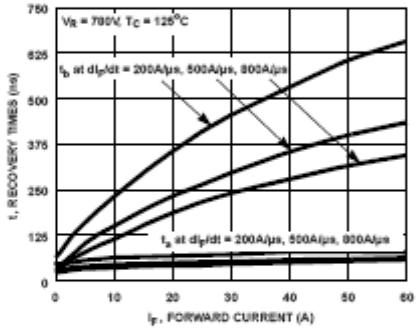

Figure 3. t_a and t_b Curves vs Forward Current

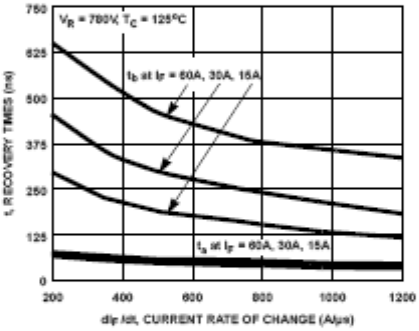

Figure 4. t_a and t_b Curves vs dI_F/dt

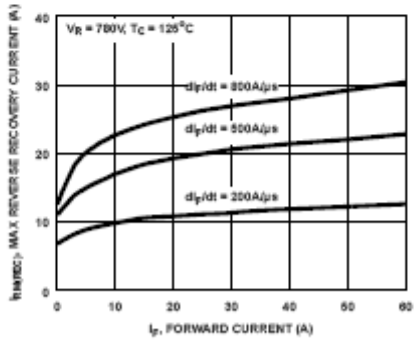

Figure 5. Maximum Reverse Recovery Current vs Forward Current

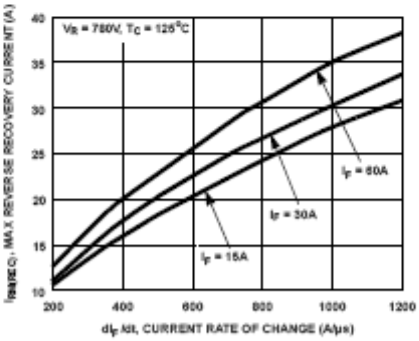

Figure 6. Maximum Reverse Recovery Current vs dI_F/dt

Typical Performance Curves (Continued)

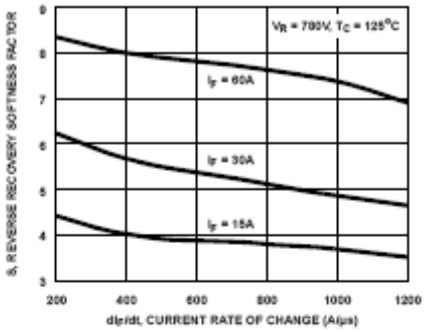

Figure 7. Reverse Recovery Softness Factor vs dI_F/dt

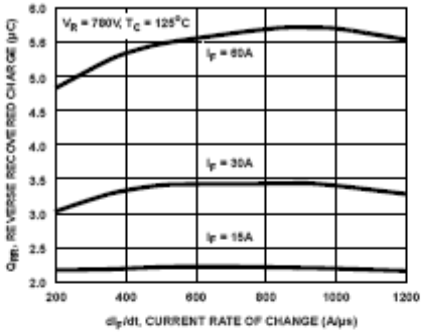

Figure 8. Reverse Recovery Charge vs dI_F/dt

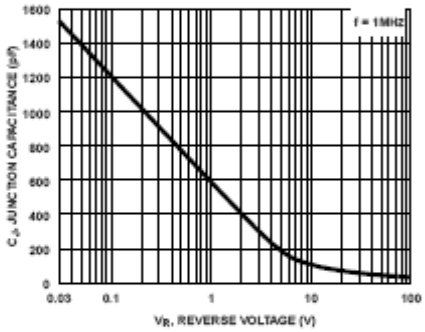

Figure 9. Junction Capacitance vs Reverse Voltage

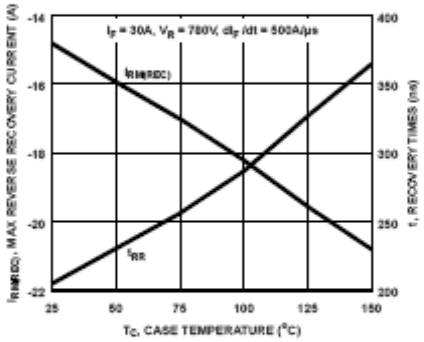

Figure 10. Maximum Reverse Recovery Current and t_{rr} vs Case Temperature

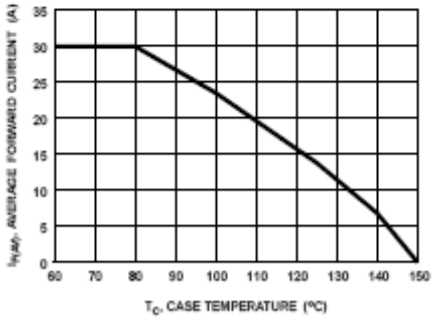

Figure 11. DC CURRENT DERATING CURVE

Typical Performance Curves (Continued)

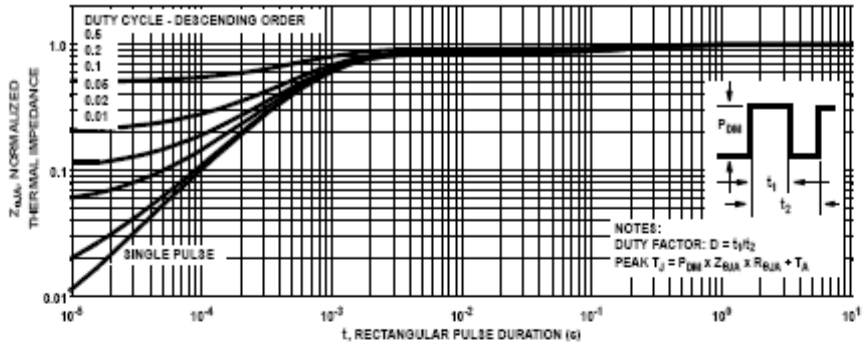

Figure 12. Normalized Maximum Transient Thermal Impedance

Test Circuit and Waveforms

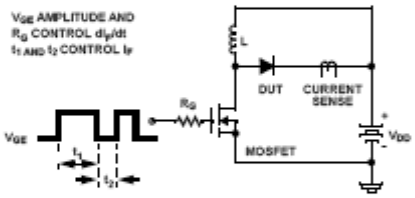

Figure 13. t_{rr} Test Circuit

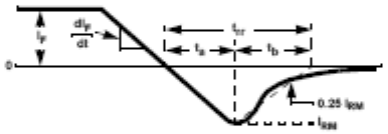

Figure 14. t_{rr} Waveforms and Definitions

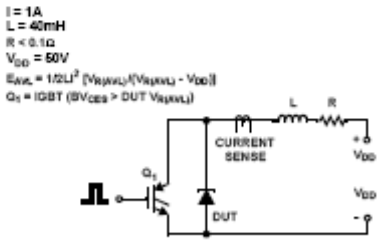

Figure 15. Avalanche Energy Test Circuit

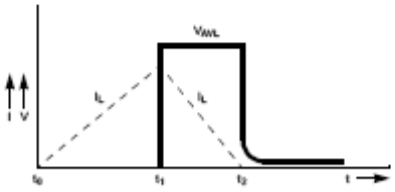

Figure 16. Avalanche Current and Voltage Waveforms